One figure missing

W. H. WARREN

L ENGINEERING STUDIES
TRUCTURAL RESEARCH SERIES NO. 92

STATIC AND DYNAMIC LOAD-DEFLECTION TESTS OF STEEL STRUCTURES

By
F. L. HOWLAND, W. EGGER
R. J. MAYERJAK and R. J. MUNZ

Approved by
N. M. NEWMARK

Final Report for the Period from
15 September 1953 to 1 September 1954
to
WRIGHT AIR DEVELOPMENT CENTER
UNITED STATES AIR FORCE
Contract No. AF 33(616)-170
Expenditure Order No. R 449-37 AW-7

UNIVERSITY OF ILLINOIS
URBANA, ILLINOIS

DISTRIBUTION LIST

Commander
Wright Air Development Center
Wright-Patterson AFB, Ohio
ATTN: WCRRN - Blast Effects Research (5)

The Chief
Armed Forces Special Weapons Project
Washington 25, D. C.
ATTN: Weapons Effects Division (1)

Director of Intelligence
Headquarters, USAF
Washington 25, D. C.
ATTN: Mr. R. G. Grassy - AFOIN-3B (1)

Commander
Wright-Air Development Center
Wright-Patterson AFB, Ohio
ATTN: Maj. Andrew Boreske, WCOES-2 (1)

Commander
Air Research and Development Command
P. O. Box 1395
Baltimore 3, Maryland
ATTN: Col. Delmar Crowson (1)

The Rand Corporation
1700 Main Street
Santa Monica, California
ATTN: Dr. Marc Peter (1)

Massachusetts Institute of Technology
Department of Civil and Sanitary Engineering
Room 1-232
Cambridge 39, Massachusetts
ATTN: Dr. Charles Norris (1)

Drexel Institute
Philadelphia, Pennsylvania
ATTN: Professor Harry Bowman (1)

Armour Research Foundation
35 W. 33rd Street
Chicago 16, Illinois
ATTN: Dr. S. J. Fraenkel (1)

DISTRIBUTION LIST (Cont'd)

American Machine and Foundry Co.
Mechanics Research Department
1104 S. Wabash Ave.
Chicago 5, Illinois
ATTN: Mr. J. E. Fitzgerald (1)

Professor Lynn S. Beedle
Fritz Laboratory
Lehigh University
Bethlehem, Pennsylvania (1)

Document Service Center (DSC)
U. B. Building
Dayton, Ohio (1)

Dean W. L. Everitt
University of Illinois (1)

Professor N. M. Newmark
University of Illinois (2)

Professor W. H. Munse
University of Illinois (1)

N. Brooks
Project Supervisor of AF 24994
University of Illinois (1)

F. L. Howland
Project Supervisor (2)

Project Personnel (6)

Project Files (10)

FINAL REPORT FOR THE PERIOD FROM
15 SEPTEMBER 1953 TO 1 SEPTEMBER 1954

Contract No. AF 33(616)-170
Expenditure Order No. R 449-37 AW-7

STATIC AND DYNAMIC LOAD-DEFLECTION TESTS OF STEEL STRUCTURES

by

F. L. Howland, W. Egger
R. Mayerjak and R. Munz

Approved by

N. M. Newmark

University of Illinois
Urbana, Illinois

February 1955

ABSTRACT

The results of four phases of a study of the resistance of structural steel frames and frame components are described in this report. Three of the phases, the study of full-scale beam-columns laterally loaded in a principal direction, the model frame study, and the study of obliquely loaded full-scale beam-columns, are concerned with the investigation of static resistance. The fourth phase is concerned with the nature of dynamic resistance of beams. The purpose of this program is to obtain the structural parameters necessary to define the resistance of buildings and building components to blast loading.

The static resistances, as measured in tests of the beam-columns and frames, are compared with the resistances predicted using the elasto-plastic theory and an extension of this theory to include the effect of strain hardening. In all studies described the influence of constant axial loads is discussed and techniques for including this effect in the analysis are presented except for the case of the oblique loading study.

The last section of this report describes the results of a dynamic test of a simply-supported beam and the analytical studies undertaken in conjunction with this test. A criterion for determining the dynamic yield stress, based on available information on the delay time for yielding, is described and applied to the data obtained in the test. Two possible forms for the dynamic resistance of the beam after yielding are discussed and a comparison of the measured response with the response predicted assuming these forms of the resistance is made.

ACKNOWLEDGMENT

This report is a final report for the period from 15 September 1953 to 1 September 1954 of a research project conducted in the Engineering Experiment Station of the University of Illinois, Department of Civil Engineering, and sponsored by the Wright Air Development Center, Department of the Air Force, under Contract AF 33(616)-170.

The work constitutes a part of the structural research program of the Department of Civil Engineering under the general direction of N. M. Newmark, Research Professor of Structural Engineering. The research program is under the direct supervision of F. L. Howland, Research Associate in Civil Engineering. The research described was performed by W. Egger, R. J. Munz, R. J. Mayerjak, C. L. Wilkenson, and R. F. Wojcieszak, Research Assistants in Civil Engineering. In addition to the members of the regular project staff, considerable assistance in this work was given by L. Olson and A. Wainscott, then undergraduates in the Department of Civil Engineering.

The authors wish to acknowledge the assistance of W. H. Munse, Research Associate Professor of Civil Engineering, W. J. Hall, Research Assistant Professor of Civil Engineering, and J. M. Massard, Research Associate in Civil Engineering, in the planning of the program and in the interpretation of the test results.

The recording instruments used in the dynamic test program were assembled and operated by V. J. McDonald, Research Assistant Professor of Civil Engineering, and R. J. Craig, Senior Electrical Technician, whose attention to these and other phases of the instrumentation problems has been of considerable assistance throughout the program.

TABLE OF CONTENTS

TABLE OF CONTENTS (Cont'd)

TABLE OF CONTENTS (Cont'd)

TABLE OF CONTENTS (Cont'd)

LIST OF TABLES

LIST OF FIGURES

LIST OF FIGURES (Cont'd)

LIST OF FIGURES (Cont'd)

LIST OF FIGURES (Cont'd)

LIST OF FIGURES (Cont'd)

LIST OF FIGURES (Cont'd)

1. INTRODUCTION

1.1 INTRODUCTION

The object of this program is to obtain the parameters necessary for the computation of blast effects on buildings and structures by determining the load-deflection characteristics, under both static and dynamic conditions, of steel structures and elements.

In this program the parameters and their relationship with one another in the formulation of the resistance have been studied through experimental investigations of the response of structural frame elements to static and dynamic loads. In these studies the experimentally measured response, as revealed by the load-deflection and moment-curvature relationships, has been compared with the predicted response based on an elementary theory of plasticity. This comparison of the experimental and predicted response permits an estimate of the error that is inherent in the theory, and helps to determine other variables which may be of importance but which have not been included in the analysis. This procedure has been satisfactory for the static loading conditions. For dynamic loading, a further approximation has been made in that the actual structure, for the analysis only, has been replaced by a simple single-degree-of-freedom model which, when loaded, exhibits the same response as the load point of the actual structure. However, the resistance of the model is to be correlated with the resistance predicted by the elementary theory through the introduction of parameters which indicate the time dependence of the resistance.

1.2 SURVEY OF THE LITERATURE

The application of the procedure outlined above has been used frequently in the past for the evaluation of static response parameters. In Great Britain, extensive tests of beams and frames have been conducted by Baker[1,2,3,4]*, Horne[5,6,7] and Neal[8]. These tests have included many model beams and several full scale portal frames. In this country extensive experimental investigation of frames, knee connections, and beam columns have been studied at Lehigh University[9,10,11,12,13,14,15,16,17]. These tests have indicated that in many cases the response of structures can be predicted satisfactorily by means of the elasto-plastic theory of inelastic action which neglects strain hardening of the material. The analytical aspects of the inelastic behavior problem have been treated by the group at Brown University[18,19,20,21] and many techniques for the analysis of structures and some general theorems for certain classes of problems have been obtained. More recently, Lazard[22] has published the results of an extensive series of tests on beams which include many variables such as the influence of a reversal of the direction of loading and cyclic loading on the static response of beams. A rather extensive survey of the literature has been summarized by Steele, Liu, and Smith[23].

Unfortunately, much of the past work on the static response problem has been limited to the investigation of the response in the

---

* Numbers in parenthesis refer to corresponding numbered entries in the Bibliography at the end of this section.

initial phases of the inelastic deformation before strain hardening occurred. In the recent portal frame tests by Baker[3,4] the influence of strain hardening on the response of frames in which the columns were oriented in the weak direction has been reported. These tests indicate that when the columns are oriented in the strong direction the effects of strain hardening are hidden by the development of lateral failures of the columns. The studies[2,13,17] have indicated the importance of the residual stresses and stress concentrations at the boundary in the determination of the elastic limit and the response of the structures for the early phases of the inelastic deformations.

When attention is turned from the static response problem to the dynamic problem the amount of available information decreases and a relatively unexplored field presents itself. The nature of the properties of materials for various conditions and rates of loading have been of some interest for many years. Before 1940, limited investigations of the effect of rate of loading and loading history on the stress-strain relationship for mild steel were undertaken by Manjoine[25,26] and Davis[27] and have been summarized by Nadai[28]. Since 1940, further work on the stress-strain relationship for mild steel and other materials has been done. Clark, Wood and Vreeland[29,30], using constant stress tests, have shown that mild steel can sustain a stress greater than the static upper yield point for some time before general yielding occurs. Stuart[31] reports that the stress-strain relationship for copper and similar materials, which exhibit a strain-rate effect, requires some modification to account for the observation that a

transient pulse applied to the inelastically deformed material propagates initially with the elastic velocity rather than the velocity corresponding to the tangent modulus for the strained condition of the material immediately before the pulse was applied. This strain-rate phenomenon has been simulated in an analytical study by Malvern[32] for longitudinal loading conditions.

For beam structures rather extensive literature is available on the elastic response. In the case of the inelastic response much of the literature deals with ideal rigid-plastic beams[33,34]. A limited study of the response of semi-infinite beams for constant velocity impact is available as a closed solution[35]. However, in the cases which have been reported, the form of the resisting function has been assumed and investigations similar to Malvern's, where time dependence of the dynamic resistance is included, have yet to be undertaken for the beam response problem.

1.3 SUMMARY

In this program, attention was first focused on the investigation of the static response and the further study of those variables which might be significant but which have been neglected in previous studies. In this study, the specimen configuration, the applied load, and the testing procedure have been selected to cover as wide a range of conditions as possible while simulating the loads which might be applied to an actual structure. In this way it was hoped that information on the large deflection response, where strain hardening influences and the failure conditions would be magnified, could be studied. The static

program, which is described in the first three parts of this report, can be subdivided into three phases: tests of beam-columns oriented in the principal directions with respect to the lateral load, tests of beam-columns subjected to oblique loading, and tests of model frames.

The test specimens used in the full-scale beam-column tests simulated an interior column of a structure by replacing the floor system framing into the column by a stub system fastened to the beam. The lateral load was applied to the beam through the stub. In half of the tests the beam-column was subjected to a constant axial load equal to approximately the AISC allowable load and a varying lateral load. The beam-columns subjected to an oblique lateral load were similar to the specimens tested in a principal direction except that, rather than maintaining a constant direction of load application, the specimen was constrained to deflect in a preset direction.

The model frame study was undertaken to determine if additional variables other than those noted in the beam-column tests were significant in determining the response of simple frames. In these tests, column sections which were approximately one-quarter scale models of a 6 WF 25.0 section, were fabricated into two-column bents connected by a rigid top girder. The frame formed from this bent was essentially an ideal frame with fixed column bases. The lateral load, which varied throughout the tests, was applied along the axis of the top girder. As in the case of the full-scale beam-columns, the frames were tested with the columns oriented in both the strong and the weak directions with respect to the applied load. In one half of the tests a constant axial

thrust, equal to approximately the AISC design load was applied to the columns.

From the static tests it has been found that, in addition to the dependence of the resistance on the shape of the section and the character of the loading, as revealed by the elasto-plastic theory generally applied in limit analysis, the resistance or response depends on the applied thrust, the possibility of strain hardening of the material, the mode of failure of the structure, and the direction of the applied lateral load with respect to the principal axes of the section.

The effect of the axial load is readily predicted by the elementary theory if the influence of strain hardening is included and if failure by lateral deflection and twisting does not occur. In most of the weak direction tests and some of the strong direction tests reported herein, the axial load did not significantly affect the moment-curvature relationship and had to be included only as a primary force in the computation of the moments. The agreement between the test results and the theory was best in the cases where bending about the weak axis of the section occurred. Greater divergence occurred in the strong direction tests where the specimens were subjected to lateral and twisting type failures soon after the elastic limit was exceeded.

The influence of the strain hardening of the material on the response was appreciable for most of the tests. In the model frame studies strain hardening nearly doubled the load capacity of the structures while in the full-scale beam-column tests the increase was smaller but was still significant. These differences in the contribution of

strain hardening to the load capacity was a result of the difference in the restraints against failure. Fortunately, the effect of strain hardening is readily incorporated in the theory for loading which results in bending about a principal axis of the section. The increased capacity obtained by strain hardening, however, does not continue indefinitely. In the weak direction tests, the increase in load provided by strain hardening was gradually overcome by the local buckling of the compression flanges. In the strong direction tests the increased capacity resulting from strain hardening was lessened by the development of twisting and lateral types of failures.

In all of the tests performed on this program, the mode of failure significantly influenced the static response. In the weak direction tests, the primary failure was by local buckling of the compression flange. For this direction of loading, the local buckling did not destroy the symmetry of the section and the lateral stability of the structure was not impaired so that the local buckling provided a limit to the load capacity without causing large losses in the load capacity.

In the strong direction tests, two types of failure occurred: a lateral buckling without local buckling, and local buckling followed by a final failure due to lateral buckling. The only case in which lateral buckling occurred alone was in the strong direction test of the 6 I 12.5 beam. The failure was rapid and severely limited the energy absorbing capacity of the structure.

The most common type of failure in the strong direction tests was by local buckling followed by lateral buckling. This type of failure

is dependent on many variables such as the dimensions of the section, the type of loading, the restraint conditions, intentional or accidental eccentricities of the loading, and the orientation of the loading with respect to the principal axes of the section. The lateral buckling and twisting type failures were, for these tests, triggered by anti-symmetric local buckling of the compression flange which was equivalent to an inclination of the load to the principal axes. It has been found from the oblique loading study that slight inclinations of the load from the direction causing bending about the strong axis of the section results in a rapid growth of the lateral deflection of the beam when inelastic behavior develops.

In comparing the full-scale beam-column tests with model frames, it was noted that the maximum deflection relative to the elastic limit deflection was considerably larger in the frame tests. However, the difference in the restraint conditions for the two types of tests can account for this difference.

In the oblique loading study, the elasto-plastic theory of plasticity has been extended to include the condition of simultaneous bending about both principal axes. The theory in its present form, requires that two relationships, the moment interaction and moment-curvature relationships, be known for the solution for the load-deflection relationship of the structure. The moment-interaction relationship defines the position of the neutral axes for any given combination of bending moments and the moment-curvature relationship relates the applied moment to the local curvature of the section. This theory, which at present includes the entire cross section, is too complex for

application but can be used to evaluate the accuracy of approximate analysis methods.

In order to check the theoretical study, two tests were performed: one in which only a lateral load was applied and the second in which lateral and axial loads were applied. In these tests the direction of the deflection at the center of the beam was constrained to a fixed line. Because of this constraint the direction of the applied loads with respect to the principal axes of the beams changed throughout the tests. The results indicate that the theory is reasonably accurate: the errors being the same as those found in the principal direction tests of full-scale beam-columns.

The second aspect of this program is concerned with a study of the dynamic response of structures. In this report a summary of the results of a test of a 3 I 7.5 beam loaded with a pulse applied at mid-span are described. These results are tentative and further work is required. The analysis of the data obtained from this test has indicated that the dynamic resistance can be divided into three parts: the initial elastic range, the initiation of inelastic behavior, and the resistance after yield. The nature of the elastic resistance has been studied thoroughly in many places and presents no great problem. The second part, the initiation of yielding, requires the establishment of some criterion for determining when yielding occurs. This problem has been approached by formulating a criterion, based on the results of tests by Clark and Wood, which permits other than constant stress conditions to be considered. One finds that, for the beam test, the dynamic

yield stress, as determined with this criterion, was approximately 1.75 times the static upper yield point of approximately 40,000 psi. From this test it was also noted that the dynamic resistance, after yielding occurred at the increased stress, decayed and reached a lower limit that was somewhat greater than the static capacity. However, further work on this problem is required before definite conclusions can be made

1.4 CONCLUSIONS

This program has indicated that the static response of steel frames and frame elements can be predicted with a theory that is similar to the elasto-plastic theory but which includes the effect of strain hardening of the material. However, the tests have also indicated that the mode of failure can cause significant deviations from the predicted response even though strain hardening has been included. For nearly all of the tests the experimentally determined capacity was between that predicted by the elasto-plastic theory as a lower bound and that predicted by a theory that includes strain hardening as an upper bound. In the weak direction of loading, although failures generally occurred by local buckling and the load capacity was restricted, the response nevertheless approached the upper bound. In the strong direction tests, however, the failures by lateral buckling caused significant deviations from the upper bound predictions and, in many cases, the elasto-plastic theory, which neglects strain hardening, provided the best predictions. However, the deviation depends on many factors such as the restraint conditions which are not incorporated in the theories at this time.

In the application of these theories for the prediction of response, the effect of the axial load must be included. In the weak direction tests, the thrust had only a small effect on the moment-curvature relationship and had to be included only in the computation of the applied moments. In the strong direction tests, the thrust had to be included in the computations of the bending moments and of the curvatures corresponding to these moments.

The dynamic tests of the beam specimens have indicated that the resistance to dynamic loads differs significantly from the static resistance. The change in resistance noted occurs because of an increase in the yield stress of the material. This increase is, at first, a result of the delayed yield phenomenon which extends the elastic range of the response. After yielding occurs the resistance decays to a level that is greater than the static resistance. For the beam specimens, the dynamic resistance was from 100 to 50 per cent greater than the static resistance and consequently the deflections obtained in the tests were considerably less than expected on the basis of predictions made assuming the dynamic resistance to be the same as the static resistance.

Until the nature of the dynamic resistance after yielding is more completely defined the significance of the increased load capacity in the blast loading problem is subject to question. However, these results indicate that the structure's resistance can be nearly doubled for an appreciable range of deformations. In all likelihood, an increase in capacity will accompany loading that results in continuing deformation of the structure. If the loading is such that the structure comes to

rest during the loading, the resistance probably decays to the static resistance during the periods of low or zero velocity. However, if the motion redevelops after a period of rest, the resistance probably increases as the velocity increases. Thus for long duration loadings, where rest periods may occur, the resistance of the structure can be complex but can, on the average, be significantly larger than the static resistance. Further studies of the nature of the dynamic resistance after yielding are being made at this time and more quantitative information should be available in the future.

1.5 BIBLIOGRAPHY

1. Baker, J. F., "The Design of Steel Frames," The Struct. Engn. (Br), Vol. 27, No. 10, p 397, Oct. 1949.

2. Baker, J. F. and Horne, M. R., "Effect of Internal Stresses on the Behavior of Members in the Plastic Range," Engn. 171-212-3, Feb. 1951.

3. Baker, J. F., "A Review of Recent Investigations Into the Behavior of Steel Frames in the Plastic Range," Journ. Inst. C. E. (Br), No. 3, p 185, Jan. 1949.

4. Baker, J. F. and Roderick, J. W., "Tests of Full-Scale Portal Frames," Excerpt Part I, Proceedings of the Institution of Civil Engineers, Jan. 1952.

5. Horne, M. R., "The Plastic Theory of Bending of Mild Steel Beams with Particular Reference to the Effect of Shear Forces," Proc. Royal Society, Series A, Vol. 207, 1951, pp 216-228.

6. Horne, M. R., "The Lateral Instability of I Beams Stressed Beyond the Elastic Limit," British Welding Research Assoc. Report, July 1948.

7. Horne, M. R., "Experimental Investigations Into the Behavior of Continuous and Fixed Ended Beams," Fourth Congress, International Assoc. for Bridge and Structural Engineers, 1952.

8. Neal, B. G., "The Lateral Instability of Mild Steel Beams of Rectangular Section Stressed Beyond the Elastic Limit," British Welding Research Assoc. Report, July 1948.

9. Luxion and Johnston, B. G., "Plastic Behavior of Wide Flange Beams," Progress Report No. I, Welding Journ., Nov. 1948, p 538.

10. Beedle, Ready and Johnston, B. G., "Tests of Columns Under Combined Thrust and Moment," SESA Proc. Vol. 8, No. 1, 1950, p 109.

11. Yang, Beedle and Johnston, B. G., "Plastic Design and the Deformation of Structures," Progress Report No. 3, Welding Journ., July 1951.

12. Topractsoglou, Beedle and Johnston, B. G., "Connections for Welded Continuous Portal Frames," Progress Report No. 4.

Part I. Test Results and Requirements for Connections, Welding Journ., July 1951.

Part II. Theoretical Analysis of Straight Knees, Welding Journ., August 1951.

Part III. Discussion of Test Results and Conclusions, Welding Journ., Nov. 1952.

13. Yang, Beedle and Johnston, B. G., "Residual Stress and the Yield Strength of Steel Beams," Welding Journ., April 1952.

14. Ketter, Beedle and Johnston, B. G., "Column Strength Under Combined Bending and Thrust," Welding Journ., Dec. 1952.

15. Ruzek, Knudsen, Johnston, E. R., and Beedle, "Welded Portal Frames Tested to Collapse," Progress Report No. 7, Fritz Laboratory, Lehigh University.

16. Yang, Knudsen, Johnston, B. G. and Beedle, "Plastic Strength and Deflections of Continuous Beams," Progress Report No. 9, Fritz Laboratory, Lehigh University.

17. Ketter, Kaminsky, and Beedle, "Plastic Deformation of WF Beam Columns," Proc. ASCE, Vol. 79, Separate No. 330, Oct. 1953.

18. Neal, B. G., "Plastic Collapse and Shakedown Theorems for Structures of Strain Hardening Material," Journ. of Aero Sci., Jan. 1951.

19. Neal, B. G. and Symonds, P. S., "The Calculation of Plastic Collapse Loads for Plane Frames," Fourth Congress, International Assoc. for Bridge and Structural Engineers, 1952.

20. Symonds, P. S., "A Review of Methods for the Plastic Analysis of Rigid Frame of Ductile Material," ALL-S6/86, Grad. Div. of Applied Math, Brown Univ., May 1950.

21. Greenberg, H. J. and Prager, "On Limit Design of Beams and Frames," Tech. Report No. 1, Grad. Div. of Applied Math., Brown Univ., Oct. 1949.

22. Lazard, A., "The Effect of Plastic Yield in Bending on Mild Steel Plate Girders," The Structural Engn., Vol. 23, No. 2, Feb. 1954.

23. Steele, M. C., Liu, C. K., and Smith, J. O., "Critical Review and Interpretation of the Literature on Plastic (Inelastic) Behavior of Engineering Metallic Materials," Contract No. AF 33(038)-15677, Dept. of Theo. and Applied Mech., Engn. Exper. Station, Univ. of Illinois, Sept. 1952.

24. Elam, C. F., "The Influence of Rate of Deformation on the Tensile Test with Special Reference to the Yield Point in Iron and Steel," Proc. of the Royal Society, Ser. A., Vol. 165, 1938.

25. Nadai, A. and Manjoine, M. J., "High Speed Tension Tests at Elevated Temperatures"

Part I. Proc. ASTM, Vol. 40, 1940, pp 822-837.

Parts II and III. Trans ASME, Vol. 63, 1941, p A-77.

26. Manjoine, M. J., "Influence of Rate of Strain and Temperature on Yield Stresses of Mild Steel," Journ. Applied Mech., Dec. 1944.

27. Davis, E. A., "The Effect of the Speed of Stretching and Rate of Loading on the Yielding of Mild Steel," Journ. of Applied Mech., Vol. 5, Dec. 1938.

28. Nadai, A., "Theory of Flow and Fracture of Solids," Vol. 1, Second Edition, McGraw-Hill, 1950.

29. Wood, D. S. and Clark, D. S., "The Influence of Temperature Upon the Time Delay for Yielding in Annealed Mild Steel," Proc. ASM, 1951.

30. Vreeland, T., Wood, D. S., and Clark, D. S., "A Study of the Mechanism of the Delayed Yield Phenomenon," Proc. ASM, 1952.

31. Stuart, D. A., "The Propagation of Large Amplitude Longitudinal Strains in a Work Hardenable Material," Cornell University, Final Report for Contract DA 30-115-ORD-424, Proj. TB2-0001, 27 Feb. 1954.

32. Malvern, L. E., "Propagation of Longitudinal Waves of Plastic Deformation in Bar of Material Exhibiting Strain-Rate Effect," Journ. Applied Mech., Vol. 18, No. 2, June 1951.

33. Conroy, M., "Plastic Rigid Analysis of Long Beams Under Transverse Impact," Journ. Applied Mech., 1952.

34. Lee, E. H., and Symonds, P. S., "Large Plastic Deformations of Beams Under Transverse Impact," Journ. Applied Mech., Vol. 19, No. 3, Sept. 1952.

35. Duwez, P. E., Clark, D. S., and Bohenblust, H. F., "The Behavior of Long Beams Under Impact Loading," Journ. of Applied Mech., Trans. ASME, Vol. 72, 1950.

2. STATIC TESTS TO FAILURE OF STEEL BEAM-COLUMNS

2.1 INTRODUCTION

2.1.1 Introductory Statement

The static response of a member subjected to both bending and axial loads can best be described by its load-deflection relationship. To predict the response of a member for both the elastic and inelastic ranges, the relationship between the resisting moment of the member and the curvature associated with that moment must be known. For the elastic range, this relationship is linear and is well known. In the inelastic range, the relationship between moment and curvature at any section depends upon the magnitude of the axial load, the properties of the cross section of the member, and the degree of inelastic action. Until recently, the direct determination of the moment-curvature relationship for a beam-column loaded inelastically was feasible only for a rectangular section. It was felt therefore that the development of a procedure for the determination of the moment-curvature relationship for wide flange beam-columns would be of considerable value.

The main objectives of this study were: first, to develop a method by which the moment-curvature relationship for a wide-flange beam-column could be obtained; second, to ascertain, both experimentally and analytically, the effect of an axial load on the response of certain wide-flange beam-columns; and third, to make comparisons between the predicted responses and those derived from the tests. The procedure developed for obtaining the desired moment-curvature relationship makes

use of two expressions which relate the thrust and the resisting moment to the curvature for various degrees of inelastic action. However, although the approach described herein was developed independently, a similar approach has recently been published by Lehigh University.(1)*

The experimental phase of the study consisted of twelve tests using three sizes of standard rolled section - 6 B 15.5, 4 M 13.0, and 6 I 12.5. All of the members were tested in the as-rolled condition as pin-ended members. A single concentrated load was applied at mid-span, in each case, through a welded connection detail. Six of the beam-columns were tested with a constantly applied axial thrust and their companion members were tested as simply supported beams. In all cases, the tests were carried either to the limit of the testing apparatus or to the point of collapse, whichever occurred first. The magnitude of the axial loads to which the beam-column members were subjected was approximately the allowable loads which the current AISC Specifications(2) permit for axially loaded members.

2.1.2 Summary of Results

From the experimental and analytical investigations, the influence of the axial load on the beam-column is realized in two ways: first, the thrust reduces the moment-carrying capacity of the member, the reduction depending upon the shape of the cross section and on the magnitude of the axial load; and second, the axial load causes a drop-off in the lateral load soon after the peak load is reached. Agreement between

---

* Numbers in parentheses refer to correspondingly numbered entries in the Bibliography at the end of this section.

the moment-strain, i.e., the moment-curvature, relationships determined by test and theory is, in most cases, reasonable. These results are shown in Figs. 2.22 to 2.27. A major deviation between test and theory occurs during the early stages of the inelastic action. This deviation is evidenced by yielding of the test members at loads approximately 15 percent lower than predicted by the elementary theory of plasticity. It is believed that this reduction in the yield load of the test members resulted from the presence of residual stresses and stress concentrations arising from the welded connection detail at the center load point.

Load-deflection relationships were derived from the theoretical moment-strain relationships for each of the sections tested. The deflections corresponding to particular loads were obtained by numerical integration[5] of the curvatures associated with these loads. Agreement between the derived load-deflection relationships and those obtained from the tests is fair. These results are shown in Figs. 2.28 to 2.33. In each case, the predicted deflection at a particular load is less than the measured value for loads up to the peak of the curve. In the drop-off portion of the load-deflection relationship, the predicted relationship appears to give a reasonable approximation to the test results. It should be noted, however, that this region of the curve represents an unstable condition in the member and the determination of theoretical points along this curve is impossible for purely static conditions. For this reason, this portion of the load-deflection relationship was approximated by a curve passing through the peak load and

through the predicted collapse deflection. The collapse deflection was chosen such that the thrust alone developed the fully plastic moment of the member; any strain-hardening of the member was neglected. It is interesting to note that only in specimen 4Y1S6 I did the actual collapse deflection exceed the predicted value.

Lateral buckling failures occurred in specimens 4lS4 M and 4lS6 I before the lateral load had dropped to zero. These failures developed quite suddenly and resulted in a very sudden drop-off in the applied load. Similar failures also developed in the members which were loaded in the strong direction without axial load. However, in these cases the failure was gradual and no appreciable decrease in the lateral load capacity was noted. Two important observations can be drawn from these tests:

(1) For the magnitude of the axial loads and the span length considered, strain-hardening could be neglected in the determination of the collapse deflection.

(2) For those members which were tested without axial load, strain-hardening appeared to be of considerable importance in the member's ability to sustain the load even after considerable lateral buckling had taken place.

A more detailed discussion of the results presented here is given in the following sections. The presentation of test results in dimensionless form is for convenience since the analytical study is most easily expressed in this form.

2.1.3 Notation

The following notation has been used in this report:

Cross-Sectional Constants

f = thickness of flange for wide-flange sections; average flange thickness for rolled I sections

w = thickness of web

b = width of flange

b' = distance between flanges

c = distance from centerline of section to extreme fiber

d = $2c$ = total depth of section

h_1 = depth of penetration of inelastically strained material from the top fiber

h_2 = depth of penetration of inelastically strained material from the bottom fiber

A = total cross-sectional area

A^e = area of cross section which is elastically strained

A_1^P = area of cross section which is inelastically strained in the same sense as the axial thrust

A_2^P = area of cross section which is inelastically strained in the opposite sense of the axial load

Q^e = the first moment of A^e about the centerline

Q_1^P = the first moment of A_1^P about the centerline

Q_2^P = the first moment of A_2^P about the centerline

I = the moment of inertia of the cross section about the centerline

I^e = the moment of inertia of A^e about the centerline

Loads

T = applied axial thrust

T_e = the axial thrust which would stress the entire cross section to the yield stress

M = total bending moment on the section

M_e = the bending moment corresponding to the yield point of the material with no thrust applied

M_{FP} = the fully plastic resisting moment of the cross section neglecting strain hardening

P = applied lateral load

P_e = applied lateral load which would initiate inelastic behavior of the beam-column with no thrust applied

Stresses

σ = tensile or compressive stress on any fiber

σ_e = yield stress of the material

E = modulus of elasticity

Strains

ϵ = total strain on any fiber

ϵ_f = component of the total strain resulting from bending of the member

ϵ_d = component of the total strain resulting from the axial thrust on the member

ϵ_e = yield strain of the material

Deflections

δ = total deflection at the center of the span

δ_e = center of span deflection corresponding to the yield point of the material

δ_c = deflection at which collapse of the member is impending

2.2 ANALYTICAL STUDY OF THE EFFECT OF AXIAL LOAD ON THE RESPONSE OF WIDE-FLANGE BEAMS

2.2.1 The Problem Defined

The problem of determining the response of a member subjected to both lateral and longitudinal forces resolves itself into the determination of the following:

(1) The relationship between the axial thrust, T, and the resisting moment, M, as a function of the extreme fiber strains and of the inelastically strained material. This relationship may be used to determine the interaction between applied thrust and total resisting moment for any constant fiber strain or any depth of inelastic action.[3]

(2) A relationship between the total resisting moment and the flexural component of the fiber strain. This relationship is of value in determining the load-deflection relationship for the member.

These two relationships are determined by the same equations. Since the primary interest of this investigation is to determine the load-deflection relationship for a beam-column, the moment-strain relationship, i.e., the moment-curvature relationship, is of primary importance. Also of interest is the effect of the axial thrust upon the moment-strain and load-deflection relationships for various values of the applied thrust.

2.2.2 Assumptions Made In the Analysis

The analysis is based upon the elementary theory of plasticity. The assumptions which were used in the analysis are:

a. The material is homogeneous and isotropic.

b. The loading process is always increasing and in the same direction.

c. The stress-strain relationship for the material is assumed to be independent of strain rate.

d. The cross section is symmetrical about its centroidal axis.

e. The Bernoulli-Navier hypothesis that the bending strain is proportional to the distance from the neutral axis can be extended to include inelastic deformations.

f. The stress-strain relationship is based on the relationship determined during a static tension test of a coupon of the material. In the following analysis this assumption has been further simplified by assuming the material to act as a perfect elasto-plastic material. The idealized stress-strain relationship used is shown in Fig. 2.2. However, when necessary the stress-strain relationship has been modified to include the effect of strain hardening of the material.

2.2.3 Derivation of the General Equations for Combined Bending and Axial Loads

The cross section used in this derivation together with an arbitrary strain distribution across this section are shown in Fig. 2.1-A and Fig. 2.1-B respectively. With this strain distribution and the assumed stress-strain relationship of Fig. 2.2, the resulting stress distribution across the section will be as shown in Fig. 2.1-C. From the assumed strain distribution it is quite obvious that a relationship exists between the components of strain ϵ_d and ϵ_f and the depths of inelastic action, h_1, and h_2. This relationship is useful in the derivation of the moment-strain relationship and is presented here as:

$$\epsilon_f/\epsilon_e = \frac{1}{1 - h_1/2c - h_2/2c} \qquad (1)$$

and

$$\epsilon_d/\epsilon_e = 1 - (1 - h_1/c)\epsilon_f/\epsilon_e \qquad (2)$$

When $\epsilon_d + \epsilon_f > \epsilon_e$ and $\epsilon_d - \epsilon_f < -\epsilon_e$, Eq. (1) may be used. However, when $\epsilon_d + \epsilon_f > \epsilon_e$ and $\epsilon_d - \epsilon_f > -\epsilon_e$, no independent relationship exists between ϵ_f and h_1 with the result that Eq. (2) must be used. Since the moment, M, and the axial thrust, T, at a section are functions of the stress on the section, it follows that:

$$T = \int_{-c}^{+c} \sigma\, b\, dy = -\int_{-c}^{-c+h_2} \sigma_e\, b\, dy + E \int_{-c+h_2}^{c-h_1} \left(\epsilon_d + \frac{Y}{c}\epsilon_f\right) b\, dy + \int_{c-h_1}^{c} \sigma_e\, b\, dy$$

$$= \sigma_e \left[A_1^P - A_2^P\right] + E\left[\epsilon_d\, A^e + \left(\frac{\epsilon_f}{\epsilon_e}\right) Q^e\right] \qquad (3)$$

where T is positive if the thrust is compressive

$$M = \int_{-c}^{+c} \sigma\, b\, y\, dy = -\int_{-c}^{-c+h_2} \sigma_e\, b\, y\, dy + E \int_{-c+h_2}^{c-h_1} \left(\epsilon_d + \frac{Y}{c}\epsilon_f\right) b\, y\, dy + \int_{c-h_1}^{c} \sigma_e\, b\, y\, dy$$

$$= \sigma_e \left[Q_1^P - Q_2^P\right] + E\left[\epsilon_d\, Q^e + \left(\frac{\epsilon_f}{c}\right) I^e\right] \qquad (4)$$

where M is positive if the top fiber is in compression. A more convenient form of these expressions results when Eq. (3) is divided by $T_e = \sigma_e A$ and Eq. (4) is divided by $M_e = \sigma_e I/c$. The equations then become:

$$\frac{T}{T_e} = \frac{A_1^P - A_2^P}{A} + \left(\frac{\epsilon_d}{\epsilon_e}\right)\frac{A^e}{A} + \left(\frac{\epsilon_f}{\epsilon_e}\right)\frac{Q^e}{cA} \qquad (5)$$

$$\frac{M}{M_e} = \frac{c(Q_1^P - Q_2^P)}{I} + \frac{\epsilon_d}{\epsilon_e}\frac{cQ^e}{I} + \left(\frac{\epsilon_f}{\epsilon_e}\right)\frac{I^e}{I} \tag{6}$$

These equations can be transformed into expressions involving only h_1, h_2, and ϵ_f by substituting Eq. (2) into Eqs. (5) and (6). The resulting expressions become:

$$\frac{T}{T_e} = \frac{(A_1^P - A_2^P) + A^e}{A} + \frac{\epsilon_f}{\epsilon_e}\left[\frac{Q^e}{cA} - \left(1 - \frac{h_1}{c}\right)\frac{A^e}{A}\right] \tag{7}$$

$$\frac{M}{M_e} = \frac{c}{I}\left[Q_1^P - Q_2^P + Q^e\right] + \frac{\epsilon_f}{\epsilon_e}\left[\frac{I^e}{I} - \left(1 - \frac{h_1}{c}\right)\frac{cQ^e}{I}\right] \tag{8}$$

Before these expressions can be used to determine the M, ϵ_f relationship for any value of T/T_e, the magnitude of h_1 and h_2 must be determined. Also, some criterion must be established which tells when $h_2 \geq 0$. The required criterion is to determine when $\epsilon_d - \epsilon_f \geq -\epsilon$ since if:

$$\begin{aligned}
&\epsilon_d - \epsilon_f < -\epsilon_e && h_2 > 0 \text{ and } A_2^P \text{ exists} \\
&\epsilon_d - \epsilon_f = -\epsilon_e && h_2 = 0 \text{ and } A_2^P = 0 \\
&\epsilon_d - \epsilon_f > -\epsilon_e && \text{only } A_1^P \text{ exists}
\end{aligned} \tag{9}$$

Of interest therefore is that combination of h_1 and ϵ_f for which A_2^P exists. This condition is satisfied when $\epsilon_d - \epsilon_f = -\epsilon_e$. Substitution of Eq. (2) into this expression gives as the required criterion:

$$\frac{\epsilon_f}{\epsilon_e} = \frac{1}{1 - \frac{h_1}{2c}} \tag{10}$$

The value of h_1 associated with this condition on h_2 is hereafter referred to as the critical depth of penetration and the value of axial thrust compatible with this limit on h_2 is similarly referred to as the critical thrust. The complete statement of the conditions is:

$$\text{for} \quad \frac{\epsilon_f}{\epsilon_e} < \frac{1}{1 - \frac{h_1}{2c}} \qquad \text{only } A_1^P \text{ exists}$$

$$\text{for} \quad \frac{\epsilon_f}{\epsilon_e} = \frac{1}{1 - \frac{h_1}{c}} \qquad h_2 = 0 \text{ and } A_2^P \text{ is pending} \tag{11}$$

$$\text{for} \quad \frac{\epsilon_f}{\epsilon_e} > \frac{1}{1 - \frac{h_1}{c}} \qquad h_2 > 0 \text{ and } A_1^P \text{ and } A_2^P \text{ exist.}$$

With Eqs. (7), (8), and (11), the M/M_e, ϵ_f/ϵ_e relationship can be established. For h_1/c less than the critical value, only one plastic area exists and Eq. (7) can be used directly to relate ϵ_f/ϵ_e, h_1/c, and T/T_e. For h_1/c greater than the critical value, two plastic areas occur and Eq. (1) must be introduced into Eq. (7) before h_1 and h_2 can be related. When the relationship between h_1 and ϵ_f or h_1 and h_2 is known, Eq. (8) can be solved for M.

The use of these equations for determining the moment-curvature relationship is not difficult, for the rectangular cross section.[4]

However, the application of these expressions to a wide flange beam becomes very involved because of the many changes in the section. For a wide flange beam-column loaded in either its strong or weak direction, seven expressions of the form of Eq. (7) and (8) are required to relate completely T, M, ϵ_f, h_1, and h_2 for all possible stress distributions across the section. For this reason, the direct determination of the moment-strain relationships for wide-flange sections becomes very troublesome. The desired relationship between moment and the flexural component of strain can be derived with the use of two auxiliary curves.

This procedure has recently been presented independently in reference (1) and with the exception of a different nomenclature, the method of attack presented here is similar to that of the reference. The method makes use of the following relationships:

(1) The relationship between the axial thrust and the flexural component of the strain for various values of h_1 and h_2.

(2) The relationship between the total resisting moment and the flexural component of the strain for various values of h_1 and h_2.

These relationships have been constructed for all of the sections which were tested and are presented in Figs. 2.3 to 2.14. It should be noted that all of these curves are based on idealized sections, i.e., the wide flange and standard I sections have been reduced to a system of three rectangles. This approximation of the shape of the cross section is nearly exact in the case of a wide flange beam but only a rough approximation in the case of a standard I section.

The required equations for the determination of the above relationships have been summarized in Appendix 2.A. Each of the T/T_e, ϵ_f/ϵ_e relationships was first evaluated for the critical values of h_1/c. In the case of the strong direction of loading, it was observed that in each case T/T_e was restricted to rather small values for h_1/c at the critical value. Since any point to the right of this critical condition falls in a region where only one plastic area occurs, h_2 does not exist and the relationship between T/T_e and ϵ_f/ϵ_e is a simple linear expression. Hence, in the case of the strong direction, the important equation relating T/T_e, ϵ_f/ϵ_e, and h_1/c is case 2 given in Appendix 2.A. This is true only as long as T/T_e is equal to or greater than approximately 0.2. For thrusts less than this value, the region where two plastic areas exist will become more important and hence those equations which contain both h_1 and h_2 must be used.

In the case of the weak direction of loading, inspection of the T/T_e, ϵ_f/ϵ_e relationship for critical values of h_1/c indicates that the region where two plastic areas exist is of importance for values of thrust within the working range. Hence all of the equations presented in Appendix 2.A for the weak direction of loading must be used.

With axial load-flexural strain curves it is possible to obtain the desired moment-strain relationship for any value of the axial thrust. The procedure to obtain one point on the moment-strain curve is as follows:

(1) Determine the magnitude of T/T_e acting on the member.

(2) For any depth of penetration, h_1/c find the value of ϵ_f/ϵ_e, compatible with the assumed value of thrust.

(3) Enter the M/M_e, ϵ_f/ϵ_e relationships with this value of ϵ_f/ϵ_e and obtain the value of M/M_e corresponding to that assumed depth of penetration.

These points plus the value of the resisting moment at the fully plastic condition as given by the appropriate expression in Appendix 2.A will completely define the desired moment-strain relationship. The effect of axial load on this relationship is shown for the 4 M 13.0 section in Fig. 2.15. The fact that the tension flange becomes plastic for only small values of axial load is quite clearly shown in this figure.

2.2.4 Determination of the Load-Deflection Relationship

The load-deflection relationship is of primary importance in describing the behavior of the member under load and to determine the total energy-absorbing capacity of that member. For the case of an elastic beam subjected to flexure only, this relationship may be determined by integration of the curvatures of the member along its length. In this range the curvature is expressed as M/EI. When inelastic action occurs within the member, the curvature is no longer a linear function of the bending moment and hence this simple relationship does not hold. For the case of combined flexure with axial load, the curvature at any section along the member may be approximated by dividing the flexural component of strain of that section by half the depth of the member. This approximation is limited to small deflections, i.e., deflections which do not appreciably change the geometry of the member.

With this restriction on the curvature, the conversion of the derived moment-flexural strain relationships to moment-curvature relationships for all values of axial thrust is very simple.

The load-deflection relationship is determined by the integration of the derived moment-curvature expressions. However, the curvature is dependent upon the bending moment which in turn is dependent upon the deflection. A numerical integration procedure[5] may be used in a problem of this type. A deflected shape is assumed and the total resisting moments are then computed. The values of curvature corresponding to these moments are then obtained from the derived moment-curvature relationship. These curvatures are then integrated and a new deflected shape is obtained. If the assumed deflected shape is correct for the applied thrust on the member, the deflection values obtained will be identical with those which were assumed. This method was applied to the analytically derived moment-curvature relationships in order that a comparison between the test and the derived values could be made. A discussion of the results thus obtained is presented with the test results.

2.3 DESCRIPTION OF SPECIMENS, TEST APPARATUS, AND INSTRUMENTATION

2.3.1 Test Specimens

Three rolled steel sections were used in the testing program. The sections which were used are listed in Table 2.1, together with their properties as given in the AISC Manual of Steel Construction.[2] Also, listed in this table are the properties of each section as determined from actual measurements of the test specimens. The essential features

of each test are summarized in Table 2.2.

In the early phases of the test program two beams of 12 ft span were used. These two tests were conducted on a 6 I 12.5 section which was loaded about each of its principal axis. It was noted that in the strong direction of loading for this section, failure by lateral buckling occurred at a relatively low maximum fiber strain. For this reason it was decided that a shorter span length should be used for the remainder of the program. Some consideration was also given to the matter of shear as related to the span length. It was felt that the inclusion of the shear problem would complicate the study of the effect of axial load on the response and it was decided that the specimen length should be such that the shear forces would not influence the results appreciably. A span length of approximately 8 ft was used as a compromise in order to achieve sufficient lateral stability and at the same time in order that the shear stresses should not be excessive.

The beam-column specimens were fabricated in such a way that they would simulate a single pin-connected column from a structural steel frame. A stub beam section was fastened to the center portion of each test column to simulate the effect which the floor or roof framing system might have in an actual frame structure. This stub connection detail was made as rigid as possible in order that full restraint might be afforded to the column section at this center section. A detail of this connection is shown in Fig. 2.16. Inspection of this figure shows that the detail is more rigid than might be found in actual practice. It was felt however, that the use of such a connection would insure that

the desired inelastic response within the member would occur outside the connection detail. In addition, this connection afforded a relatively simple means for applying the lateral load to the specimen.

For each of the sections tested, it was desirable to have some information as to the mechanical properties of the section. Of particular interest was the information regarding the distribution of these mechanical properties through the cross section. To obtain this information a 9 in. length of the section was removed from its central position. Standard 0.5 to 0.25 in. tension coupons with a 2 in. gage length were sawed from these sections. The number of such coupons used varied from nine to thirteen depending upon the size of the cross section. Each of these coupons was tested statically and their stress-strain curve for tensile loading was obtained. These results are summarized in Table 2.3 where the average yield stress is shown for various locations within the cross section.

The specimen designation which was used may be explained by considering a few of the specimens. For example, specimen 40 S 6B refers to a 6B section loaded statically in the strong direction, i.e., about the x-x axis, with no axial load and has a half span of approximately 4 ft. Specimen 41 S 6B refers to the same member loaded with axial load. Specimens 4Y0 S 6B and 4Y1 S 6B refer to the same section loaded in the weak direction, i.e., about the y-y axis.

2.3.2 Test Apparatus and Instrumentation

A complete description of the test apparatus and instrumentation used in this study is given in reference (6). However a brief

description is presented here for convenience.

Essentially, the apparatus consisted of the following systems: the lateral loading system, the center restraining system, the end reaction system, and the axial loading system. The lateral load was applied through a tension jacking system mounted between a hold-down point in the floor of the laboratory and the bottom stub beam of the specimen. This arrangement is shown in Fig. 2.17. The applied lateral load was measured by dynamometers located in the hanger rods which suspended the end reaction systems from the testing frame. A detail of the end reaction system is shown in Fig. 2.18. This end reaction system was chosen because it provided a minimum of constraint to the ends of the specimen and therefore allowed the beam-columns to act as pin-ended members.

An A-frame center support was used in order that no premature lateral buckling would occur. A detail of this frame assembly is shown in Fig. 2.19. The restraining system permitted the specimen to move vertically downward by adding restraining forces to the upper stub beam through a roller and guide assembly. The forces which were introduced by this arrangement were of no consequence since the laterally applied load was measured at the end reactions.

The axial load was applied through a system of two U-shaped members connected by four tie rods as shown in Figs. 2.20 and 2.21. The axial load was applied by a hydraulic jack placed between one end reaction and its corresponding U beam. At the other end of the specimen the load was transferred directly from the U beam to the end reaction.

In both cases the linkage between these U beams and the end reaction plates was accomplished with knife edges which permitted the specimen to deflect in the direction of the lateral load. The axial load was measured by four dynamometers, one located in each of the tie rods.

The major problem encountered in the axial loading system was maintaining the applied thrust at a nearly constant magnitude. In the first beam-column test, that of specimen 4IS6 I 12.5, the applied thrust was controlled by the indicated pressure in the hydraulic system. It was found that this system was very insensitive and as a result large fluctuations in the thrust occurred. This difficulty was overcome by use of a null type system activated by the total output of the four dynamometers. A complete description of this control system can be found in reference (6).

Rather complete information regarding the deflected shape of each specimen was obtained with the use of two deflection measuring systems. The first of these systems made use of Ames dials which were mounted on a beam connected to the lower stub. These dials were used to measure the deflections relative to a line through the stub and approximately parallel to the undeformed axis of the beam-column. This system afforded a fairly accurate means for measuring the deflected shape of the specimen when the deflections were small. For large deflections and when the lateral movements of the specimen produced noticeable rotation of the Ames dial system, a precision level was used to measure the deflected shape of the specimen relative to the floor of the laboratory.

Strain measurements were made with SR-4 electrical strain

gages of types A-5 and A-7. These gages were mounted at four or five sections along each specimen such that the extreme fiber strains and the strain distribution across the section could be determined. A Baldwin-Southwark portable strain indicator was used to measure all strains.

2.3.3 Testing Procedure

All of the specimens were tested in essentially the same manner. Each test was controlled by the center deflection of the specimen. When a desired increment of deflection had been applied to the specimen, the lateral loading was stopped and the load was allowed to decrease slightly until the deflection of the specimen stopped. For those tests which included an axial thrust, the thrust was maintained at a constant magnitude throughout the test. All of the specimens were loaded until either the limit of the testing apparatus for sideward or vertical deflections had been reached or until the lateral load capacity had decreased to zero. In no case was a beam-column test carried past the deformation which resulted in a drop-off of the axial thrust on the member.

2.4 RESULTS OF BEAM-COLUMN STUDY

2.4.1 Test Results

A summary of the more important test results is given in Table 2.4. The failure conditions for all of the specimens are summarized in Table 2.5. Also included in this table are the ratios of collapse to yield deflection which were observed for those members subjected to axial thrusts. For the range of axial loads which were used in these

tests, this ratio varied from approximately 6 to 13.

The experimentally determined moment-strain curves for the sections which were tested are presented in Figs. 2.22 to 2.27. In order that these results might be correlated with the theoretically determined relationships, it was found convenient to reduce the test curves to a dimensionless form. The yield values of moment and strain, in terms of which these results are expressed, are those values which correspond to the specimens without axial load. With the experimental results expressed in this form, direct comparison can be made between the axially loaded and non-axially loaded specimens corresponding to a particular cross section and orientation.

In order that direct comparison between each pair of tests could be made it was necessary to adjust, in some cases, the values of yield moment and strain such that each pair of tests were expressed in terms of a common yield stress. This adjustment had to be made for specimens 4Y1S4 M, 4lS6 I, and 4Y1S6 I shown in Figs. 2.23, 2.24, and 2.25 respectively. For specimen 4Y1S4 M, inspection of the coupon data showed that the yield strength of its companion member, 4Y0S4 M, was about 10 per cent higher. Hence, the values of M_e and ϵ_e for 4Y0S4 M, were reduced by 10 per cent for the dimensionless moment-strain results of 4Y1S4 M. Similar adjustments to the values of M_e and ϵ_e were made for specimens 4lS6 I and 4Y1S6 I. The values of M_e and ϵ_e which were used to reduce the test results to their appropriate dimensionless form are given in each figure.

In each of the tests it was observed that the moment-strain relationship obtained for a section one inch from the stub beam indicated

a much lower yield moment than was obtained at the 3 in. and 6 in. sections. It is possible that this may have resulted from high stress concentrations caused by the welded connection detail. It is interesting to note, however, that this localized effect was overcome after sufficient inelastic action had taken place. Figures 2.22 and 2.26 clearly show that the reduced stiffness of the one inch section was overcome as the members approached the fully plastic condition.

The experimentally determined load-deflection relationships for each of the sections tested are shown in Figs. 2.28 to 2.33. These figures clearly show the effect which the axial load had upon the response of each member. For these specimens which were tested in the strong direction without axial load a limiting value of the lateral load capacity was reached. Reference to Table 2.5 will show that in each of the strong direction tests, final failure resulted from lateral buckling. This mode of failure did not occur, however, until after the fully plastic moment had been developed and the material was well into the strain-hardening region of the stress-strain relationship. An actual decrease in the lateral load for a strong direction test without axial load was noticed only in specimen 60S6 I shown in Fig. 2.30. This evidently resulted from the fact that the twelve foot span of the member was too large for its small moment of inertia about the weak axis.

The load-deflection relationships obtained for the specimens tested in the weak direction without axial load show a considerable increase in load-carrying capacity above the fully plastic condition.

The ability of these members to strain-harden and resist increasing loads resulted from their large resistance to lateral buckling. A reduction in load-carrying capacity for a weak direction test was noted only for specimen 4Y0S6 B shown in Fig. 2.33. Local flange buckling developed very early in the test and did not appear to influence the response of the member until considerale strain-hardening had been developed.

The effect of the axial load on the load-deflection relationships was to cause a decrease in the lateral load-carrying capacity of each member. This drop-off in load occurred shortly after the fully plastic moment had been reached in each case. Further deformation of the member past this point resulted in an increased thrust moment and if equilibrium was to be maintained, a decrease in the lateral load was necessary. It should be pointed out that if the specimens had been tested at constant load, the peak load on the load-deflection curve would have corresponded to collapse of the member. However, since the tests were run by increments of deflection and the load was applied with a hydraulic jack, it was possible to obtain the drop-off portion to the load-deflection relationship.

The members which were tested in the strong direction with axial load failed by lateral buckling with the exception of specimen 41S6 B, Fig. 2.32. This specimen developed local flange buckling very early in the test and although this local failure became quite severe near the end of the test there were no signs of lateral buckling present. The extent of the flange buckling for this specimen is shown

in Fig. 2.34. The lateral buckling failures which developed in specimens 41S4 M and 41S6 I, Figs. 2.28 and 2.30, respectively, caused a very sudden decreased load-carrying capacity. However, these failures did not occur until after the peak value of the lateral load had been applied.

The effect of the axial load on those members which were loaded in the weak direction is shown in Figs. 2.29, 2.31, and 2.33. These curves show that the thrust caused a more rapid decrease in lateral load capacity than was evidenced in the strong direction tests. This was effected by the decreased strength of the member for this orientation which resulted in a large axial load moment component of the total bending moment.

2.4.2 Comparison of Experimental and Analytical Studies

The analytically determined moment-strain relationships are presented with the experimental results in Figs. 2.22 to 2.27. For the most part, reasonable agreement was obtained between test and theory. Major deviation between the test and analytical results occurs during the early stages of inelastic action in each test. In all of the tests, this deviation from the theory is most noticeable for the moment-strain relationships which were obtained from the gages mounted one inch from the face of the stub. This deviation however becomes less noticeable for the sections which were 3 in. and 7 in. from the face of the stub. As was mentioned in the previous section, it is possible that this deviation is a result of the presence of cooling residual stresses and stress concentrations in the material. The

effect of such stresses is to initiate yielding at a load which is lower than that predicted from the stress-strain relationship as determined from a tension coupon.(7)

In comparing the test moment-strain relationships to those derived from theory, some mention must be made regarding the tensile properties of the members. Referring to Table 2.3, it is obvious that a marked non-uniformity of yield strength existed for all of the 4M section specimens. This very marked non-uniformity of the yield strength may have resulted from severe cold rolling of the member during its manufacture. As a result, the stress-strain relationship obtained from these specimens differed considerably from that which is normally associated with A-7 steel. The material exhibited a strain-hardening characteristic immediately after the yield point had been reached. This then might explain why the experimentally determined moment-strain curves for the 4M section fell above those predicted on the basis of a material having a flat yield characteristic. In the case of specimen 41S 4 M, Fig. 2.22, the departure from theory for large values of strain was increased further because of a drop-off in the applied axial load. Control of the axial load for this test was maintained by the hydraulic pressure in the jack which, as mentioned previously, afforded a rather poor regulation of the thrust. The gradual decrease of the axial load amounted to 10 per cent of the initial axial load.

Some of the differences between the moment-strain relationships, as derived by test and analysis, may be also attributed to the manner in which the yield moments were taken. These values were taken

as the point of departure from the initial straight-line portion of the moment-strain relationship. Since this departure usually occurred at different values of moment for the 1, 3, and 6 in. sections, the choice of the yield moment, in each case, was quite uncertain. Realizing that the value of M_e obtained from the 1 in. section was quite probably reduced by local conditions, it was felt that a more reasonable approximation to the yield point might be obtained at the 3 or 6 in. sections. For this reason, the values of yield moment reported for these tests represent an average value obtained on the basis of measurements made at sections 3 in. and 6 in. from the load. Because of the uncertainty in the yield point, some of the test curves may be too low or too high at the full plastic condition. This then may account for some of the discrepancies encountered between the test and theoretical moment-strain relationships.

With the exception of the 4M section specimens, the moments obtained in the tests at the fully plastic condition usually fell below those predicted on the basis of the tensile stress-strain properties of the material. This discrepancy cannot be attributed to the presence of residual stresses since at the fully plastic condition a fully developed stress block exists within the member. It is possible that this reduction in moment capacity may have resulted from plastic flow of the material. After the yield point load had been exceeded, a slight drop-off in the lateral load was noted after each increment of deflection had been applied. The amount of this drop-off could not be determined with the load measurement system which was used. The loads which were measured

therefore correspond to values which were lower than the actual maximum for any increment. This phenomenon of plastic flow, or time-dependent yielding, was present in all of the tests.

An attempt was made to derive the load-deflection relationship for specimen 4Y0 S 6B from the moment-strain relationship obtained experimentally. The experimental moment-strain curve was first extended to include the strain-hardening range of the stress-strain relationship as determined from the tension coupons. The load-deflection relationship which was derived, using the numerical integration procedure,[5] is shown in Fig. 2.33. Up to the fully plastic condition, which occurred at the knee of the curve, the derived deflections were found to be smaller than actually occurred at any particular load. This departure from the measured values may be attributed to the fact that the moment-strain relationship obtained from the 3 in. section was used in the computations, the premature yielding which occurred at the 1 in. section was not considered and hence the computations are based on a beam which was stronger than actually existed. Had this effect been taken into account, closer agreement would have resulted. It is interesting to note, however, that good agreement was obtained past the fully plastic condition indicating that the effect of the reduced stiffness of the 1-in. section had been overcome. Agreement existed up to the point where local buckling of the flanges finally reduced the load capacity of the member.

The load-deflection relationships were predicted for each of the axially loaded test members on the basis of the derived moment-strain relationships and the stress-strain properties for each member. These

predicted load-deflection curves are presented together with their corresponding experimental curves in Figs. 2.28 to 2.33. In each case, with the exception of specimen 4Y1S4 M, the derived values of deflection are less than those which actually occurred for loads less than the peak load. Again this may be attributed to the residual stresses and stress concentrations which apparently influenced the response of the test members. For all of the beam-columns studied, the error in the predicted yield load varied from 14 per cent to 17 per cent on the high side while the error in the predicted maximum load was as much as 25 per cent on the high side.

The peak value of the load on the derived load-deflection relationship represents the limit at which the deflections may be determined. If a value of load larger than the peak value is assumed to be acting, the value of deflection determined by the numerical procedure will become larger and larger. This indicates that the total bending moment on the member is greater than its fully plastic resisting moment and a state of instability exists.

An approximation of the deflection corresponding to the end point of each test was obtained by dividing the fully plastic moment by the value of the axial load. This approximation assumes that the material has not strain-hardened and neglects any reduction in moment capacity as a result of either local or lateral buckling. This procedure was applied to each of the beam-columns and the values of deflection thus obtained are indicated as collapse deflections, δ_c, on the derived load-deflection curves. An approximation to the drop-off portion of

the load-deflection relationship was then obtained by passing a curve through the value of δ_c and tangent to the peak value of load.

Agreement between the predicted and the test curves is fair. However, it should be noted that the best agreement exists for those beam-columns which were tested in the weak direction. In the case of the strong direction specimens rather poor agreement exists owing to the fact that lateral buckling caused a sudden decrease in the lateral load-carrying capacity. Of particular interest with regard to these comparisons is the fact that the observed collapse deflection exceeded the predicted value in just one test. This would tend to indicate that the neglect of strain-hardening from the determination of the collapse deflection in the axially loaded beam-columns was reasonable for the cases studied.

Considerable departure of the derived load-deflection relationship from the test curve was observed for specimen 4IS6 B, Fig. 2.32. This departure may be attributed to the early flange buckling which developed in the member. Near the peak load this buckling became quite pronounced and apparently reduced the load-carrying capacity of the member considerably.

2.5 SUMMARY AND CONCLUSIONS

The effect of an axial load on the static response of a member may be realized in two ways. First, the addition of a thrust reduces the moment-carrying capacity of the member; second, this thrust reduces the lateral load-carrying capacity of the member by directly adding to the bending moment at any section along the member. This reduction in the

lateral load-carrying capacity is a function of the magnitude of the axial load and the orientation of the specimen with respect to the lateral load.

The procedure used for the development of theoretical moment-strain relationships for any value of axial load appears to check the test results reasonably well. However, major discrepancies between test and theory exist during the early stages of the inelastic deformation. These differences result from premature yielding of the test members caused by either the presence of residual stresses in the material or local stress concentrations from the welded connection detail. No information regarding the possible magnitude of such stresses is available from these tests. The inclusion of residual stress in the determination of theoretical moment-strain relationships has been done at Lehigh University.(1) These findings indicate that closer agreement between test and theory can be obtained if these stresses are known and are included in the analysis. However, because of the uncertainty of the effect of the welding operation on the member, it was felt that such refinements to the analysis were unwarranted and were therefore not considered.

With the theoretically determined moment-strain relationships based on some value of axial thrust and an assumed or known yield stress, it is possible to predict a load-deflection relationship for a given member. In this study the deflections corresponding to arbitrarily chosen lateral loads were computed by a numerical integration procedure.(5) The load-deflection relationships thus derived could only be

determined to the peak value of the lateral load. To obtain some measure of the drop-off portion to the load-deflection curve, the collapse deflection was approximated by dividing the fully plastic moment by the value of the axial load. A curve passing through this point and tangent at the peak load was used as an approximation to the decay portion of the curve.

Agreement between the derived and experimental load-deflection relationships is reasonable for those members which did not fail by lateral buckling. For those members which failed in this manner, a very rapid decrease in the lateral load-carrying capacity and a marked departure from the predicted curve resulted at the point of failure. This is to be expected since there is no failure criterion in the simple plastic theory upon which the derived results are based. This is perhaps one of the more serious deficiencies of the theory and until such time as these failure criterion are developed, a more exact procedure for the determination of the load-deflection relationship is not warranted.

The predicted collapse deflections exceeded the test values in every test but one. For these tests, therefore, the neglect of strain-hardening in the determination of the collapse deflection appears to be reasonable. For the members which were loaded in the weak direction without axial load, considerable increase in the lateral load-carrying capacity above the fully plastic condition was observed. Evidently, strain-hardening was of considerable importance in the response of these members. In the case of the members which were loaded in the strong

direction without axial load, the strain-hardening effect was not observed by an increased load-carrying capacity of the member. Each of these members buckled laterally with no appreciable reduction in the lateral load-carrying capacity below the fully plastic condition. The strain-hardening effect in these members evidently overcame any tendency of the lateral load capacity to decrease as a result of the lateral buckling failure.

2.6 BIBLIOGRAPHY

1. Ketter, R., Kaminsky, E., and Beedle, L., "Plastic Deformation of Wide-Flange Beam-Columns," Proceedings of the ASCE, Vol. 79, Separate No. 330, Oct. (1953).

2. American Institute of Steel Construction, "Steel Construction Manual,"New York, 5th Ed., (1951).

3. Seely,F., and Smith, J., "Advanced Mechanics of Materials," John Wiley and Sons, Inc., New York, 2nd Ed., (1952).

4. Bleich, F., "The Buckling Strength of Metal Structures," McGraw-Hill Book Company, New York, 1st Ed., (1952).

5. Newmark, N. M., "Numerical Procedure for Computing Deflections, Moments, and Buckling Loads," Transactions of the ASCE, Vol. 108, ppl161-1234, (1945).

6. Howland, F. L., "Static Load-Deflection Tests of Beam-Columns," Structural Research Series No. 65, University of Illinois, Sept. (1953).

7. Yang, C., Beedle, S., and Johnston, B., "Residual Stress and the Yield Strength of Steel Beams," Progress Report No. 5, The Welding Journal 31(4), Research Supplement, 205-s to 229-s (1952).

APPENDIX: 2.A

ANALYTICAL EXPRESSIONS FOR THE DETERMINATION OF THE MOMENT-STRAIN RELATIONSHIPS

Strong Direction of Loading

Case I. $0 \leqq h_1 \leqq f$ $\qquad \varepsilon_d - \varepsilon_f \leqq -\varepsilon_e$

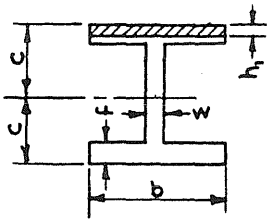

$$T/T_e = 1 + \frac{\varepsilon_f}{\varepsilon_e}\left[\frac{h_1}{c} - \frac{bc}{2A}\left(\frac{h_1}{c}\right)^2 - 1\right]$$

$$M/M_e = \frac{\varepsilon_f}{\varepsilon_e}\left[1 + \frac{bc^3}{6I}\left\{\left(\frac{h_1}{c}\right)^3 - 3\left(\frac{h_1}{c}\right)^2\right\}\right]$$

Case II. $f \leqq h_1 \leqq 2c - f$ $\qquad \varepsilon_d - \varepsilon_f \leqq -\varepsilon_e$

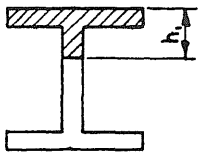

$$T/T_e = 1 + \frac{\varepsilon_f}{\varepsilon_e}\left[\frac{h_1}{c}\left(\frac{bf + w(2c-f)}{A}\right) - 1 + \frac{f^2}{2cA}(b-w) - \frac{wc}{2A}\left(\frac{h_1}{c}\right)^2\right]$$

$$M/M_e = \frac{\varepsilon_f}{\varepsilon_e}\left\{1 + \frac{c^2}{I}\left[\left[\frac{w}{6}\left(\frac{h_1}{c}\right)^3 - \frac{w}{2}\left(\frac{h_1}{c}\right)^2 + \frac{f}{c}(b-w)\left[\frac{h_1}{c}\left(\frac{1}{2}\frac{f}{c} - 1\right) + \frac{1}{2}\frac{f}{c}\left(1 - \frac{2}{3}\frac{f}{c}\right)\right]\right]\right\}$$

Case III. $2c-f \leqq h_1 \leqq 2c$ $\qquad \varepsilon_a - \varepsilon_d \leqq -\varepsilon_e$

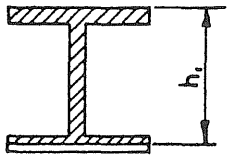

$$T/T_e = 1 - \frac{\varepsilon_f}{\varepsilon_e}\left[\frac{1}{2}\frac{bc}{A}\left(\frac{h_1}{c}-2\right)^2\right]$$

$$M/M_e = \frac{\varepsilon_f}{\varepsilon_e}\left\{\frac{bc^3}{I}\left[\frac{2}{3} - \frac{1}{2}\left(\frac{h_1}{c}\right)^2 + \frac{1}{6}\left(\frac{h_1}{c}\right)^3\right]\right\}$$

Case IV. $0 \leqq y_m \leqq c-f$

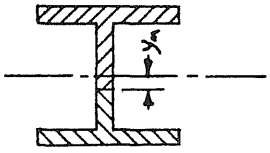

$$T/T_e = \frac{2y_m w}{A}$$

$$M/M_e = \frac{2bcf}{I}\left(c-\frac{f}{2}\right) + \frac{wc}{I}\left[(c-f)^2 - y_m^2\right]$$

Case V. $0 \leqq K \leqq 1$

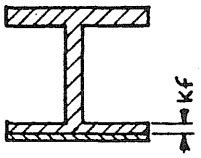

$$T/T_e = 1 - \frac{2bf}{A}(1-K)$$

$$M/M_e = \frac{2bcf}{I}(1-K)\left[c - \frac{1}{2}f(1-K)\right]$$

Case VI. $0 \leqq h \leqq f$

(No Axial Load)

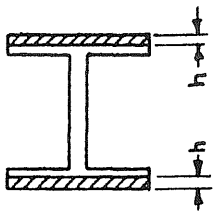

$$M/M_e = \frac{1}{1-\frac{h}{c}} + \frac{bc^3}{I\left(1-\frac{h}{c}\right)}\left[\frac{1}{3}\left(\frac{h}{c}\right)^3 - \left(\frac{h}{c}\right)^2\right]$$

Case VII. $f \leqq h \leqq c$

(No Axial Load)

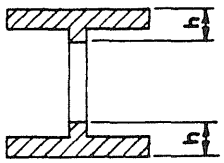

$$M/M_e = \frac{c^3}{I}\left[w\left(\frac{2}{3}\frac{h}{c} - \frac{1}{3}\left(\frac{h}{c}\right)^2 + \frac{2}{3} - \frac{2f}{c} + \left(\frac{f}{c}\right)^2\right) + \frac{bf}{c}\left(2 - \frac{f}{c}\right)\right]$$

Weak Direction of Loading

Case I. $0 \leq h_2 \leq c - \frac{w}{2}$ $\qquad h_2 \leq h_1 \leq c - \frac{w}{2}$

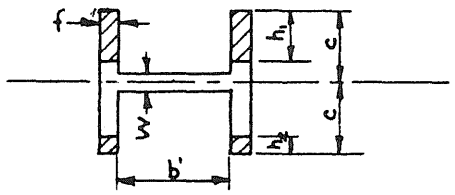

$$\frac{T}{T_e} = 1 - 4\frac{f_c}{A}\left(\frac{h_2}{c}\right) + \frac{\varepsilon_f}{\varepsilon_e}\left\{\frac{h_1}{c} + \frac{f_c}{A}\left[4\frac{h_2}{c} - \left(\frac{h_1}{c} + \frac{h_2}{c}\right)^2\right] - 1\right\}$$

$$\frac{M}{M_e} = \frac{c^3}{I}\left[4f\left(\frac{h_2}{c}\right)\left(1 - \frac{1}{2}\frac{h_2}{c}\right)\right] + \frac{\varepsilon_f}{\varepsilon_e}\left\{1 + \frac{f c^3}{I}\left[\left[\frac{1}{3}\left[\left(\frac{h_1}{c}\right)^3 - 2\left(\frac{h_2}{c}\right)^3\right] - \left[\frac{h_1}{c} - \frac{h_2}{c}\right]^2 + \left(\frac{h_2}{c}\right)^2\left(4 - \frac{h_1}{c}\right) - 4\left(\frac{h_2}{c}\right)\right]\right]\right\}$$

Case II. $0 \leq h_2 \leq c - \frac{w}{2}$ $\qquad c - \frac{w}{2} \leq h_1 \leq c + \frac{w}{2}$

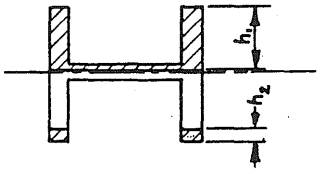

$$\frac{T}{T_e} = 1 - 4\frac{f_c}{A}\left(\frac{h_2}{c}\right) + \frac{c}{A}\frac{\varepsilon_f}{\varepsilon_c}\left\{-f\left[\left(\frac{h_1}{c} + \frac{h_2}{c}\right)^2 - 4\left(\frac{h_2}{c}\right) + 4\right] - \frac{1}{2}b'\left[\left(\frac{h_1}{c}\right)^2 + \left(\frac{1}{2}\frac{w}{c} + 1\right)^2\right] + \frac{h_1}{c}\left[4f + b'\left(1 + \frac{1}{2}\frac{w}{c}\right)\right]\right\}$$

$$\frac{M}{M_e} = \frac{c^3}{I}\left[4f\left(\frac{h_2}{c}\right)\left(1 - \frac{1}{2}\frac{h_2}{2}\right)\right] + \frac{\varepsilon_f}{\varepsilon_e}\left\{1 + \frac{c^3}{I}\left[\left[\left(f + \frac{1}{2}b'\right)\left[\frac{1}{3}\left(\frac{h_1}{c}\right)^3 - \left(\frac{h_1}{c}\right)^2\right] - \frac{2}{3}f\left(\frac{h_2}{c}\right)^3 + f\left(\frac{h_2}{c}\right)^2\left(3 - \frac{h_1}{c}\right) + 2f\frac{h_2}{c}\left(\frac{h_1}{c} - 2\right) + \frac{1}{2}b'\frac{h_1}{c}\left[1 - \frac{1}{4}\left(\frac{w}{c}\right)^2\right] + \frac{1}{24}b'\left[3\left(\frac{w}{c}\right)^2 - \left(\frac{w}{c}\right)^3 - 4\right]\right]\right]\right\}$$

Case III. $c+\frac{w}{2} \leq h_1 \leq 2c \qquad 0 \leq h_2 \leq 2c-h_1$

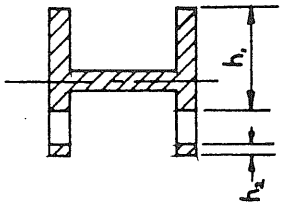

$$\frac{T}{T_e} = 1 - 4\frac{f_c}{A}\left(\frac{h_2}{c}\right) - \frac{4f_c}{A}\frac{\varepsilon_f}{\varepsilon_e}\left[\frac{1}{4}\left(\frac{h_1}{c}+\frac{h_2}{c}\right)^2 - \left(\frac{h_1}{c}+\frac{h_2}{c}\right) + 1\right]$$

$$\frac{M}{M_e} = \frac{4c^3 f}{I}\left(\frac{h_2}{c}\right)\left(1-\frac{1}{2}\frac{h_2}{c}\right) + \frac{\varepsilon_f}{\varepsilon_e}\left\{1 + \frac{c^3}{I}\left[\left[\frac{1}{3}f\left[\left(\frac{h_1}{c}\right)^3 - 2\left(\frac{h_2}{c}\right)^3\right] - f\left[\left(\frac{h_1}{c}\right) - \left(\frac{h_2}{c}\right)\right]^2 + 4f\frac{h_2}{c}\left[\frac{h_2}{c} - \frac{1}{4}\left(\frac{h_1}{c}\right)\left(\frac{h_2}{c}\right) - 1\right] - \frac{1}{12}b'\left(\frac{w}{c}\right)^3\right]\right]\right\}$$

Case IV. Fully Plastic Condition

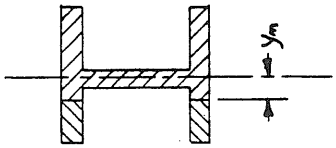

$$\frac{T}{T_e} = \frac{2y_m d}{A}$$

$$\frac{M}{M_e} = \frac{c}{I}\left[b'\left[\left(\frac{w}{2}\right)^2 - y_m^2\right] + 2f\left(c^2 - y_m^2\right)\right]$$

Case V. Neutral Axis Below The Web

$$\frac{T}{T_e} = \frac{b'w + 4y_m f}{A}$$

$$\frac{M}{M_e} = \frac{2cf}{I}\left(c^2 - y_m^2\right)$$

TABLE 2.1

AVERAGE SECTION PROPERTIES

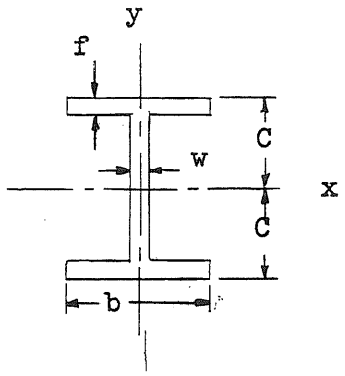

Section	Area	C	f	b	w	I_x	I_y
4M 13.0*	3.71	2.00	0.370	3.85	0.263	10.18	3.52
4M 13.0**	3.82	2.00	---	3.94	0.250	10.4	3.4
6I 12.5*	3.51	3.04	0.353	3.26	0.225	21.72	2.04
6I 12.5**	3.61	3.00	0.359	3.33	0.230	21.80	1.8
6B 15.5*	4.89	3.04	0.291	6.03	0.251	32.9	10.64
6B 15.5**	4.62	3.00	0.269	6.00	0.240	30.3	9.69

* Measured Values

** Values Given In AISC Handbook

TABLE 2.2

COMPARISON OF BEAM-COLUMN SPECIMENS

Specimen Number	Direction of Bending	Span Between Reactions	Connection* Detail	Axial** Load
40S4M 13.0	x-x	8 ft.-2 in.	A	none
41S4M 13.0	x-x	8 ft.-2 in.	A	17.3
4Y0S4M 13.0	y-y	8 ft.-2 in.	B	none
4Y1S4M 13.0	y-y	8 ft.-2 in.	B	14.8
60S6I 12.5	x-x	12 ft.-2 in.	A	none
41S6I 12.5	x-x	8 ft.-2 in.	A	10.9
6Y0S6I 12.5	y-y	12 ft.-2 in.	B	none
4Y1S6I 12.5	y-y	8 ft.-2 in.	B	7.6
40S6B 15.5	x-x	8 ft.-2 in.	A	none
41S6B 15.5	x-x	8 ft.-2 in.	A	13.5
4Y0S6B 15.5	y-y	8 ft.-2 in.	B	none
4Y1S6B 15.5	y-y	8 ft.-2 in.	B	9.0

* Details of these connections are shown in Fig. 16.

** Nominal axial stress in kips per sq. in. based on the measured areas.

TABLE 2.3

SUMMARY OF TENSILE PROPERTIES DETERMINED FROM TENSION COUPONS

(Yield Stress Based on 0.2 Offset*)

Specimen No.	Tips of Flanges Av. of 4 Coupons	Center of Flanges Av. of 2 Coupons	Junction of Flange and Web, Av. of 2 Coupons	Center of Web
4M 13.0 Section				
40S4M 13.0	57.1	42.6	67.5	66.0
41S4M 13.0	58.2	38.3	69.4	59.5
4Y0S4M 13.0	56.2	61.9	70.9	62.0
4Y1S4M 13.0	49.5	37.3	68.0	61.8
6I 12.5 Section				
60S6I 12.5	39.1	38.0	46.8	42.7
41S6I 12.5	48.2	39.2	52.7	46.6
6Y0S6I 12.5	45.6	46.6	50.9	----
41S6I 12.5	47.8	39.3	50.3	46.5
6B 15.5 Section				
40S6B 15.5	37.0	35.3	39.3	42.0
41S6B 15.5	37.8	36.7	37.1	43.0
4Y0S6B 15.5	38.2	37.9	36.0	40.7
4Y1S6B 15.5	37.5	38.0	----	----

* All values given in kips per sq. in.

TABLE 2.4

SUMMARY OF TEST RESULTS

Specimen Number	40S4M	41S4M	4Y0S4M	4Y1S4M	60S6I	41S6I
Yield load, P_e, kips	10.8	6.1	4.40	1.30	7.06	8.73
Max. load, p, kips	15.8	8.23	8.29	2.31	9.41	13.9
Yield mom., M_e, in. kips	237.5	170	96.7	58.5	240	207
Max. mom., M, in. kips	348	226	182	125	320	339
Yield defl. at center, δ_e, in.	0.64	0.55	0.75	0.31	0.71	0.30
Max. center defl., δ, in.	4.55	3.24	9.10	2.11	7.4	2.44
σ_e computed from M_e, ksi	46.7	50.7	52.8	45.8	33.5	39.8
σ_e(Av. of flange coupons), ksi	52.2	51.5	56.5	49.5	38.7	45.2
ϵ_e corresponding to observed M_e, micro in.	1650	1200	1900	1050	1250	1030
Axial thrust, T, kips	-------	64	-------	55	-------	38.1
Stress resulting from axial thrust, ksi	-------	17.3	-------	14.8	-------	10.9
AISC allow. column stress, from handbook, ksi	-------	12.8	-------	12.8	-------	10.1
T/T_e based on σ_e of coupons	-------	0.30	-------	0.32	-------	0.24

TABLE 2.4 (Cont'd)

SUMMARY OF TEST RESULTS

Specimen Number	6Y0S6I	4Y1S6I	40S6B	41S6B	4Y0S6B	4Y1S6B
Yield load, P_e, kips	1.59	1.00	14.5	9.41	5.91	5.1
Max. load, p, kips	2.85	1.57	19.4	11.2	10.5	7.0
Yield mom., M_e, in. kips	54	36	320	200	130	112
Max. mom., M, in. kips	96.9	75.4	427	284	231	199
Yield defl. at center, δ_e, in.	1.85	0.47	0.29	0.20	0.33	0.30
Max. center defl., δ, in.	14.4	2.51	2.97	2.37	9.82	3.92
σ_e computed from M_e, ksi	43.1	40.3	29.6	32.0	36.8	40.5
σ_e (Av. of flange coupons), ksi	45.6	42.5*	36.4	37.4	38.1	38.0**
ϵ_e corresponding to observed M_e, micro in.	1684	1000	880	670	1155	960
Axial thrust, T, kips	-------	26.8	-------	66	-------	44
Stress resulting from axial thrust, ksi	-------	7.6	-------	13.5	-------	9.0
AISC allow. column stress, from handbook, ksi	-------	10.1	-------	15.2	-------	15.2
T/T_e based on σ_e of coupons	-------	0.16	-------	0.355	-------	0.22

* Based on AISC handbook value for I_y

** Based on coupon strength of one flange only

TABLE 2.5

SUMMARY OF FAILURE CONDITIONS

Specimen Number	$\frac{L}{r}$*	$\frac{\delta_c}{\delta_e}$	Mode of Failure
40S4M 13.0	---	----	Lateral buckling
41S4M 13.0	93	5.8	Lateral buckling
4Y0S4M 13.0	---	----	No failure observed within the limit of the apparatus
4Y1S4M 13.0	93	6.8	Lateral load drop to zero
60S6I 12.5	---	----	Lateral buckling
41S6I 12.5	122	8.1	Lateral buckling
6Y0S6I 12.5	---	----	No failure observed within the limit of the apparatus
4Y1S6I 12.5	122	5.3	Lateral load drop to zero
40S6B 15.5	---	----	Local buckling followed by lateral buckling
41S6B 15.5	60	11.8	Local buckling followed by lateral load drop to zero
4Y0S6B 15.5	---	----	Local buckling. Test carried to limit of apparatus
4Y1S6B 15.5	60	13.1	Local buckling followed by lateral load drop to zero

* These values are approximate in that a small end restraining effect has been neglected; hence they are conservative.

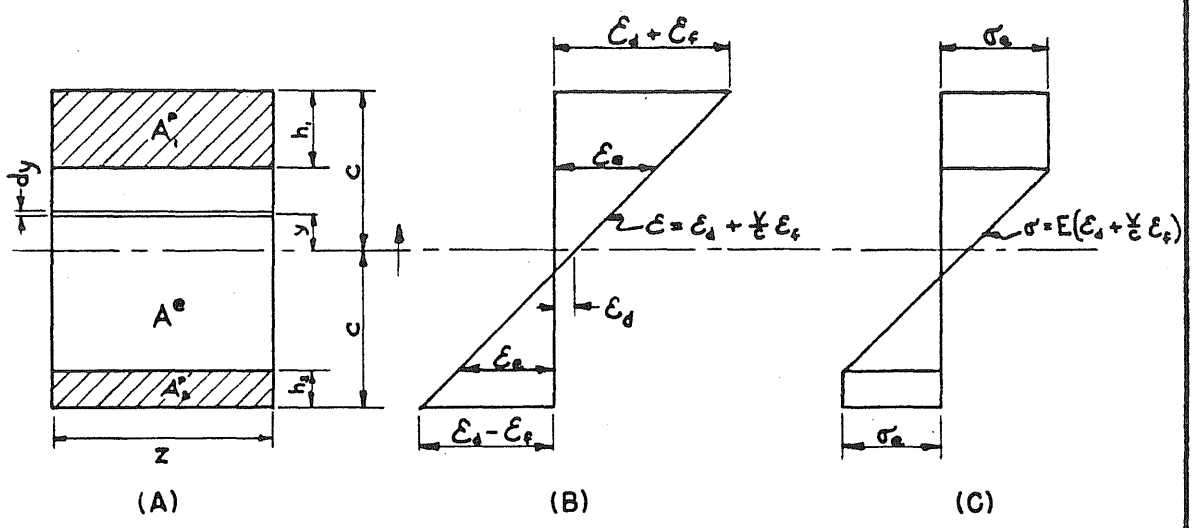

FIG. 2.1 STRESS AND STRAIN DIAGRAMS FOR SOME ASSUMED INELASTIC ACTION

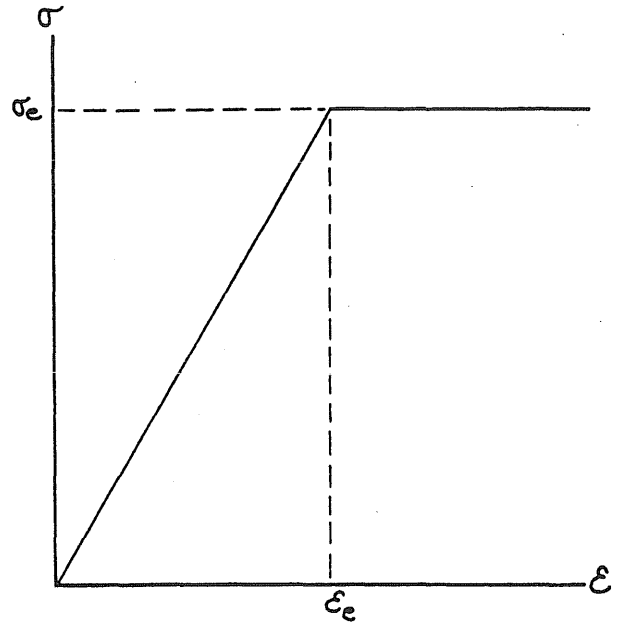

FIG. 2.2 STRESS–STRAIN RELATIONSHIP ASSUMED FOR THE ANALYSIS

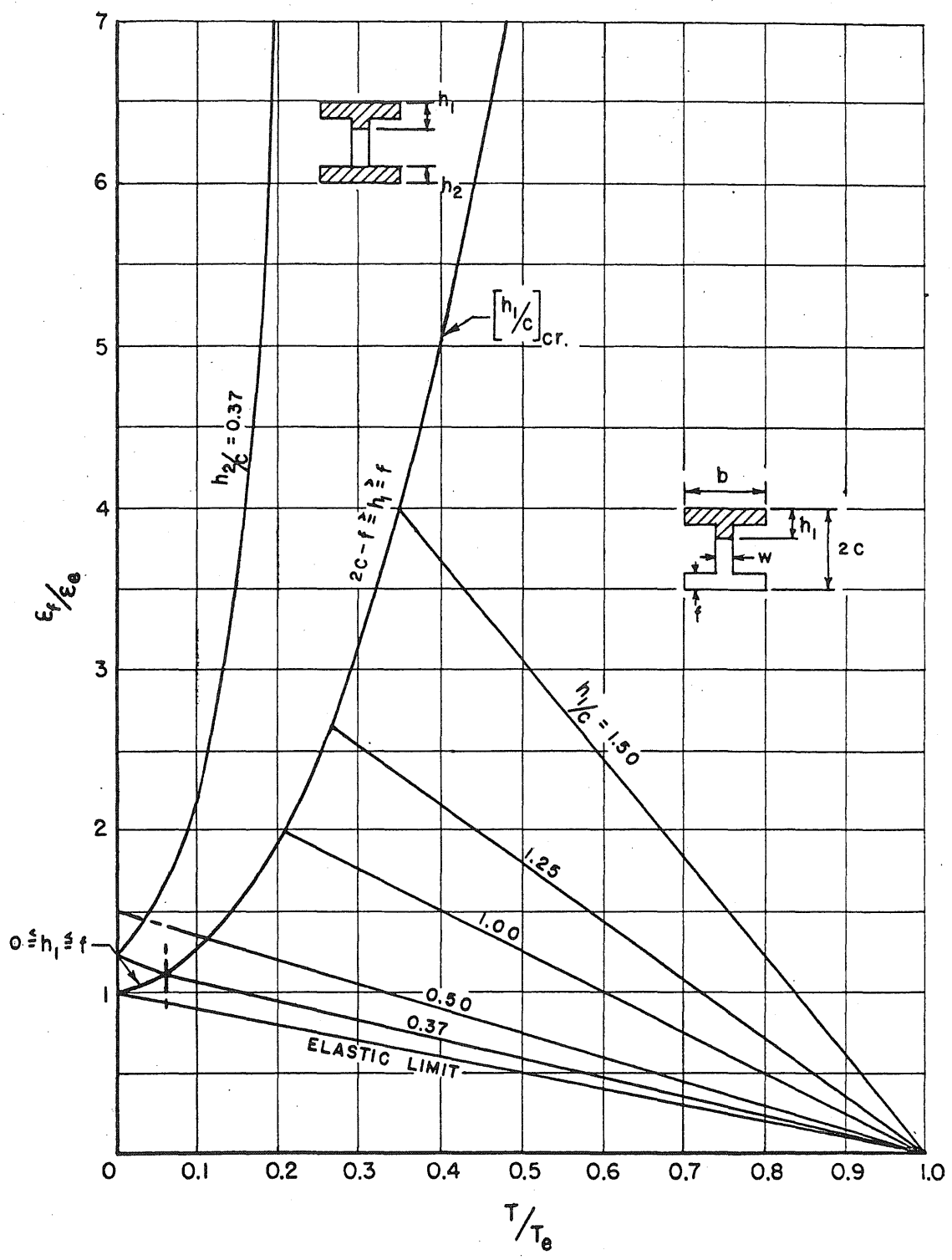

FIG. 2.3 AXIAL LOAD VS FLEXURAL STRAIN CURVES FOR 4MI3.0 ABOUT AXIS X-X

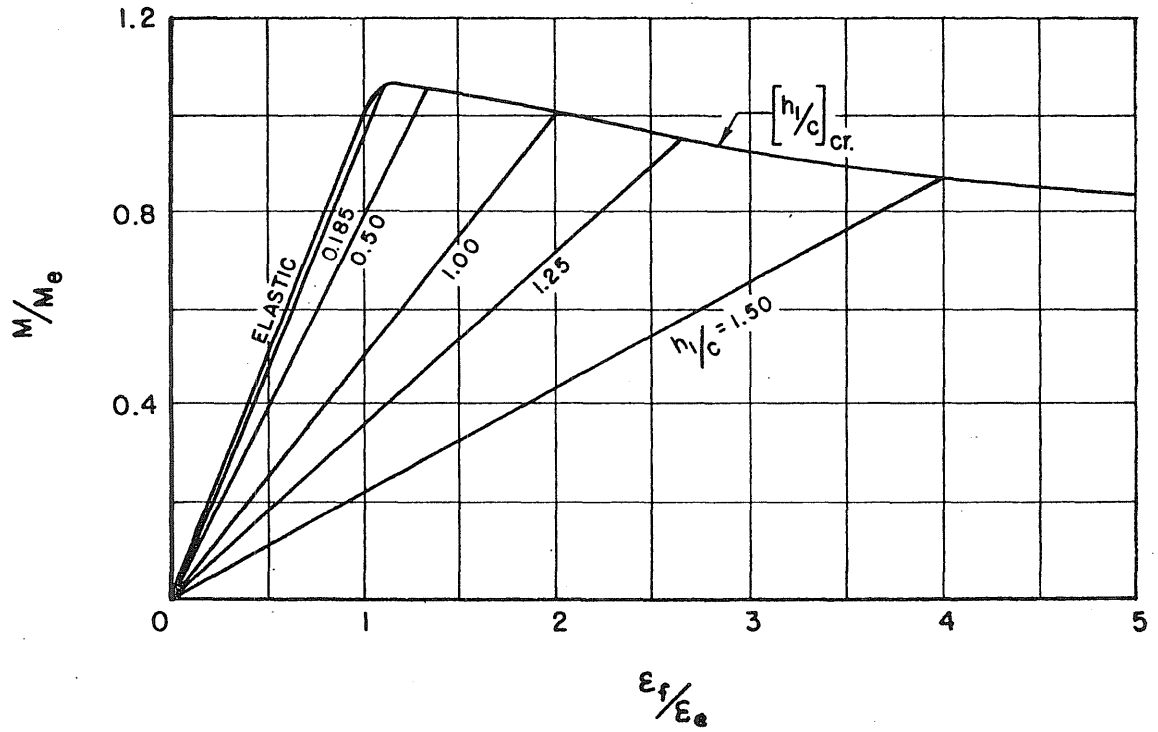

FIG. 2.4 MOMENT VS FLEXURAL STRAIN CURVES FOR 4MI3.0 ABOUT AXIS X–X

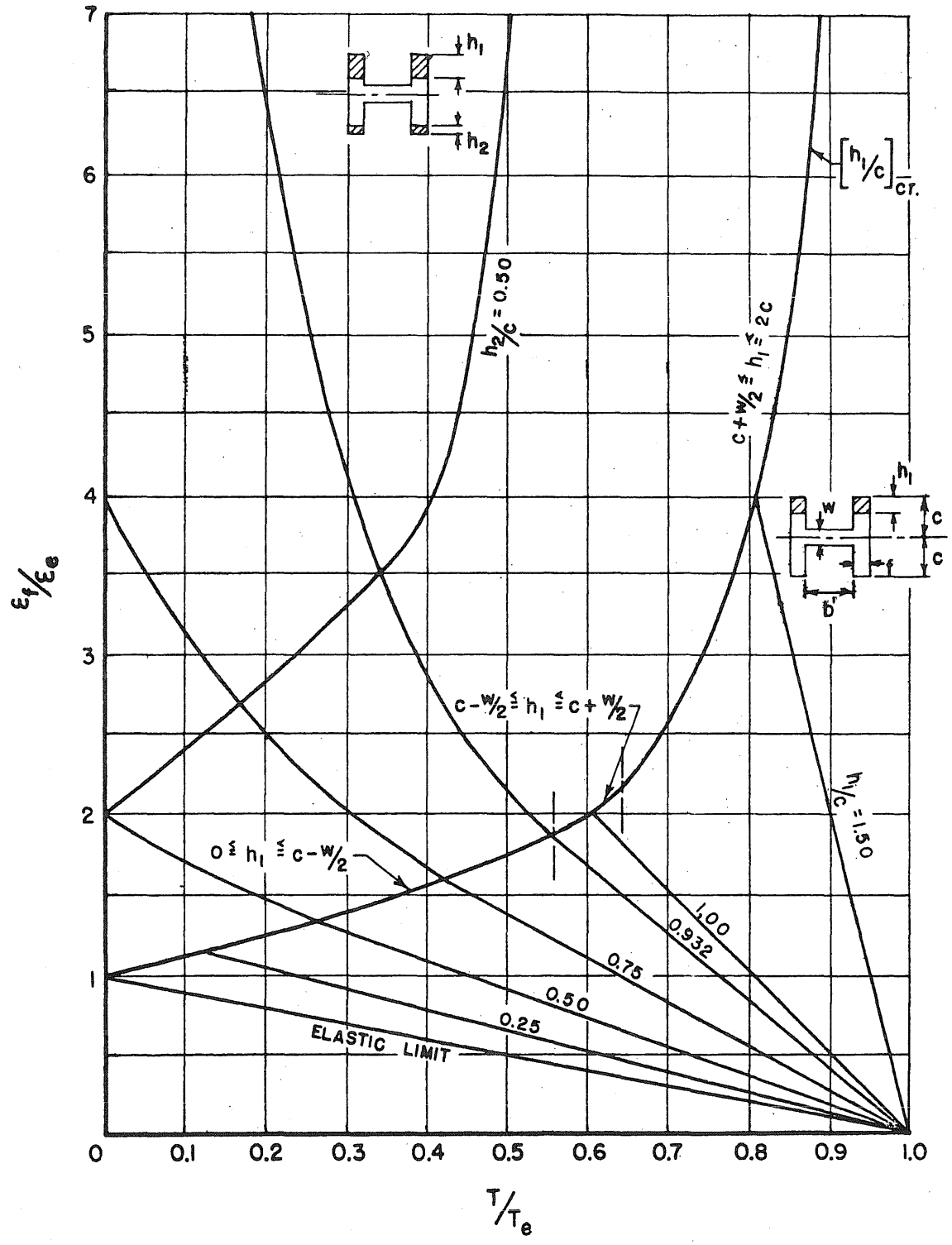

FIG. 2.5 AXIAL LOAD VS FEXURAL STRAIN CURVES FOR 4 MI3.0 ABOUT AXIS Y-Y

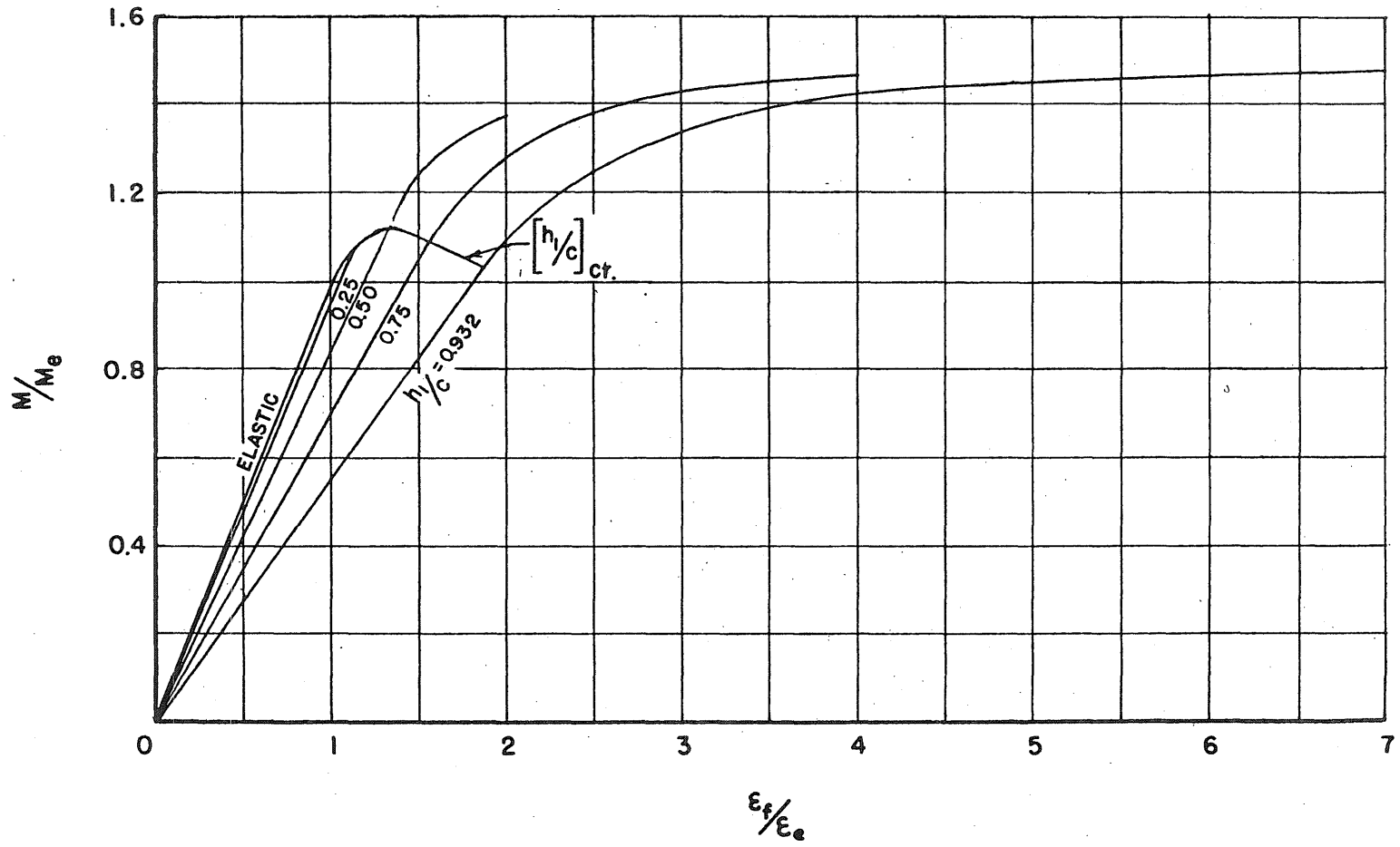

FIG. 2.6 MOMENT VS FLEXURAL STRAIN CURVES FOR 4MI3.0 ABOUT AXIS Y—Y

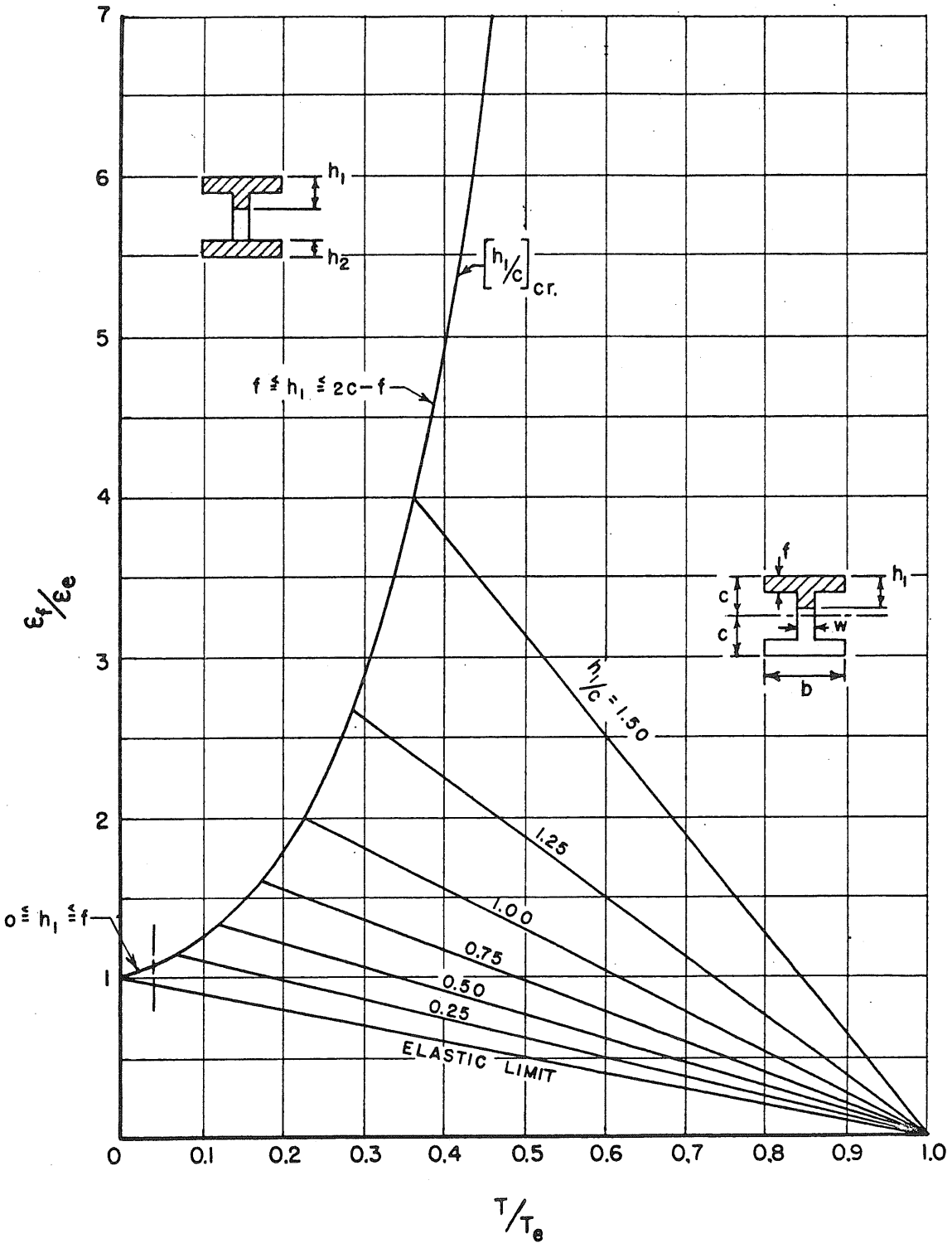

FIG. 2.7 AXIAL LOAD VS FEXURAL STRAIN CURVES FOR 6I12.5 ABOUT AXIS X-X

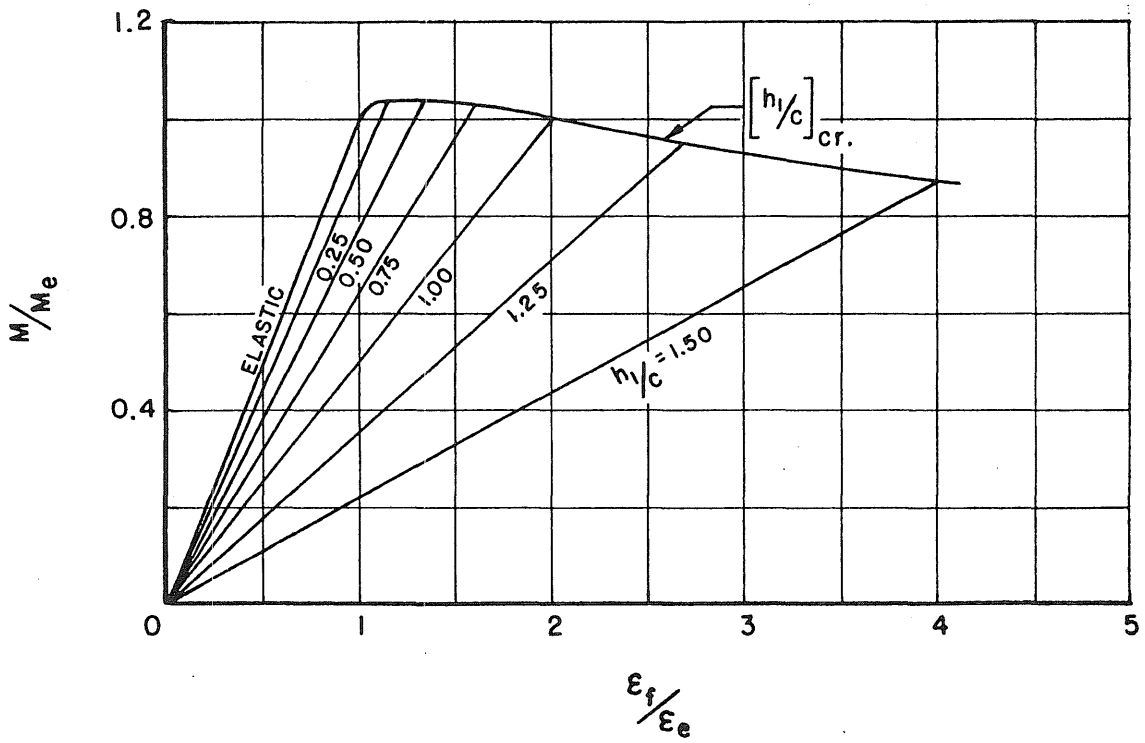

FIG. 2.8 MOMENT VS FLEXURAL STRAIN CURVES FOR 6II2.5 ABOUT AXIS X–X

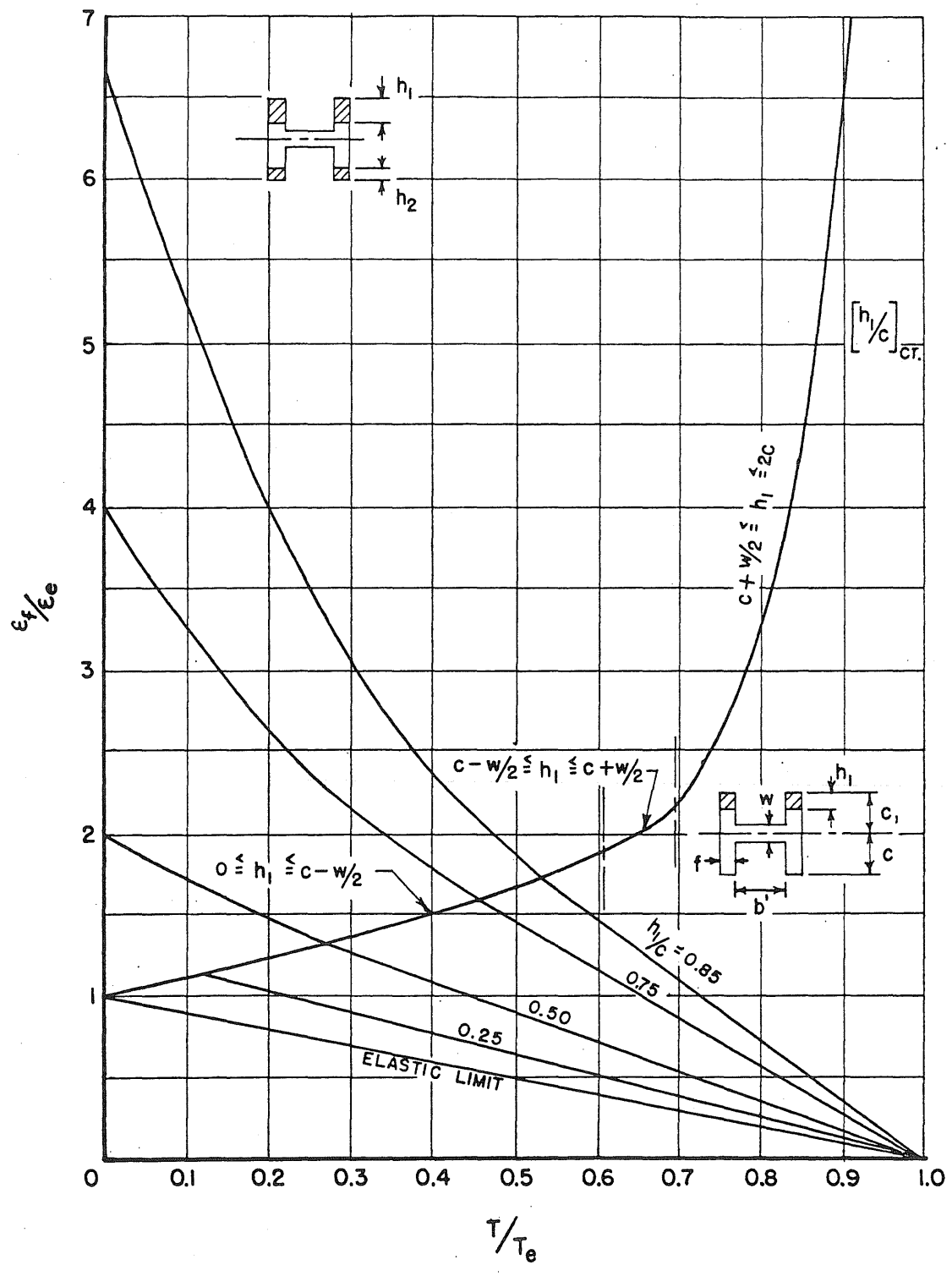

FIG. 2.9 AXIAL LOAD VS FLEXURAL STRAIN CURVES FOR 6112.5 ABOUT AXIS Y–Y

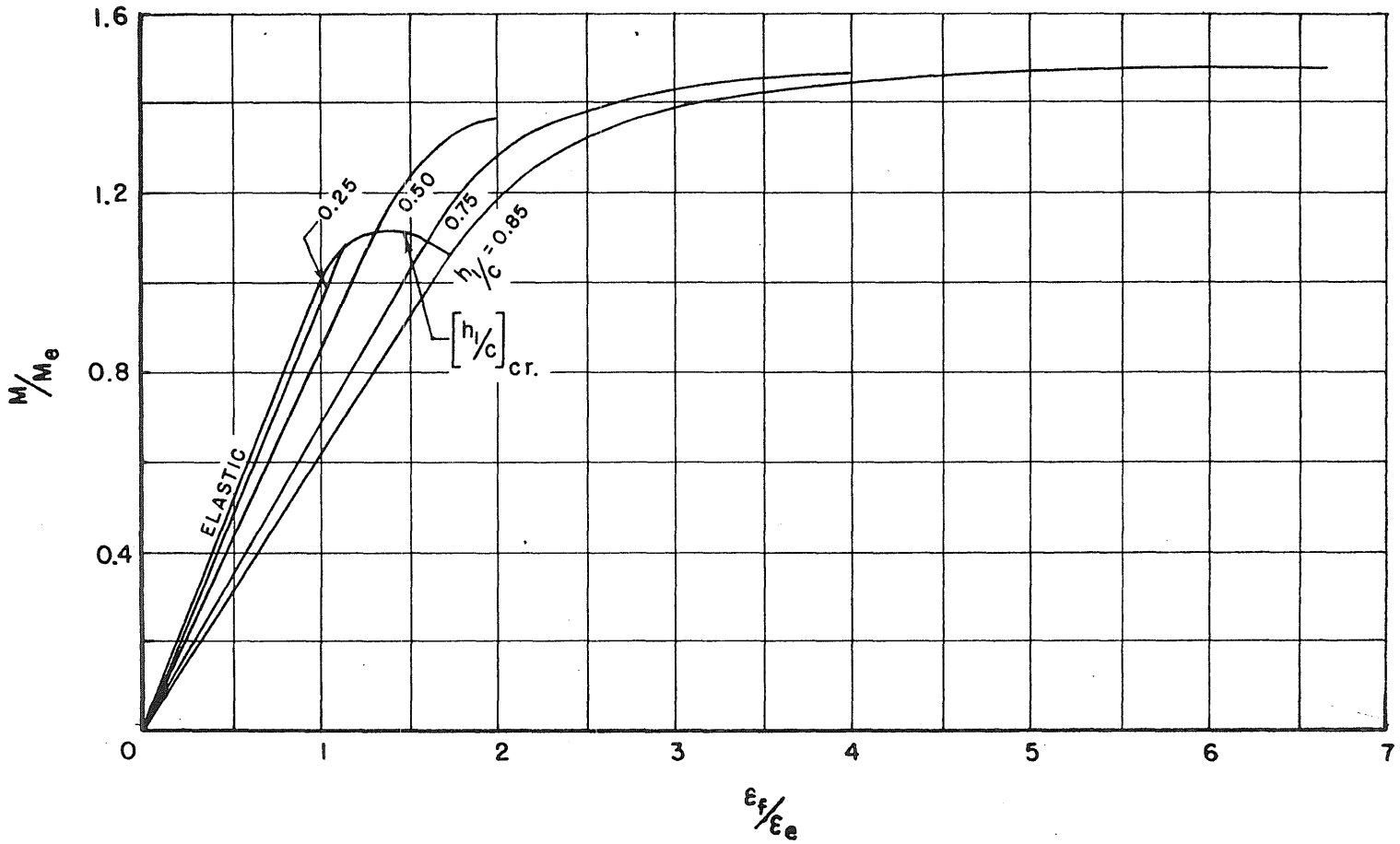

FIG. 2.10 MOMENT VS FLEXURAL STRAIN CURVES FOR 6I12.5 ABOUT AXIS Y–Y

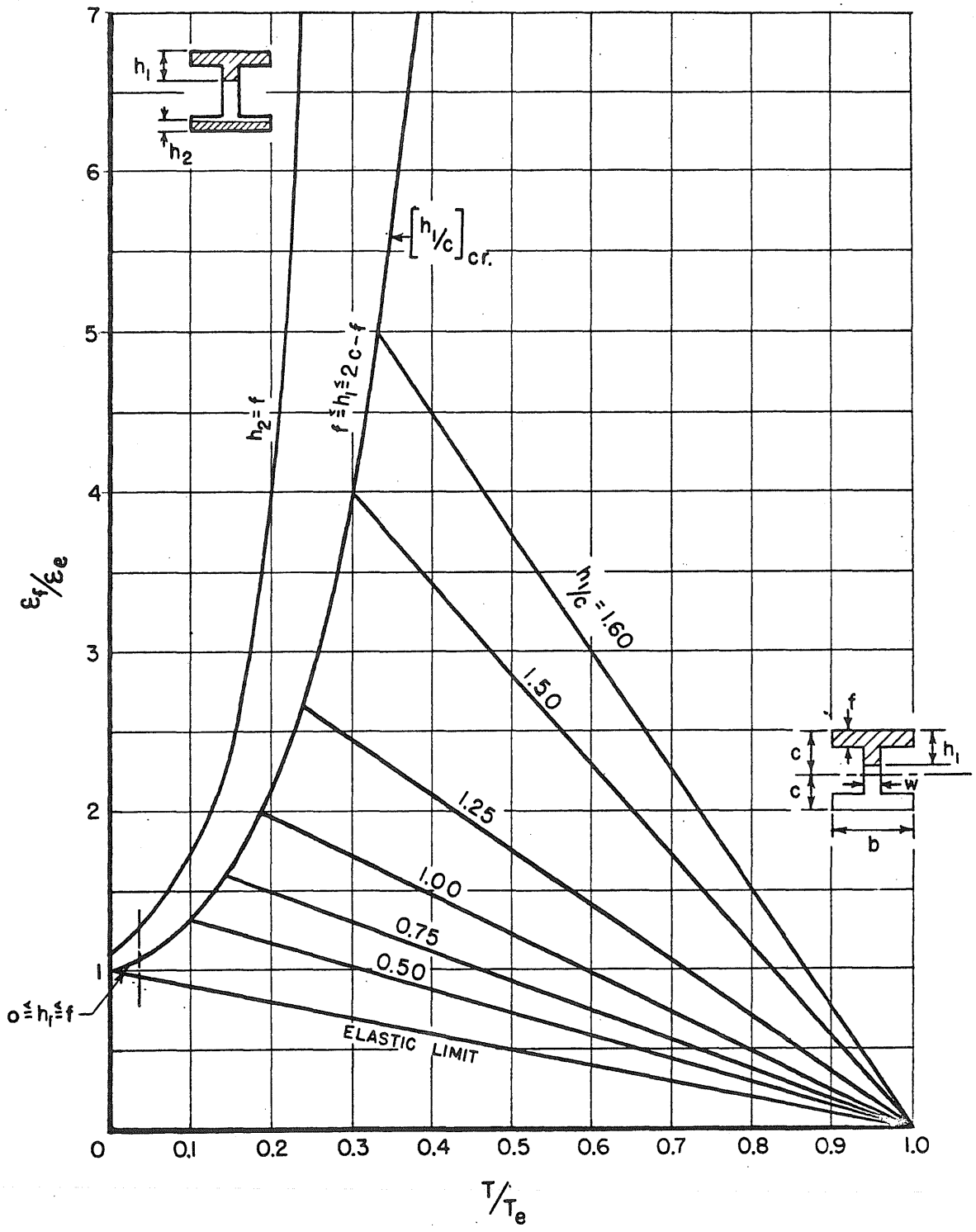

FIG. 2.11 AXIAL LOAD VS FLEXURAL STRAIN CURVES FOR 6B15.5 ABOUT AXIS X-X

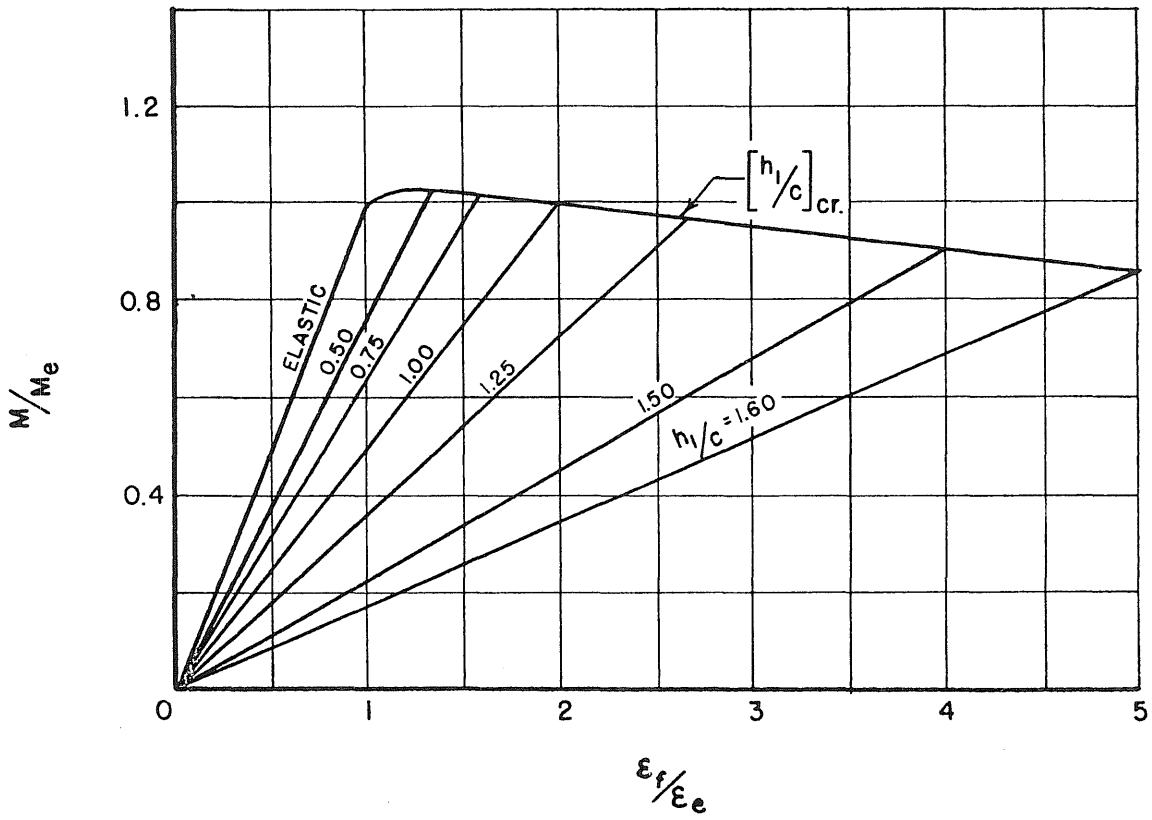

FIG. 2.12 MOMENT VS FLEXURAL STRAIN CURVES FOR 6BI5.5 ABOUT AXIS X–X

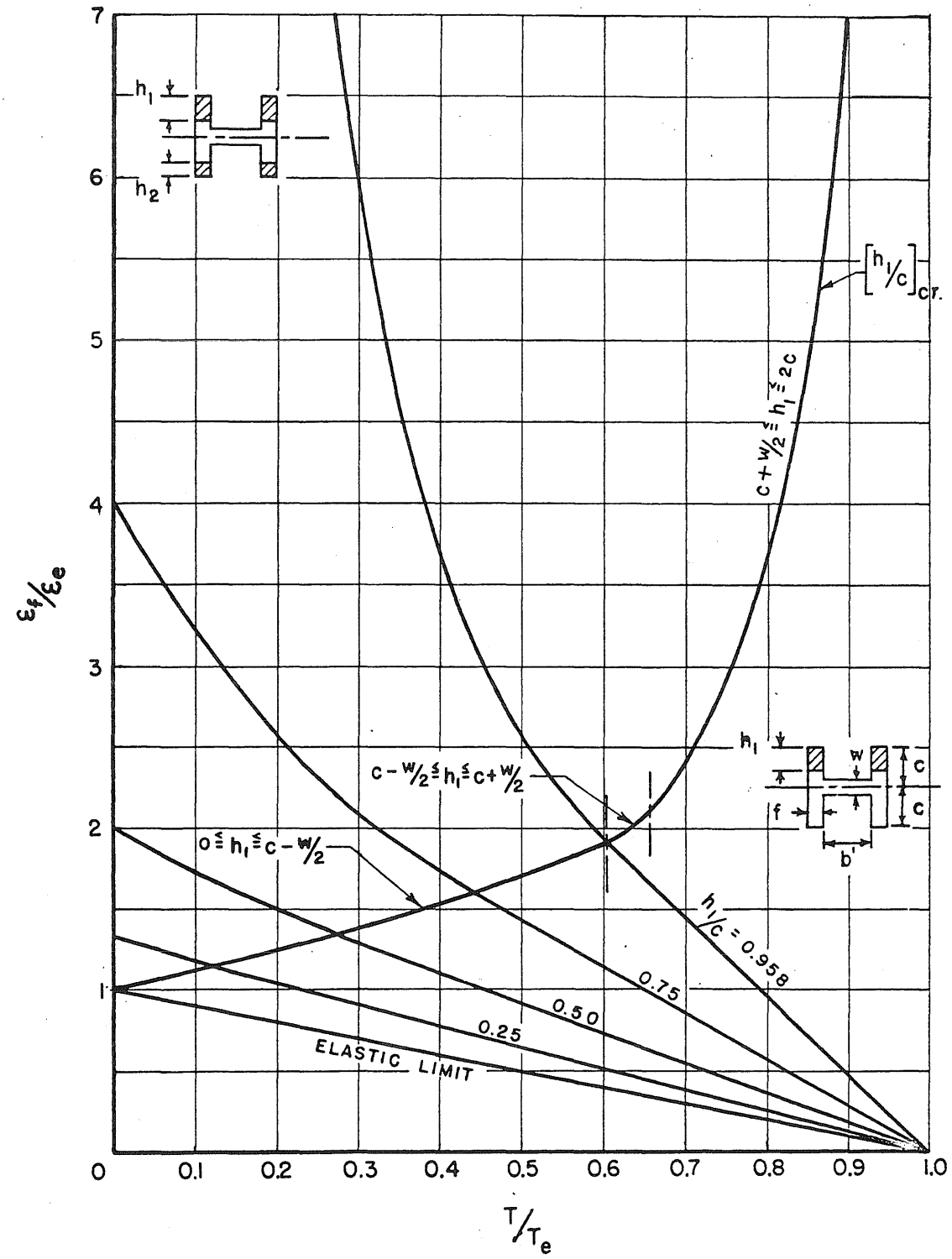

FIG. 2.13 AXIAL LOAD VS FLEXURAL STRAIN CURVES FOR 6B15.5 ABOUT AXIS Y–Y

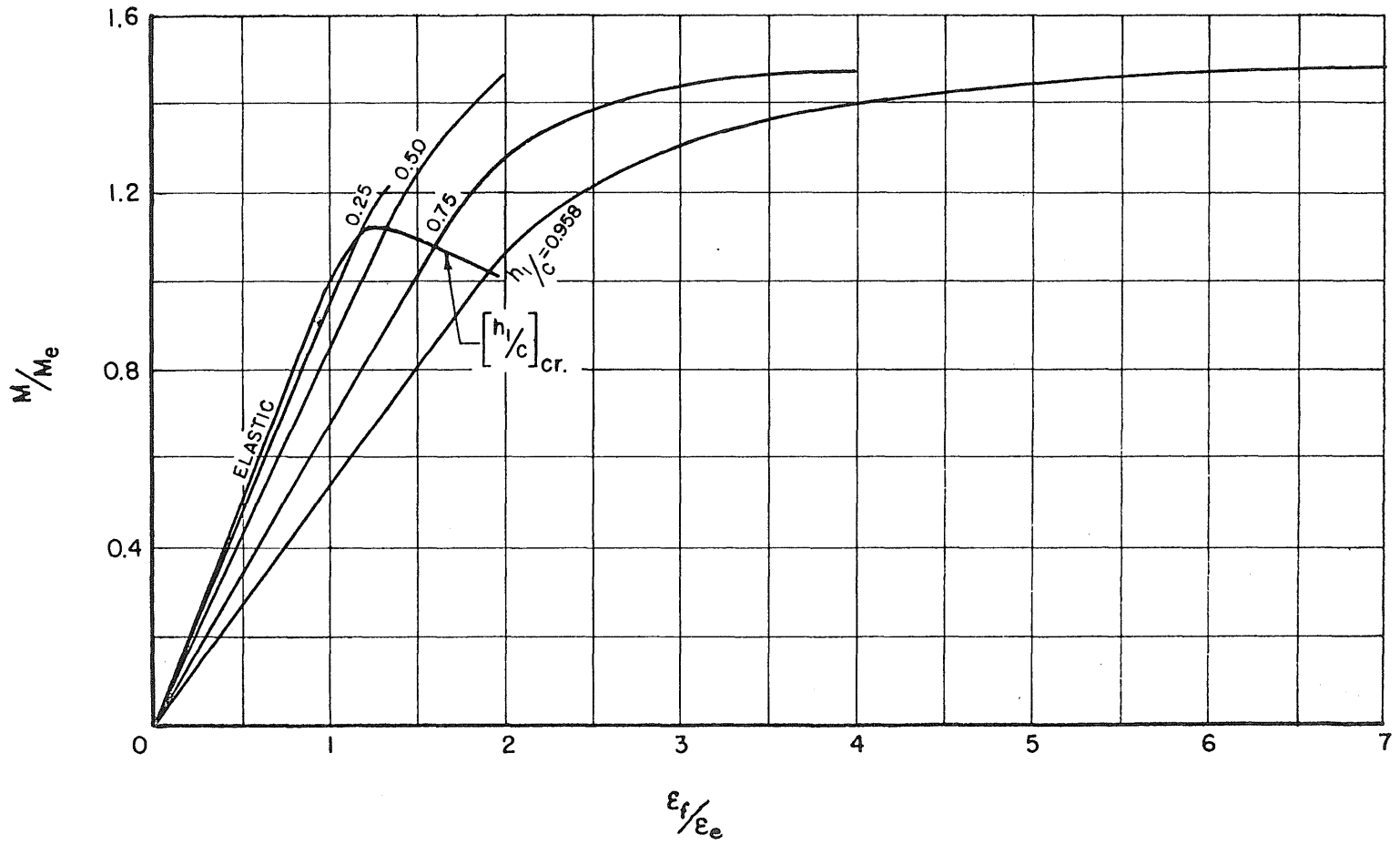

FIG. 2.14 MOMENT VS FLEXURAL STRAIN CURVES FOR 6B155 ABOUT AXIS Y-Y

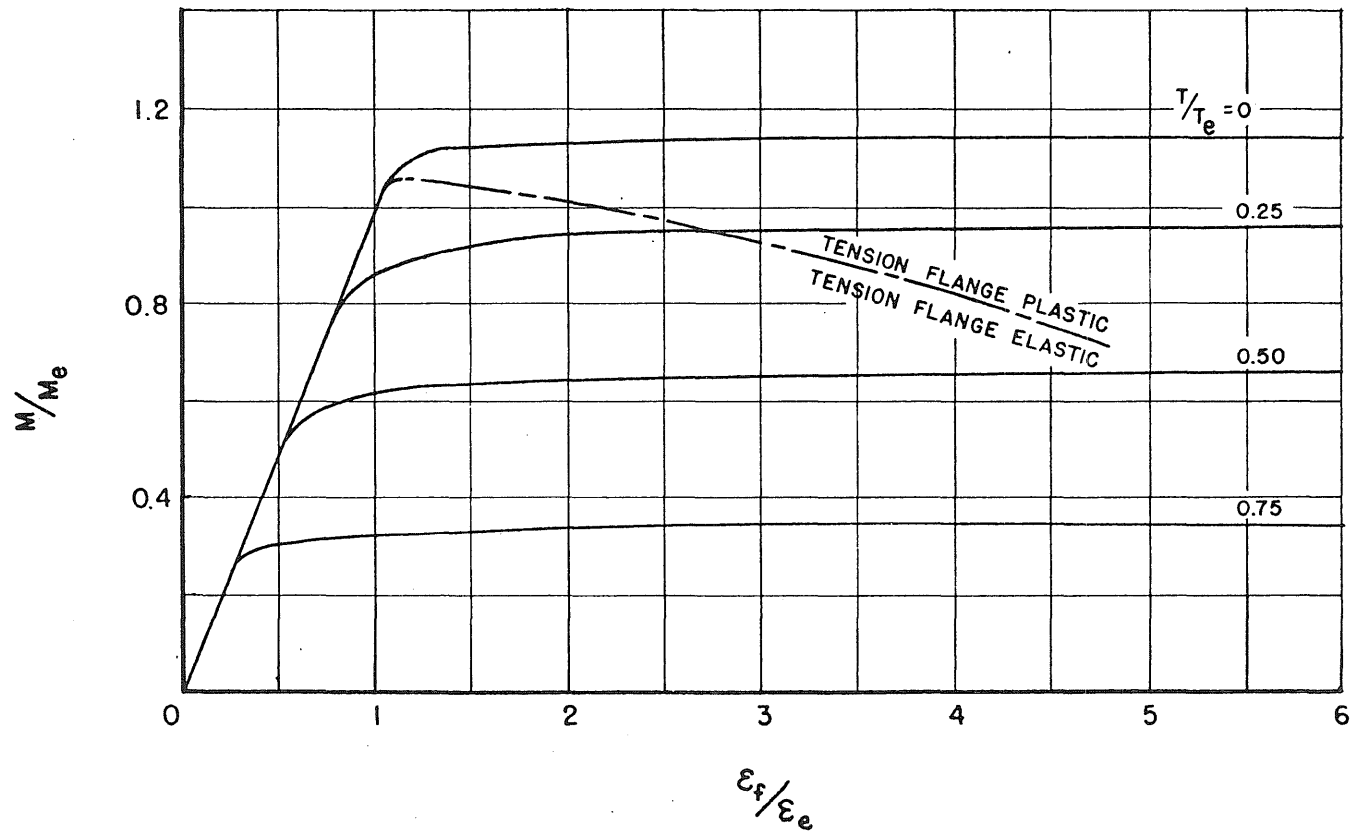

FIG. 2.15 EFFECT OF VARIOUS AXIAL LOADS ON THE MOMENT–STRAIN RELATIONSHIP FOR A 4MI3.0 SECTION ABOUT AXIS X–X

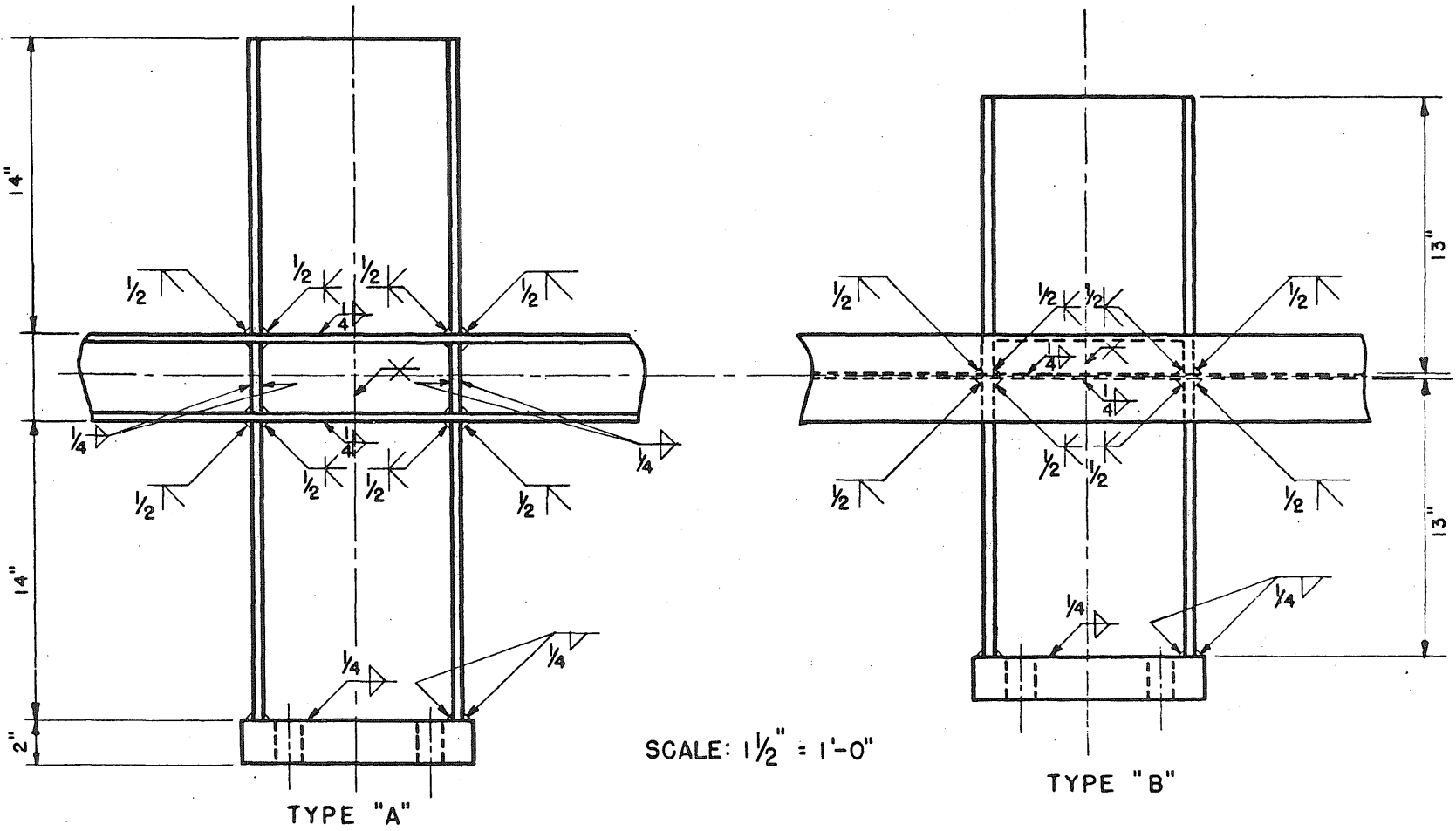

FIG. 2.16 STUB BEAM CONNECTION DETAILS

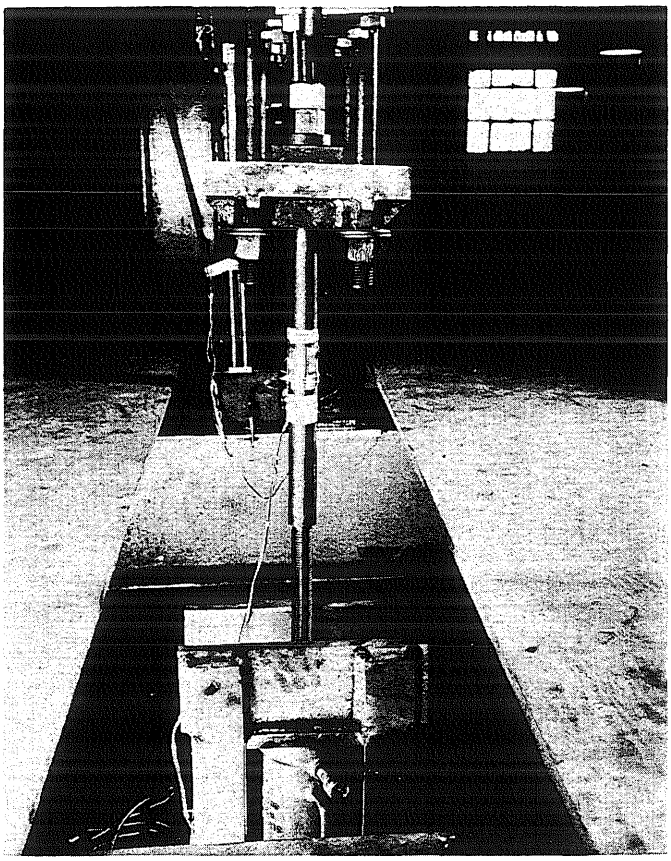

Fig. 2.17. Tension Jacking System

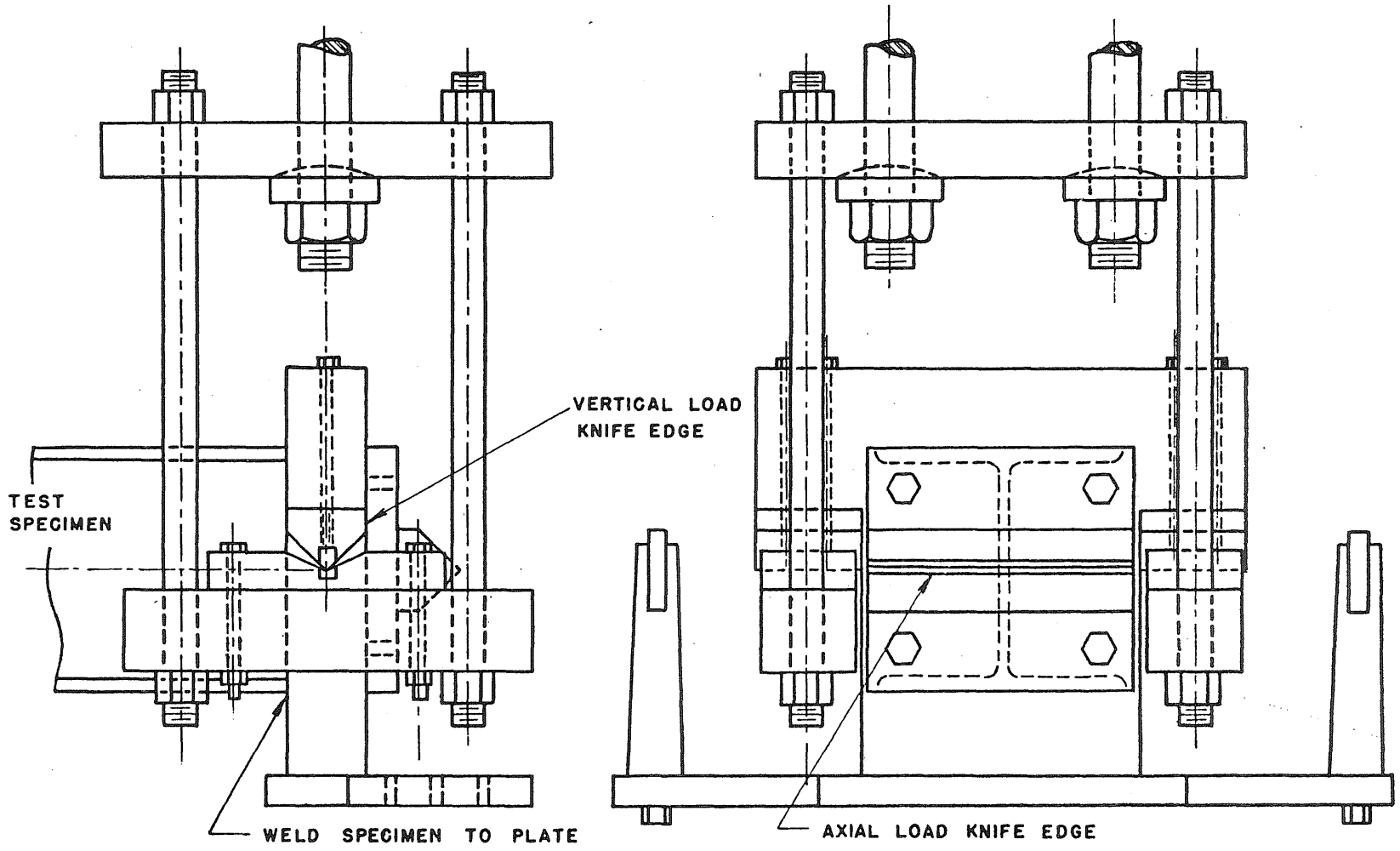

FIG. 2.18 END REACTION SYSTEM

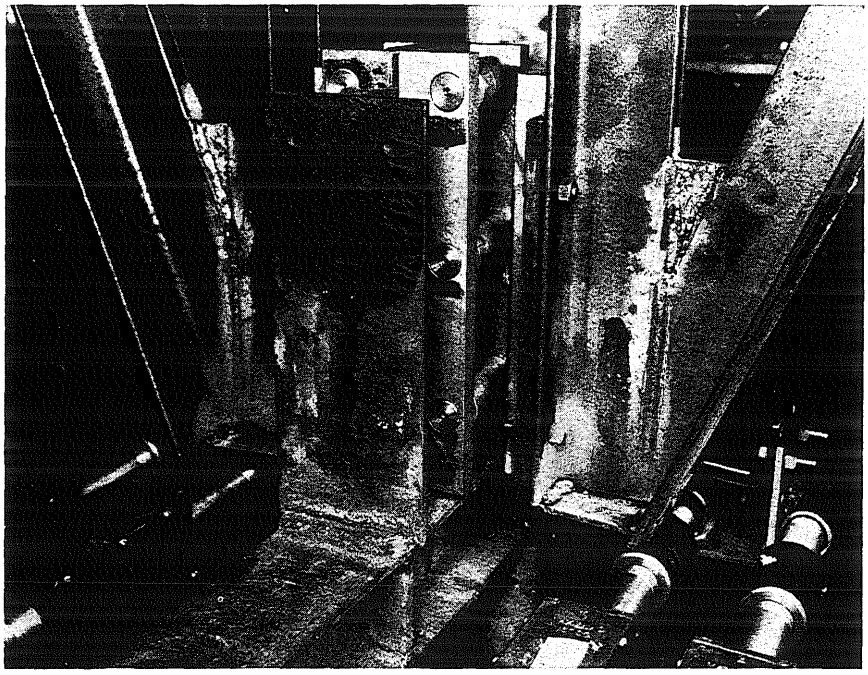

Fig. 2.19. Center Restraining System

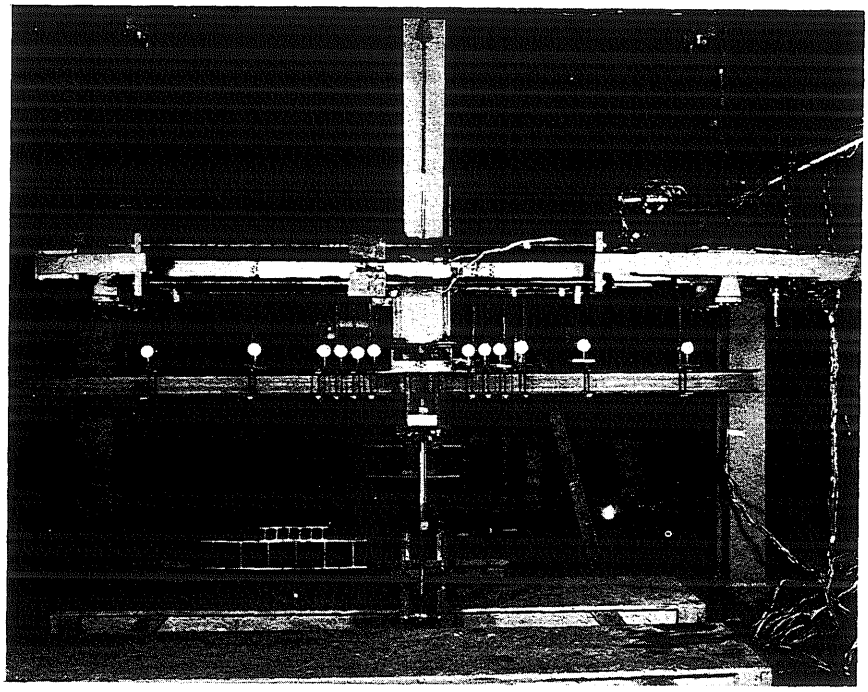

Fig. 2.20. Assembled Axial Load Apparatus

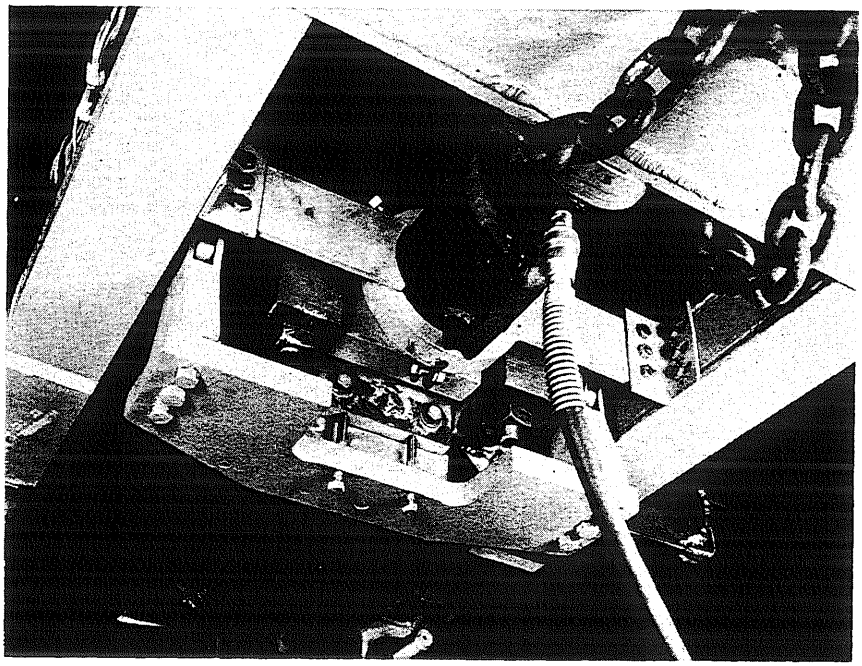

Fig. 2.21. Axial Load Jacking System

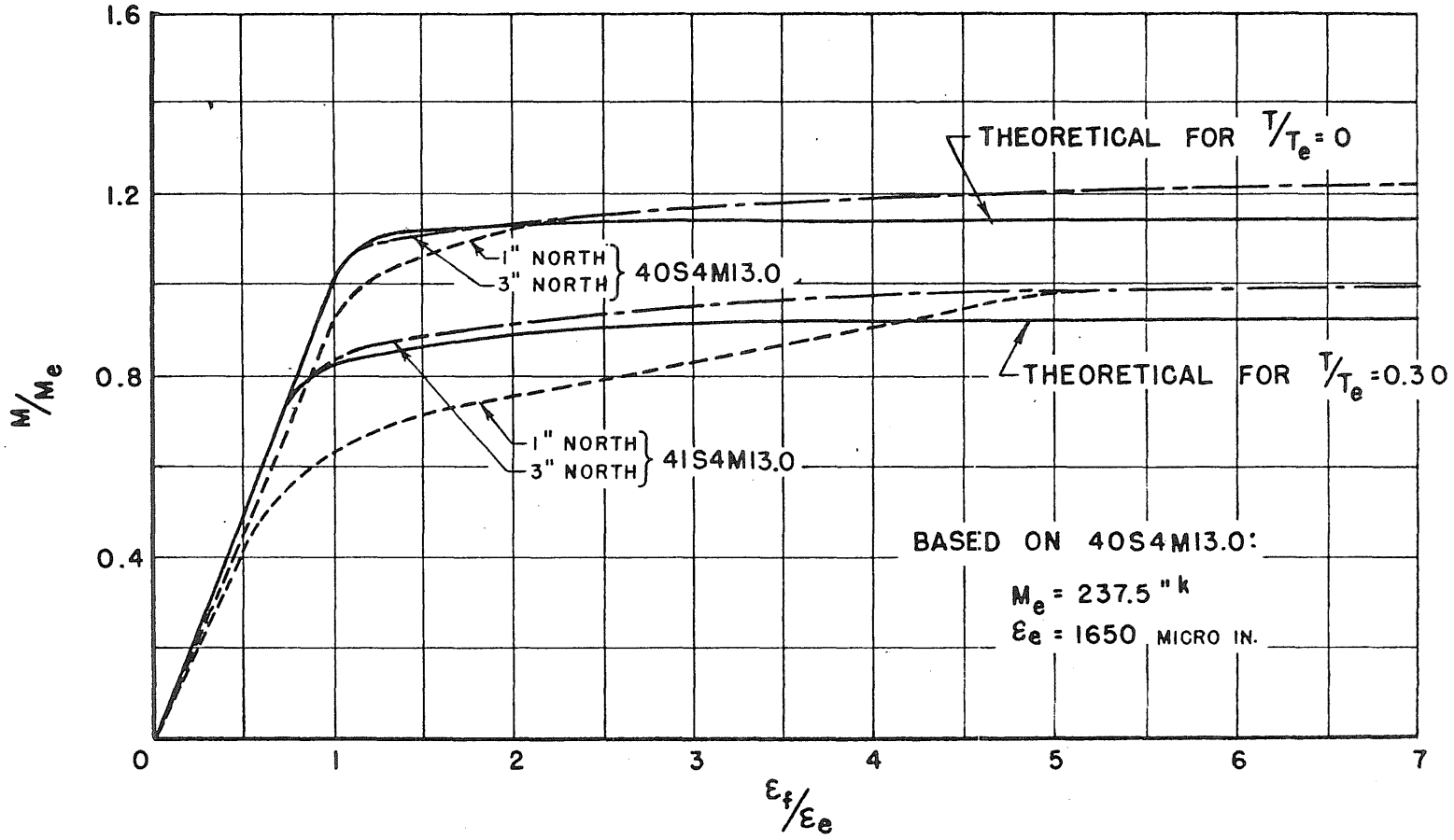

FIG. 2.22 MOMENT-STRAIN CURVES FOR SPECIMENS 40S4MI3.0 AND 41S4MI3.0

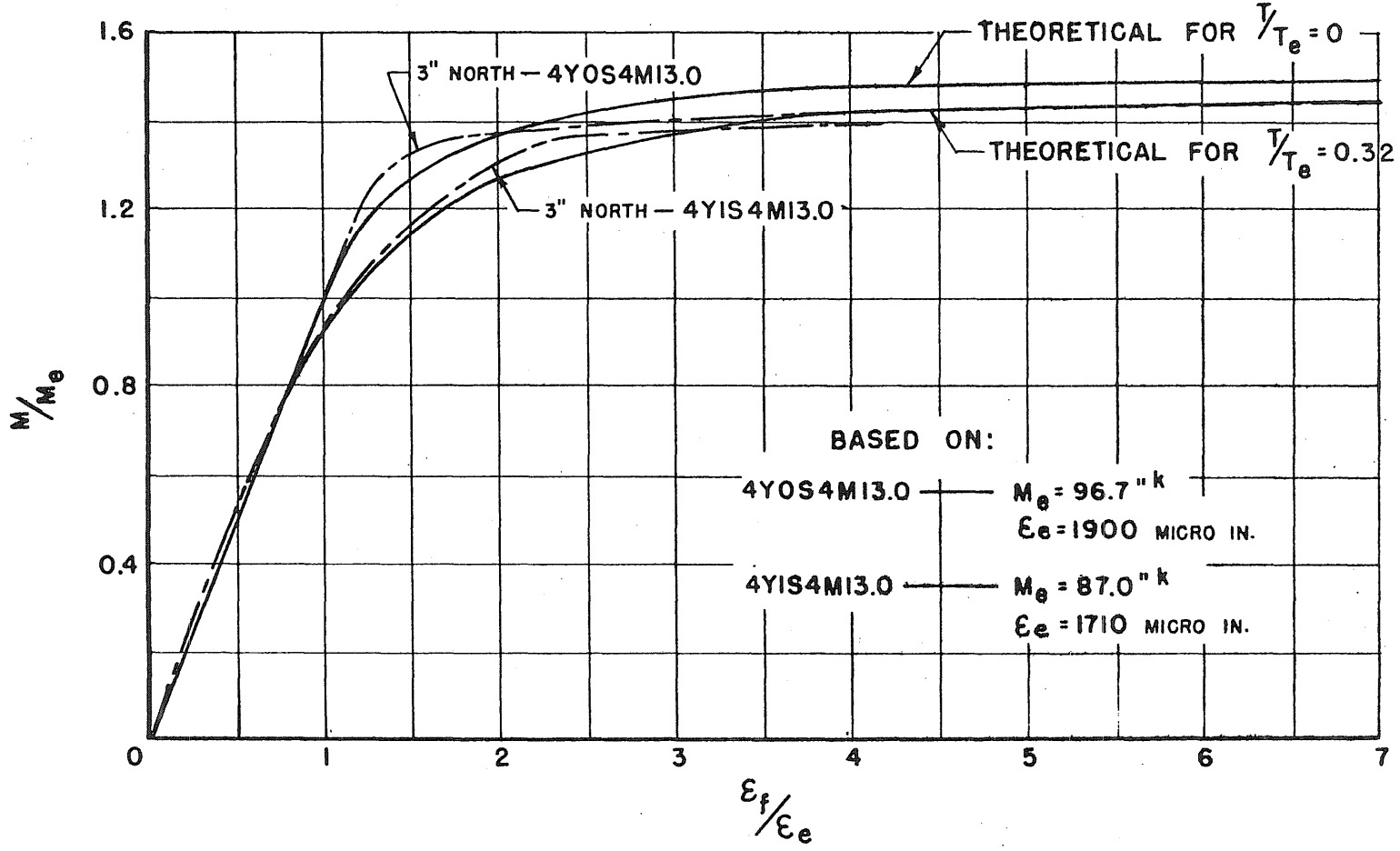

FIG. 2.23 MOMENT—STRAIN CURVES FOR SPECIMENS 4YOS4MI3.0 AND 4YIS4MI3.0

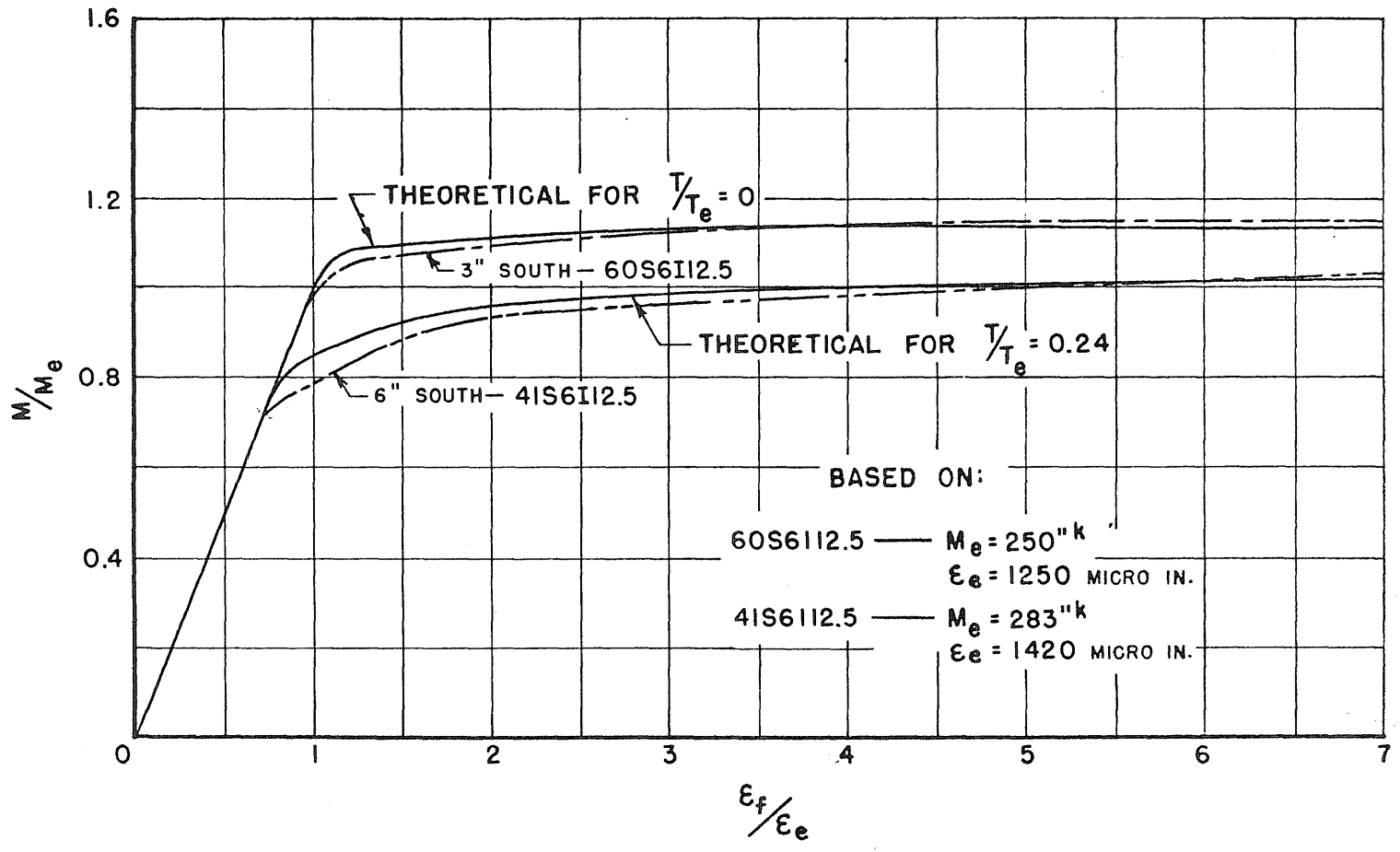

FIG. 2.24 MOMENT—STRAIN CURVES FOR SPECIMENS 60S6I12.5 AND 41S6I12.5

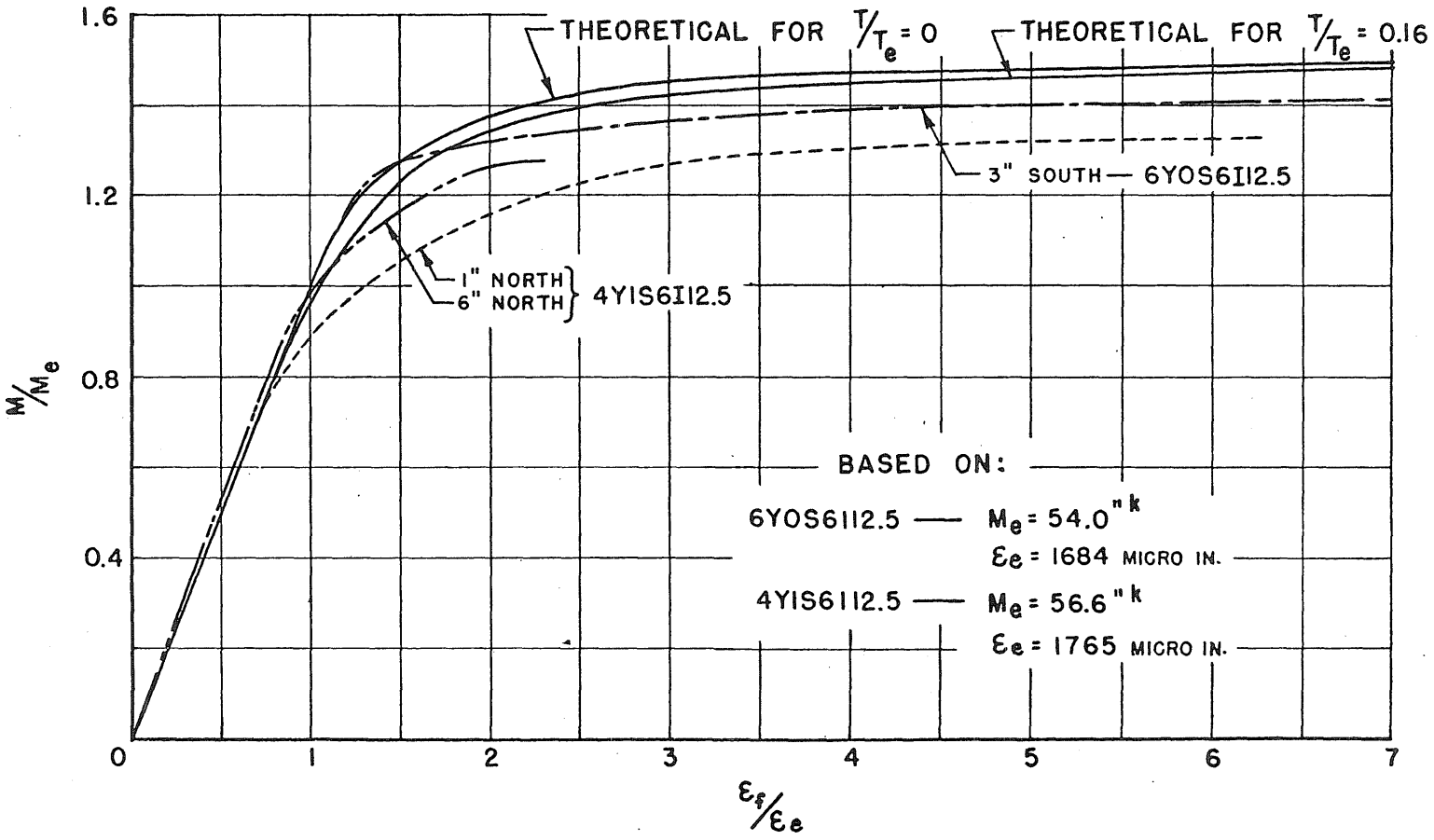

FIG. 2.25 MOMENT-STRAIN CURVES FOR SPECIMENS 6YOS6112.5 AND 4YIS6112.5

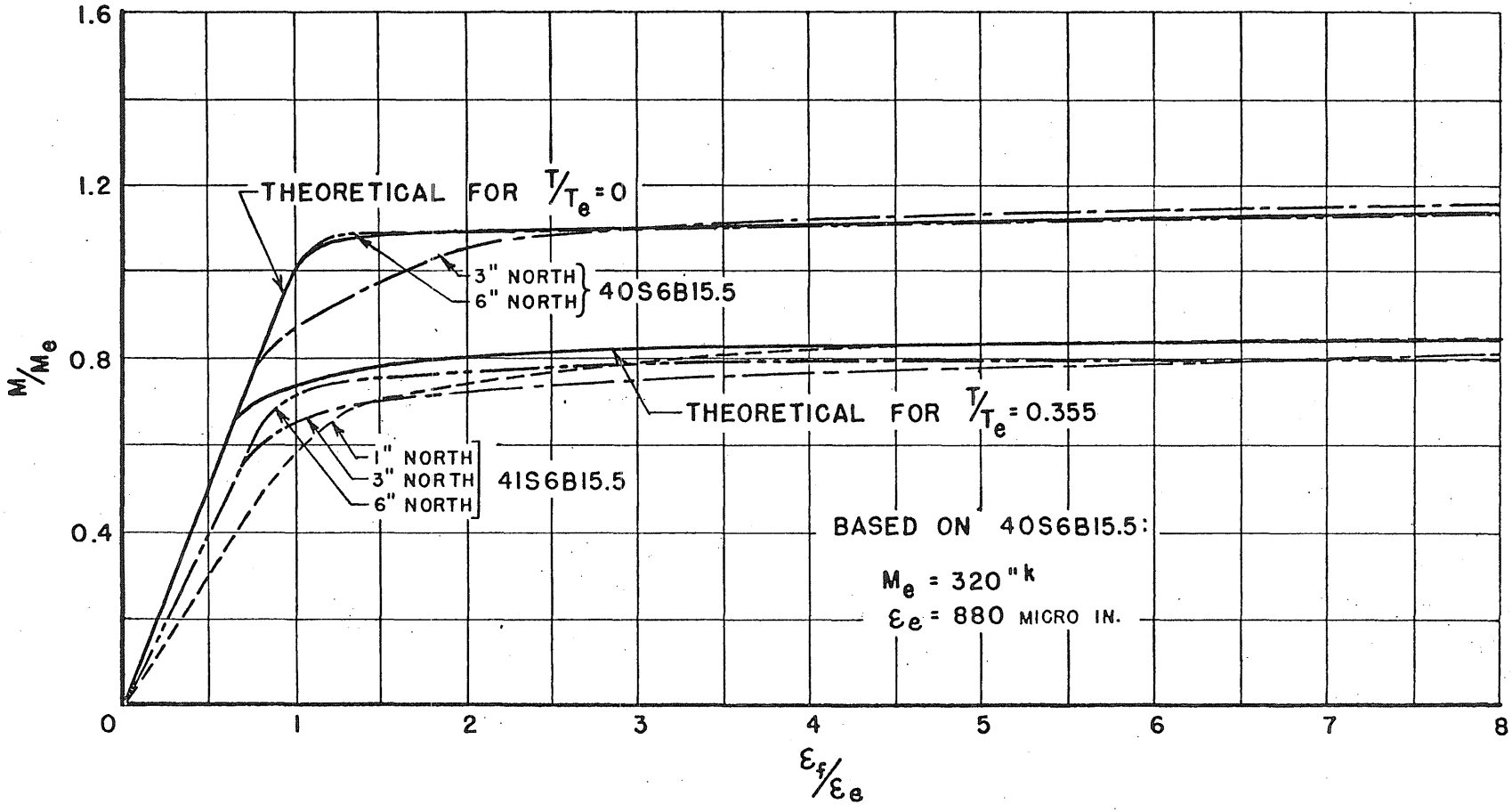

FIG. 2.26 MOMENT—STRAIN CURVES FOR SPECIMENS 40S6B15.5 AND 41S6B15.5

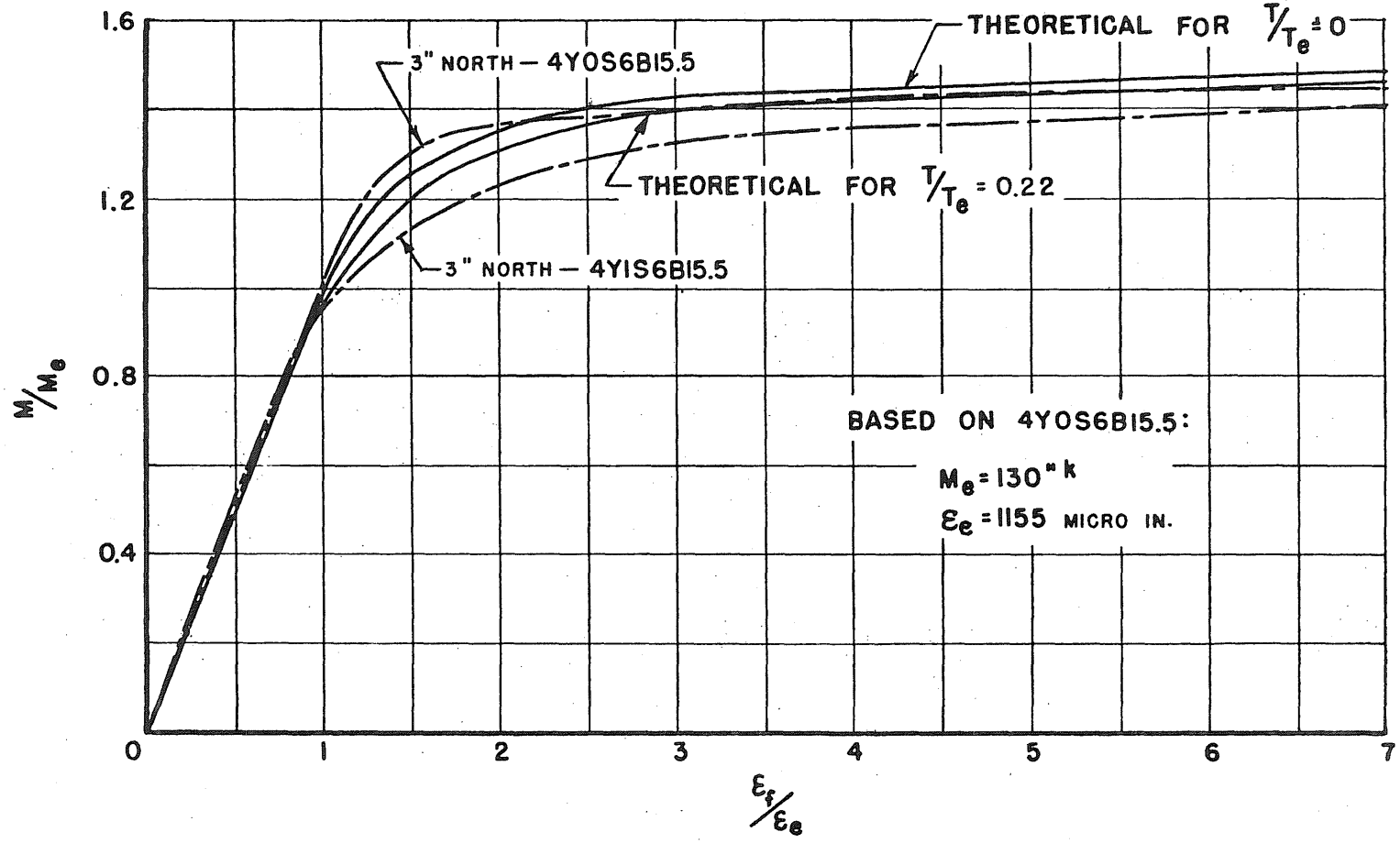

FIG. 2.27 MOMENT—STRAIN CURVES FOR 4YOS6BI5.5 AND 4YIS6BI5.5

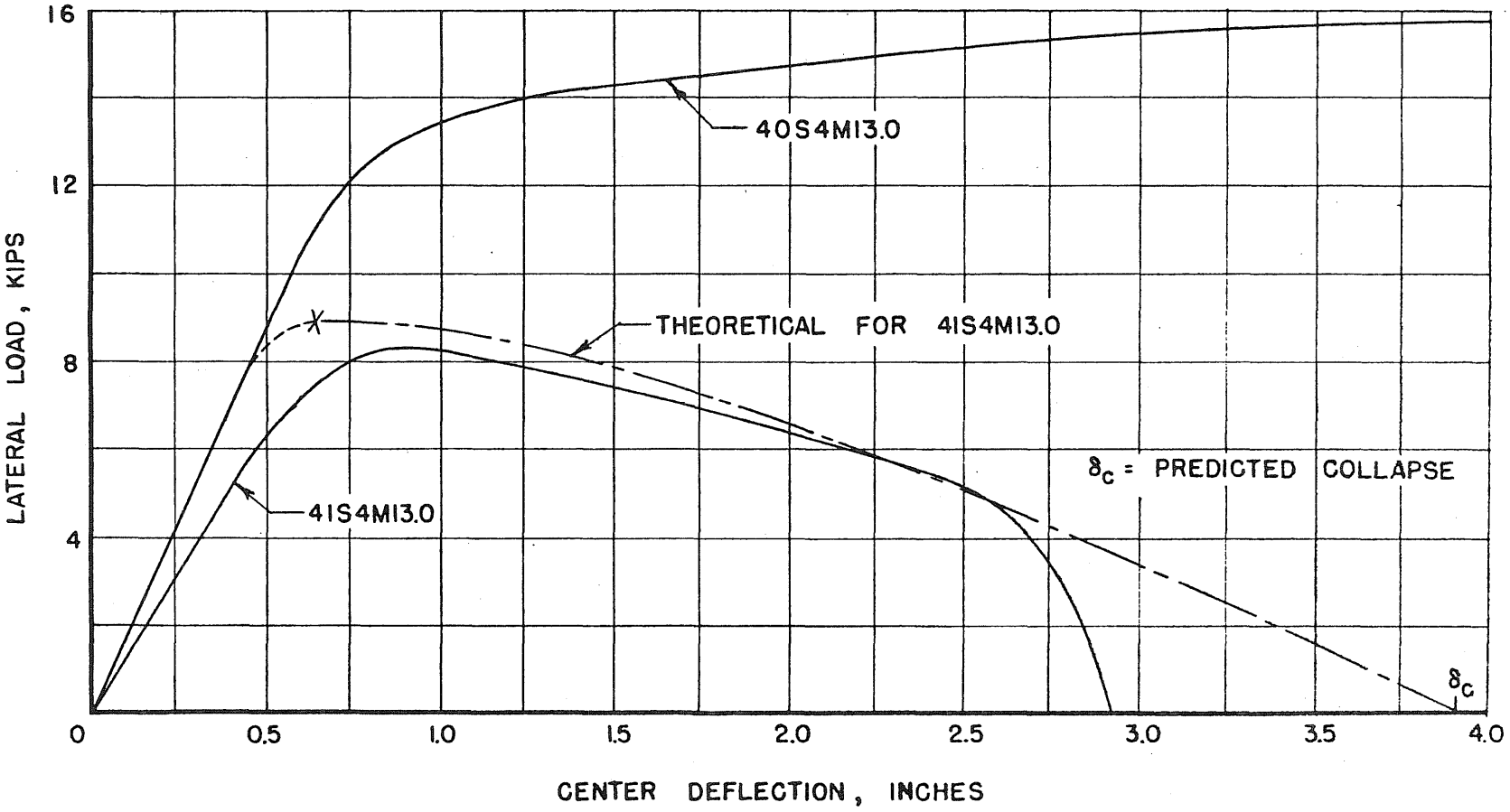

FIG. 2.28 LOAD—DEFLECTION FOR SPECIMENS 40S4MI3.0 AND 41S4MI3.0

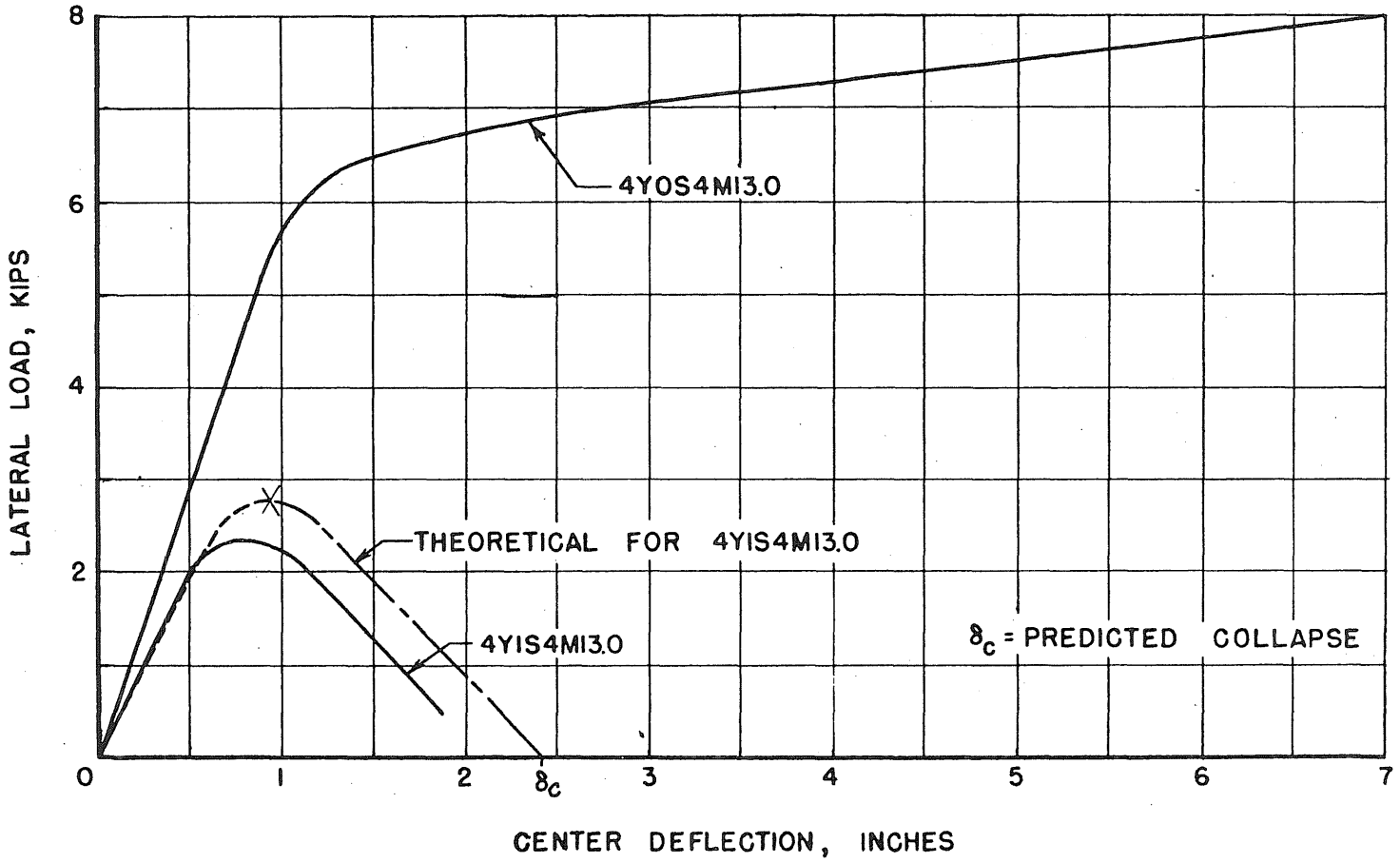

FIG. 2.29 LOAD—DEFLECTION FOR SPECIMENS 4YOS4MI3.0 AND 4YIS4MI3.0

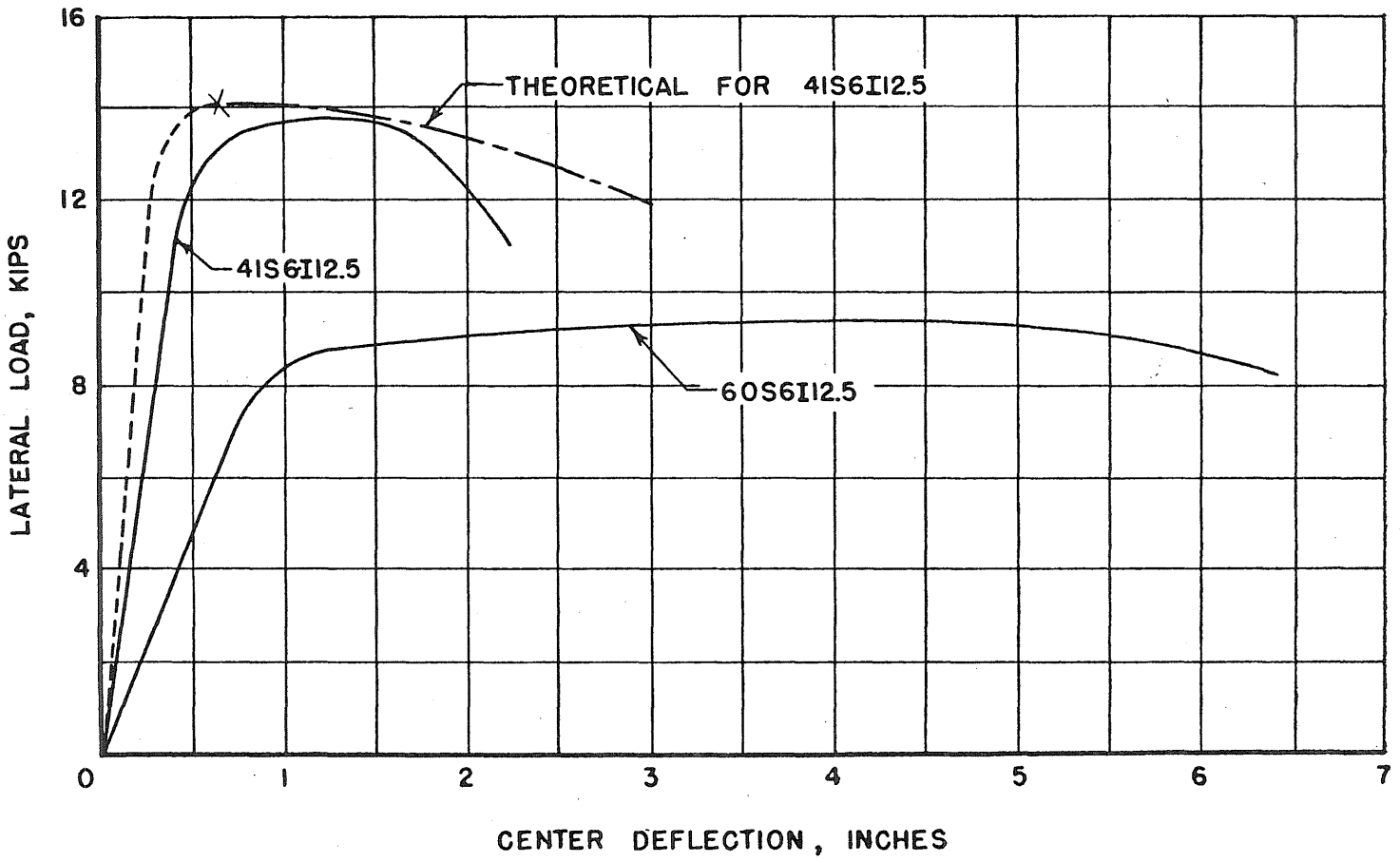

FIG. 2.30 LOAD–DEFLECTION FOR SPECIMENS 60S6II2.5 AND 41S6II2.5

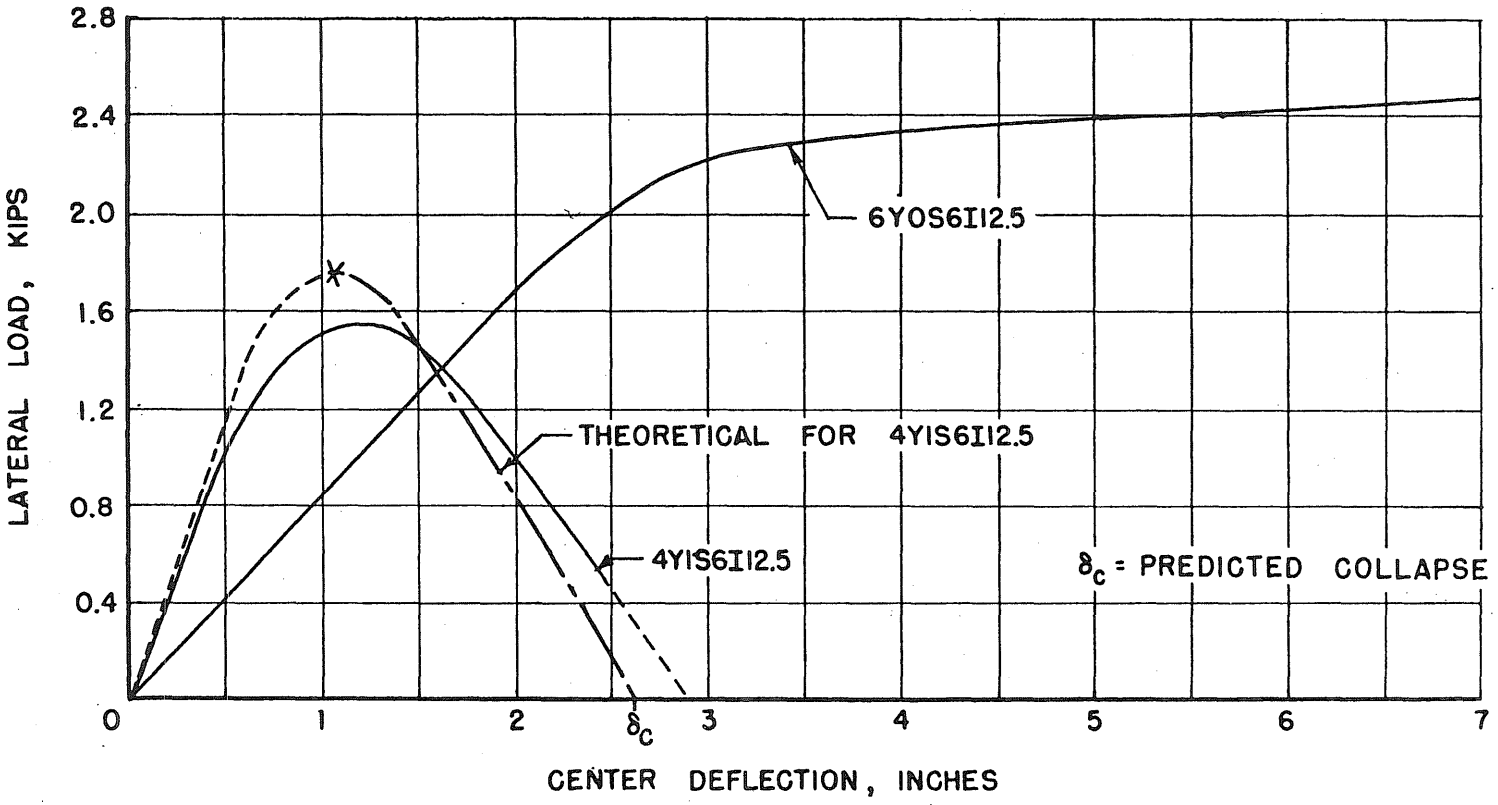

FIG. 2.31 LOAD—DEFLECTION FOR SPECIMENS 6YOS6II2.5 AND 4YIS6II2.5

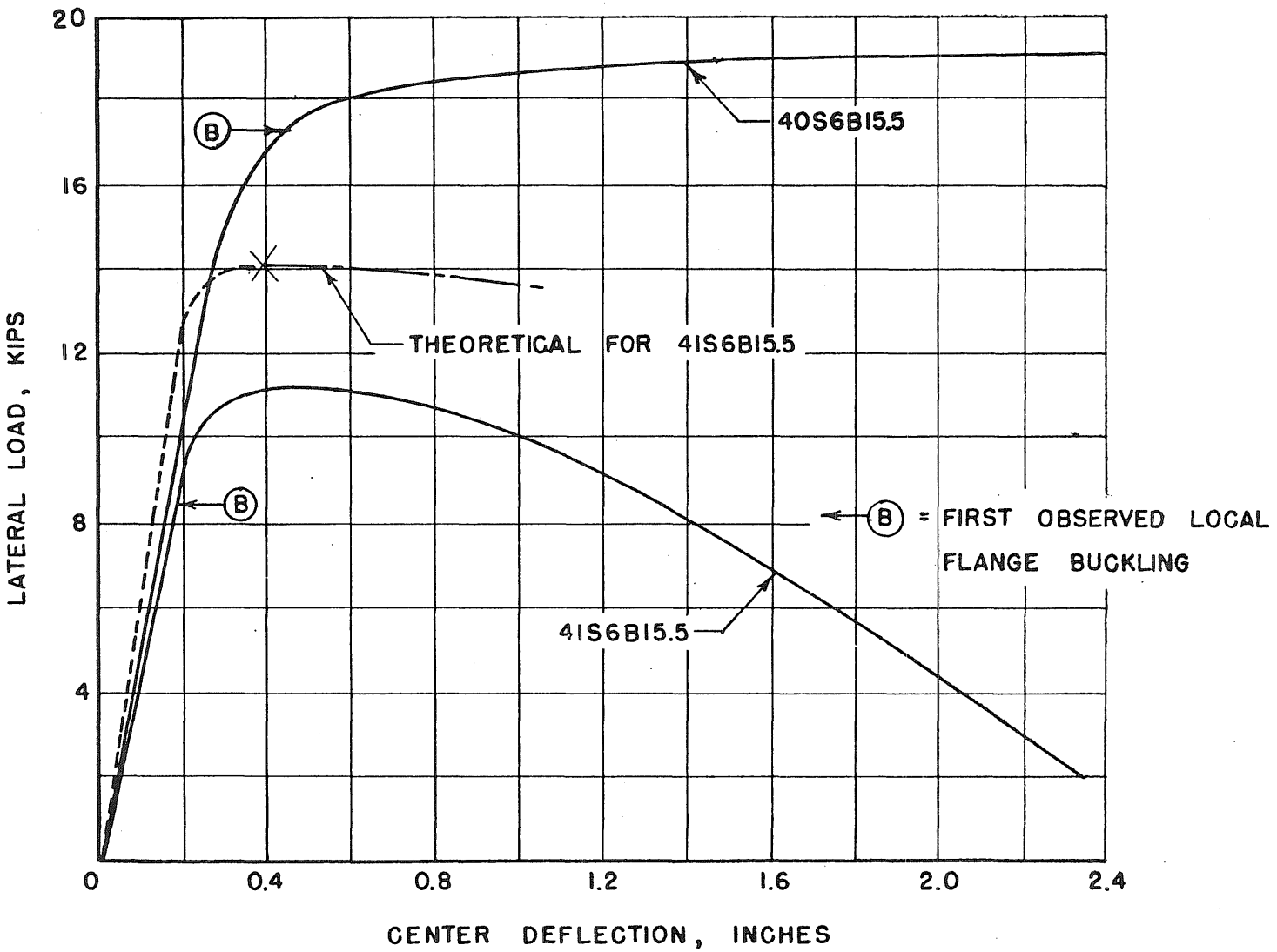

FIG. 2.32 LOAD–DEFLECTION FOR SPECIMENS 40S6B15.5 AND 41S6B15.5

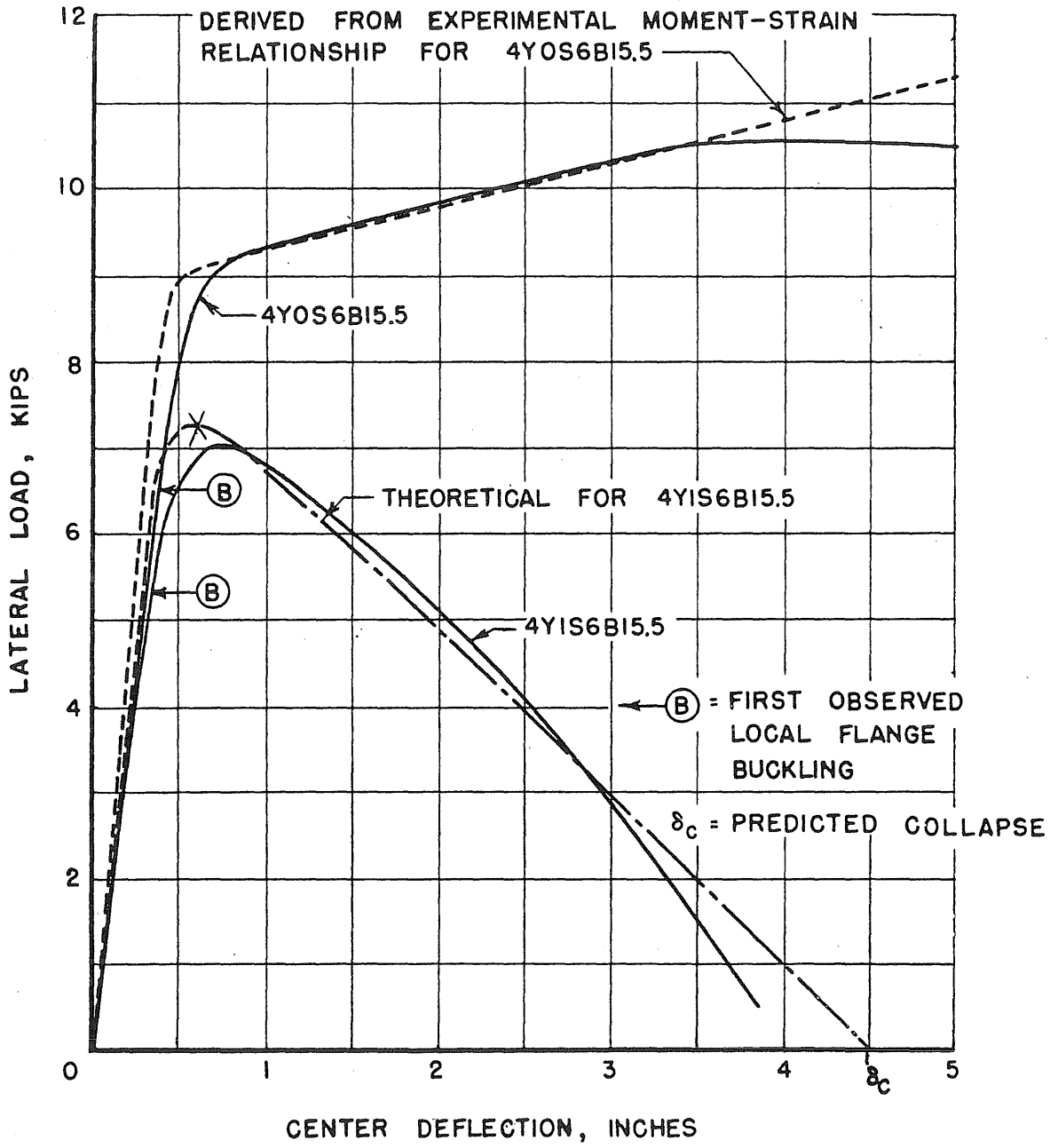

FIG. 2.33 LOAD—DEFLECTION FOR SPECIMENS 4YOS6BI5.5 AND 4YIS6BI5.5

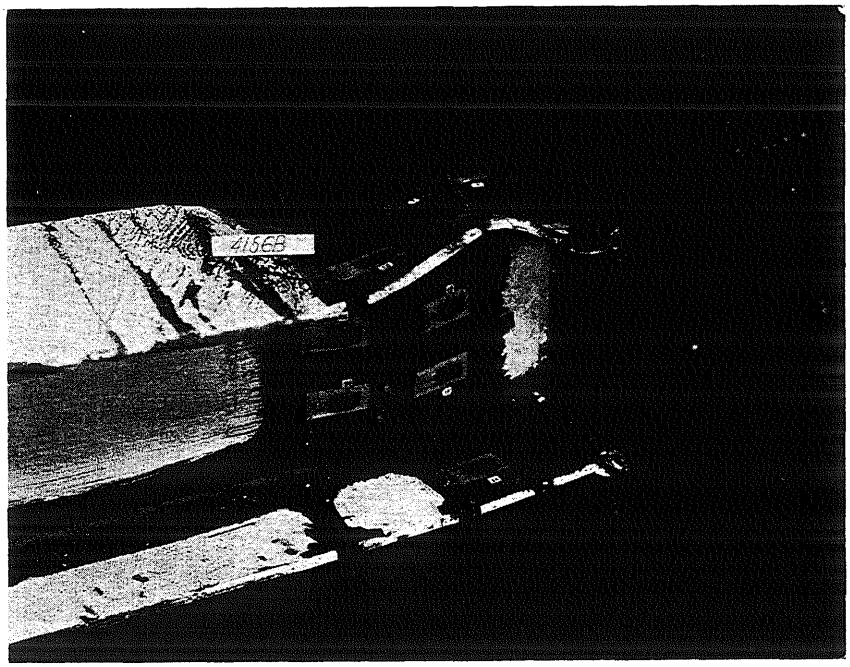

Fig. 2.34. Extent of Flange Buckling for Specimen 41 S 6 B

3. MODEL STUDIES OF FRAMES SUBJECTED TO STATIC LATERAL LOADS

3.1 INTRODUCTION

3.1.1 Introductory Statement

In order to determine the large deflection response of structures subjected to transient loadings, it is necessary to know the resisting force characteristics of the structure well beyond the elastic limit.

Much of the attention that has been given to the plastic response of structures has been directed towards the analysis of structures assumed to be constructed of a material which has no increase in strength for strains greater than the yield point strain. Such studies have provided information which is applicable to the early stages of the plastic deformation of mild steel structures since ASTM A-7 structural steel is a material that generally has a long flat region in the stress strain curve immediately following the elastic portion. However, for structures in which the maximum moment occurs along only an infinitesimal portion of the member, and where the inelastic action is confined to a short length of the beam, such as is the case in beams subjected to uniform and single concentrated loads, the deflection corresponding to large maximum strains may be only 2 to 10 times the elastic limit deflection, depending on the shape of the cross-section and the loading condition. Thus, this assumption of the stress-strain relationship confines the response study to a region where the structure's deflections cannot become large in comparison to the elastic limit deflections. In this

program the large deflection response of the structure is being studied. Since the stress-strain relationship for mild steel does show an increased capacity for strains greater than approximately 1 per cent, strain-hardening can appreciably affect the load-deflection response and must be considered in the case of large plastic deformations.

The objective of this study is to compare the large deflection response of model beams and frames subjected to static loads with the theoretical predictions of the response which can be made by using the assumptions following:

1. The stress-strain relationship for the material of the members may be obtained from standard tensile coupon specimens.

2. The strain distribution across the section is linear.

3. The curvatures are in accord with the usual small deflection flexure theory.

3.1.2 Summary of the Investigation

To evaluate the validity of the theoretical moment-curvature and load-deflection responses of the structures, model beams and frames were tested. These models had an effective length of 15 in. and were approximately 1/4 scale models of a 6 WF 25 section. The program included two series of tests, one in which the columns were oriented in their weak direction of resistance and another series in the strong direction. In each series, two model beam-columns and two frames were tested. In the model beam-column tests, no axial load was applied. One frame specimen in each series had an axial load, approximately 9 ksi; the other had no axial load.

Reasonably good agreement was found between the theoretical and observed moment-curvature relationships obtained in the beam-column tests. Tests in the weak direction of resistance gave better agreement between the theoretical and observed load-deflection response than did tests in the strong direction of resistance.

3.2 TEST SPECIMENS

3.2.1 Material

All column members were machined from adjacent strips cut from a 2 in. thick ASTM A-7[1]* steel plate. Before the column members were machined, these strips were stress-relieved and annealed in order to eliminate machining difficulties caused by warping from residual stresses and to provide a more homogeneous material. The heat treatment provided for a heating of the strips to 1300°F for three hours and then cooling them in the furnace.

Tension coupons, 0.505 in. in diameter, were machined from the center of blocks cut from each end of the stress-relieved strips. The average properties obtained from the stress-strain relationships of the coupons for each of the columns fell into three groups. A summary of the stress-strain relationships for these groups is shown in Figs. 3.1, 3.2, and 3.3.

The stress-strain curves show that the average yield strength was 35.5 ksi for the group shown in Fig. 3.1, 34.7 ksi for those in Fig. 3.2, and 37.5 ksi for those in Fig. 3.3. All coupons began to

---

* Numbers refer to entries in the Bibliography at the end of this section.

strain-harden at a strain that was lower than normal for A-7 structural steel. Several of the coupons showed an ultimate strength greater than that specified for ASTM A-7 steel. The average final elongation was 32 per cent which satisfies the ASTM A-7 standards.

Although the properties of the test material were not completely in accord with the requirements of ASTM Designation A-7, it is believed that the variations in properties of the test material from the properties of standard ASTM A-7 steel has no effect on the applicability of the theoretical procedures used in this study to the analysis of structures constructed with A-7 steel. The stress-strain relationships corresponding to the material of the particular structure must be used in the theoretical analysis.

3.2.2 Column Sizes

The columns tested were 1/4 scale models of a standard 6 WF 25[2] section except for the use of constant thickness flanges. This modification was made to facilitate machining. In addition, for some specimens the depth of the model was increased slightly (approximately 0.01 in.) in order to use the laboratory's existing machine tools more efficiently.

The dimensions of the section are shown in Fig. 3.4. The column specimens were made 17.5 in. long; however, the free length of the members during the tests was only 15 in. The remaining 2.5 in. was used in providing rigid end connections.

3.2.3 Beam-Column Specimens

Model 6 WF 25 sections with an effective length of 15 in.

were used for two types of simple beam-column specimens. Columns No. 1 and 7 were tested as simple beams subjected to two-point loadings which produced a region of pure moment. Columns No. 4 and 6 were tested with the load applied to the center of the beams. Columns No. 1 and 4 were loaded in the weak direction of resistance while Columns No. 6 and 7 were loaded in the strong direction of resistance. In all tests the loading blocks and end reaction blocks were made to fit into the column section and were rigidly brazed to the specimens. Photographs of Columns No. 1 and 4 in testing position are shown in Fig. 3.6.

3.2.4 Frame Specimens

The test frames were two legged, rigid bents whose dimensions can be found in Fig. 3.5. The column members of the frames were model 6 WF 25 sections while the top member of all frames was a 3 x 1-7/8 in. rectangular steel bar. The stiffness of this top beam may be considered infinite with respect to the column stiffness. Both the top and bottom joints of the frame were made rigid by means of additional blocking which was brazed around and into the column members at their end connections. In order to insure a strong, rigid connection, welding was used for the connections of the columns to the top beam in frame No. 3. These connections can be seen in Figs. 3.7 and 3.8.

The fabrication of the frames was begun by brazing the columns into recesses in the top beam to form a "U-shaped" structure. After these joints cooled the frame was welded to the base plate with a 1/4 in. fillet weld to complete the fabrication. This sequence and method of fabrication minimized the residual stresses, which would have

developed during the cooling of the specimen, by permitting the movements resulting from temperature differentials to occur before the ends of the frame were rigidly attached. The heat produced by the welding was small and, because of the 1-1/4 in. end blocks, was restricted to a section away from the column members for all specimens except frame No. 3, where, for strength requirements the columns were welded directly to the top beam. Consequently, for all sections except those of frame No. 3, the properties of the material in the column section were, most likely, not affected by the welding.

3.3 APPARATUS

3.3.1 Testing Apparatus

With the special jigs shown in Fig. 3.6, point loads were applied to the beam-column specimens through steel balls. The ends of the members were free to move inwards as the specimen deflected since in these jigs the end supports were on rollers. In the center-load test a center-roller guide system provided restraint against rotation and lateral displacement of the specimen. This restraint was provided to insure that lateral buckling would not occur. For the two point load test the special loading yoke shown in Fig. 3.6 was made to apply the point loads through steel balls.

With the frame testing apparatus, shown in Figs. 3.9, 3.10, and 3.11, it was possible to apply lateral and axial loads in a constant direction even after the frame had undergone large deflections. The ball assemblies at the loading points permitted the movements necessary to maintain the direction of loading constant. Springs were used to

apply the axial loads to the columns of the model frame while the lateral load was applied with a hydraulic jack. It was not necessary to provide lateral restraint for the frames No. 1 and 2, with columns oriented in the weak direction. Lateral restraint was provided for the frames with columns oriented in the strong direction. This restraint system is shown in Fig. 3.11.

3.3.2 Measuring Apparatus

Measurements of the deflections, strains, and loads were obtained with mechanical dials, SR-4 type A-7 strain gages, and electrical resistance type dynamometers respectively. The dynamometers were calibrated weigh bars on which SR-4 type AD-7 strain gages were used to measure the strains in the bar. Since these dynamometers had a high sensitivity, about 2.3 lb per micro-inch of indicated strain, it was possible to determine and control accurately the loads applied to the frame.

Strain gages were used on the beam-column specimens to obtain curvature data for the moment-curvature relationship. Strain gages on the model frame specimens provided curvature data from which the resisting moments within the frame could be calculated with the aid of the moment-curvature relationships found from the beam-column tests.

3.4 THEORETICAL RELATIONSHIPS USED IN THE ANALYSIS

3.4.1 Moment-Curvature Relationships in General

In this section the procedures which were used to determine the moment-curvature relationships are described. For sections with or

without axial load the moment is defined by:

$$M = \int_A y \, \sigma \, dA$$

where:

A is the area of the cross-section of the member

dA is an element of area in the cross-section of the member

σ is the unit stress at this element of area

y is the distance from the neutral axis to the element of area

Curvature is defined as the angle change per unit length. Therefore, with the assumption of linear strain distribution, the curvature can be found by dividing the algebraic difference of extreme fiber strains by the depth of the section. For the case of no axial load this relationship becomes the extreme fiber strain divided by 1/2 the depth of the section.

3.4.2 Moment-Curvature Relationships for No Axial Load

To determine the moment at any section subjected to a given curvature it is necessary to know how the stress varies with strain. The stress-strain relationships for the materials used in this study can be divided into three groups. Average stress-strain curves which can be seen in Figs. 3.1, 3.2, and 3.3, were used to determine the theoretical moment-curvature relationships.

The calculation of the moment-curvature relationship was begun by choosing a particular curvature. Stresses corresponding to the strains resulting from this curvature were found from the average stress-strain curves. These stresses were then integrated numerically to

determine the moment for the particular curvature chosen. This procedure was repeated to obtain other points on the moment-curvature curves.

3.4.3 Moment-Curvature Relationships for Axial Load

The average stress-strain curve shown in Fig. 3.1 was used to develop a moment-curvature relationship for the column section subjected to an axial load of 8.89 ksi and laterally loaded in the weak direction of resistance. This curve was used to predict the theoretical response of frame No. 2. Similarly, for frame No. 4, a moment-curvature curve using the stress-strain curve shown in Fig. 3.3 was found for the column section subjected to an axial load of 8.73 ksi and loaded in the strong direction of resistance. In both cases the average stress-strain curves indicated that the material had a limited range of constant stress yielding before strain-hardening began.

Munz[3] has presented equations which can be used to determine the moment-curvature relationship for I and wide-flange sections, subjected to axial load, when strain-hardening of the material is neglected. These equations were used to obtain the initial portions of the moment-curvature relationship for bending in the weak direction of resistance and are valid to a curvature of approximately 0.005 radians per inch. After this curvature, strain-hardening began to influence the moment-curvature relationship; consequently, the moment-curvature relationship was determined by means of a numerical integration procedure in which the actual average coupon stress-strain curve was used.

To obtain one point on the moment-curvature curve, an extreme fiber strain was chosen, and the strain at the other extreme

fiber was allowed to vary until the desired value of axial load was developed on the section. Then the moment and curvature were computed for this strain distribution. This moment-curvature relationship for the section in the weak direction of resistance with axial load was found to be almost identical with the moment-curvature relationship for the section with no axial load. The moment-curvature curve for the case of axial load and bending in the strong direction of resistance was computed entirely by the numerical procedure described above. This moment-curvature curve for axial load was found to differ slightly from that for no axial load.

3.4.4 Load-Deflection Relationship

The analytical expression for curvature is:

$$\text{curvature} = \frac{1}{R} = \frac{\frac{d^2y}{dx^2}}{\left[1 + \left(\frac{dy}{dx}\right)^2\right]^{\frac{3}{2}}}$$

where: R is the radius of curvature

x is the coordinate along the length of the beam

y is the deflection

If the quantity $(dy/dx)^2$ is small, the curvature is approximately d^2y/dx^2. When this approximation is made, the deflected shape can be found by solving the differential equation:

$$\frac{1}{R} = \frac{d^2y}{dx^2}$$

The curvature at any point along the length of the beam or column was determined from the moment at that point by using the theoretical moment-curvature curve. In the determination of the moments along the specimen, account was taken of the change in the length of the moment arm resulting from the deflection. The deflections were found directly from the known moments and moment-curvature curve by the use of a numerical integration procedure.(4) This method was found to be quite rapid.

3.5 BEAM-COLUMN TESTS

With the assumption of linear strain distribution, curvatures were calculated from strains measured at sections 1/2 in., 1 in., and 2 in. from the loading stub of the beam-column specimens. The relationships between these observed curvatures and moments is compared in Figs. 3.12 and 3.13 with theoretical relationships obtained from the average stress-strain curves. Figure 3.12 shows the results for the weak direction of resistance; Fig. 3.13, the strong direction.

The distribution of strains across a section will be affected by discontinuities or restraints in or near the section. Therefore, the readings of the strain gages close to the loading stub reflect the influence of the stub. In order to evaluate this influence on the moment-curvature response, beam-column No. 1 (weak direction of resistance) and beam-column No. 7 (strong direction of resistance) were tested as simple beams loaded at two points. Strains at sections approximately 2 in. from rigidly fixed loading blocks were measured within the region of pure moment. The moment-curvature curves obtained from these strain readings are in good accord with the theoretically predicted relationships.

The moment-curvature curves calculated from the strains measured at sections 1 in. and 1/2 in. from the loading stub lie considerably above the theoretical curves. This indicates that the relationship was considerably influenced by the loading block. These deviations from the theoretical moment-curvature relationship in regions near boundaries were neglected. The neglect of the "stiffening" effect of the loading stub on nearby sections of the specimen lowers the theoretical load-deflection curve.

A theoretical load-deflection relationship determined for the center loaded, simple beam-column No. 4 is compared in Fig. 3.14 with the observed load-deflection curves. In this figure, two test curves are seen because the test was performed by increments of deflection. The load required to reach each new deflection is shown in Fig. 3.14 as the high load. While the specimen was held at a particular deflection the load required to maintain this deflection decreased because of a relaxation and redistribution of stress. In a few minutes the load stabilized to a value which is shown as the drop-off load.

The fact that the observed curve intersects and then lies below the theoretical curve can be attributed to a large degree to the increase in effective length caused by the failure of the brazing material at the loading stub. This break in the bond allowed a local buckle to extend into the region of the loading block which was intended to be rigidly connected to the flanges. As a result of this break the effective length of the specimen was increased 0.75 in. It is not known when the failure at the loading stub first occurred, but it is known that it occurred before a deflection of 1.4 in.

$$\frac{\delta}{\delta_e} = \frac{\text{deflection}}{\text{elastic limit deflection}} = \text{approximately } 50,$$

since at that deflection the bond failure was noted.

For the center loaded, simple beam-column test loaded in the weak direction the computed load and deflection at initial yielding, based on a yield stress of 35.5 ksi, were 0.824 kips and 0.029 in., respectively. As yielding progressed, and if no strain-hardening were present, the stress block would have approached a limiting value, a rectangle, and the maximum load capacity would have approached only 1.5 times the load at first yielding. However, because strain-hardening did occur, the maximum load sustained by the beam was approximately 3.3 times the yield load. Thus, it can be seen that strain-hardening had an important effect on the behavior of the specimen.

The load-deflection curve for column No. 6, a simple center loaded beam-column tested in the strong direction of resistance, is compared in Fig. 3.15 to the theoretical load-deflection curve. The "stiffening" effect of the loading stub caused the test curve to lie above the theoretical curve immediately after the elastic limit was passed. At large deflections, however, the buckling and twisting which the columns experienced reduced the load capacity and the test curve then falls below the theoretical curve. At a deflection of approximately 55 times the elastic limit deflection the buckling was so severe that the load began to drop quite rapidly.

The computed load and deflection at initial yielding, based on a yield stress of 34.7 ksi, were 2.438 kips and 0.027 in. respectively.

The lateral load to cause the fully plastic moment without consideration of strain-hardening is approximately 1.13 times the elastic limit load. Strain-hardening increased the maximum load sustained by the beam-column to nearly 2.2 times the elastic limit load.

It was realized after the beam-column tests that the deflections measured included a deformation of the loading system. The deformation of the loading system was found to vary non-linearly from 0 to 0.020 in. This deformation was erratic, and no corrections for it have been made in the reported curves. The errors are not significant after large deflections have occurred. They are, however, very important to the elastic deflection measurements and the disagreement of the theoretical and observed elastic limit deflections, even after shear deformations are considered, may be attributed to these errors in measurements.

3.6 FRAME TESTS IN THE WEAK DIRECTION

3.6.1 Frame No. 1

The average stress-strain curve, shown in Fig. 3.1, was used to determine the theoretical load-deflection response of frame No. 1. The theoretical load-deflection relationship is compared in Fig. 3.16 to the observed load-deflection curve. In this figure the values of P_e and δ_e are those for no axial loads. These curves show reasonably good agreement between the theoretical and observed response. Since the theoretical curve was computed neglecting the stiffening effect of the rigid boundaries it is somewhat below the observed response. The final deflected shape can be seen in Fig. 3.17.

In this test axial loads were produced in the columns by the overturning effect of the lateral load. Tension was produced in the windward column, and compression in the leeward column. These axial loads affected the moment-curvature relationship; however, since the axial stresses were small, less than 3.5 ksi, their effect on the moment-curvature relationship was small and has been neglected. As a result of this simplification the curvature at any section became a function only of the total moment.

Theoretically, as the deflections became large, the induced axial loads should have increased the percentage of the total shear carried by the windward column because the axial tension load in this column produced a moment that opposed the lateral shear moment. Since theoretically the end moments were approximately equal in both columns for the same deflection, the shear was larger in the windward column. In the leeward column the axial load had the opposite effect; it reduced the shear in this column. The net result was that the induced axial loads changed only the distribution of lateral resistance and did not significantly affect the total resistance of the frame. To a small extent the axial loads did affect the moment-curvature relationship and thus the load-deflection response. If these effects had been included, the theoretical lateral load resistance would have been reduced slightly.

With data from the strain gages placed at the third points of the columns it was possible to determine the resisting forces within the frame. The measured strains were used to determine curvatures, and the moments corresponding to these curvatures were found from Fig. 3.12.

Shears computed from these measured moments show that the percentage of shear carried by the windward column was about 50 per cent of the total in the elastic stage of the test, dropped to about 35 per cent in the early plastic stage, and then began to rise. Although the shear distribution to the windward column did not increase continuously from 50 per cent as theoretically predicted, the theoretical load-deflection behavior of the frame was in accord with the observed behavior.

The theoretical load-deflection response of frame No. 1 was found by considering a cantilever beam of 1/2 the column height, loaded at the end with a single concentrated force. When twice the load on this beam was plotted against twice the corresponding deflection, the load-deflection curve for the frame was obtained. The shortening of the moment arm of the force, because of the deflections, was considered in the calculation of moments.

It is apparent that this frame test and the center load beam-column test are directly related. If the deflections of the beam-column are doubled the load-deflection curve will be the same as that for this frame. The results of this study are in good agreement with this fact. Consequently, it appears that the behavior of the frame with column oriented in the weak direction of resistance can be determined in terms of the behavior of a beam-column member.

3.6.2 Frame No. 2

The columns of frame No. 2 were subjected to an axial load of 4.03 kips; this corresponds to an axial stress of 8.89 ksi. During the test the external load of 4.03 kips was kept constant and maintained

in a vertical direction with the apparatus described in Section 3.3.1. However, the total axial load in the columns actually varied somewhat because the overturning effect of the lateral load produced additional compressive stress in the leeward column. Since these induced axial forces were small, the maximum being less than 0.7 kips, in comparison with the external load of 4.03 kips, the theoretical moment-curvature relationship was computed for 4.03 kips, neglecting the variations caused by the overturning effect. Even the 4.03 kips load had little effect on the moment-curvature relationship for this section.

The load-deflection curves for this frame are shown in Fig. 3.16. In the deflection calculations the moment was assumed to be linearly distributed along the columns. The linearizing of the distribution of the moment is an approximation because the axial load contribution to the total moment depends upon the deflected shape of the columns. However, after inelastic action had become extensive, the deflected shape was approximately a straight line since the curvature was concentrated predominately at the ends. For this reason, the deflections of the frame calculated from the linear moment distribution were nearly identical to those which would have been obtained if the actual deflected shape of the columns were used in the computation of the moments. With the above approximation it was possible to compute a load-deflection curve for frame No. 2 by considering a cantilever beam, 1/2 the column height in length, loaded by a concentrated lateral force and an axial force of 4.03 kips applied at the end. The deflection of the frame is twice that of this beam for twice the lateral force.

The lateral elastic limit load and deflection for the sections used in the frame without axial loads were 0.824 kips and 0.058 in., respectively, based on a 35.5 kip yield stress. The maximum load was approximately 1.68 times the yield load, and the deflection at the maximum load was approximately 12 times the yield deflection.

If there were no strain-hardening, the maximum lateral load would have been approximately 1.13 times the elastic limit lateral load for the frame without axial load, since the contribution of the axial loads to the moments is negligible for deflections in this range. The maximum lateral force which was resisted by the axially-loaded frame was increased by strain-hardening; however, the increase was much less than that for frame No. 1, which carried no axial loads. This occurred because, in order to develop the increased strength resulting from strain-hardening, the frame had to resist additional moments resulting from the large deflections and axial loads. In a frame with axial load the large deflections produce additional moment because of the corresponding eccentricity of the axial load. For axial loads as great as those in this test the amount of additional moment caused by the eccentricity of the axial loads was nearly as great as the amount of increased strength resulting from strain-hardening; therefore, the maximum load capacity did not increase greatly because of strain-hardening.

The strain-hardening was important, however, because it did increase the energy absorbed by the frame before collapse; the observed collapse deflection was approximately 73 times the yield deflection.

By taking strain-hardening into account, one obtains a predicted collapse deflection approximately 80 times the yield deflection. Had a stress-strain relationship with no strain-hardening been used, the predicted deflection at collapse would have been only approximately 39 times the yield deflection. Thus, it is apparent that the energy-absorbing capacity of the frame is greatly increased by strain-hardening of the material. This fact is especially important in the consideration of loadings to cause total collapse of frames.

It is important to note also that, after the maximum lateral resistance had been reached, the theoretical load-deflection response was above the observed response. This suggests that a reduction of capacity, because of local buckling, may be accentuated by the axial load.

The final deflected shape of frame No. 2 can be seen in Fig. 3.17.

3.7 FRAME TESTS IN THE STRONG DIRECTION

3.7.1 Frame No. 3

The average stress-strain curve shown in Fig. 3.3 was used to determine the response of frame No. 3. The induced axial loads resulting from the overturning effect of the lateral load varied from 0 at the beginning of the test to 4.1 kips at a deflection of 50 times the yield deflection. Account was taken of the effect of these axial loads on the moment-curvature relationships which were used to determine the theoretical deflections.

Shear stresses were large, with a maximum of 30 ksi, in this test. Hall[4] has determined the shear-detrusion curve for a specimen

of ASTM A-7 steel. With this information, the additional deflections caused by shear deformations were considered. The load-deflection relationships both with and without consideration of shear deformation are compared in Fig. 3.18 to the observed responses. In this figure, the values of P_e and δ_e are those for no axial loads. The comparison shows that the observed loads are less than the theoretical load at the same deflection. Since the stiffening effect of the boundary on the moment-curvature relationships and the load-deflection relationship was observed in the strong direction beam-column tests it can be expected that the observed response for this frame would also lie above the theoretical relationship which did not take the stiffening into account. This difference in behavior between the beam-column and corresponding frame test was caused, to a great extent, by the difference in the restraint against twisting and lateral buckling that each type of test provides. In the beam-column testing apparatus, the tension flanges were held in line to prevent twisting and lateral buckling at points 7.5 in. apart while this distance was increased to 15 in. in the frame specimens.

The drop in lateral load which occurred after a deflection of 50 times the yield deflection is attributed to twisting and local buckling of the columns aggravated by a tearing of the flange material at the edge of the heat-affected zone of the welding. The picture of the final deflected frame, in Fig. 3.19, shows the buckling, twisting, and rupture that occurred.

3.7.2 Frame No. 4

Frame No. 4 was similar to frame No. 3 with the exception that all joints in frame No. 4 were brazed together. The stress-strain relationships for the columns used in this frame are shown in Fig. 3.3. Axial loads of 4.03 kips, or 8.73 ksi, were applied to each of the columns of the frame in addition to the lateral load. The same lateral restraining system that was described in Section 3.3.1 was used for this frame.

The theoretical load-deflection of this frame is compared in Fig. 3.18 to the observed load-deflection relationship. The curves show that the observed load is smaller than the theoretical load. However, if the resistance of the frame to lateral load is considered to be that observed in the test of frame No. 3, the observed response of frame No. 4 can be predicted quite accurately. Figure 3.20 shows this comparison. Since frame No. 4 was completely of brazed construction, there was no tearing of the flanges near the weld as there was in frame No. 3; this accounts for the fact that the load capacity obtained from frame No. 3 decreases rapidly after deflections of approximately 70 times the elastic limit deflection. It is believed that the response would follow the dashed line in Fig. 3.20 if the tearing had not occurred in frame No. 3. By observing the load-deflection curves, it can be reasoned that the effect of axial loads was to reduce the moment capacity of the members of the frame only slightly. The same phenomenon was found in the weak direction tests. As an approximation, the small reduction can be neglected, and the effect of the axial loads needs to be taken into account only in the calculation of primary forces acting on the frame.

Apparently the mode of failure of these frames was not significantly changed by the addition of axial forces. If the mode of failure for columns with and without axial loads is found to be the same for all structural shapes, the problem of predicting the response of axially-loaded sections can be reduced to a study of the simple non-axially-loaded case.

3.8 CONCLUSIONS

Good agreement between the theoretical and the observed load-deflection and moment-curvature response was found for beam-column and frame specimens tested in the weak direction of resistance. This agreement indicates that the assumptions listed in the Introductory Statement are reasonable approximations when the short-time static response is desired for laterally-loaded frames tested in the weak direction.

The tests of columns oriented in the strong direction did not show agreement as good as that found for the weak direction tests. The observed load for these tests was considerably less than the theoretically predicted loads for corresponding deflections. Figures 3.15 and 3.18 show a comparison between the observed and theoretical response.

It was observed in both the strong and weak direction tests that the mode of failure was nearly the same for frames with or without axial loads on their columns. This is significant because if it is true for the ordinary rolled sections, the action of axially-loaded members will be known from a study of non-axially-loaded members.

There was no significant difference in the behavior of a centrally-loaded beam-column specimen and a fixed-ended, laterally-loaded frame

when the specimens were loaded in the weak direction of resistance. There was, however, considerable difference between the responses found for the strong direction specimens. It is believed that the cause of this discrepancy lies in the differences in restraint provided against buckling and twisting. Since the restraints in the beam-column tests were higher than those for the corresponding frame, the resistance was also greater.

The effect of strain-hardening on the response of the structures was considered also in this study. Strain-hardening increased the energy-absorbing capacity of all frames tested, by increasing the maximum lateral load and, in the case of the frames with high axial loads, increasing the collapse deflection.

The collapse deflection for the weak direction frame was predicted with considerable accuracy by considering strain-hardening. The load-deflection response in the strong direction of resistance, however, was not predicted as well as that in the weak direction since twisting, combined with the local buckling occurred.

The load-deflection results show that the moment resistance for a particular curvature was not appreciably affected by axial loads. The observed load corresponding to a given deflection was found to be slightly lower than that which would be predicted even when the effect of the thrust on the moment-curvature relationship is taken into account. Some of this discrepancy can be attributed to the assumption of linearly distributed moments along the length of the column. The analysis, however, would be complicated considerably by the introduction of a

refinement in the distribution of moments and it is thought that the procedures outlined were sufficiently precise.

3.9 BIBLIOGRAPHY

1. American Society for Testing Materials, "ASTM Specifications for Rolled Structural Steel," Philadelphia, Pa., (1952).

2. American Institute of Steel Construction, "Steel Construction Manual," New York, 5th Ed. (1952).

3. Munz, R., "Static Tests to Failure of Steel Beam-Columns," M. S. Thesis, University of Illinois, Department of Civil Engineering, (1954).

4. Newmark, N. M., "Numerical Procedure for Computing Deflections, Moments, and Buckling Loads," Transactions ASCE, Vol. 108, pp. 1181-1234, (1945).

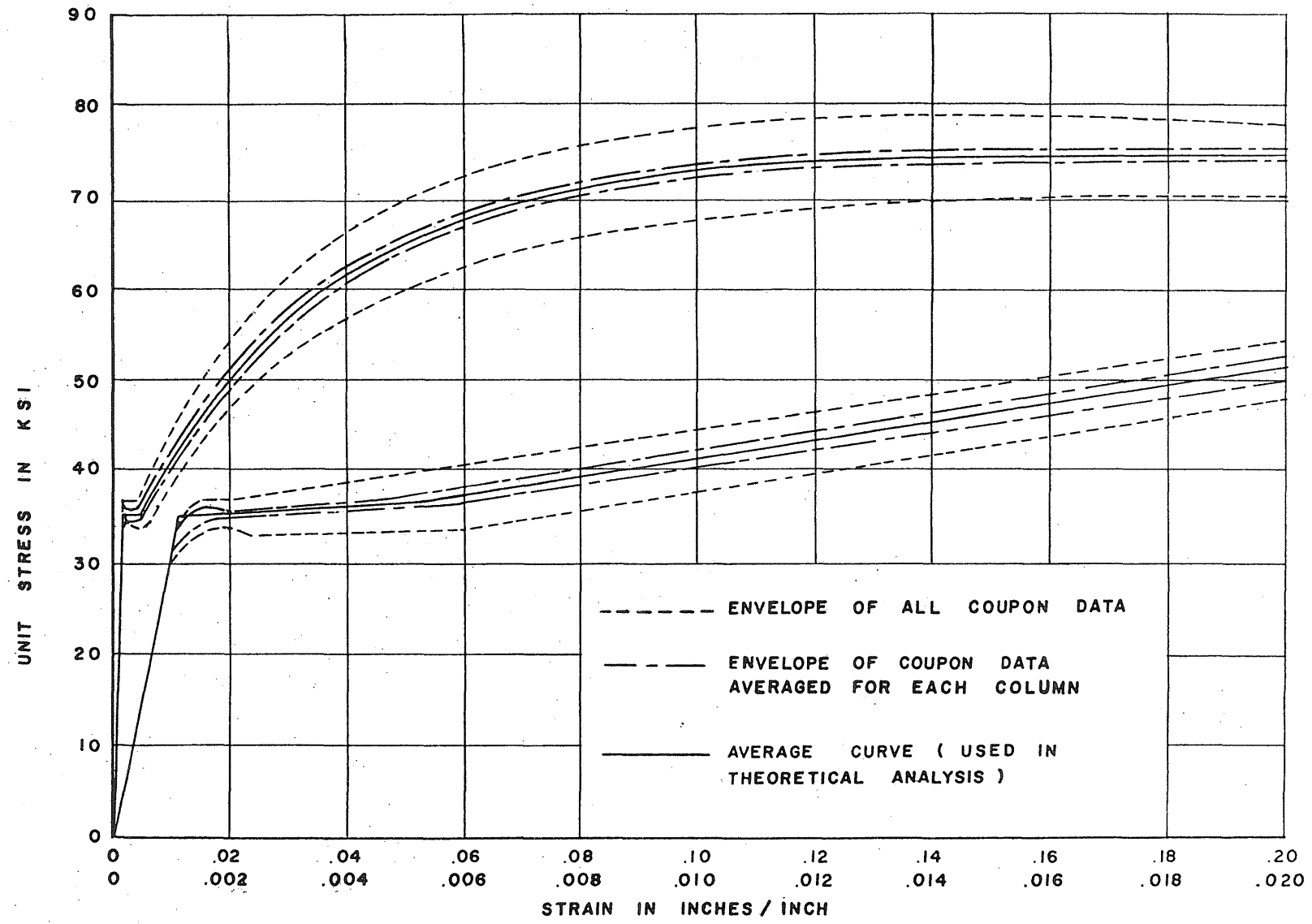

FIG. 3.1 STRESS—STRAIN RELATIONSHIPS FOR COLUMNS 1, 2, 3, 4, 8, & 11

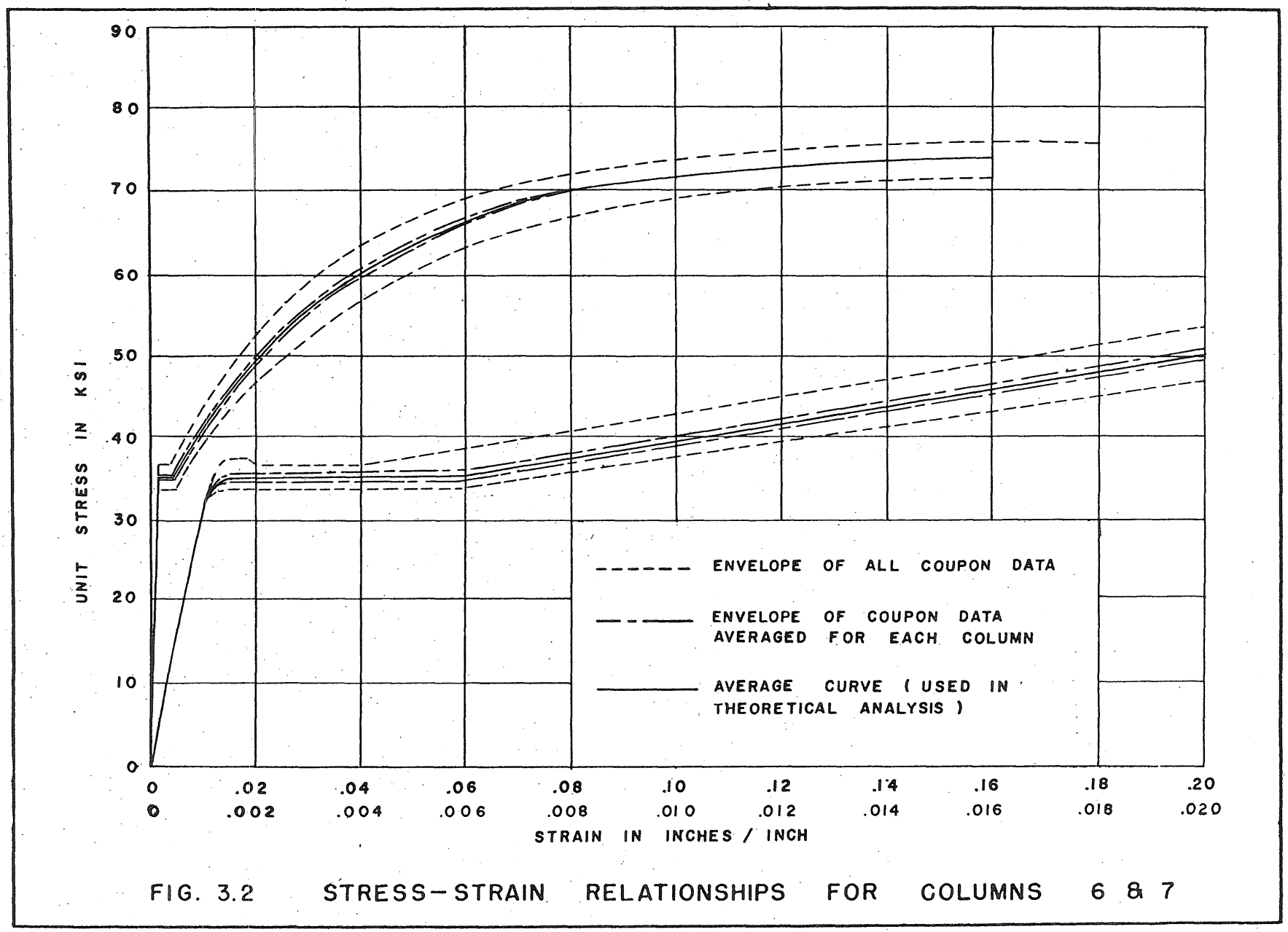

FIG. 3.2 STRESS–STRAIN RELATIONSHIPS FOR COLUMNS 6 & 7

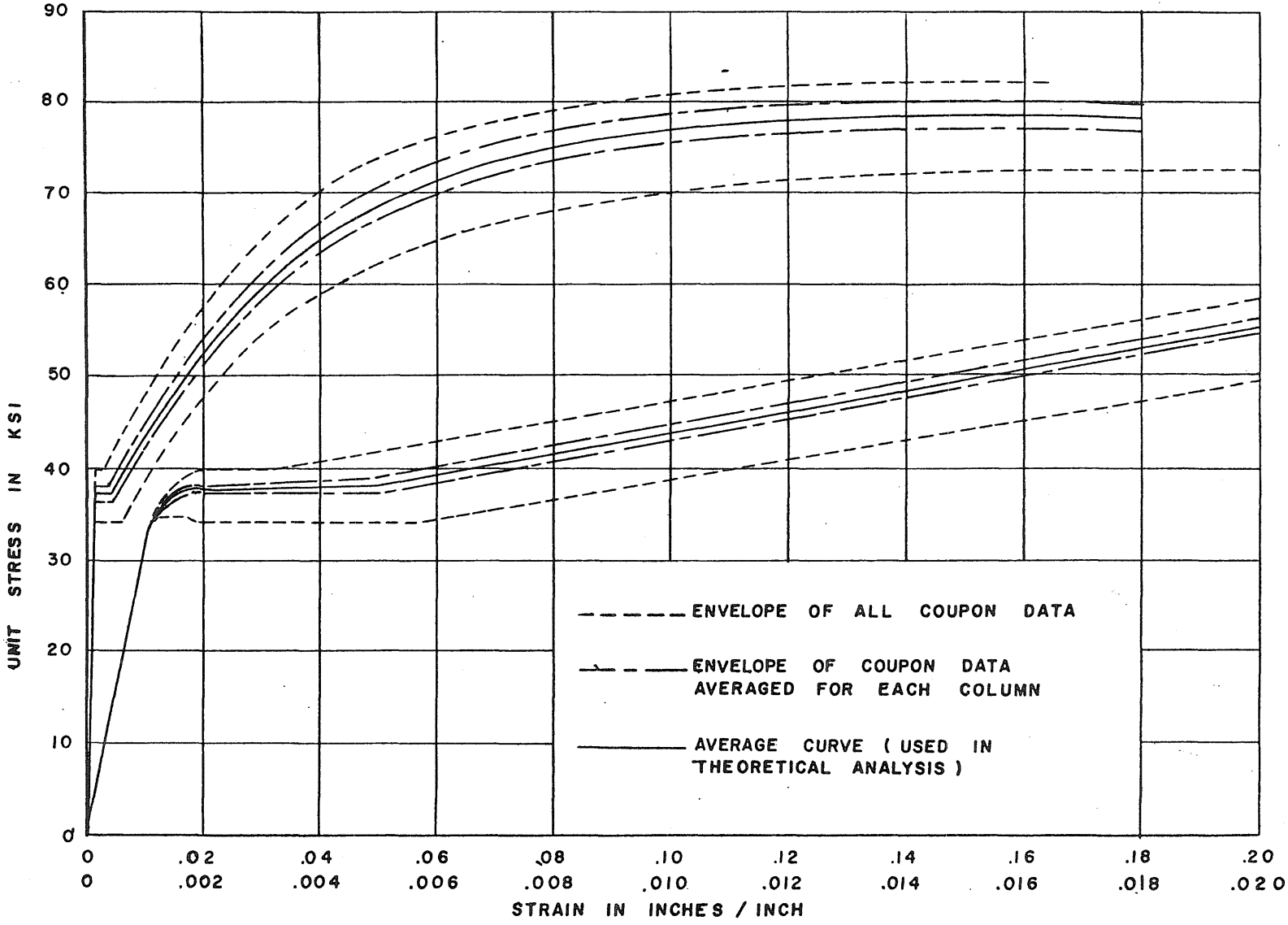

FIG. 3.3 STRESS-STRAIN RELATIONSHIPS FOR COLUMNS 18, 20, 21, & 23

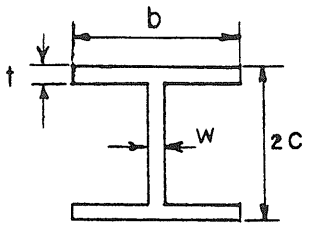

COLUMN NUMBER	b"	2c"	t"	w"
SPECIMENS TESTED IN WEAK DIRECTION				
1,2,3,4	1.520	1.592	0.114	0.080
8,11	1.520	1.602	0.112	0.080
SPECIMENS TESTED IN STRONG DIRECTION				
6,7,20,23	1.523	1.606	0.114	0.080
18, 21	1.520	1.605	0.116	0.080

FIG. 3.4 DIMENSIONS OF SECTIONS

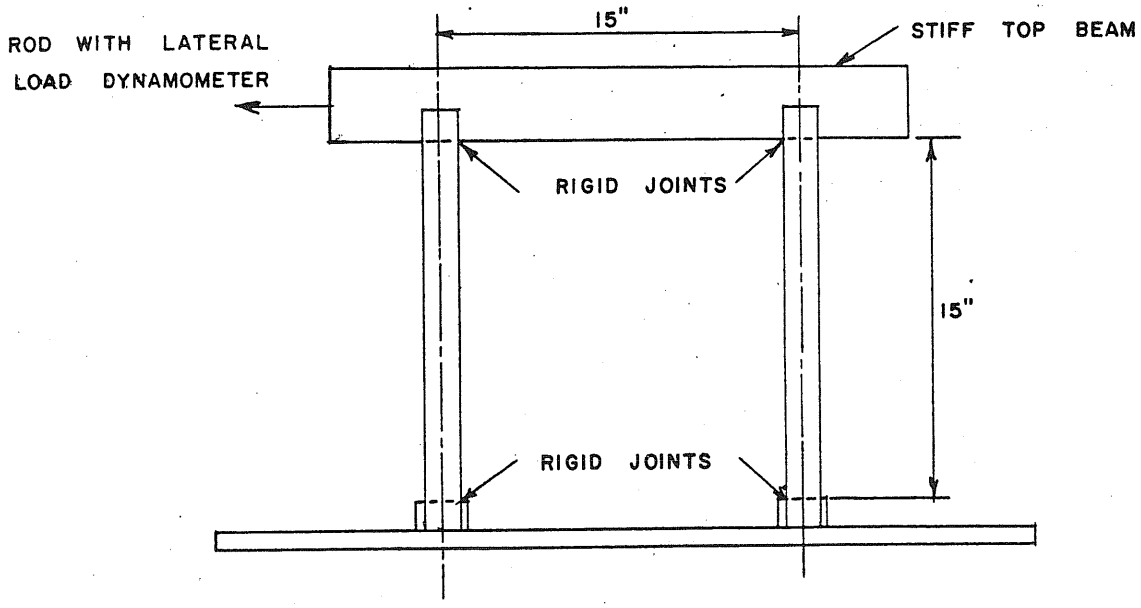

FIG. 3.5 DIMENSIONS OF FRAMES

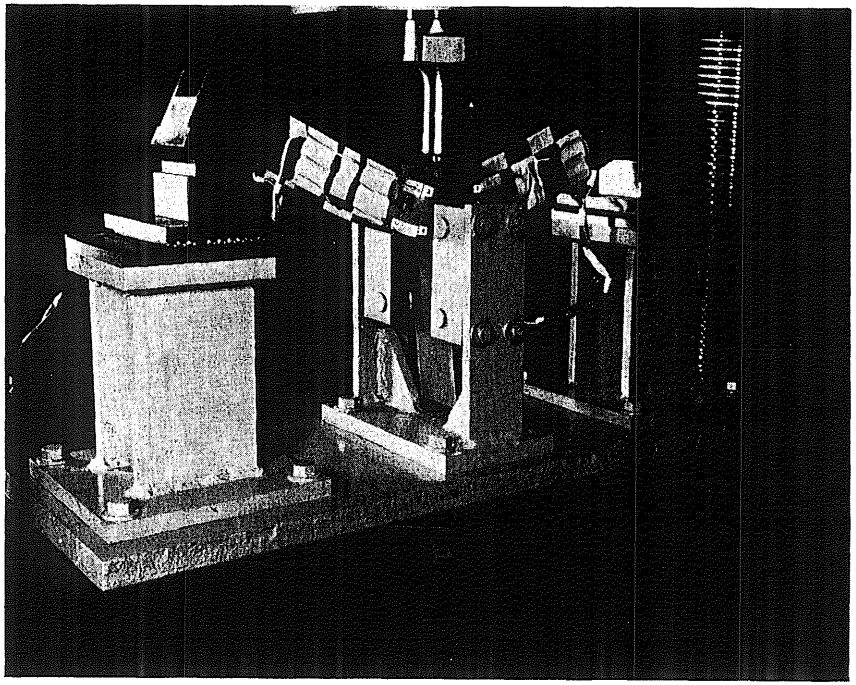

BEAM-COLUMN NO. 4 (CENTER LOAD)

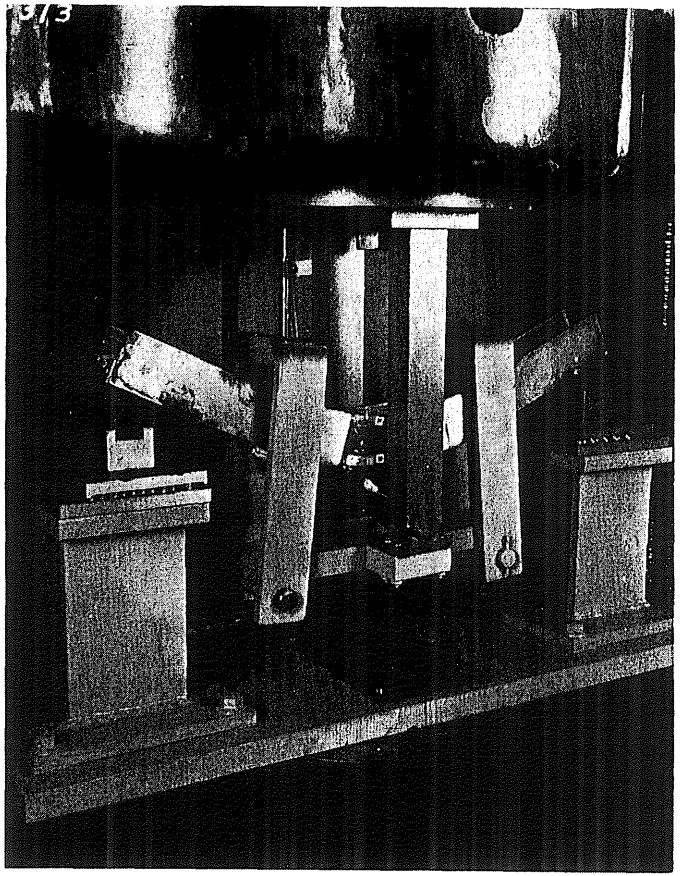

BEAM-COLUMN No. 1 (PURE MOMENT)

FIG. 3.6. BEAM-COLUMNS NO. 1 AND 4 IN TESTING POSITION

FRAME NO. 1
CONNECTION TO
RIGID BEAM

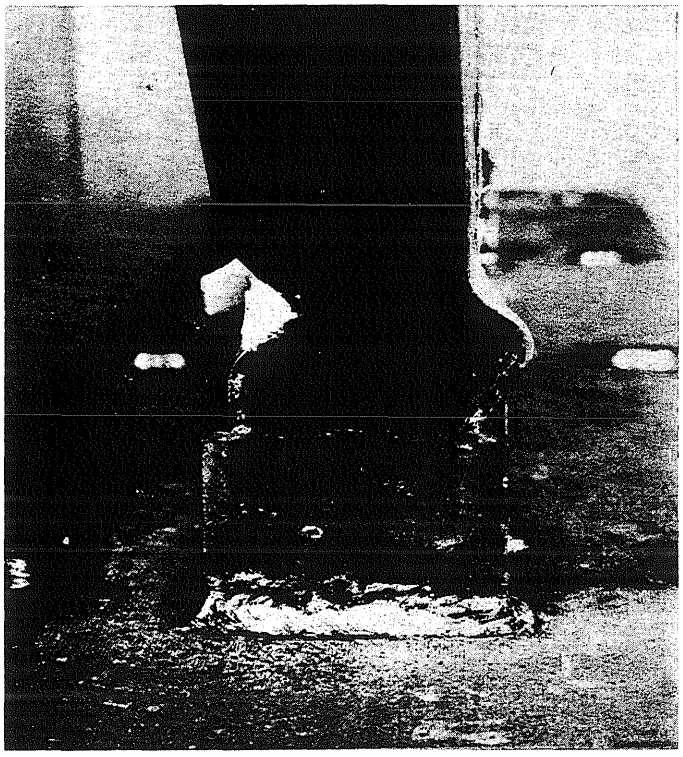

FRAME NO. 1
CONNECTION TO
BASE PLATE

FIG. 3.7. WEAK DIRECTION CONNECTIONS

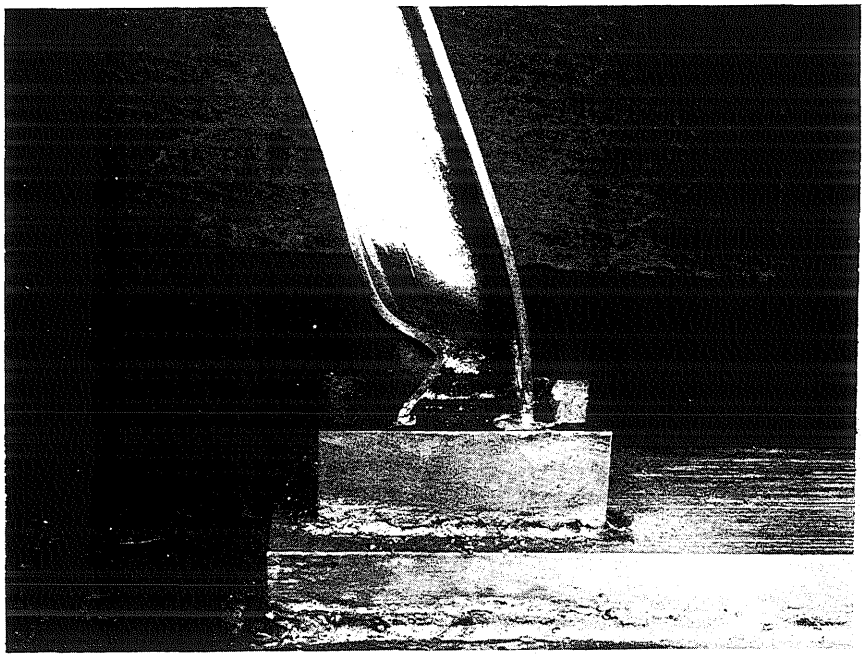

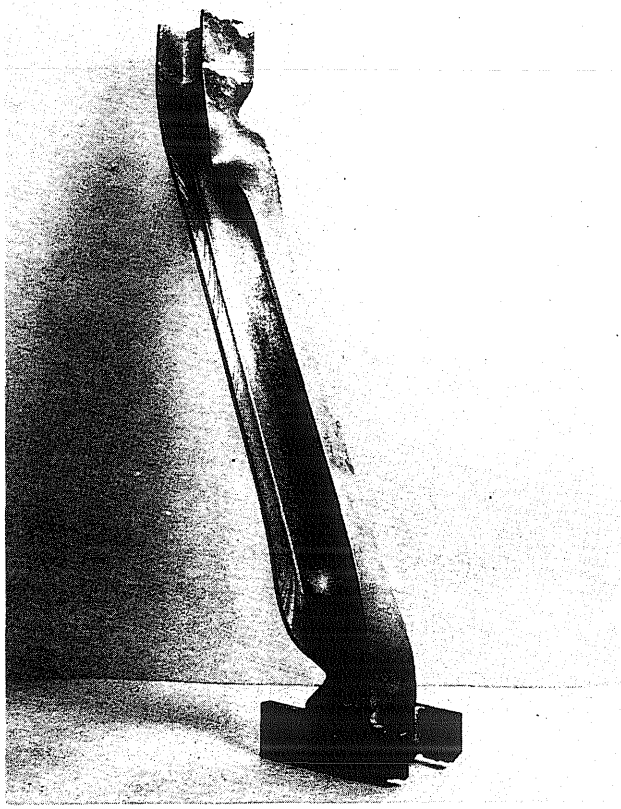

FIG. 3.8 STRONG DIRECTION CONNECTIONS

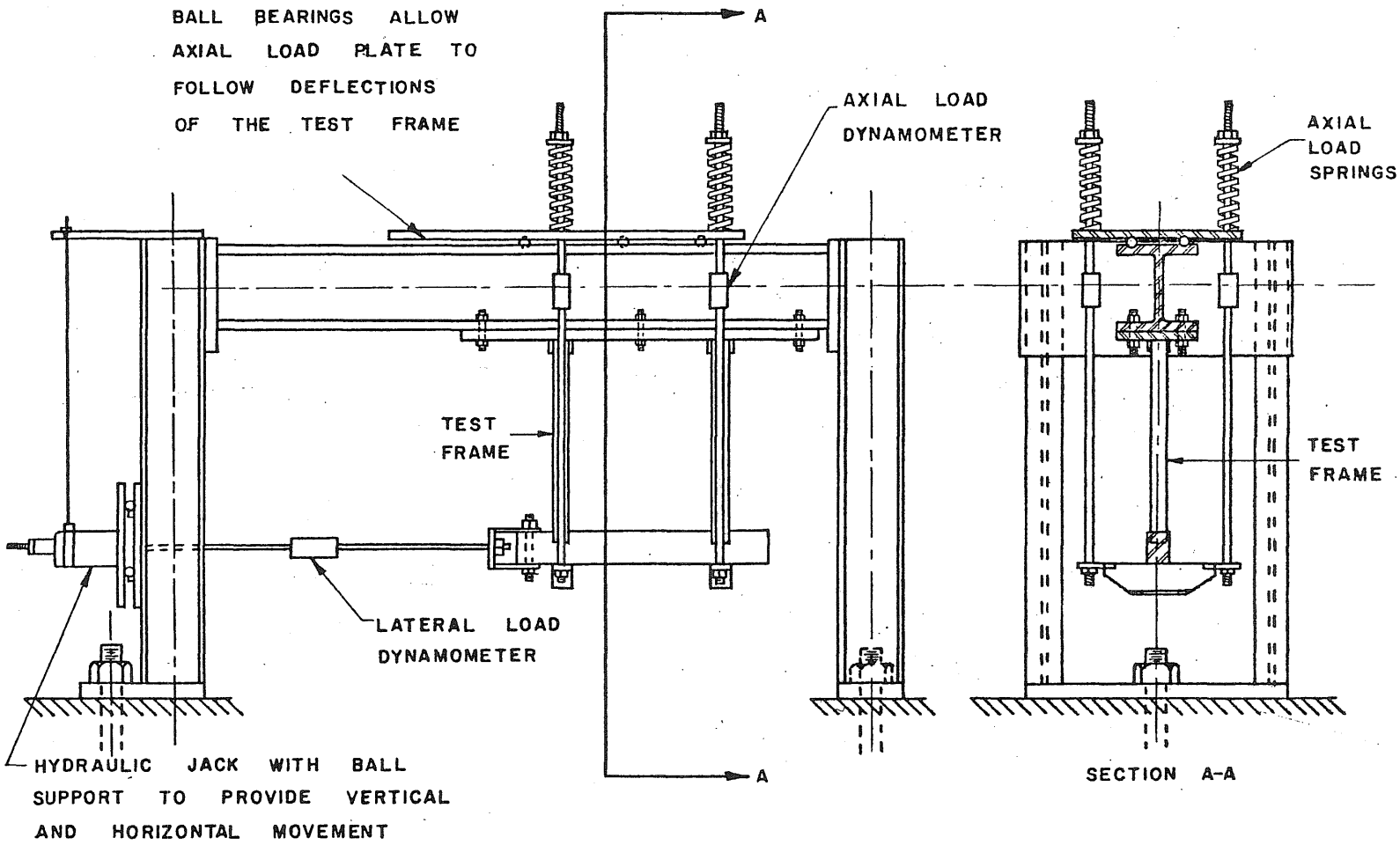

FIG. 3.9 FRAME TESTING APPARATUS

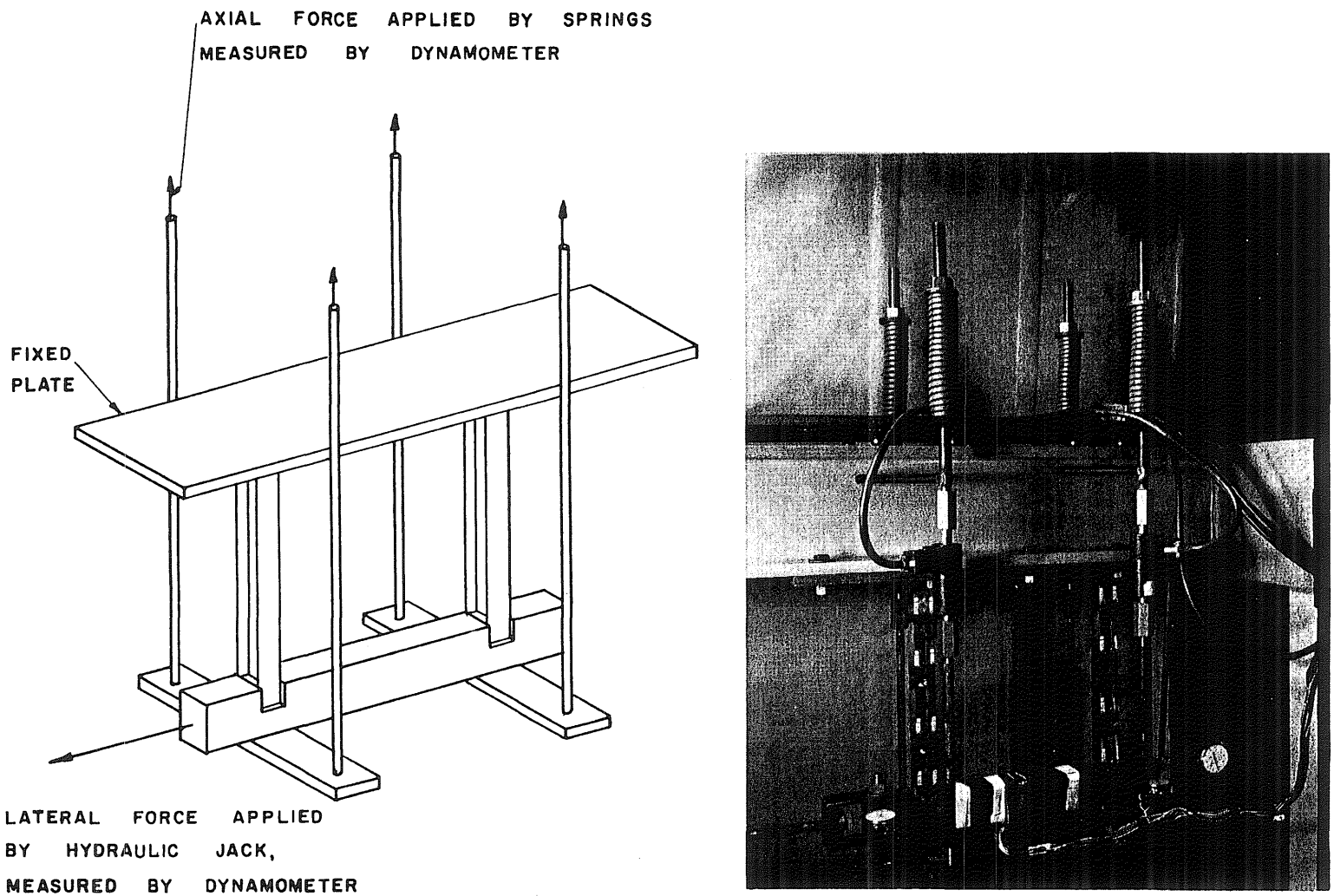

FIG. 3.10. DETAILS OF LOADING APPARATUS

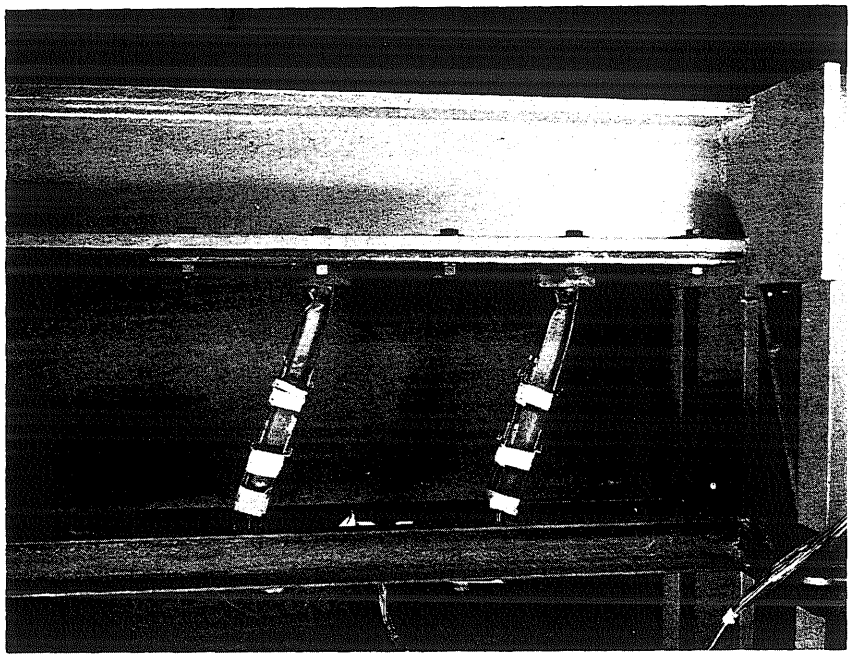

FIG. 3.11 LATERAL RESTRAINT SYSTEM

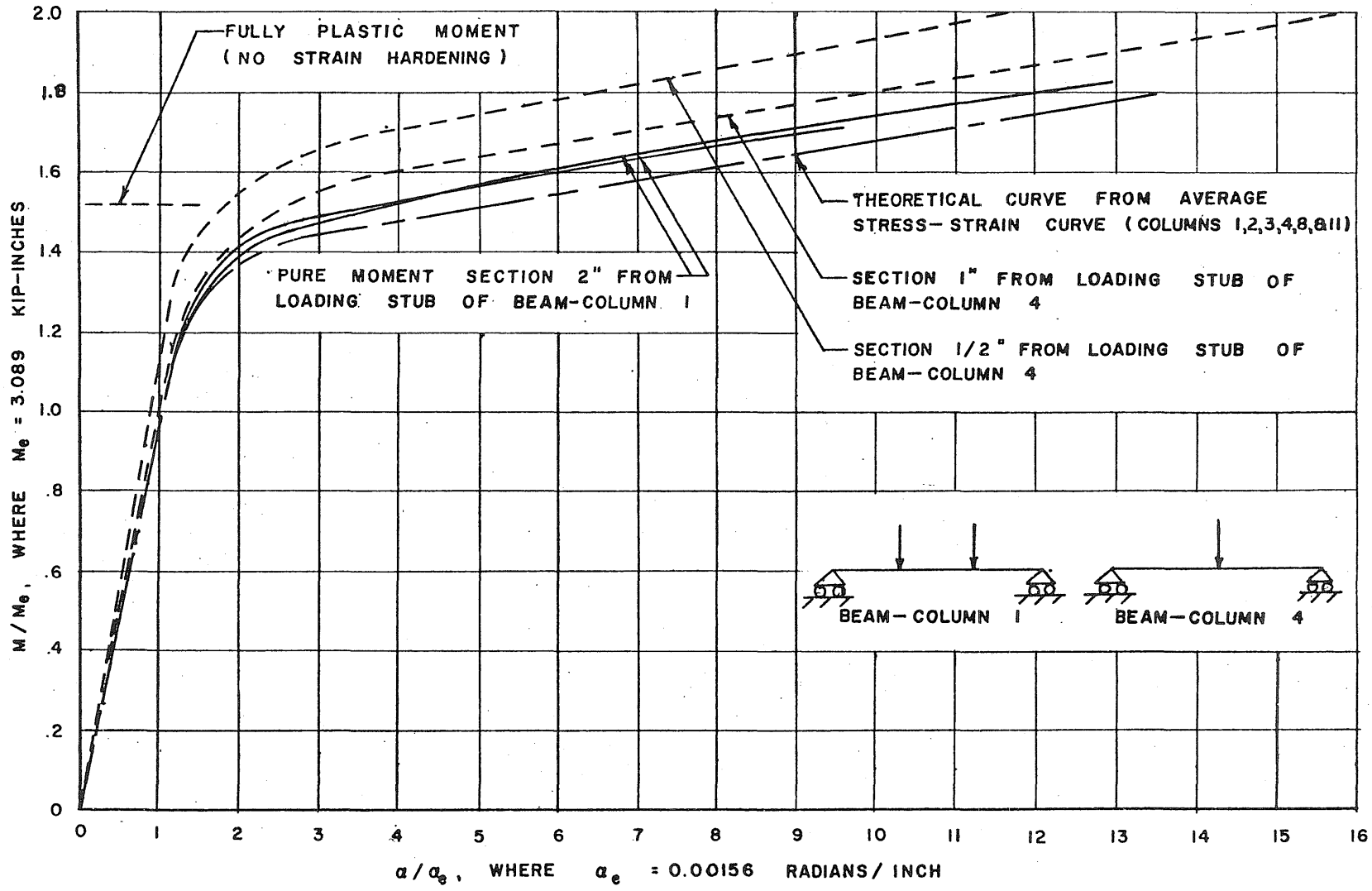

FIG. 3.12 DIMENSIONLESS MOMENT-CURVATURE RELATIONSHIPS FOR THE WEAK DIRECTION OF RESISTANCE

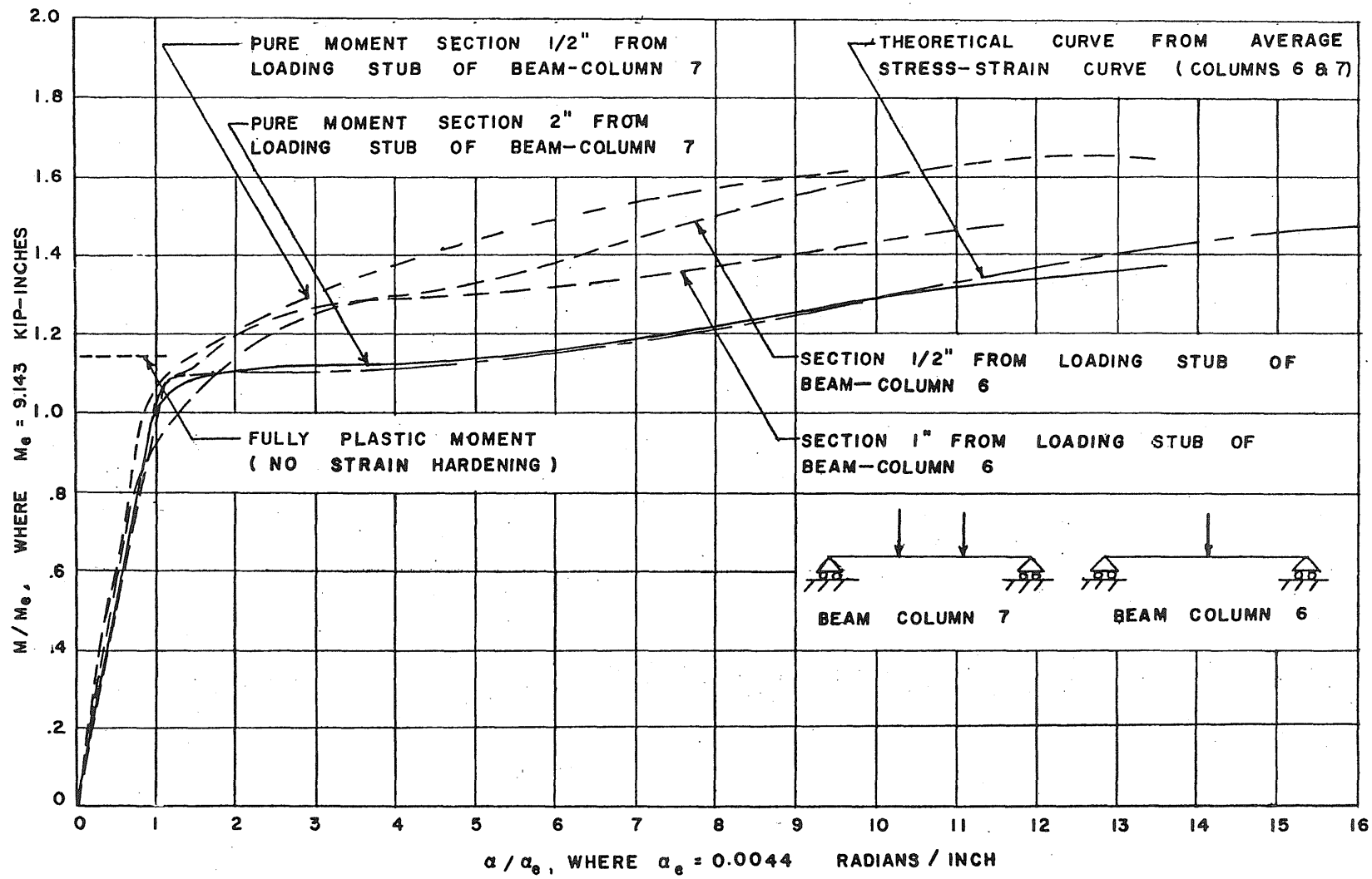

FIG. 3.13 DIMENSIONLESS MOMENT-CURVATURE RELATIONSHIPS FOR THE STRONG DIRECTION OF RESISTANCE

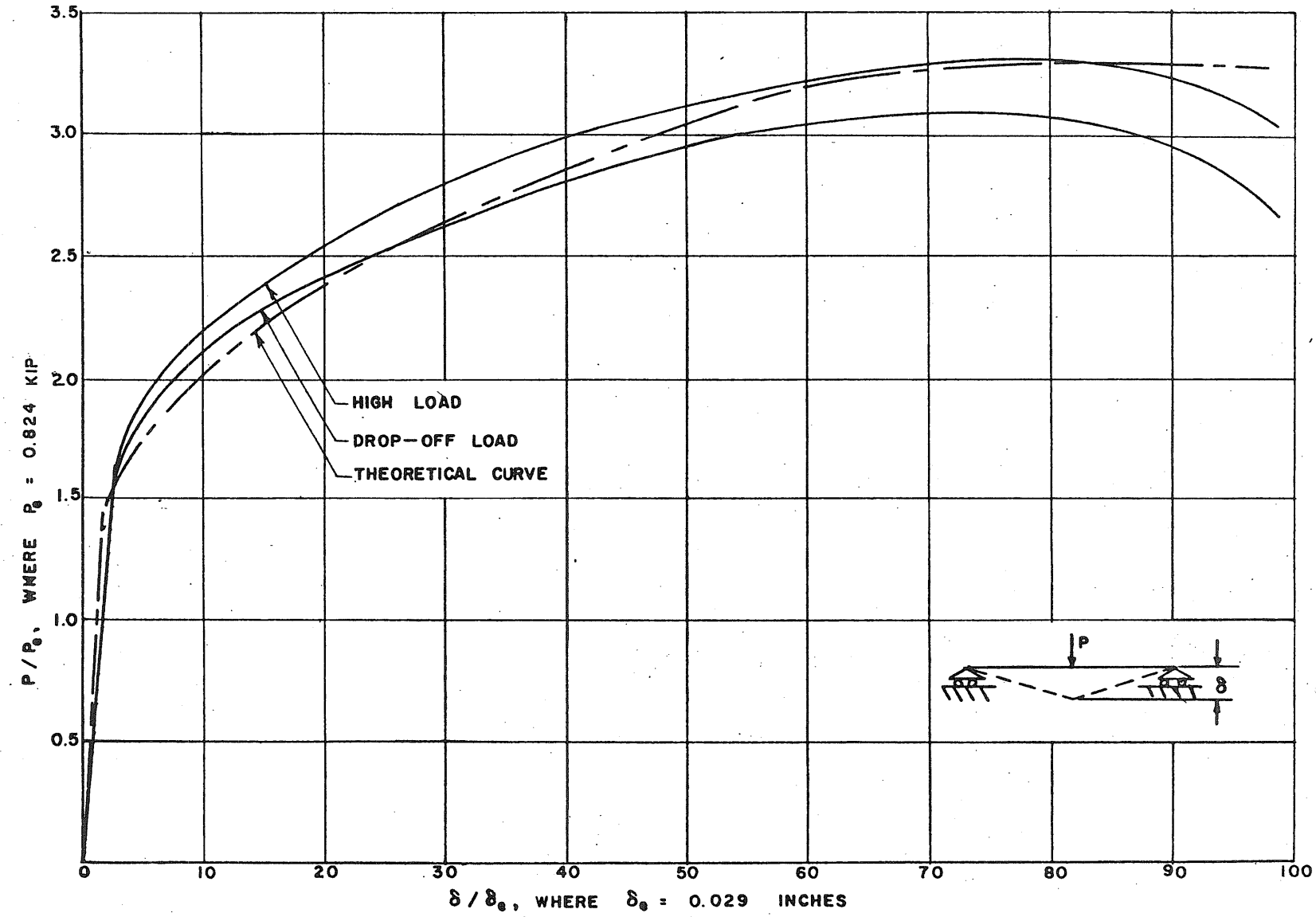

FIG. 3.14 DIMENSIONLESS LOAD-DEFLECTION CURVES FOR BEAM—COLUMN NO. 4

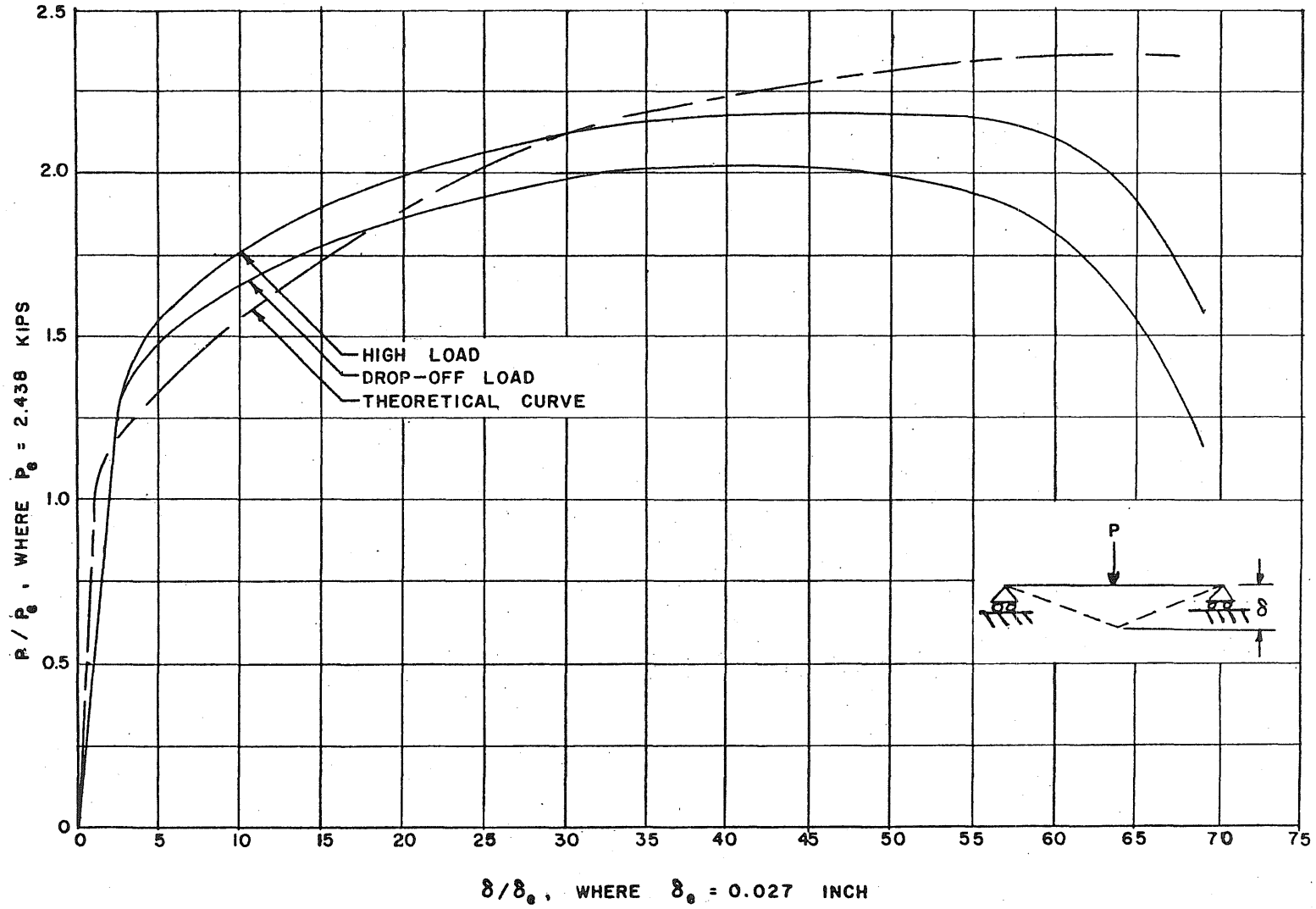

FIG. 3.15 DIMENSIONLESS LOAD—DEFLECTION CURVES FOR BEAM-COLUMN NO. 6

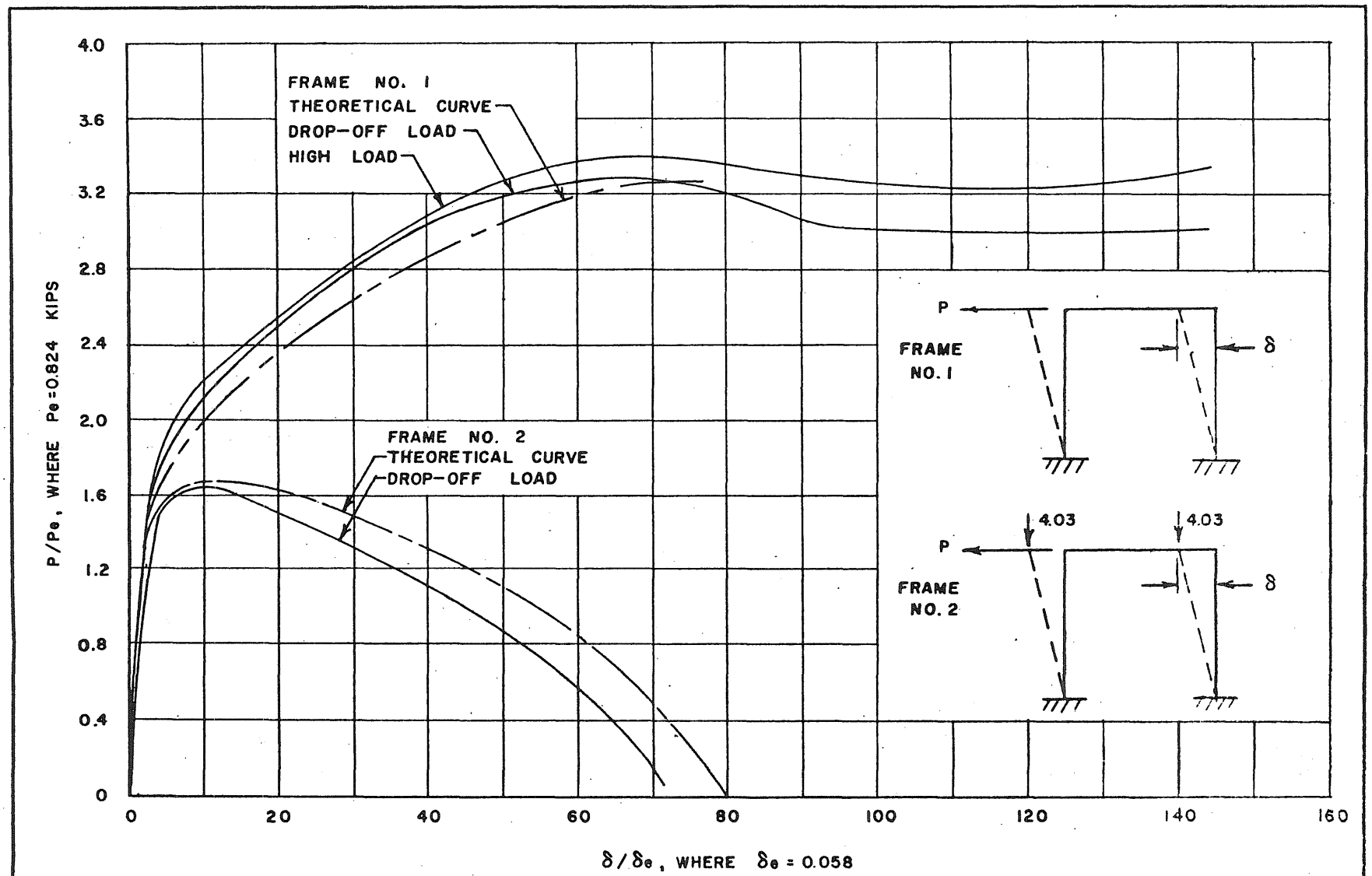

FIG. 3.16 DIMENSIONLESS LOAD-DEFLECTION CURVES FOR FRAMES NO. 1 AND 2

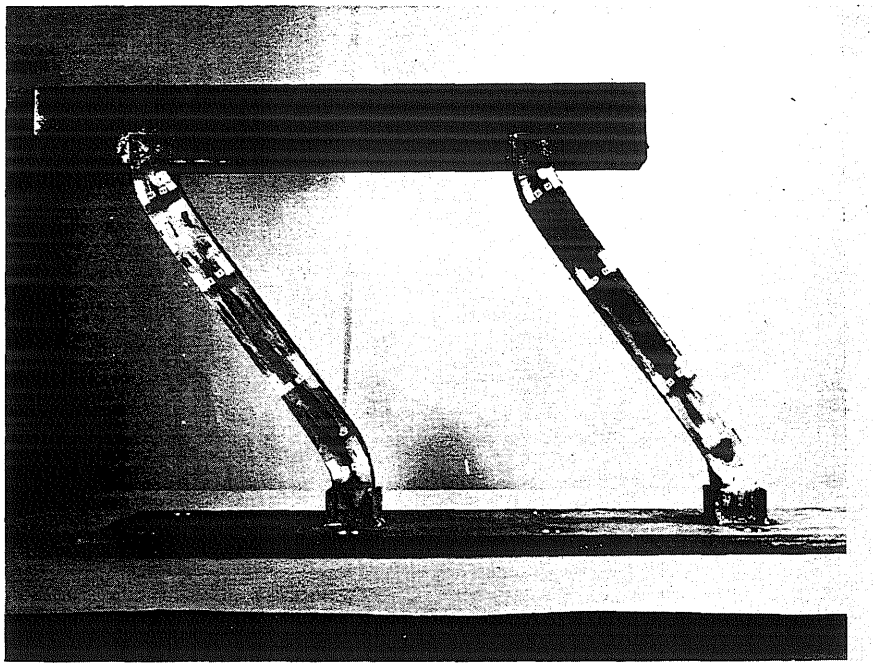

FRAME NO. 1

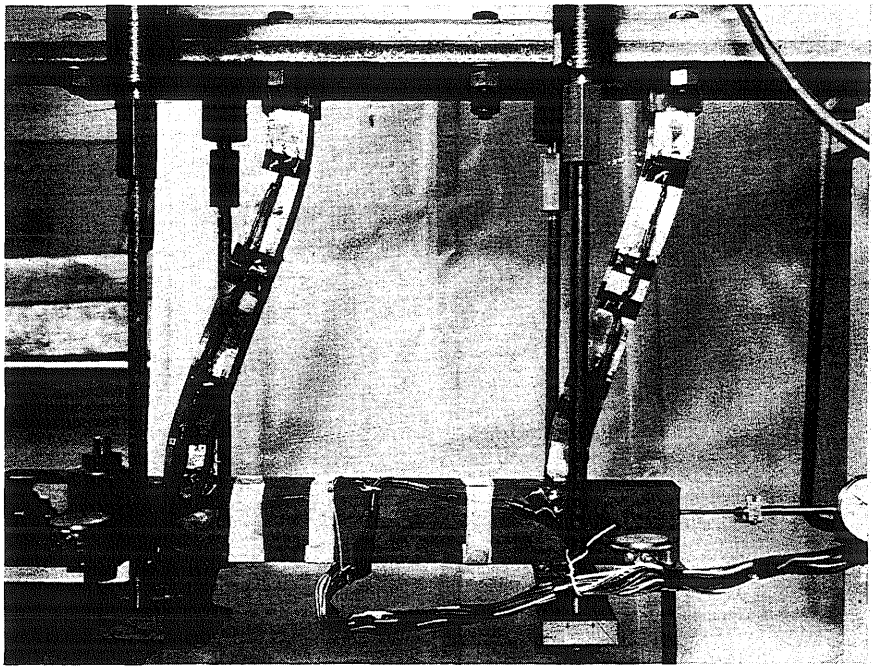

FRAME NO. 2

FIG. 3.17. FINAL DEFLECTED SHAPE OF FRAMES NO. 1 AND 2

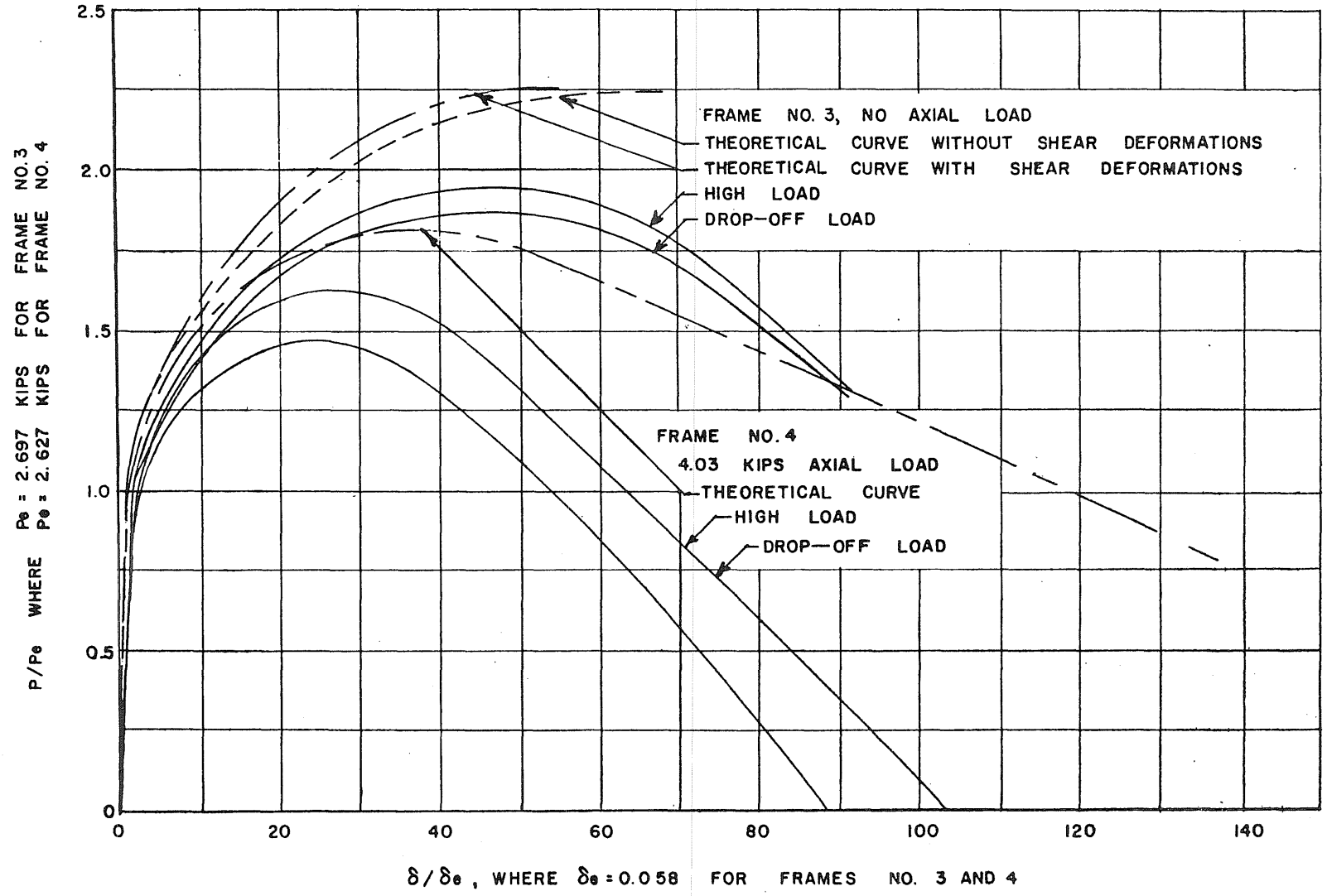

FIG. 3.18 DIMENSIONLESS LOAD-DEFLECTION CURVES FOR FRAMES NO. 3 AND 4

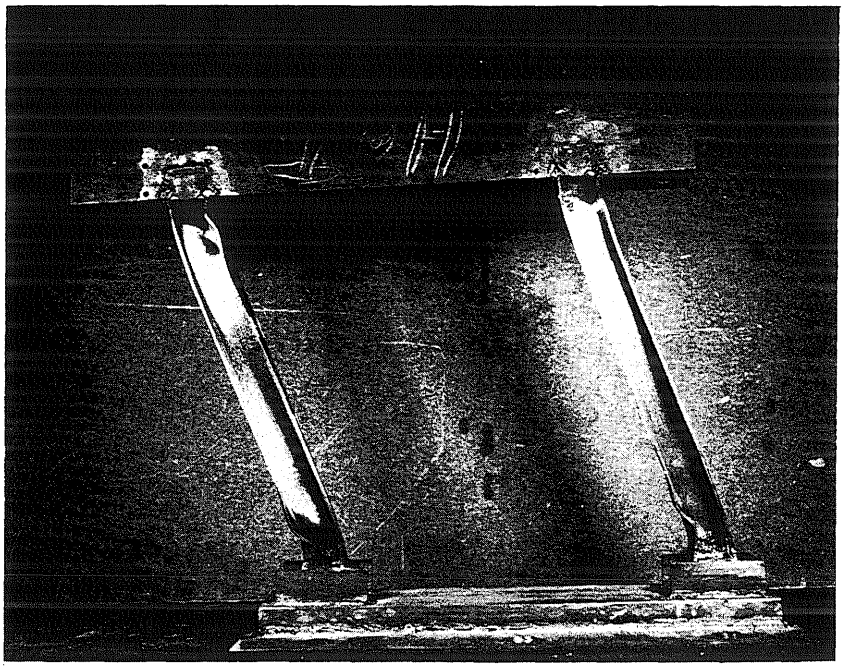

FRAME NO. 3

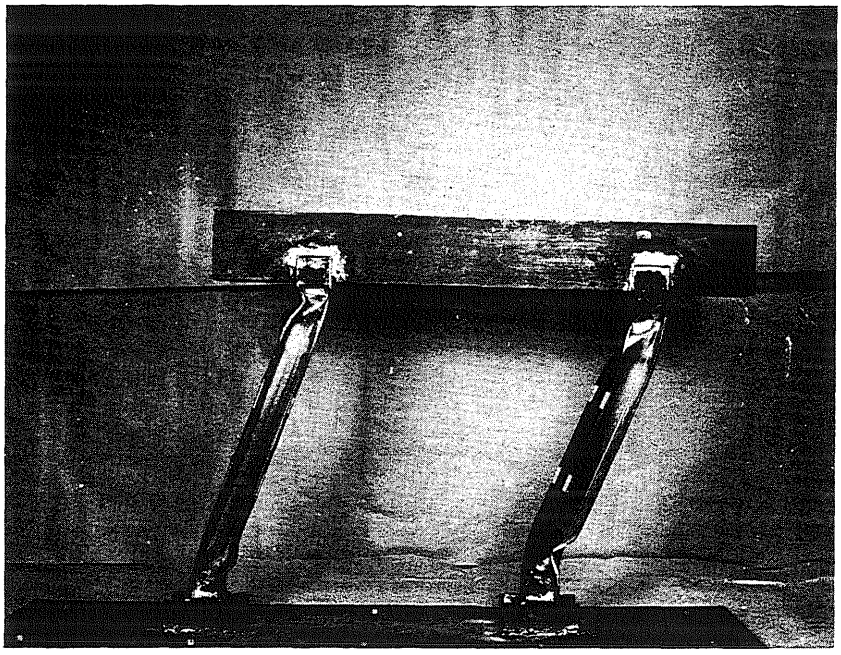

FRAME NO. 4

FIG. 3.19 FINAL DEFLECTED SHAPE OF FRAMES NO. 3 AND 4

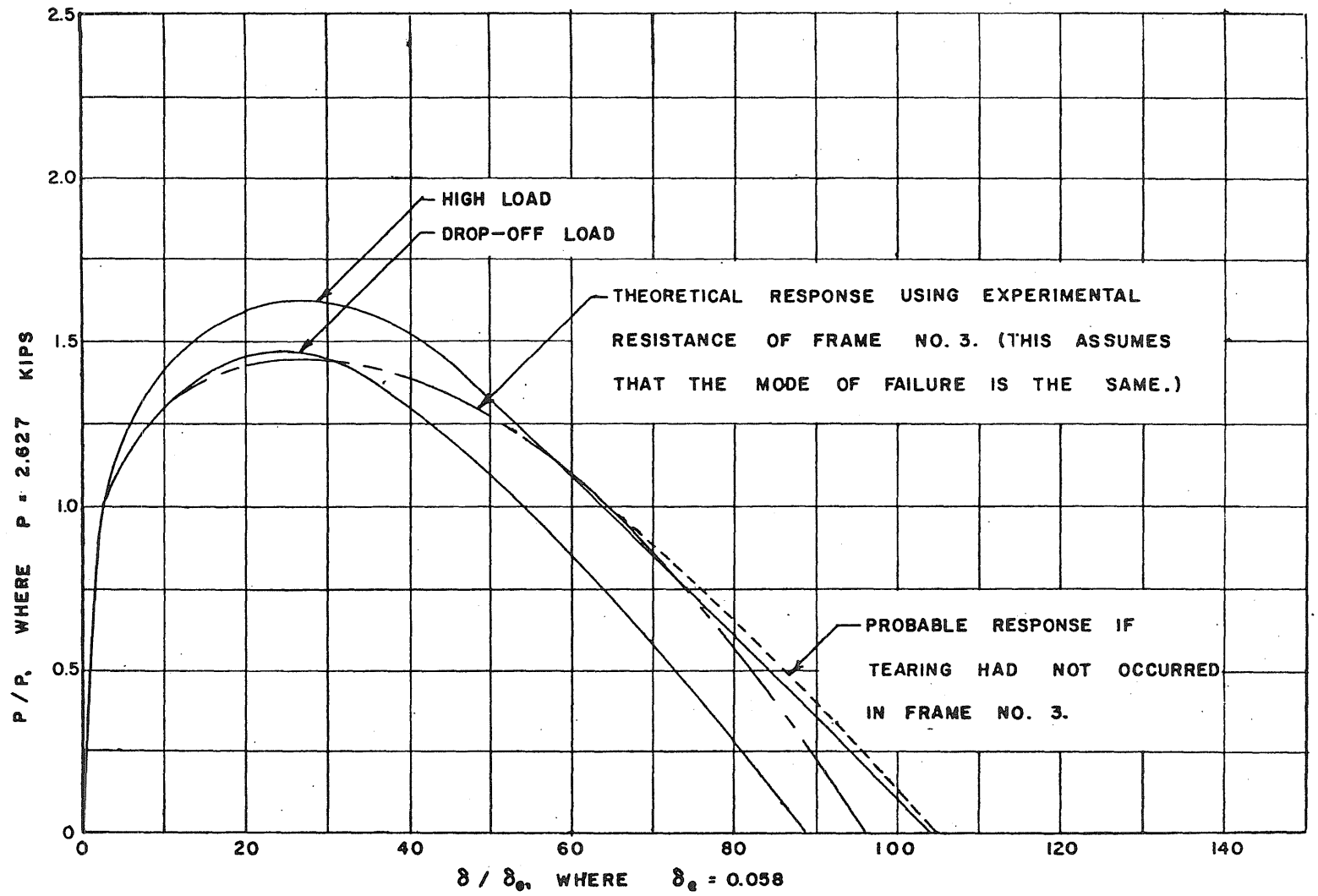

FIG. 3.20 DIMENSIONLESS LOAD–DEFLECTION CURVES FOR FRAME NO. 4

4. STATIC OBLIQUE LOADING TESTS OF STEEL BEAM-COLUMNS

4.1 INTRODUCTION

The elastic load-deflection response of a member subjected to a static lateral load not in the direction of a principal axis has been treated in many references[4]*. However, very little work has been done on the inelastic response to a static oblique load, the major sources being the theoretical and experimental results for rectangular and triangular sections presented in a paper by H. A. Williams[5] and a thesis by B. W. Anderson[1].

In the present report a method of analysis is presented for the determination of the load-deflection response of rolled I or WF beams subjected to obliquely applied lateral loads which result in inelastic deformation. The prediction of the response is approached through the use of relationships between the moments about the principal axes for specific neutral axis positions and moment-curvature relationships for these neutral axis positions. The analysis is based on the following assumptions:

(1) The stress-strain curve of the material can be represented by two straight lines which neglects the strain-hardening of mild steel.

(2) The strains are distributed linearly across the section.

(3) The effect of shear is negligible.

(4) The curvatures are in accord with the small deflection theory.

---

* Numbers in parentheses refer to correspondingly numbered entries in the Bibliography at the end of this section.

(5) The torsional moment can be neglected.

Since the analysis is cumbersome, an attempt was made to simplify it by neglecting the web of the section. The results obtained using this approximation differed considerably from the results obtained when the web was included.

The experimental portion of the investigation consisted of two tests of beams with an as-rolled 6 B 15.5 section. In order to simplify the apparatus the specimens were restrained so that the deflection was essentially in one direction, at 45 degrees to the principal axes. As a result of this restraint condition the direction of lateral loading changed throughout the tests.

One specimen was loaded only laterally and the other was loaded both laterally and with a constant axial thrust of approximately 65 per cent of the AISC allowable. The results obtained from these two tests are compared with the results obtained from tests of specimens loaded in the strong and weak directions of resistance.

The experimental load-deflection relationship of the specimen without axial load is compared with the theoretical curve. The difference between the two curves is of the same magnitude as has been reported elsewhere for members loaded in the strong and weak directions of resistance. However, because the theory does not include strain-hardening of the material, the analysis only covers 12 per cent of the total range of deflections. For deflections greater than this, it is possible that strain-hardening of the material will significantly affect the load-deflection relationship. However, the development of local failures

will, in all likelihood, tend to reduce the influence of the strain-hardening and the response of the structure will be between that given by the elasto-plastic theory, which neglects strain-hardening, and the response obtained assuming strain-hardening of the material. This problem is now being considered.

4.2 ANALYTICAL INVESTIGATION

4.2.1 Introduction

The theoretical static load-deflection relationship or the static response of obliquely loaded I or WF beams in the inelastic range has been obtained from a moment-curvature relationship. Since the deflection of the beam will, in all likelihood, have a component perpendicular to the plane of loading, a torsional moment will exist, changing the direction of loading with respect to fixed coordinates in the cross-section. In this analysis, the torsional effect is neglected; consequently, the direction of loading is constant and only one moment-curvature relationship is necessary for any specific direction of loading.

In order to compute the magnitude of the deflection by numerical integration, the direction of the curvature must be known as well as the moment-curvature relationship. For beams loaded in the principal planes of the cross-section the direction of the deflection is known. For an obliquely loaded beam in the elastic range, the direction of the deflection is related to the principal moments of inertia of the section and the direction of loading. In the inelastic range this relationship may be determined by the moment interaction diagram which relates the moments about the principal axes of a section, for various neutral axis

where

σ_e = the stress at the elastic limit

ϵ_e = the strain at the elastic limit

v_e = the distance from the neutral axis to where the elastic limit strain occurs.

With this stress distribution the moments about the X and Y principal axes, assuming positive bending moments as shown in Fig. 4.1, can be determined as follows:

$$M_x = -\int_A \sigma\, y\, da$$

or

$$M_x = -\int_{A_e} \frac{-\sigma_e}{|v_e|}(y^2 \cos\varphi - xy \sin\varphi)\, da - \int_{A_p} -\sigma_e \left|\frac{v}{v}\right| y\, da$$

which can be written symbolically as:

$$M_x = \sigma_e\left[\frac{I_x^e \cos\varphi}{|v_e|} - \frac{I_{xy}^e \sin\varphi}{|v_e|} + Q_x^P\right] \qquad (2\text{-a})$$

In the same manner the moment about Y can be written:

$$M_y = \sigma_e\left[\frac{I_{xy}^e \cos\varphi}{|v_e|} - \frac{I_y^e \sin\varphi}{|v_e|} + Q_y^P\right] \qquad (2\text{-b})$$

where

M_x = the component of the resisting moment of the cross section about the X axis.

M_y = the component of the resisting moment of the cross section about the Y axis.

A = the total area of the cross section.

A_e = the area of the cross section strained elastically.

A_p = the area of the cross section strained inelastically.

I_x^e = the second moment of the elastic area about the X axis.

I_y^e = the second moment of the elastic area about the Y axis.

I_{xy}^e = the product of inertia of the elastic area.

$$Q_x^p = \int_{A_p} \frac{v}{|v|}\, y\, da$$

$$Q_y^p = \int_{A_p} \frac{v}{|v|}\, x\, da$$

For a section symmetrical about the X and Y axes these equations have the following form:

For the elastic limit case:

$$M_x^e = \sigma_e\, I_x \cos \varphi \;/\; |v_e|$$

$$M_y^e = -\,\sigma_e\, I_y \sin \varphi \,/|v_e|$$

For the fully plastic case:

$$M_x^P = \sigma_e\, Q_x^P$$

$$M_y^P = \sigma_e\, Q_y^P$$

The moment relations, in general form, are presented in Appendix B for an idealized I or WF shape composed of three rectangular elements.

4.2.3 Moment Interaction Relationships

The moment interaction diagram obtained from the equations in Appendix 4.B is shown in Fig. 4.3, in dimensionless form, for an idealized 6 B 15.5 section. The moments about the X and Y axes are divided by the elastic limit moment about the X axis (M_x^e) for which the neutral axis is coincident with the X axis. By plotting the moment interaction diagram in this way, the lines of constant resultant applied moment (M_r) take the form of circles or ellipses, depending upon the scales, and are shown in the figure.

For a constant direction of loading, represented on the diagram by a radial line from the origin, α, the angle between the direction of load the the Y axis, is given by

$$\tan \alpha = \frac{M_y}{M_x}$$

It is evident from the diagram that for a constant loading direction the neutral axis rotates in the inelastic range and that for small angles of loading, the rotation can become quite large. For instance, if a cantilever 6 B 15.5 section is loaded at 10.6 deg and the load is increased so that the maximum moment increases from the elastic limit moment to the fully plastic moment, the neutral axis at the fixed end rotates from 30 deg at the elastic limit moment to 50 deg at the fully plastic moment.

4.2.4 Moment-Strain Relationships

As a consequence of computing the moment interaction curves, the values for the moment-curvature relationship are also obtained.

The curvature is determined in a dimensionless form (v''/v''_e) and the numerical values are identical with the dimensionless extreme fiber strain values (ϵ/ϵ_e). It is more convenient to use the dimensionless strain values in the numerical integration procedure since the elastic limit strain is a constant quantity whereas the elastic limit value of curvature (v''_e) varies for each neutral axis position. With a sufficient number of moment interaction and moment-strain curves for various angles of the neutral axis, the moment-strain relationship can be constructed for a specific direction of loading.

The moment-strain relationship shown in Fig. 4.4 has been plotted on the basis of total moment (M_r), in order to show the relationship for all neutral axis positions from 0 to 90 deg. However, when a particular direction of loading is considered, the more practical value to use is the dimensionless moment used in plotting the moment interaction diagram. The moment-strain curves for loads at 10.6 and 45 deg to the Y axis are shown in the figure.

4.2.5 Deflections

From the moment-strain relationship corresponding to a specific direction of loading, the deflections can be computed using numerical integration. The neutral axis position for corresponding moments may be found from the moment interaction relationship either directly or by interpolation between curves. From the neutral axis position the distance to the extreme fiber can be computed. The strains for corresponding moments are found from the moment-strain relationship.

Assuming a linear distribution of strain and small deflections the curvature takes the form:

$$\epsilon_m / v_m \cong d^2v/dz^2 = v'' \tag{3}$$

where

ϵ_m = the extreme fiber strain

v_m = the distance to the extreme fiber

z = the coordinate axis along the length of the beam.

The curvatures for the deflections in the direction of a set of reference axes ζ and η rotated an angle β from the X and Y axes respectively are related to the curvature of the neutral axis by the following relationships: (See Fig. 4.5)

$$\begin{aligned} \eta'' &= v'' \cos(\beta-\varphi) \\ \zeta'' &= v'' \sin(\beta-\varphi) \end{aligned} \tag{4}$$

where η'' and ζ'' are components of the curvature referred to the η and ζ reference axes. Using these relationships, the curvatures, slopes, and deflections in the plane of the set of reference axes can be computed.

The elastic limit deflection for a cantilever with a concentrated load at the end is found from the relationships: (See Fig. 4.6)

$$\delta^e_\zeta = \sin(\beta-\varphi)\, L^2\, \epsilon_e / 3\, v_m$$

$$\delta^e_\eta = \cos(\beta-\varphi)\, L^2\, \epsilon_e / 3\, v_m$$

where

δ^e_ζ = the elastic limit deflection in the direction of the ζ coordinates.

δ^e_η = the elastic limit deflection in the direction of the η coordinates.

When the elastic limit deflections are exceeded, the solution of the deflection Eqs. (4) are required to obtain the deflected shape of the beam. The relationship of the deflection of a cantilever 6 B 15.5 section in the directions of the X and Y axes is shown in Fig. 4.7 for loads at 10.6 and 45 deg to the Y axis. Since the strain-hardening portion of the stress-strain curve for mild steel begins at strains in the order of 10 to 20 times the yield strain, an upper limit of 20 ϵ_e is used as the maximum strain on the beam. This is done in order to obtain the maximum possible deflection and still be within the range of applicable values of the stress-strain relationship for mild steel. The moment at this value of strain differs from the fully plastic moment by something less than one per cent. Therefore, a strain of 20 times the elastic limit strain corresponding to the fully plastic moment is used in calculating the "fully plastic deflection". In general, φ varies along the length of the beam when the elastic limit is exceeded. However, since the rotation of the neutral axis is only about plus or minus one deg for the load application at 45 deg, the deflection relationship shown in the figure is nearly linear. For the load application of 10.6 deg, a non-linear relationship exists between the deflections in the X and Y directions because of the 20 deg change in the direction of the neutral axis.

4.2.6 Simplified Analysis

Two attempts were made to simplify the analysis by assuming the section to be made up of two rectangular flange plates. This eliminated all the terms in the equations shown in Appendix 4.B which

involved the thickness of the web. The method materially reduced the amount of work involved. However, the errors involved in determining both the load and the deflection are larger than are desirable.

In the first attempt to simplify the analysis, Case B, the web of the 6 B 15.5 section was neglected. The moment interaction diagram for this case is compared in Fig. 4.8 with Case A, the section with the web. The moments about the X and Y axes are divided by the elastic limit moments about the X axis (M_x^e) for Case A. The error in the elastic limit moments decreases from 11 per cent to less than one per cent as φ increases from 0 to 90 degrees. The error in the fully plastic moments for φ from 0 to 75 deg is about 18 per cent and for 90 deg is less than one per cent.

Case C, the second attempt to simplify the analysis, was studied to eliminate the error in the elastic limit moments found in Case B. This was accomplished by increasing the depth of the section used in Case B so that the elastic limit moment about the X axis (M_x^e) was the same as for Case A, the section with the web. The effect of increasing the depth is to rotate the moment relationships for constant angles of the neutral axis toward the strong direction of resistance. The elastic limit moments are approximately correct because of the increased depth of the section. The errors in the fully plastic moments, in this case, range from about 1 to 13 per cent.

The deflections in the directions of the X and Y axes for loading directions of 10.6 and 45 deg are shown in Fig. 4.7 for the three cases considered. The errors in the deflections range from

20 to 32 per cent in the X direction and 0 to 21 per cent in the Y direction. The error in the resultant deflection, neglecting the fact that they are in different directions, ranges from 18 to 23 per cent.

4.2.7 General Discussion

The deflections determined by the approximate methods are smaller than those determined by the more exact method. This is a result of the shorter length of the beam which is inelastically deformed. For the 10.6 deg loading the inelastic length of the beam, when the fully plastic moment exists, is 0.245L for Case B as compared to 0.323L for the more exact method, Case A. The ratio of the length of the beam inelastically strained to the total length of a cantilever beam loaded at the free end is given by:

$$L_p/L = 1 - M^e/M^m$$

where

L = the length of the beam

L_p = the length of the beam strained inelastically

M^e = the elastic limit moment

M^m = the maximum moment on the beam.

It was noticed in the moment interaction relationship that, for a loading direction just slightly asymmetric to the strong direction of resistance, the rotation of the neutral axis from the strong direction at the fully plastic condition could be as large as 42 deg instead of at 0 deg as is usually assumed. The deflections in the X and Y directions were computed for a loading direction of approximately 0.2 deg from

the Y axis and are shown in Fig. 4.7. The deflection in the x direction was found to be approximately 25 per cent of the deflection in the y direction for the fully plastic condition which might possibly explain the initiation of the lateral buckling and torsional type failures which are common for members loaded in the strong direction of resistance.

4.3 EXPERIMENTAL INVESTIGATION

4.3.1 Test Specimens

The test specimens simulated interior building columns pinned at the base and fixed at the floor or roof framing members. The specimens were each cut from a 10 ft length of a 6 B 15.5 section. After cutting and removing a 9 in. length from the center for tension coupons, the specimen was welded back together. A stub beam of a 10 WF 77 section, which simulated the floor beams, was welded to the specimen at the center line (Fig. 4.9) so that the longitudinal axis of the stub was 45 deg to the principal axes of the specimen. Plates were welded between the flanges of the specimen and the flanges of the stub so that the stub became a continuous member through the specimen. Then the stub was stiffened with plates in the directions of the principal axes of the specimen in order to simulate the stiffness of framing members in those directions. The stub provided a convenient method for applying the lateral load to the specimen and also for restraint against lateral movement. The ends of the specimen were welded to end reaction plates. The specimens measured 43.5 in. from the center line of the end reactions to the face of the stub, and, therefore, had an effective span of 87 in. between end reactions.

4.3.2 Specimen Properties

The measured dimensional properties for the two specimens are shown in Table 4.1 along with the values given in the AISC handbook.

Thirteen tension coupons from each specimen were tested in a 120,000 lb hydraulic testing machine. The strains were recorded automatically with a 2 in. gage length recording extensometer up to strains of about one per cent, at which time the load was allowed to drop off slightly and a "C" type extensometer, using SR-4 strain gages, was used until the maximum load was reached.

It was necessary to idealize the stress-strain curve of the material in order to obtain a stress-strain relationship that could be used to compare the test results with the theoretical work. Therefore, the yield stress was selected as that value of stress which corresponded to a 0.2 per cent offset and the yield strain was selected as that value of strain for which a projection of the truly elastic portion of the curve intersected the selected yield stress. A stress-strain curve for each specimen was derived from an average of all of the yield stresses and strains selected in this way. The two idealized relationships for the specimens are shown in Figs. 4.10 and 4.11 with the curves which show the maximum deviation of these curves from the individual stress-strain relationships.

4.3.3 Test Apparatus

The load was applied to the specimen through the stub by means of a hydraulic tension jack. Since the jack had only a 6 in. stroke, a frame was made by which the specimen could be held in place

while the jack was readjusted. In this way it was possible to continue the deflection of the specimens beyond 6 in. This loading frame, shown in Fig. 4.12, was anchored to the floor.

On either side of the loading frame, a 10 in. I section was placed vertically to restrain the specimen. Rollers attached to the stub above and below the specimen rode on a 1/2 in. round rod which had been tack-welded to the flange of the restraining I section. The restraining system may be seen in Figs. 4.13, 4.16, and 4.17.

The end reaction system was composed of three basic parts: the vertical reaction system, horizontal reaction system, and the axial load unit.

The vertical support for each end reaction assembly (See Fig. 4.14) was provided by two vertical tension rods. Knife edges and seats provided the necessary freedom for rotation of the end reaction assembly in a vertical plane.

Two horizontal rods connected above and below the specimen by means of spherical bearings provided the horizontal support and freedom for rotation in a horizontal plane. No provision was made for torsional rotation of the specimen.

The axial load was applied through ball joints at each end reaction plate by a hydraulic jack placed at one end of the specimen. A "U" yoke at each end carried the axial load reaction to the outside of the end reaction plate where the yokes were tied together by tension rods making the unit independent of the other reaction supports. The weight of the axial load unit was supported by bearings on the end

reaction plate. The system was balanced on these supporting bearings before the test so that the line of action of the axial load was at or very near to the centroid of the section. An isometric detail of the end reaction system is shown in Fig. 4.14. The reaction systems for each end of the specimen are shown in Figs. 4.15 and 4.16, with and without the axial load units in place.

The vertical and horizontal end reaction rods and the center restraint were connected to a supporting four column, main test frame. The entire test set-up may be seen in Fig. 4.17.

4.3.4 Instrumentation

The lateral loads were measured with calibrated weight-bars which were inserted as a part of the horizontal and vertical reaction systems. Similarly, the axial load was measured with weigh-bars included in the tension rod system of the axial load unit. The weigh-bars were calibrated tension rods in which the strains were measured by means of electrical resistance type strain gages.

The extreme fiber strains in the test specimen were determined with SR-4 type electrical resistance type strain gages at 1.5, 3, 6, 12, and 20 in. from the stub on the north side and at 6, 12, and 20 in. stations on the south side. Specimen 4XY0 S 6 B (without axial load) was instrumented heavily at each station in order to have an approximate measurement of the neutral axis position.

The vertical deflections were measured with mechanical dials on each side of the stub at 3, 6, 9, 12, 20 and 43.5 in. from the stub. It was necessary to offset these dials from the vertical because of the

interference of the flange of the beam with the wire from the dial to the centroid of the section. Horizontal deflections were measured at the same sections as the vertical deflections for specimen 4XY0 S 6 B. However, the error in these deflections was of the same order of magnitude as the actual deflection because of the vertical deflection of the specimen. Therefore, for the specimen with axial load (4XY1 S 6 B) the horizontal deflection was measured only at the stub and end reactions. The vertical deflection at the centerline of specimen 4XY0 S 6 B was measured with a mechanical dial on the stub.

4.3.5 Test Procedure

The lateral load was applied to the specimens in such a way that the extreme fiber strains increased in increments of about 100 microin. for each increment of load, until the specimens showed signs of inelastic action. When this occurred, the test was monitored by increments of deflection and the specimen was allowed to creep, thereby producing a decrease in the load until the deflection became nearly steady at which time the measurements were made. The greatest waiting period amounted to less than about 5 min. The axial load on specimen 4XY1 S 6 B was kept very nearly constant throughout the test by means of a null type system activated by the total output of the four weigh-bars. The variation in the axial load from the initially applied load was only plus 0.8 per cent and minus 1.2 per cent.

4.3.6 Method of Testing

The more obvious method of testing obliquely-loaded beams is to apply a load in some constant direction. In the present tests, the

applied lateral load changed direction in the inelastic range as a result of restraining the stub section so that the deflection at the stub was in a vertical direction and 45 deg to the principal axes of the specimen. This made it possible to use a lateral loading unit that was stationary.

In the test without axial load, it was planned that the direction of curvature in the elastic range would be at 45 deg to the principal axes of the beam and the deflection would be vertical. In the inelastic range, if the same neutral axis position existed at the stub, the deflection of the beam would not be vertical but would have some horizontal component. Thus, in order for the deflection to be only vertical at the stub, the neutral axis at the stub would have to be rotated through an angle greater than 45 deg. Thus, the experimental moment interaction curve would follow the theoretical curve for 45 deg neutral axis position in the elastic range and, in the inelastic range, the angle would be slightly greater than 45 deg.

4.3.7 Test Results of Specimen 4XY0 S 6 B

A small horizontal load was initially applied to specimen 4XY0 S 6 B through the end reactions in order to counteract the horizontal deflection produced by the weight of the specimen. This applied load was not sufficient to take up all the slack in the horizontal reaction assembly and a relaxation occurred which resulted in a rotation of the neutral axis at the stub from the intended 45 deg to about 54 deg. This relaxation continued throughout the test because of the continually increasing horizontal loads and deflections at the stub resulting from the formation of grooves in the rollers of the restraining system. The effect of the

relaxation in the inelastic range is to rotate the moment interaction relationship toward the relationship for a constant direction of loading.

From the dimensional properties of specimen 4XY0 S 6 B, a theoretical moment interaction relationship was obtained. The experimental and theoretical relationships are compared in Fig. 4.18. The experimentally determined moments about the X and Y axes are divided by M_x^e, the elastic limit moment about the X axis for φ = 0 degrees, which was computed from the dimensional properties of the section and the average yield stress of the tension coupons.

The experimental curve follows the theoretical relationship for a 53.6 deg neutral axis position and is nearly linear in the elastic range. The small discrepancy near the elastic limit is probably caused by the variation in the true stress-strain relationships from the one on which the theoretical work is based. In order to satisfy the restraint condition and the relaxation which occurred in the horizontal reactions, the experimental curve in the plastic range deviates from the moment relationship for a 53.6 deg neutral axis position and approaches the theoretical relationship for a 56 deg neutral axis position.

Local buckling as observed visually began at about M_x/M_x^e = 0.80 and M_y/M_y^e = 0.25. The effect of the local buckling condition was sufficient to overcome the effect of strain-hardening; thus the curve rotates toward the moment relationship for the strong direction of resistance instead of nearly radially outward as should be expected if only strain-hardening had occurred.

In Fig. 4.19 the observed moment-extreme fiber strain relationships are compared with the theoretical curves. The experimentally determined strains are divided by the average elastic limit strain of the tension coupons. The moments about the X axis are used rather than the resultant moments in order that there be a common basis between the moment interaction and moment-strain relationships.

It is not possible to compare the theoretical and experimental curves directly since the neutral axis for the theoretical curves has a fixed position whereas the experimental relationships do not. If the specimen were to respond according to the theory, the strains for the 1.5 in. section should fall between the theoretical curves for the 52 and 56 deg. positions of the neutral axis for the range in which the gages were in operation. The actual curves for this and the 3 in. section show a considerably larger strain for corresponding moments than the theory predicts. This phenomenon has been observed[2][3] in tests of beams in the strong and weak directions of resistance and may be attributed to residual stress and stress concentration.

The resultant lateral load-vertical deflection relationship for the specimen without axial load is shown in Fig. 4.20a. The elastic limit and the theoretical fully plastic loads are noted. The maximum load of 22.1 kips corresponding to a deflection of 7.56 in. is about 21 per cent greater than the theoretical fully plastic load. The ductility factor (δ/δ_e) at the maximum load is 29. At the end of the test where the ductility factor was 39 the lateral load had dropped off only slightly. The deflected shape of the specimen at the end of the test is shown in Fig. 4.21.

The load at the fully plastic condition represents the maximum load which can be calculated from the theory without taking strain-hardening into account. In Fig. 4.20b the load deflection curve for this range is shown along with the curves computed from the theoretical and observed moment-strain relationships. An extreme fiber strain of 20 ϵ_e was used in calculating the deflection corresponding to the fully plastic moment. The experimental moment-strain relationship was extrapolated slightly in order to calculate the deflection at the fully plastic moment.

The errors in the computed and the experimental curves at the elastic limit are not too alarming in that the 24 per cent error in deflection is of the same order of magnitude as has been noticed in other tests. The effect of the residual stress and stress concentration on the deflections can be seen by comparing the computed deflections with the observed value for the fully plastic load. At this load, there is virtually no difference between the deflection computed from the actual moment-strain relationships and the observed deflection but the deflection computed from the theoretical moment-strain curves is in error by about 45 per cent.

It was possible to determine a torsional moment at the end reactions because of the weigh-bar system used to measure the horizontal and vertical loads. The torsional moments are shown in Fig. 4.23 plotted to the vertical deflection of the beam. No attempt is made to explain these twisting moments since it was impossible to trace them to their source. It is felt that these moments are of major consequences in

oblique loading of I or WF shapes and more work should be done on this aspect of the problem.

4.3.8 Test Results Specimen 4XY1 S 6 B

The 50 kip axial load applied to specimen 4XY1 S 6 B resulted in a stress of approximately 10 kips per sq. in., which corresponds to about 63 per cent of the allowable AISC value.

The horizontal reactions were adjusted after the axial load and a small lateral load had been applied so that the neutral axis position in the elastic range would be approximately the same as for the specimen without axial load. This procedure eliminated the initial relaxation caused by the slack in the horizontal reactions which occurred in the test of the specimen without axial load, and since the maximum horizontal load was only about 75 per cent of that for the specimen without axial load the relaxation problem was never as severe.

The moment interaction relationship is shown in Fig. 4.24 for the experimentally determined moments which include the lateral and axial moments. The moments are divided by M_x^e, the elastic limit moment for the strong direction of resistance without axial load on the section, determined from the dimensional properties and the average yield stress of the tension coupons. The theoretical moment interaction relationships for the specimen without axial load are also shown in the figure.

The relationship of the moments along the length of the beam are shown on the figure for various loads. The distribution of the moment along the length of the beam is very nearly linear up to the load at which the maximum resultant moment on the specimen is reached, at

which point the web of the section is affected by local buckling and the distribution becomes non-linear. At failure the specimen still carried a horizontal load but the vertical load had dropped to zero and the specimen could not sustain the axial load.

The relationship between the moments about the X and Y axes and the vertical deflections at the stub are shown in Fig. 4.25. The contribution of the axial and lateral loads to the total moments about the X and Y axes are also shown in the figure. For comparison the moments for the specimen without axial load are shown. There is virtually no difference in the total moment about the Y axis for the two specimens. The total moments about the X axis are very nearly the same up to a moment of approximately 350 kip in. At about that moment the specimens were both affected by local buckling. The local deformation reduced the rate of increase in the moment-carrying capacity of the axially-loaded specimen much more than it did the specimen without axial load.

The strains which contribute to lateral deflections (flexural strains, ϵ_f) were determined from the average of the difference of the two extreme fiber strains. The moment-flexural strain relationships, shown in Fig. 4.26, for the various sections using this definition of flexural strain are similar to the curves for the specimen without axial load. Again the effect of residual stress and stress concentrations on the relationships for the 1.5 and 3 in. sections are evident. The moment-flexural strain relationships for specimen 4XY1 S 6 B are compared in Fig. 4.26 with the theoretical relationships for

specimen 4XY0 S 6 B. The experimental curves have been placed in dimensionless form by dividing the strains by the average yield strain determined from the tension coupons and the moments about the X axis have been divided by M_x^e. As in the specimen without axial load, the moments about the X axis have been used rather than the resultant moment in order to have a common basis with the moment interaction diagram.

The resultant lateral load-vertical deflection relationship for the axially-loaded specimen is compared in Fig. 4.27 with the relationship for the specimen without axial load. The maximum resultant lateral load of 15.4 kips for specimen 4XY1 S 6 B is about 70 per cent of the maximum resultant load of the specimen without axial load. The ductility factor (δ/δ_e) based on the elastic limit deflection of the specimen without axial load was 5.2 at the maximum lateral load or 18 per cent of the ductility factor at the maximum load for the specimen without axial load. At failure, the specimen still carried a horizontal load of 9.6 kips which amounts to 62 per cent of the maximum load on the specimen. The deflection at failure could not be measured precisely because the specimen was lifted from the knife edge supports at one end. However, the deflection was estimated at 6.03 in. which makes the ductility factor about 23 at failure. The final deflected shape of the specimen is shown in Fig. 4.28.

4.4 SUMMARY

The objective of this report is to present an analysis which can be used to determine the load-deflection response into the inelastic range of structural I or WF shapes when subjected to obliquely applied

lateral loads. The analysis is based upon an elasto-plastic stress-strain relationship which does not take into account the additional energy absorption capacity of a member caused by strain-hardening of the material. Although experimental results were obtained for a beam loaded with both lateral and axial loads, no analysis was developed to handle this problem.

The load-deflection relationship computed from the elasto-plastic theory differs considerably from the experimental relationship. The theoretical deflection at the elastic limit load is only about 80 per cent of the corresponding experimental deflection, and, at the fully plastic load, which is the maximum load which can be computed from the elasto-plastic theory, only 56 per cent of the experimental deflection was obtained. Differences of these magnitudes have been reported elsewhere and may be explained in part by residual stress and also by the way in which the yield strain was approximated in order to obtain an elasto-plastic stress-strain relationship. However, when the deflection is computed from the observed moment-strain relationship the deflection at the fully plastic load is in very good agreement with the experimentally measured deflection. Before these differences can be considered significant, the analysis should be extended to include the effect of strain-hardening since only about 12 per cent of the experimental deflection range can be determined with the present elasto-plastic analysis. The theoretical response of the member may be entirely satisfactory when the effect of strain-hardening is introduced even though the initial range is somewhat in error.

The 6 B 15.5 section was tested in both the strong and weak directions of resistance, with and without axial loads by R. J. Munz. The results of these tests and the oblique loading tests are presented in Table 4.2. The values have been adjusted for the average yield stress of the tension coupons determined on the basis of a 0.2 per cent offset in order to place them on a common basis for comparison. The yield load and moments for the tests without axial load were determined from the average yield stress. Since there was very little non-linearity in the oblique and weak directions of loading at these computed values, they were considered satisfactory to designate the beginning of inelastic action. For the strong direction of resistance, these computed yield values were far into the non-linear range of the test because of the greater effect of local buckling; therefore, the yield values from this test are based on the beginning of non-linearity as observed from the moment-strain relationship.

The maximum value of load, moment and deflection are not comparable to the theoretical values since the specimens were affected in different ways by local buckling, strain-hardening and the restraint conditions of the tests. The local buckling had its greatest effect on the specimen loaded in the strong direction of resistance since it resulted in a final failure by lateral buckling. The obliquely loaded specimen was prevented from failing laterally by the restraints provided by the vertical and horizontal loads on the specimen, thus making it possible for the maximum load to exceed that of the strong direction of resistance test.

The lateral load capacity of the specimens with axial load was reduced appreciably from the load capacity when no axial thrust was applied. The amount of thrust applied to the three specimens differed considerably, making a comparison between them difficult. The specimen loaded in the strong direction of resistance was affected more by local buckling than the weak and oblique directions of loading tests. However, the restraints applied to the oblique direction test make it possible for the maximum values of that specimen to exceed those for the specimen loaded in the strong direction of resistance.

One of the more important features of the analysis presented is the insight that the moment interaction relationship gives into the behavior which can be expected when an oblique load is applied to a member. If the load is applied at a very small angle, for the 6 B 15.5 section less than one degree to the Y axis of the specimen it is possible with unsymmetrical yielding conditions to build up a lateral deflection of considerable magnitude. Another feature is the insight into the effect that torsional moments, which may be caused by deflections perpendicular to the direction of loading, can have on the direction of loading along the length of the beam. Although the effect of torsional moments has been neglected in the analysis it is felt that it is of major consequence and more work should be done on this aspect of the problem.

4.5 BIBLIOGRAPHY

1. Anderson, B. W., "Unsymmetrical Pure Bending of Beams Having Rectangular Cross Sections Under Loads Which Produce Inelastic Strains," M. S. Thesis, University of Illinois, Department of Theoretical and Applied Mechanics, (1951).

2. Ketter, R., Kaminsky, E., and Beedle, L., "Plastic Deformation of Wide Flange Beam-Columns," Proceedings of the ASCE, Vol. 79, Separate No. 330, Oct. (1953).

3. Munz, R. J., "Static Test to Failure of Steel Beam-Columns," M. S. Thesis, University of Illinois, Department of Civil Engineering,(1954).

4. Seely, F. B. and Smith, J. O., "Advanced Mechanics of Materials," 2nd ed., New York, John Wiley and Sons, (1952).

5. Williams, H. A., "Investigation of Pure Bending in Plastic Range When Loads Are Not Parallel to Principal Plane," NACA Tech. Note n 2287 (1951).

APPENDIX 4.A

The following notation is used in this report:

X, Y	Rectangular coordinate system in which X, and Y denote the principal axes of a WF or I section.
U, V	Rectangular coordinate system of which the U axis is the neutral axis.
ξ, η	Rectangular coordinate system used as a reference in space.
z	Coordinate axis along the length of the beam.
φ	Angle between the X, Y and U, V coordinate systems.
β	Angle between the X, Y and ξ, η coordinate systems.
α	Angle between the Y axis and the applied load.
σ	Stress
σ_e	Yield Stress
ϵ	Strain
ϵ_e	Yield strain
ϵ_m	Extreme fiber strain
ϵ_f	Extreme fiber flexural strain

v_e	Distance to the elastic limit strain line from the neutral axis
v_m	Distance to the extreme fiber from the neutral axis
h	Distance to the elastic limit strain line along the X axis
h_m	Distance to the extreme fiber strain line along the X axis
k	Distance to the elastic limit strain line along the Y axis
k_m	Distance to the extreme fiber strain line along the Y axis
v''	Curvature referred to the U and V coordinate system
v''_e	Elastic limit curvature referred to the U and V coordinate system
ξ'', η''	Curvatures referred to the ξ and η coordinate system
δ	Deflection in the direction of the axis indicated by the subscript
δ^e	Elastic limit deflection in the direction of the axis indicated by the subscript
L	Length of the beam
L_p	Length of the beam strained inelastically
2a	Thickness of the web
2b	Width of the section
2c	Depth of the section
2d	Distance between flanges
A	Area of the section
A_e	Area of the section subjected to elastic strains
A_p	Area of the section subjected to inelastic strains
P	Component of the applied concentrated load in the direction of the axis indicated by the subscript
P_r	Applied concentrated load

P_e Elastic limit load

P_{fp} Fully plastic load

M Moment of the applied load about the axis denoted by the subscript

M^e Elastic limit moment about the axis denoted by the subscript and for a neutral axis position indicated in the following way:

$$M^e_x \Big|_{\varphi = 50^o} \quad , \quad M^e_y \Big|_{\varphi = 50^o}$$

When the neutral axis is coincident with a principal axis, the notation is as follows:

$$M^e_x \Big|_{\varphi = 0^o} = M^e_x$$

$$M^e_y \Big|_{\varphi = 90^o} = M^e_y$$

M^p Fully plastic moment about the axis denoted by the subscript and for a neutral axis position indicated in the same way as for M^e

M_r Resultant moment

M^m Maximum moment on a cantilever beam about the axis indicated by the subscript

I Moment of inertia of the total area about the axis denoted by the subscript

I^e Moment of inertia of the area strained elastically about the axis denoted by the subscript

I^e_{xy} Product of inertia of the area strained elastically about the X and Y axes

$$Q^p_x = \int_{A_p} \frac{v}{|v|}\, y\, da$$

$$Q^p_y = \int_{A_p} \frac{v}{|v|}\, x\, da$$

APPENDIX 4.B

For a WF or I section idealized, as shown in Fig. 4.B-1, the moment relations about the X and Y principal axes derived in the text (2-a, 2-b) can be related to the depth of inelastic penetration, the angle of the neutral axis and the dimension of the section. The line through the point h and k and having a slope φ determines the elastic limit strain line. This line cuts the section in one of five ways, neglecting the cases in which the line cuts the section at the ends of the flanges or at the junction of the flanges and web. In Fig. 4.B-2, the five cases are shown. The moments about the X and Y axes are found by integrating the elastic and plastic areas within the limits shown in the figure.

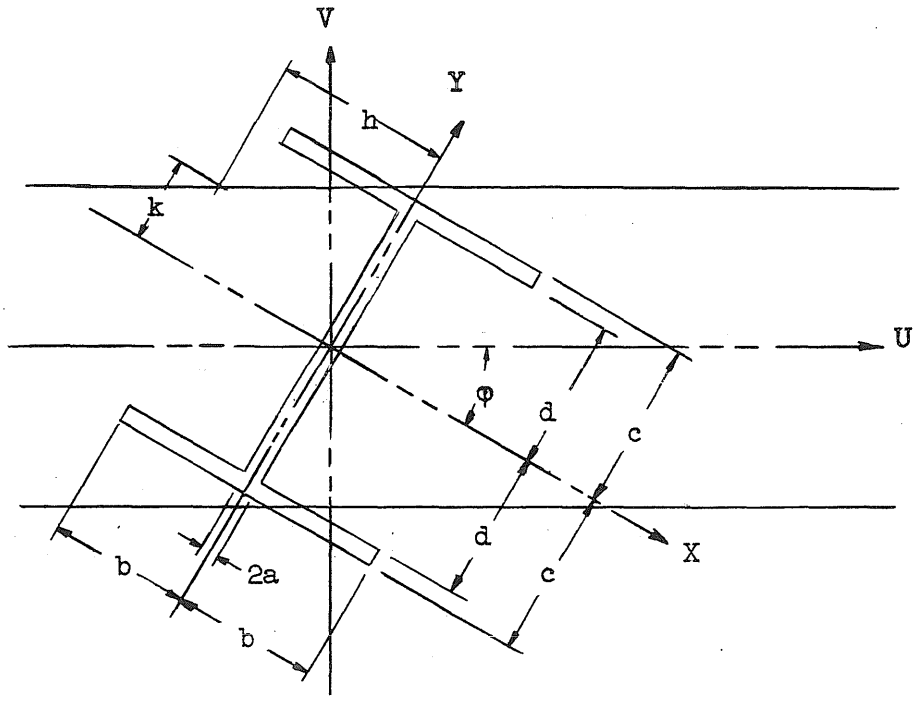

FIG. 4.B-1

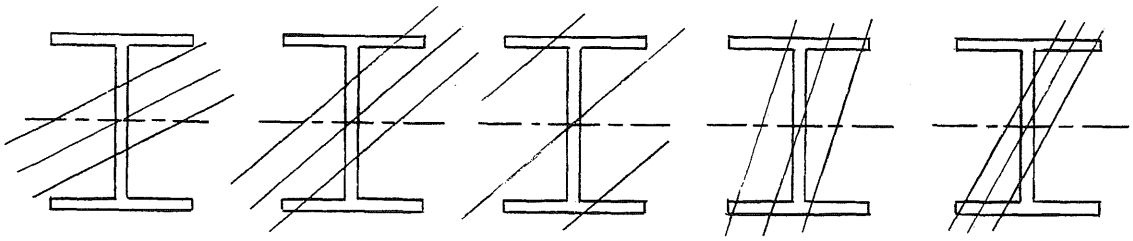

Case A Case B Case C Case D Case E

Case A: $0^{o} < \varphi < \tan^{-1} \frac{d-k}{b+h}$

Case B: $\tan^{-1} \frac{c-k}{b+h} < \varphi < \tan^{-1} \frac{d-k}{h+a}$

Case C: $\tan^{-1} \frac{d-k}{h-a} < \varphi < \tan^{-1} \frac{d+k}{b-h}$

Case D: $\tan^{-1} \frac{c+k}{b-h} < \varphi < 90^{o}$

Case E: $\tan^{-1} \frac{c}{b} < \varphi < \tan^{-1} \frac{d}{a}$

FIG. 4.B-2

If we let $k = 0$ and $v_e = h \sin\varphi$, we can write the equations for the moments in terms of the depth of yielding along the X axis (h), and the angle of the neutral axis (φ) and the dimensions of the cross section. These relations are shown below, where a, b, c, d and h are absolute quantities, a, b, c and d refer to the dimensions of the cross section and h refers to the depth of inelastic penetration along the X axis of the section. Moments determined from these equations will have positive values. The proper sign must be determined from the geometry of the problem.

Case A

$$\frac{M_x}{\sigma_e} = \frac{1}{12h}\left\{ h^3 \left[-8a \tan^2\varphi\right] + h\left[24b(c^2-d^2) + 24ad^2 - 8a^3 \tan^2\varphi\right]\right\}$$

$$\frac{M_y}{\sigma_e} = \frac{1}{12h}\left\{ h\left[16a^2 \tan\varphi\right]\right\}$$

$$d \cot\varphi - b \geq h \geq 0$$

Case B

$$\frac{M_x}{\sigma_e} = \frac{1}{12h}\left\{ h^3\left[-8a \tan^2\varphi\right] + h^2\left[-6(c^2-d^2)\right] + h\left[-8a^3 \tan^2\varphi + 8(c^3-d^3)\cot\varphi + 12b(c^2-d^2) + 24ad^2\right] + \left[-3(c^4-d^4)\cot^2\varphi + 8b(c^3-d^3)\cot\varphi - 6b^2(c^2-d^2)\right]\right\}$$

$$\frac{M_y}{\sigma_e} = \frac{1}{12h}\left\{ h^3\left[-4(c-d)\right] + h^2\left[6(c^2-d^2)\cot\varphi\right] + h\left[-4(c^3-d^3)\cot^2\varphi + 12b^2(c-d) + 16a^3 \tan\varphi\right] + \left[(c^4-d^4)\cot^3\varphi - 6b^2(c^2-d^2)\cot\varphi + 8b^3(c-d)\right]\right\}$$

$$d \cot\varphi - b \geq h \geq \left\{\begin{matrix} c\cot\varphi - b \\ b - d\cot\varphi \end{matrix}\right\} \text{ whichever is larger}$$

Case C

$$\frac{M_x}{\sigma_e} = \frac{1}{12h}\left\{ h^2\left[-6(c^2-d^2)\right] + h\left[8(c^3-d^3)\cot\varphi + 12b\,(c^2-d^2)\right] + \left[-3(c^4-d^4)\cot^2\varphi + 8b(c^3-d^3)\cot\varphi - 6b^2(c^2-d^2) + 16ad^3\cot\varphi\right]\right\}$$

$$\frac{M_y}{\sigma_e} = \frac{1}{12h}\left\{ h^3\left[-4(c-d)\right] + h^2\left[6(c^2-d^2)\cot\varphi\right] + h\left[-4(c^3-d^3)\cot^2\varphi + 12b^2(c-d)\right]\right.$$

$$+ \left[(c^4-d^4)\cot^3\varphi - 6b^2(c^2-d^2)\cot\varphi + 8b^3(c-d) + 16a^3d\right]\Big\}$$

$$b + d\cot\varphi \geq h \geq \left\{\begin{matrix} d\cot\varphi + a \\ b - d\cot\varphi \end{matrix}\right\} \text{ whichever is larger}$$

Case D

$$\frac{M_x}{\sigma_e} = \frac{1}{12h}\left\{h\left[16(c^3-d^3)\cot\varphi\right] + \left[16ad^3\cot\varphi\right]\right\}$$

$$\frac{M_y}{\sigma_e} = \frac{1}{12h}\left\{h^3\left[-8(c-d)\right] + h\left[-8(c^3-d^3)\cot^2\varphi + 24b^2(c-d)\right] + \left[16a^3d\right]\right\}$$

$$b - c\cot\varphi \geq h \geq a + d\cot\varphi$$

Case E

$$\frac{M_x}{\sigma_e} = \frac{1}{12h}\left\{h^3\left[-8a\tan^2\varphi\right] + h\left[16(c^3-d^3)\cot\varphi + 24ad^2 - 8a^3\tan^2\varphi\right]\right\}$$

$$\frac{M_y}{\sigma_e} = \frac{1}{12h}\left\{h^3\left[-8(c-d)\right] + h\left[-8(c^3-d^3)\cot^2\varphi + 24b^2(c-d) + 16a^3\tan\varphi\right]\right\}$$

$$\text{whichever is smaller } \left\{\begin{matrix} b - c\cot\varphi \\ d\cot\varphi - a \end{matrix}\right\} \geq h \geq 0$$

For small angles of φ, h becomes exceedingly large for cases A, B and C; therefore, it may be desirable to indicate the depth of inelastic penetration by k, the depth of yielding along the y axis. This can be done by letting $h = 0$ and $v_e = k\cos\varphi$.

Case A

$$\frac{M_x}{\sigma_e} = \frac{1}{12k}\left\{k^3\left[-8a\right] + k\left[24b\,(c^2-d^2) + 24ad^2 - 8a^3\tan^2\varphi\right]\right\}$$

$$\frac{M_y}{\sigma_e} = \frac{1}{12k}\left\{ k\left[16a^3 \tan\varphi\right]\right\}$$

$$d - b\tan\varphi \geq k \geq 0$$

Case B

$$\frac{M_x}{\sigma_e} = \frac{1}{12k}\left\{k^3\left[-8a\right] + k^2\left[-6(c^2-d^2)\cot\varphi\right]\right.$$
$$+ k\left[-8a^3\tan^2\varphi + 8(c^3-d^3)\cot\varphi + 12b(c^2-d^2) + 24ad^2\right]$$
$$\left. + \left[-3(c^4-d^4)\cot\varphi + 8b(c^3-d^3) - 6b^2(c^2-d^2)\tan\varphi\right]\right\}$$

$$\frac{M_y}{\sigma_e} = \frac{1}{12k}\left\{k^3\left[-4(c-d)\cot^2\varphi\right] + k^2\left[6(c^2-d^2)\cot^2\varphi\right]\right.$$
$$+ k\left[-4(c^3-d^3)\cot^2\varphi + 12b^2(c-d) + 16a^3\tan\varphi\right]$$
$$\left. + \left[(c^4-d^4)\cot^2\varphi - 6b^2(c^2-d^2) + 8b^3(c-d)\tan\varphi\right]\right\}$$

$$d - a\tan\varphi \geq k \geq \left\{\begin{matrix} c - b\tan\varphi \\ b\tan\varphi - d \end{matrix}\right\} \quad \text{whichever is larger}$$

Case C

$$\frac{M_x}{\sigma_e} = \frac{1}{12k}\left\{k^2\left[-6(c^2-d^2)\cot\varphi\right] + k\left[8(c^3-d^3)\cot\varphi + 12b(c^2-d^2)\right]\right.$$
$$\left. + \left[-3(c^4-d^4)\cot\varphi + 8b(c^3-d^3) - 6b^2(c^2-d^2)\tan\varphi + 16ad^3\right]\right\}$$

$$\frac{M_y}{\sigma_e} = \frac{1}{12k}\left\{k^3\left[-4(c-d)\cot^2\varphi\right] + k^2\left[6(c^2-d^2)\cot^2\varphi\right]\right.$$
$$+ k\left[-4(c^3-d^3)\cot^2\varphi + 12b^2(c-d)\right]$$

$$+ \left[(c^4-d^4)\cot^2\varphi - 6b^2(c^2-d^2) + 8b^3(c-d)\tan\varphi + 16a^3 d\tan\varphi\right]\Big\}$$

$$d + b\tan\varphi \geq k \geq \begin{Bmatrix} d + a\tan\varphi \\ b\tan\varphi - d \end{Bmatrix} \text{ whichever is larger}$$

The strains and curvatures are related to the depth of inelastic penetration by the following relations:

$$\frac{\epsilon_m}{\epsilon_e} = \frac{v_m}{v_e} = \frac{h_m}{h} = \frac{k_m}{k} \simeq \frac{v''}{v''_e}$$

TABLE 4.1

DIMENSIONAL PROPERTIES OF SPECIMENS

	Depth	Flange		Web Thickness	I_x	I_y
		Width	Thickness			
AISC	6.00	6.00	0.269	0.240	30.3	9.69
4XY0S6B*	6.13	6.09	0.291	0.255	33.44	10.96
4XY1S6B*	6.16	6.10	0.291	0.254	34.23	11.02

* Measured Values

TABLE 4.2

RESULTS OF TESTS ON THE 6 B 15.5 SECTION IN THE STRONG, WEAK, AND OBLIQUE DIRECTIONS OF RESISTANCE

	Specimen						
	40S6B	4Y0S6B	4XY0S6B	41S6B	4Y1S6B	4XY1S6B	Units
Length	44	44	43.5	43.75	43.75	43.5	inches
Axial Load	0	0	0	66	44	50	kips
P_r^e T	19.7 (15.5)	6.48	9.38	-------	-------	-------	kips
P_r^e 0		6.48	9.38	-------	-------	-------	kips
P_r^m 0	20.9	11.0	22.0	11.8	7.4	15.4	kips
M_r^e T	434 (344)	143	204	-------	-------	-------	kip-inches
M_r^e 0		143	204	-------	-------	-------	
M_r^m 0	459	242	478	299	211	402	kip-inches
δ^e T	0.28 (0.31)	0.29	0.21	-------	-------	-------	inches
δ^e 0		0.37	0.26	-------	-------	-------	
δ^m 0	3.19	10.3	10.2	2.49	4.16	6.03	inches
ϵ_e	1330 (950)	1375	1420	1305	1285	1350	μ in./in.
σ_e	40.1 (31.8)	40.1	40.1	40	40	40	kips/in.^{2}
Failure	*	**	**	***	***	****	

* Local buckling followed by lateral buckling.

** Local buckling and deflected to the extent of the apparatus.

*** Local buckling and lateral load drop-off to zero.

**** Local buckling and vertical load drop-off to zero.

Note: The values shown for "T" are theoretical values based on the stress corresponding to a 0.2 per cent offset of strain. The values shown for "0" are the actual observed values. In order to obtain a common basis for comparison, all values have been adjusted to the yield stresses of the oblique direction tests. The values shown in parentheses are based on the yield value determined from the moment-strain relationship.

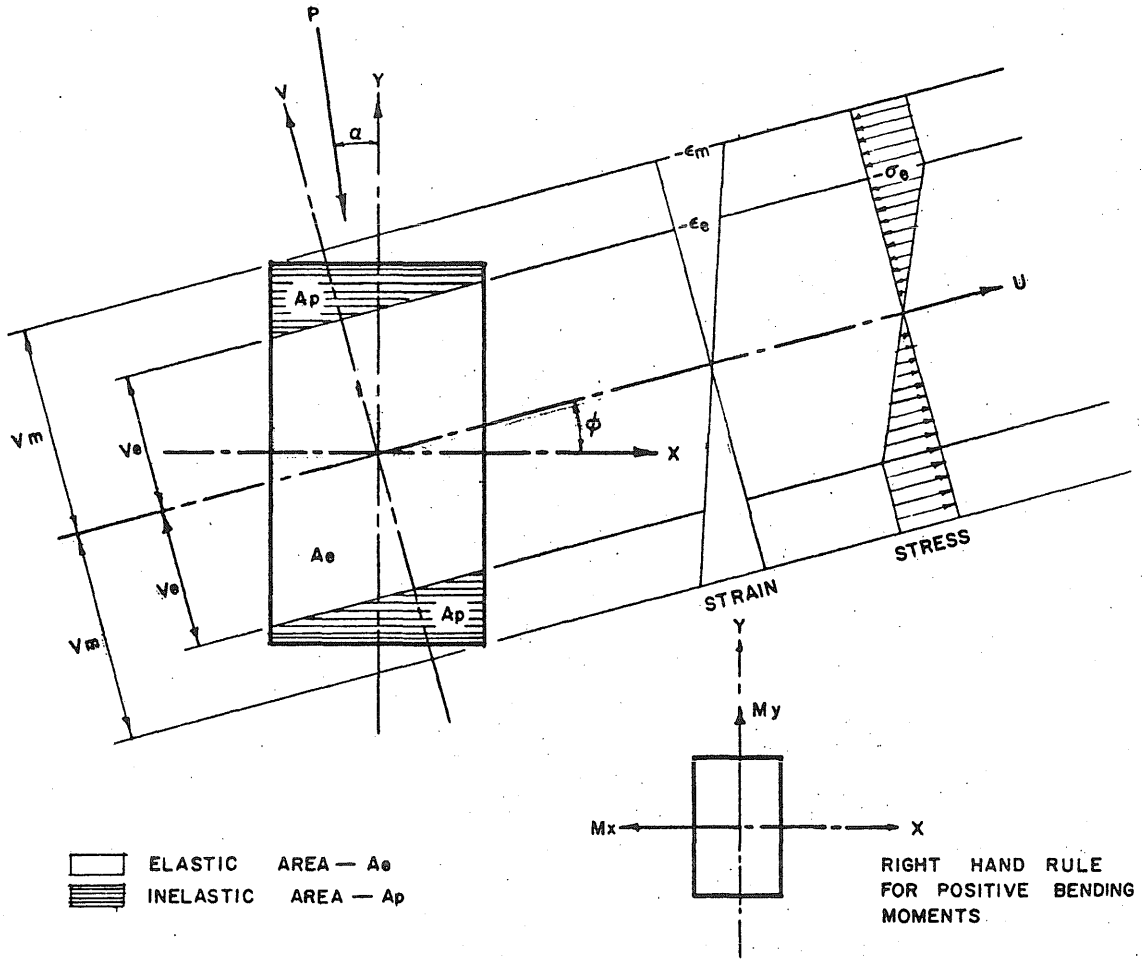

FIG. 4.1 GENERAL CROSS SECTION

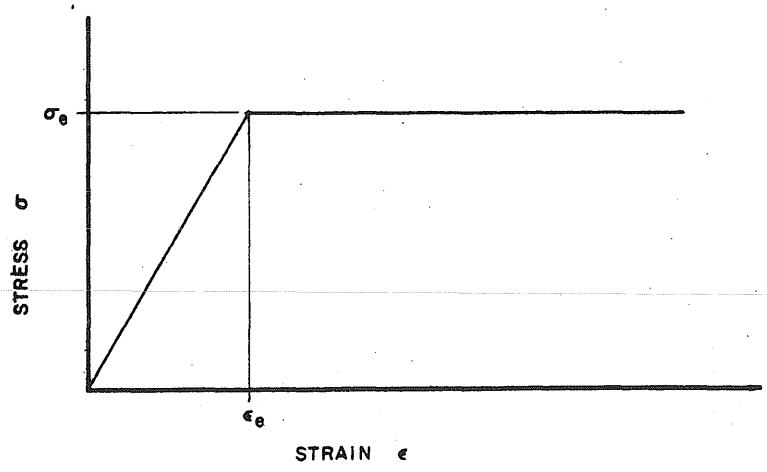

FIG. 4.2 STRESS–STRAIN RELATIONSHIP

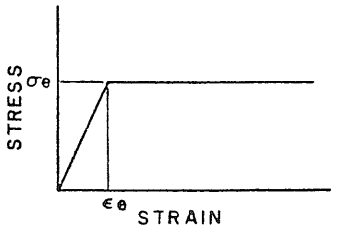

IDEALIZED STRESS STRAIN CURVE

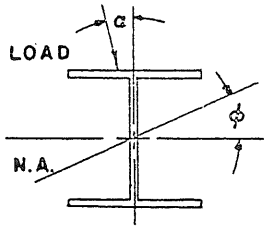

$I_x = 29.78$ IN.^{4}
$I_y = 9.69$ IN.^{4}
$M_x^e / \sigma_e = 9.93$ IN.^{3}

IDEALIZED 6 B 15.5

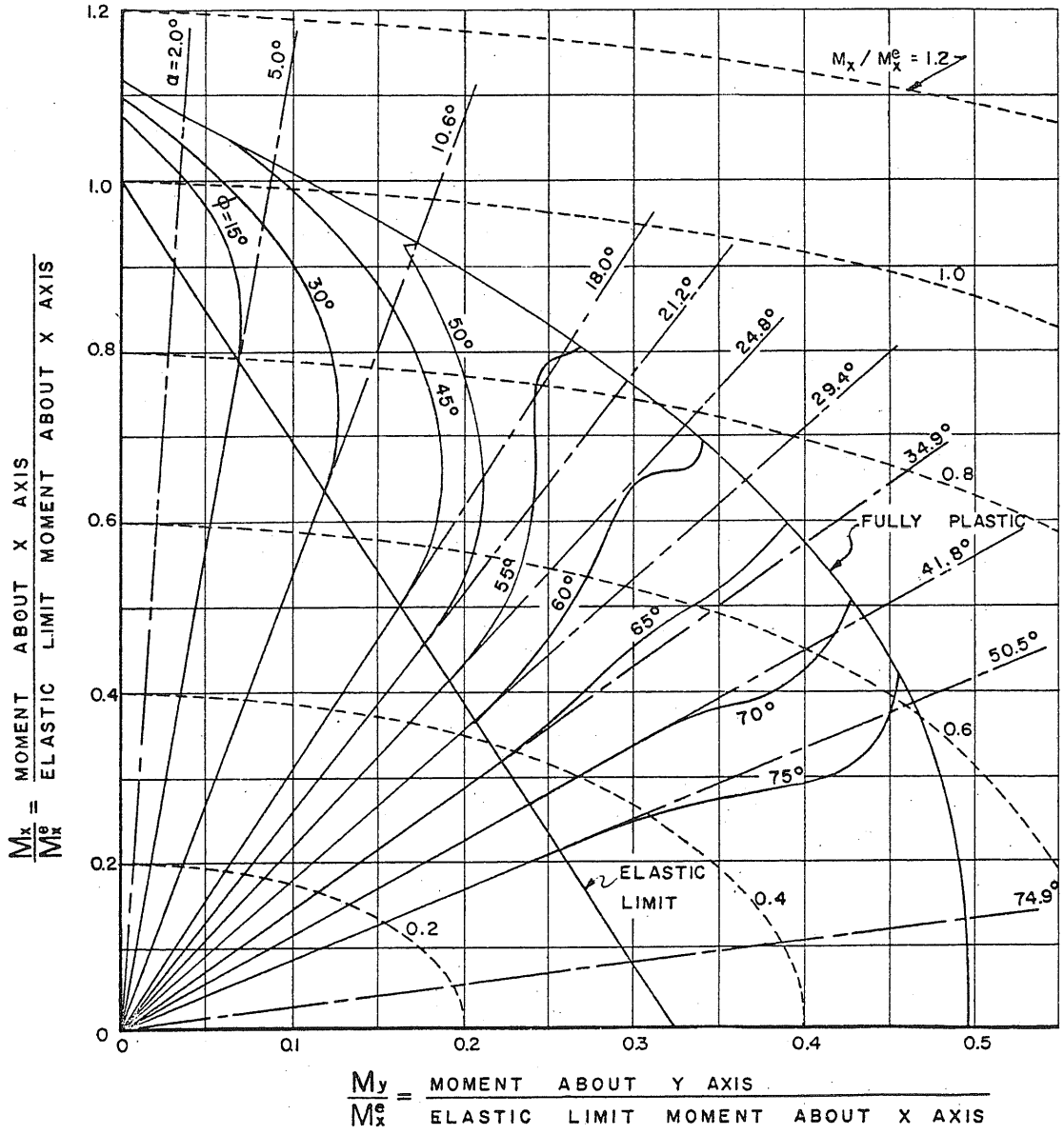

FIG. 4.3 MOMENT INTERACTION DIAGRAM FOR IDEALIZED 6 B 15.5 SECTION

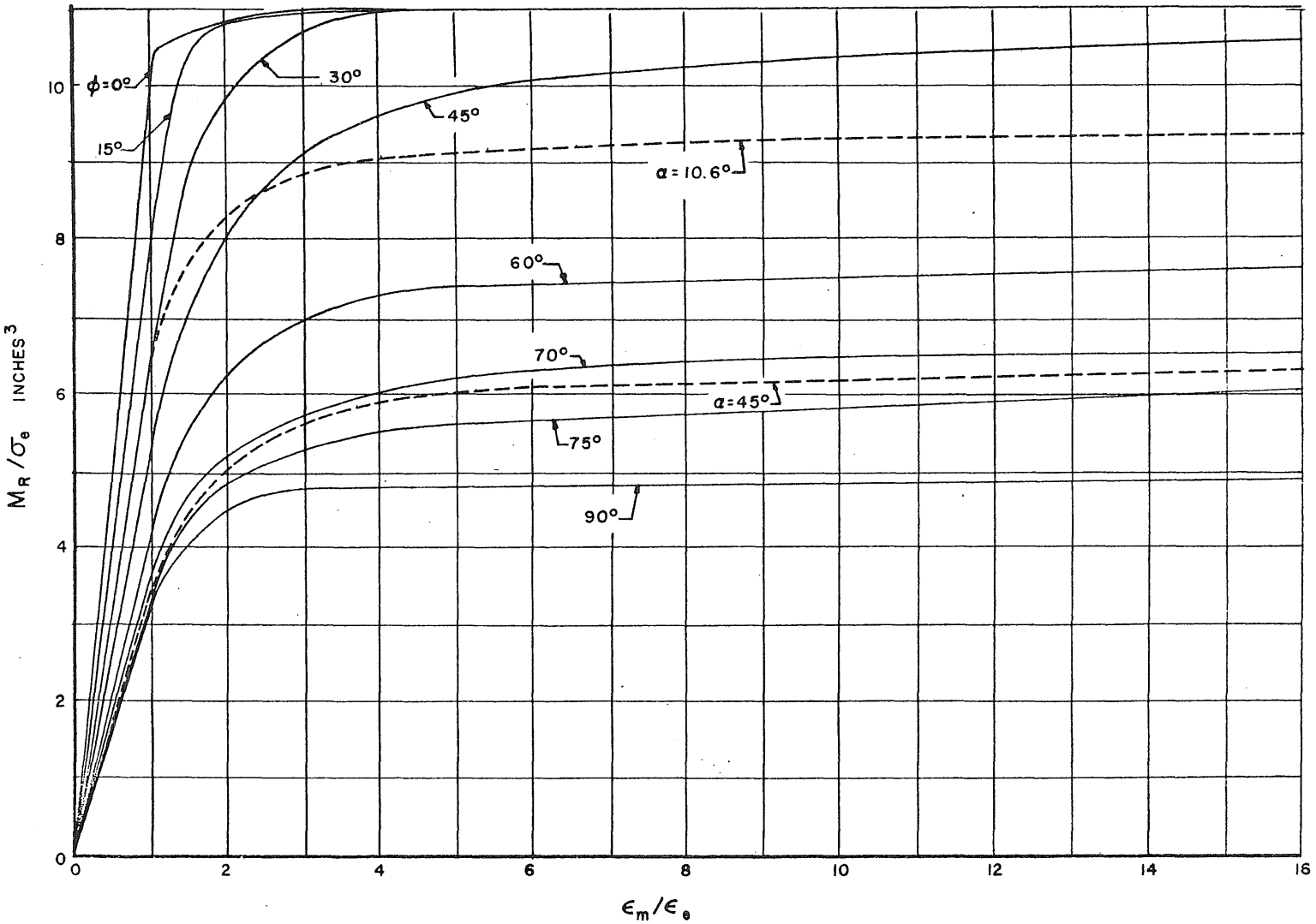

FIG. 4.4 MOMENT — STRAIN RELATIONSHIP FOR IDEALIZED 6 B 15.5 SECTION

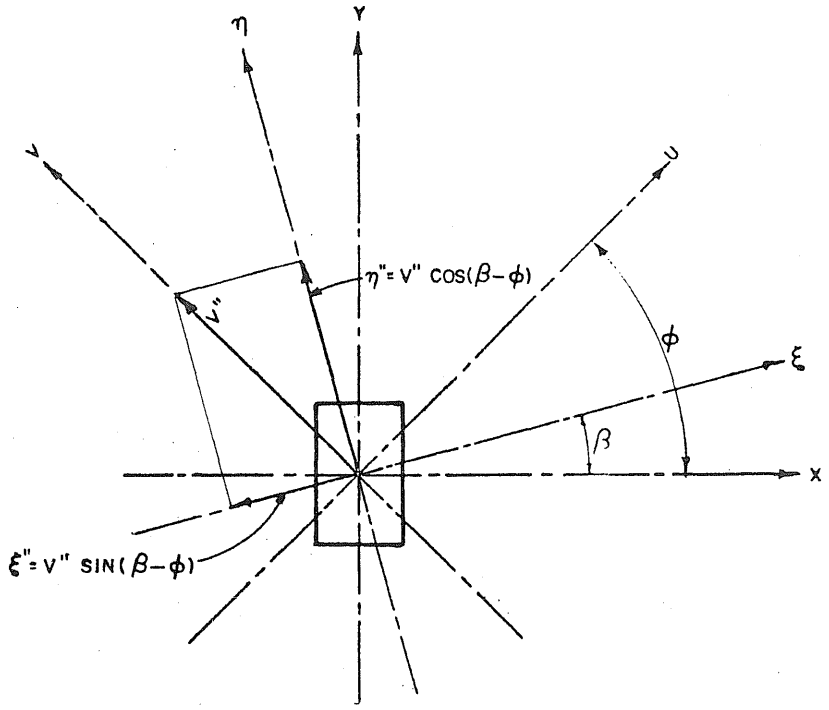

FIG. 4.5 CURVATURE RELATIONSHIPS FOR THE COORDINATE AXES

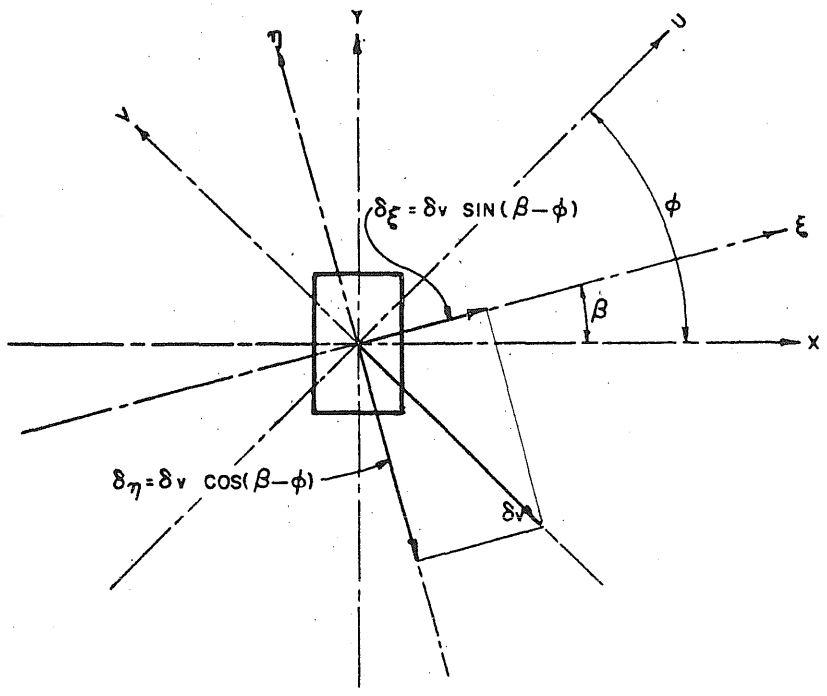

FIG. 4.6 DEFLECTION RELATIONSHIPS FOR THE COORDINATE AXES

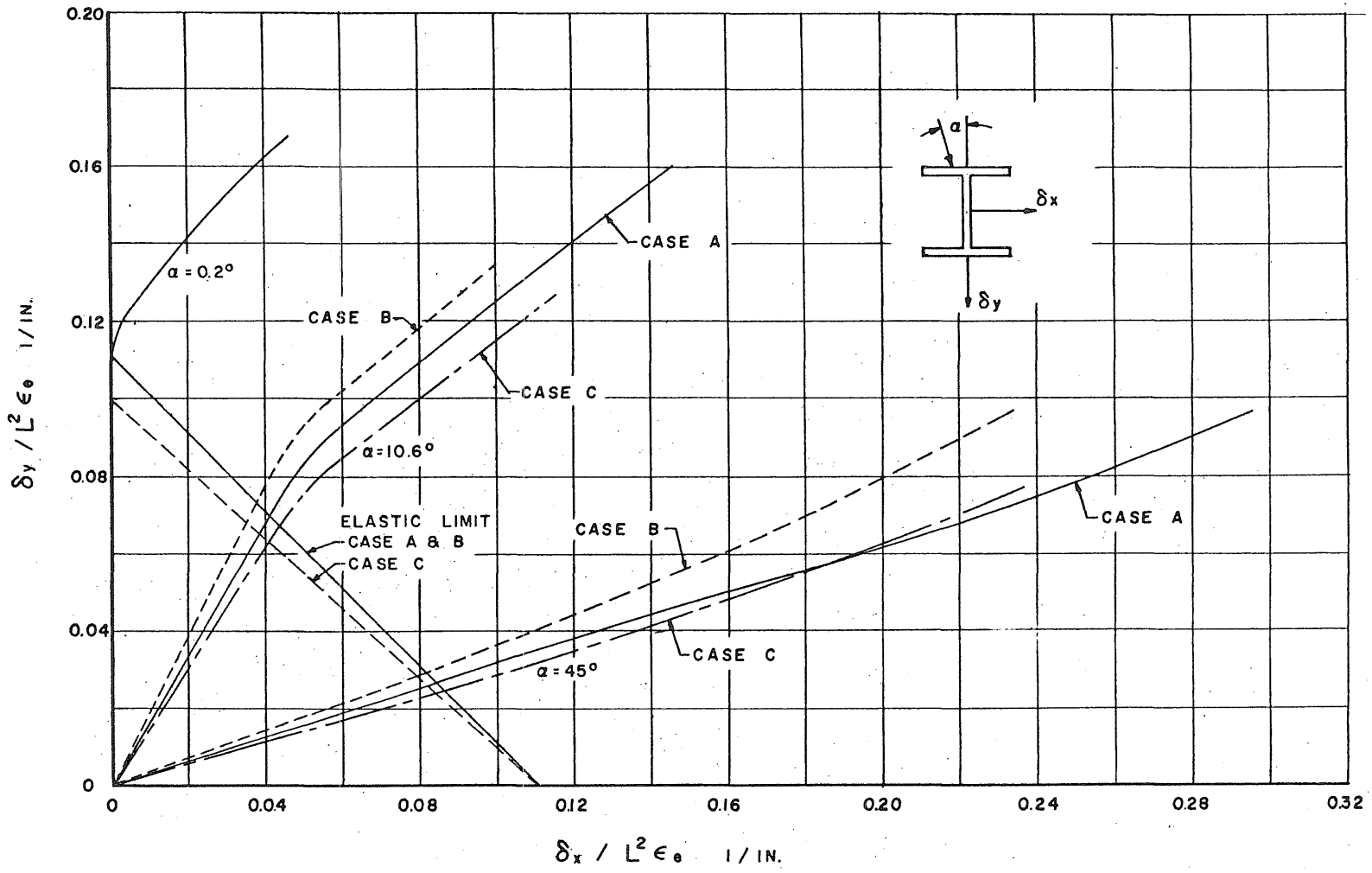

FIG. 4.7 DEFLECTION INTERACTION RELATIONSHIP FOR IDEALIZED AND SIMPLIFIED 6 B 15.5

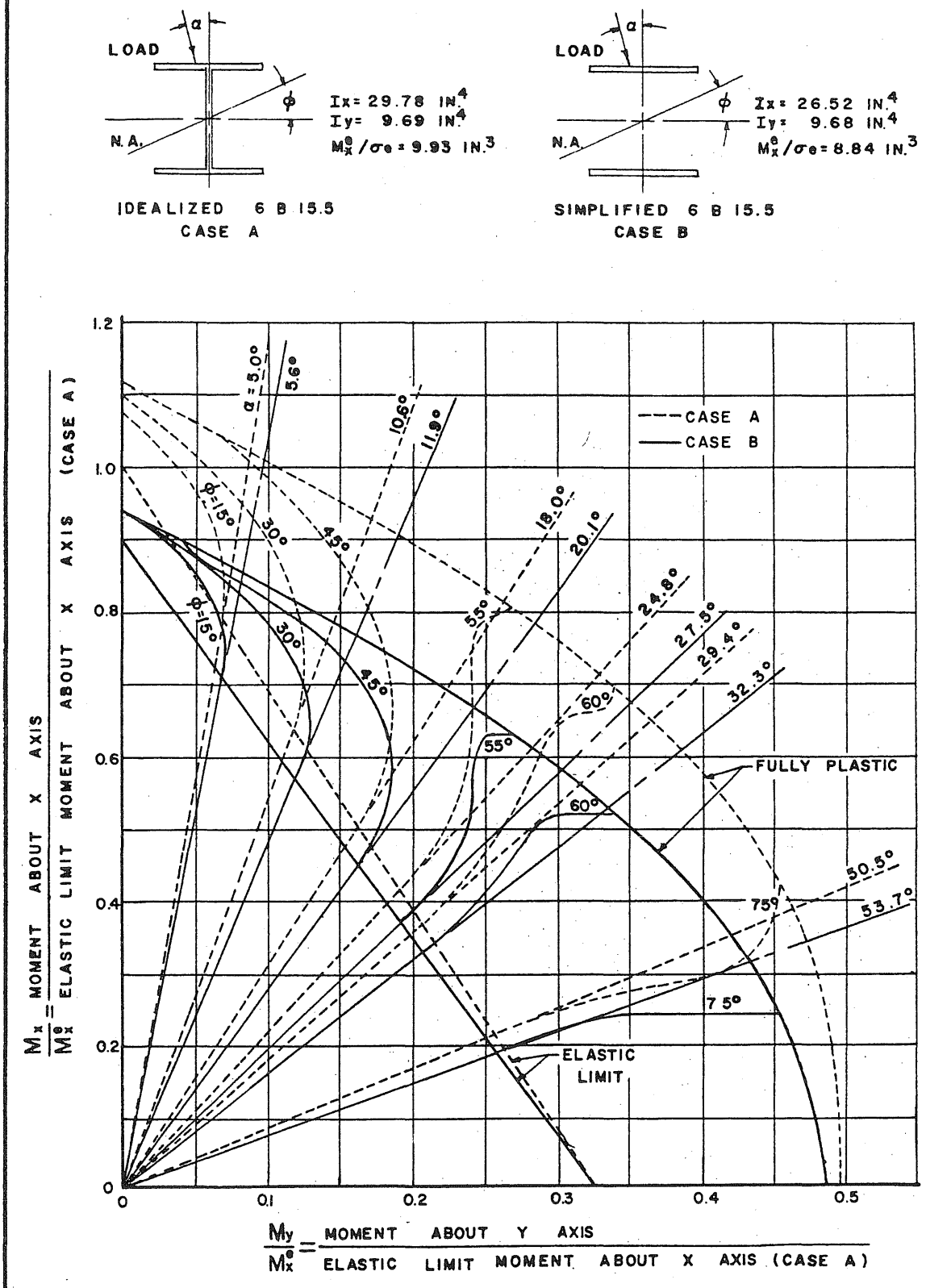

FIG. 4.8 MOMENT INTERACTION RELATIONSHIPS FOR IDEALIZED AND SIMPLIFIED 6 B 15.5

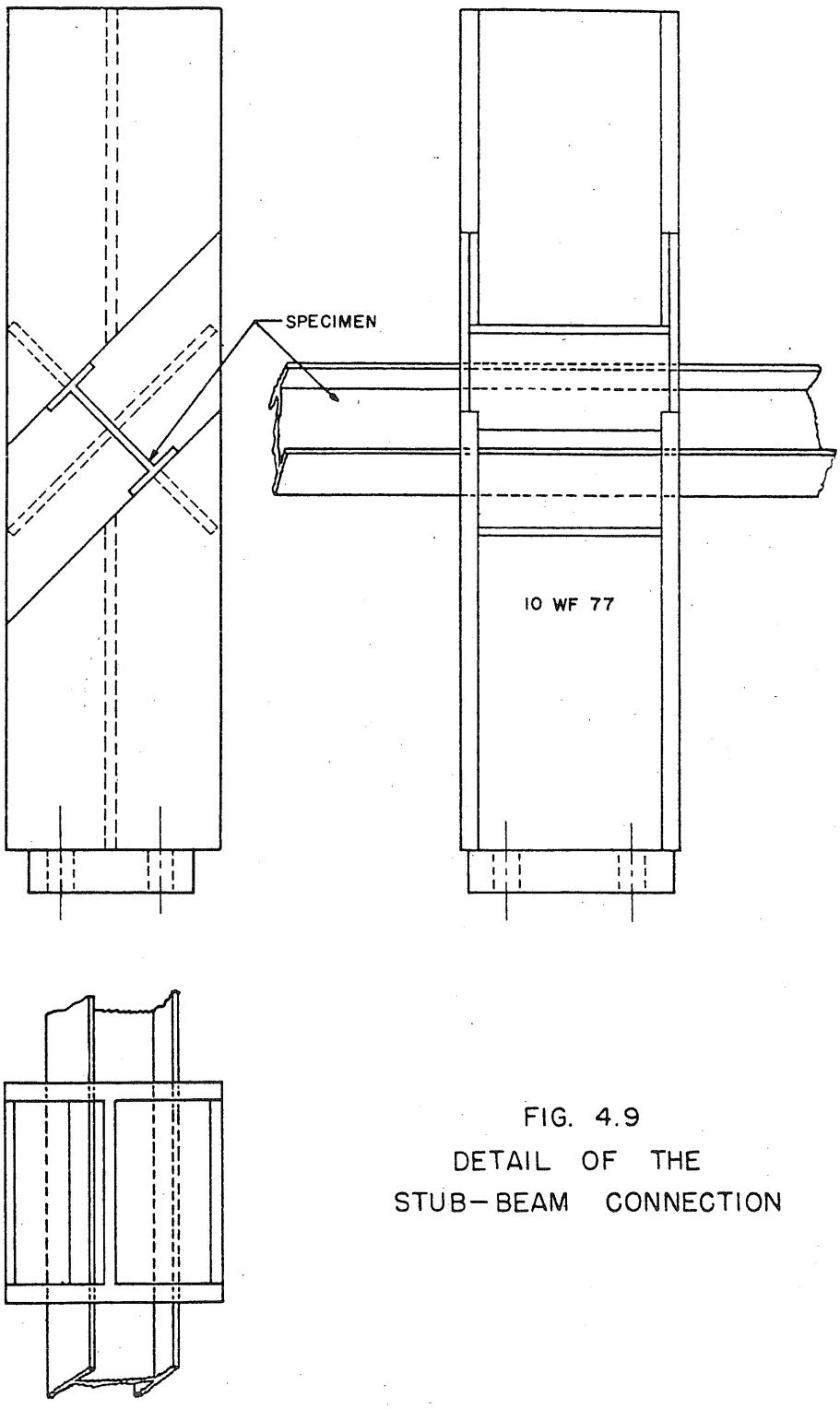

FIG. 4.9
DETAIL OF THE
STUB–BEAM CONNECTION

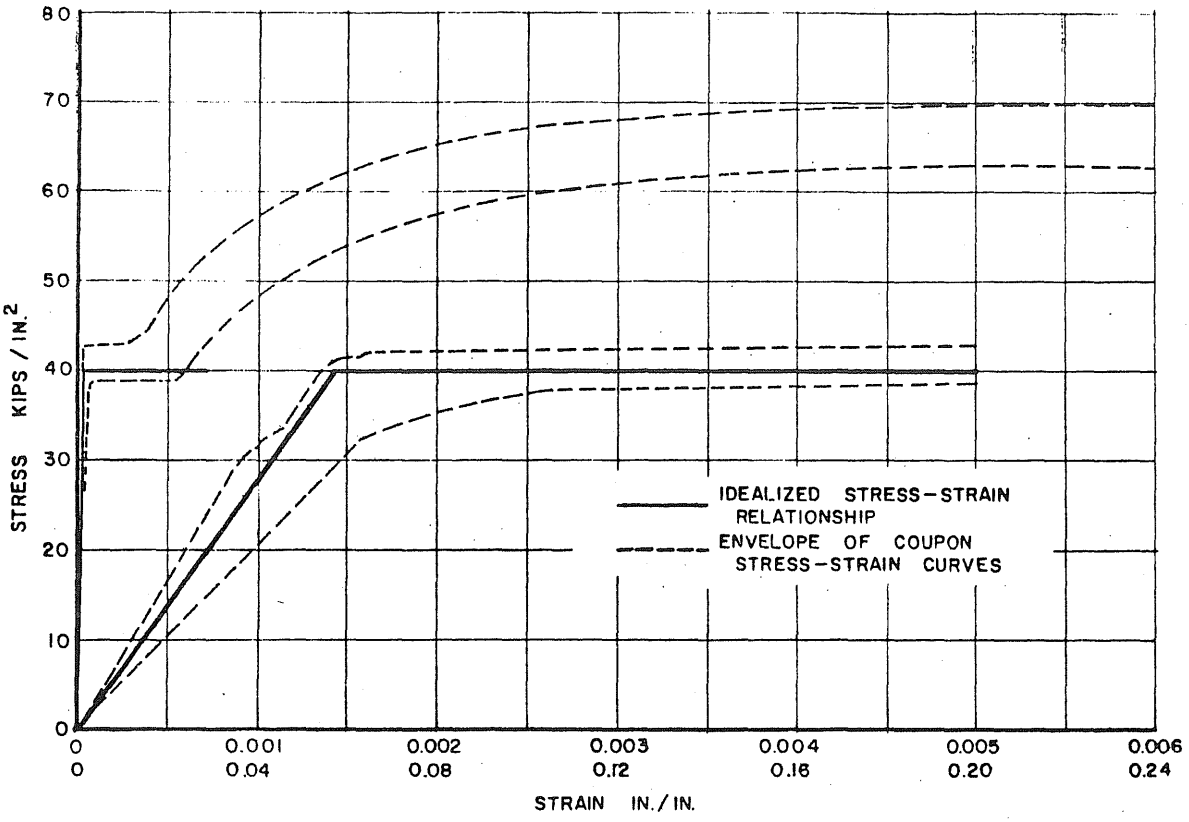

FIG. 4.10 STRESS-STRAIN RELATIONSHIP FOR SPECIMEN 4XYO S 6B

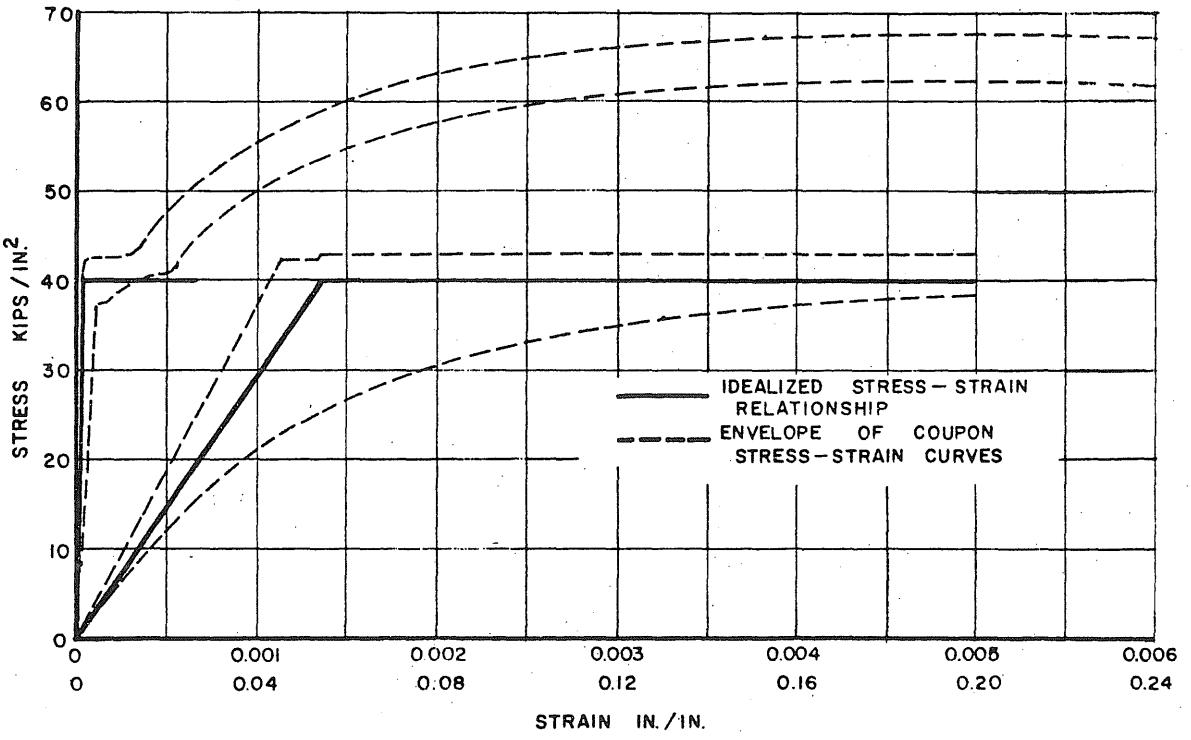

FIG. 4.11 STRESS-STRAIN RELATIONSHIP FOR SPECIMEN 4XYI S 6B

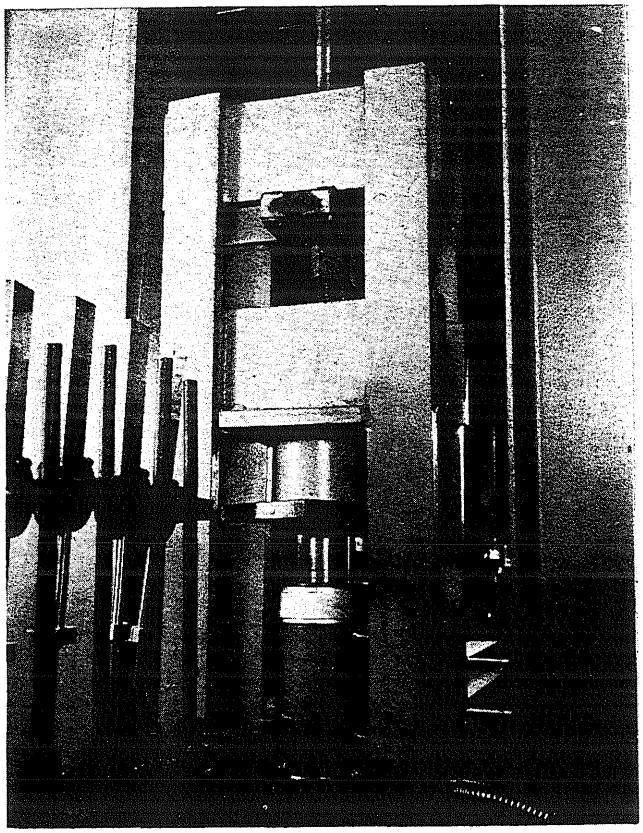

Fig. 4.12

Lateral Loading Unit

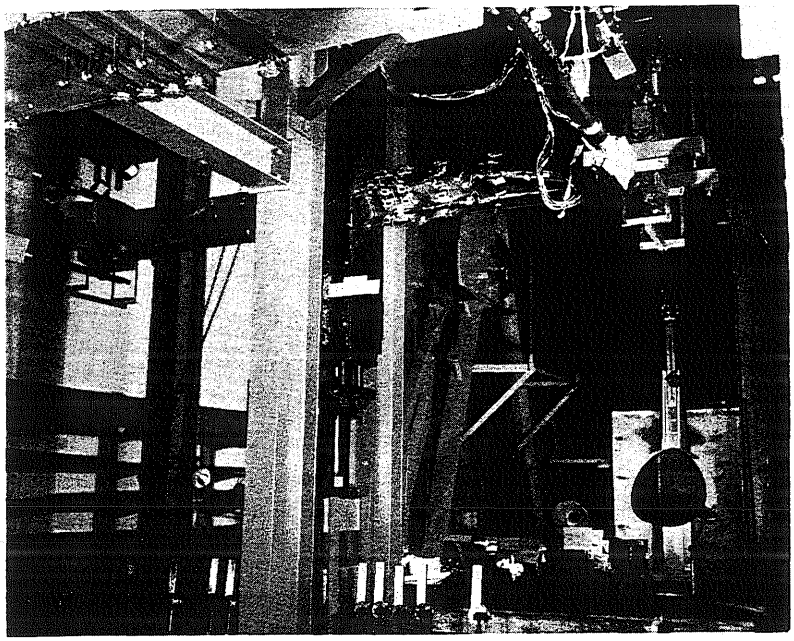

Fig. 4.13 Center Restraining System

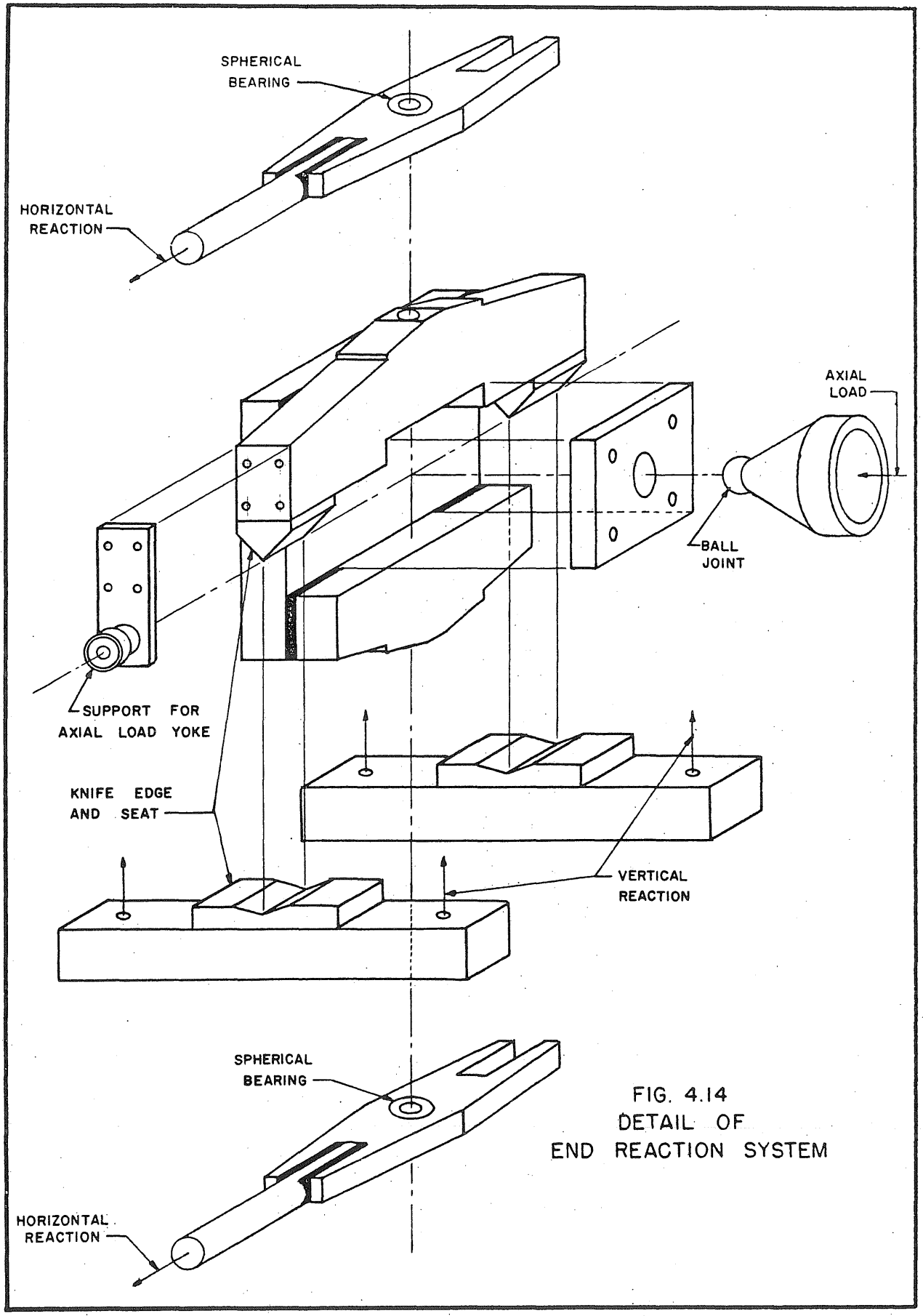

FIG. 4.14
DETAIL OF
END REACTION SYSTEM

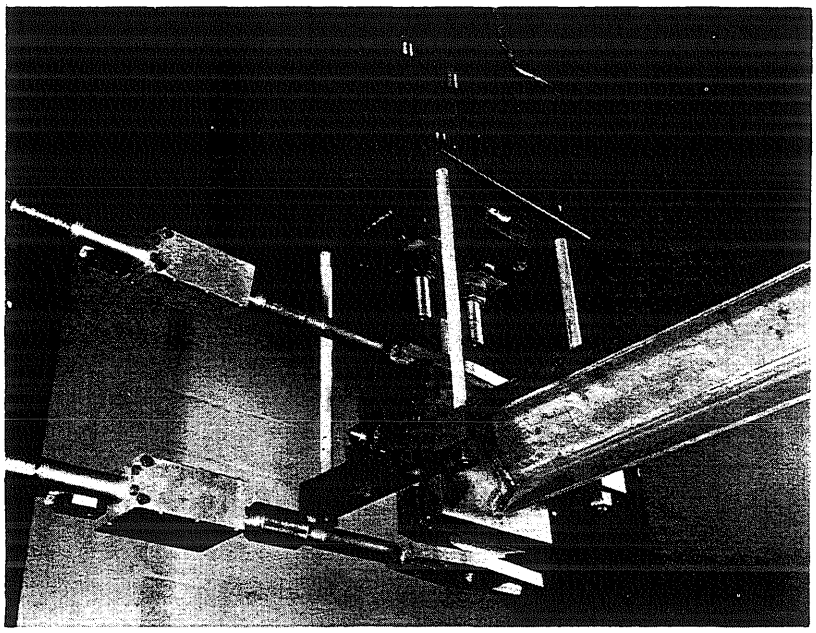

(a)

(b)

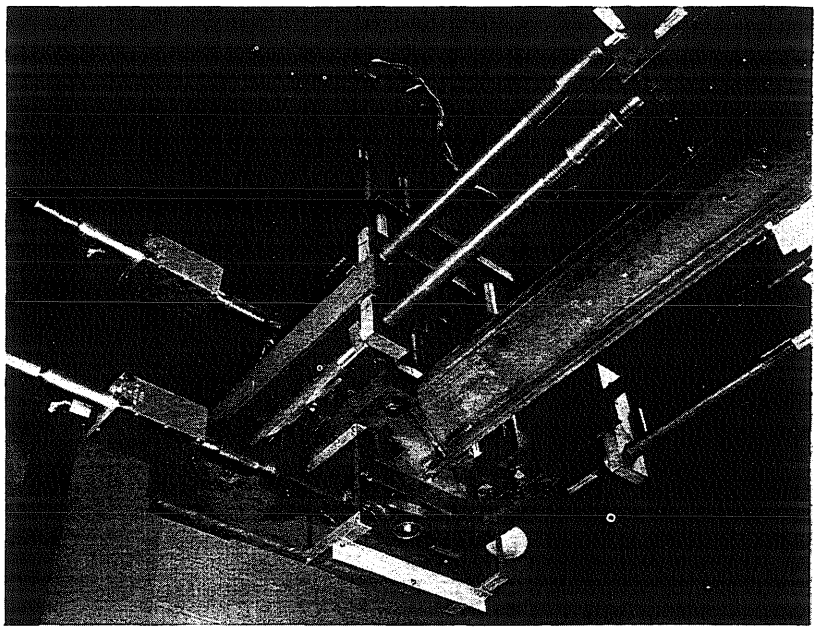

Fig. 4.15 South End Reaction System
(a) Without Axial Load
(b) With Axial Load

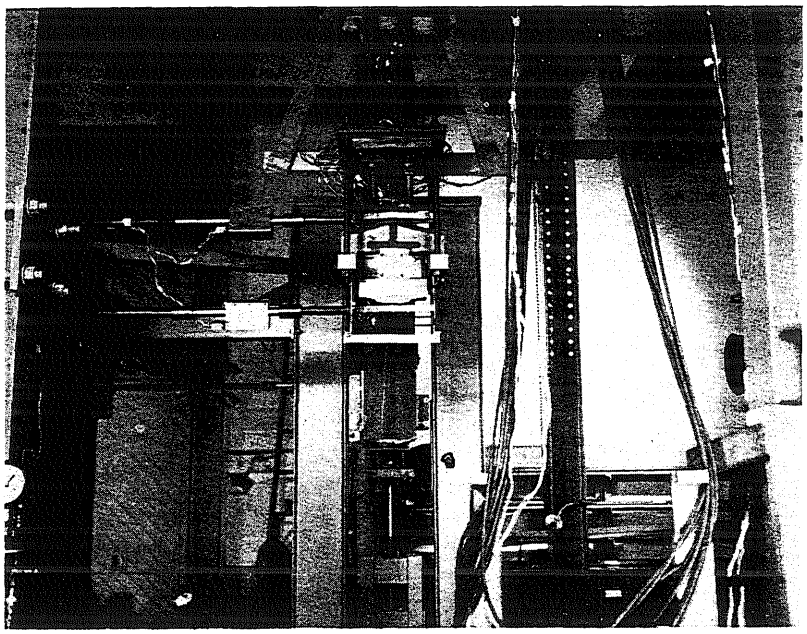

(a)

Fig. 4.16

North End Reaction System
(a) Without Axial Load
(b) With Axial Load

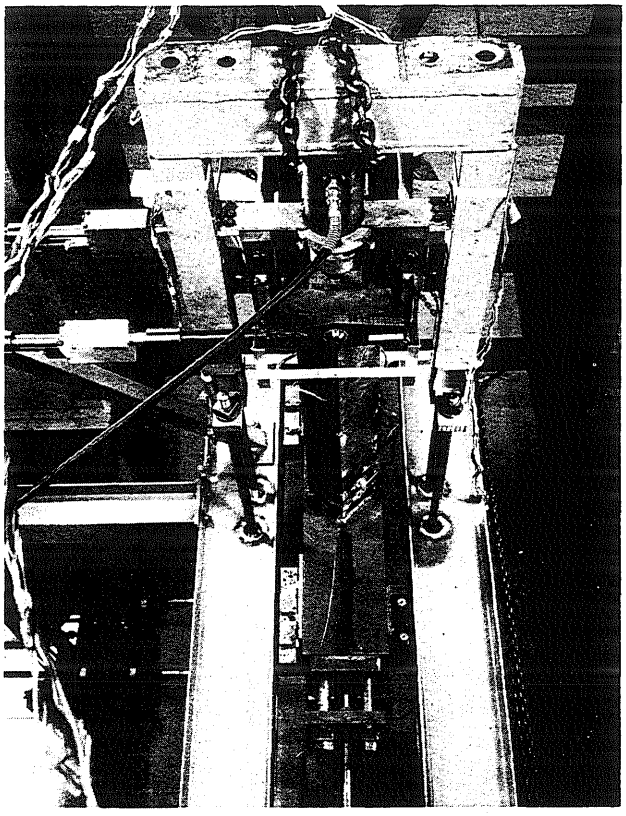

(b)

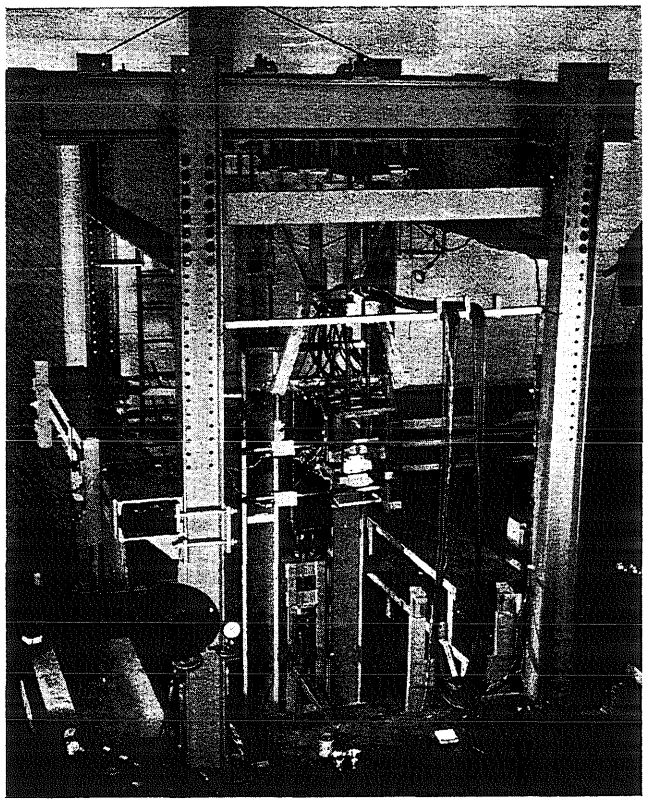

Fig. 4.17 The Entire Test Set-up

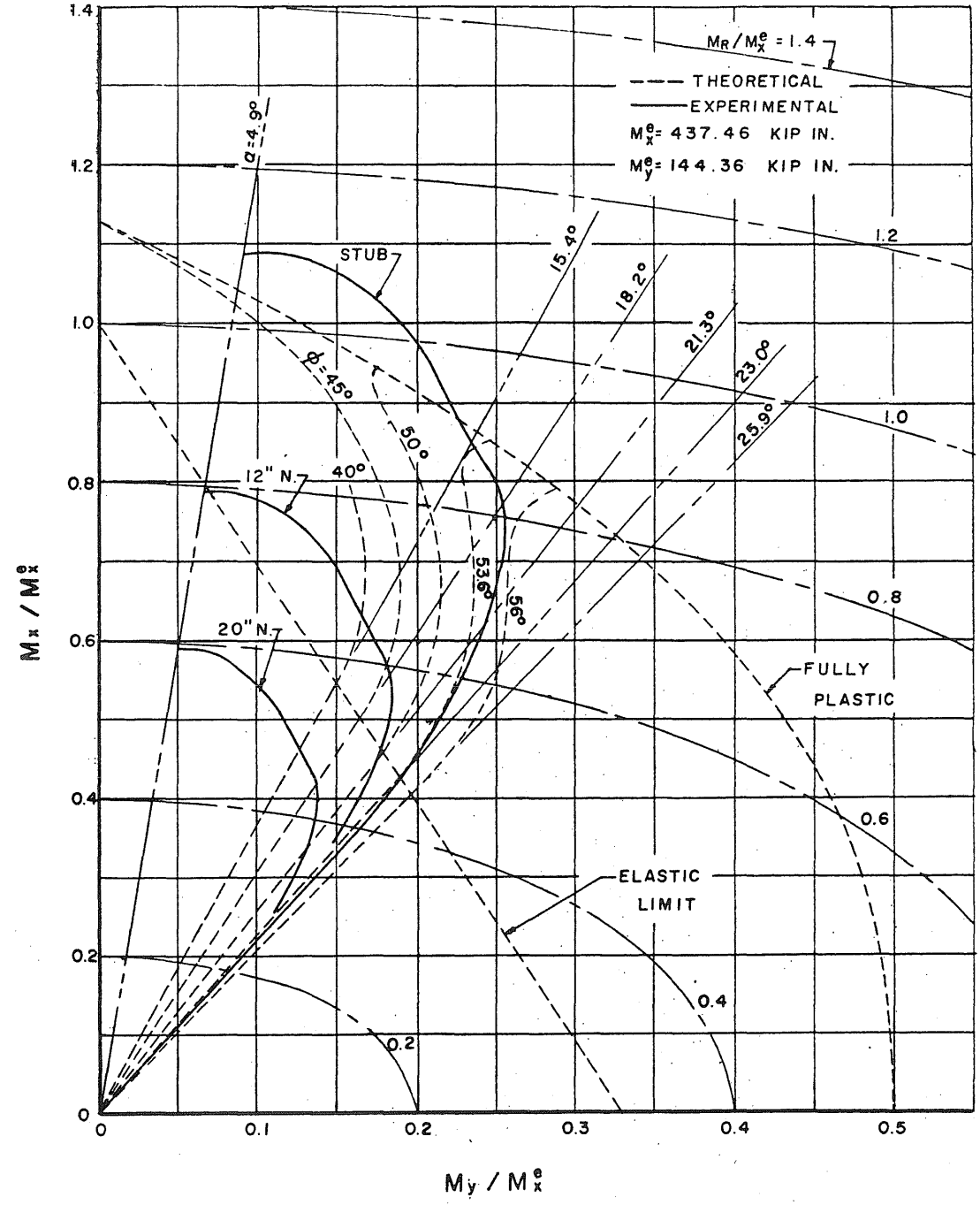

FIG.4.18 MOMENT INTERACTION RELATIONSHIP FOR SPECIMEN 4XYOS6B

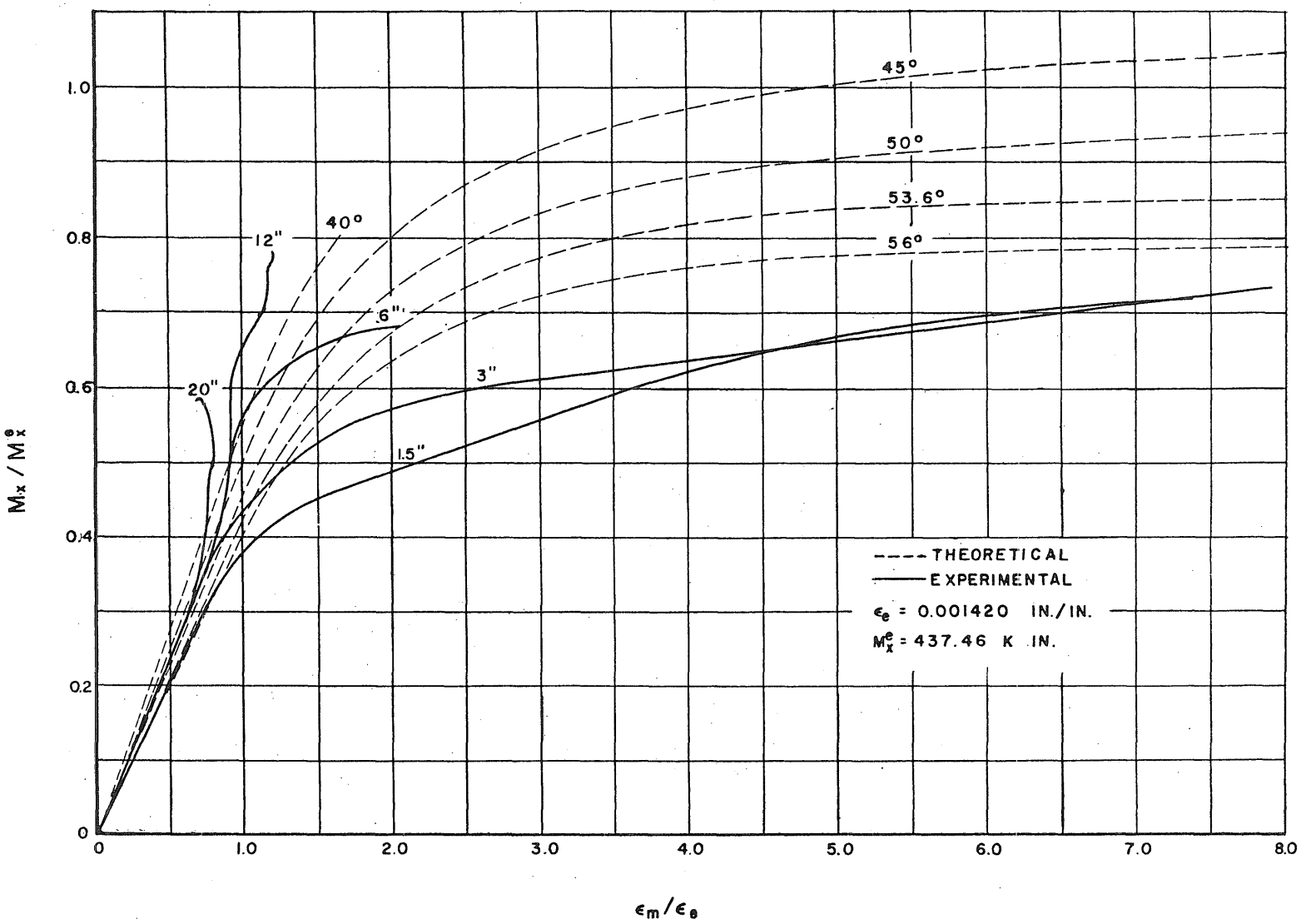

FIG. 4.19 MOMENT — STRAIN RELATIONSHIP FOR SPECIMEN 4XYOS6B

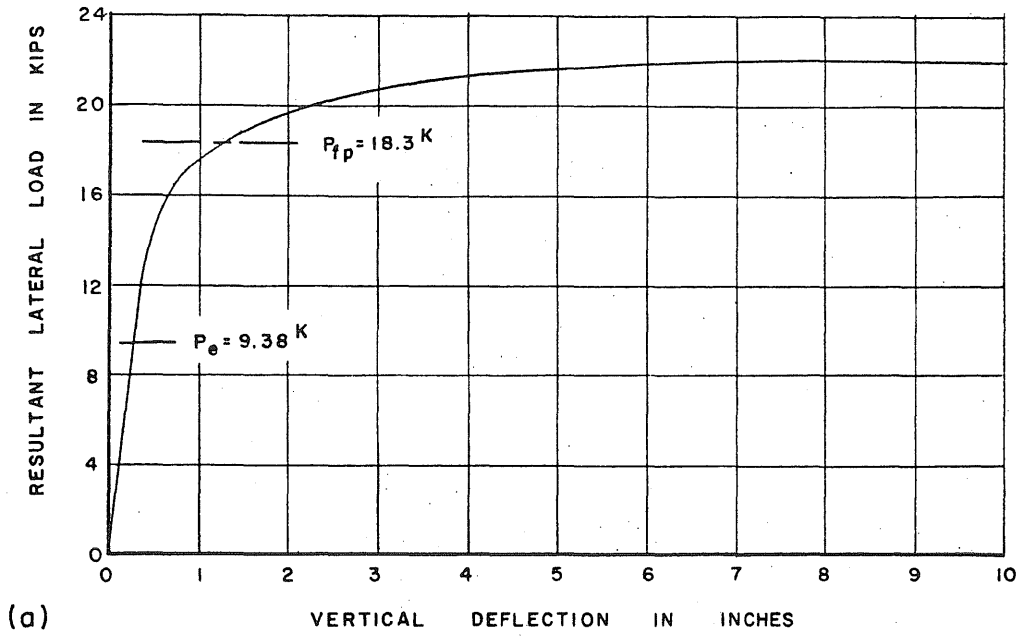

(a)

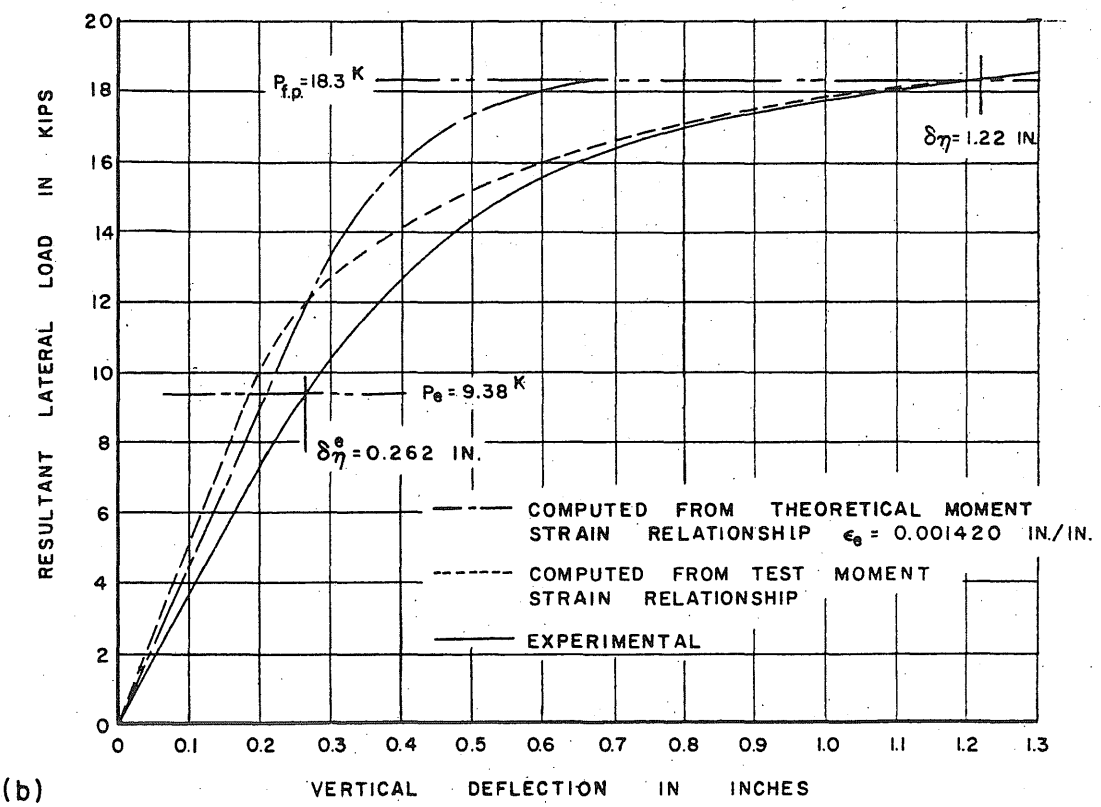

(b)

FIG. 4.20 RESULTANT LATERAL LOAD — VERTICAL DEFLECTION RELATIONSHIP FOR SPECIMEN 4XYOS6B

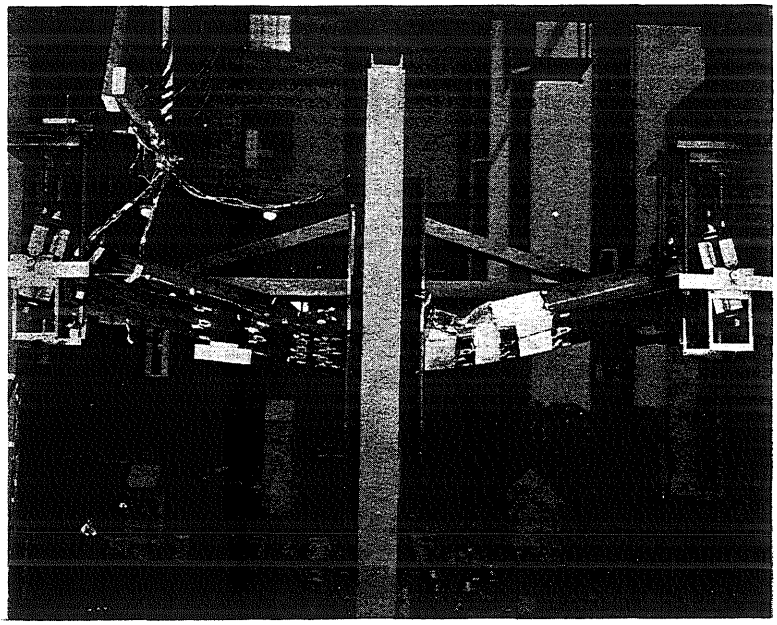

Fig. 4.21 Specimen 4XYO S 6 B After the Test

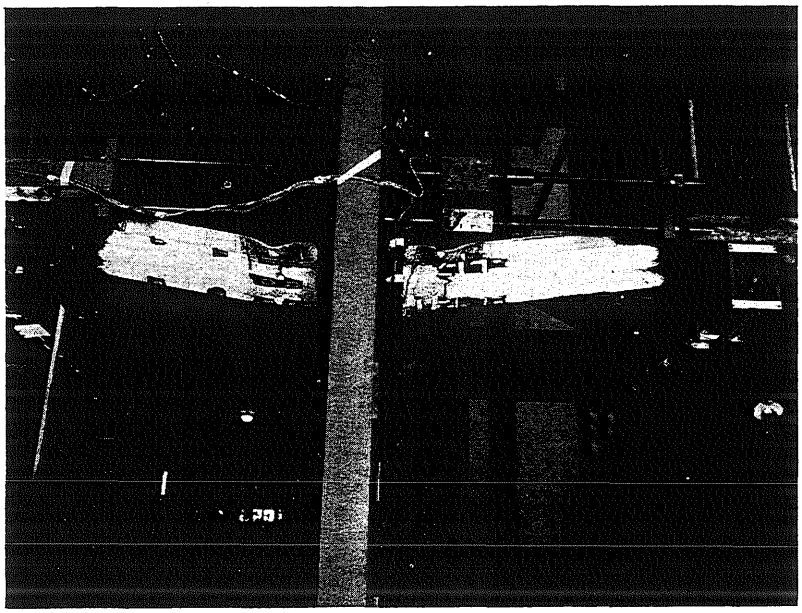

Fig. 4.22 Specimen 4XY1 S 6 B After the Test

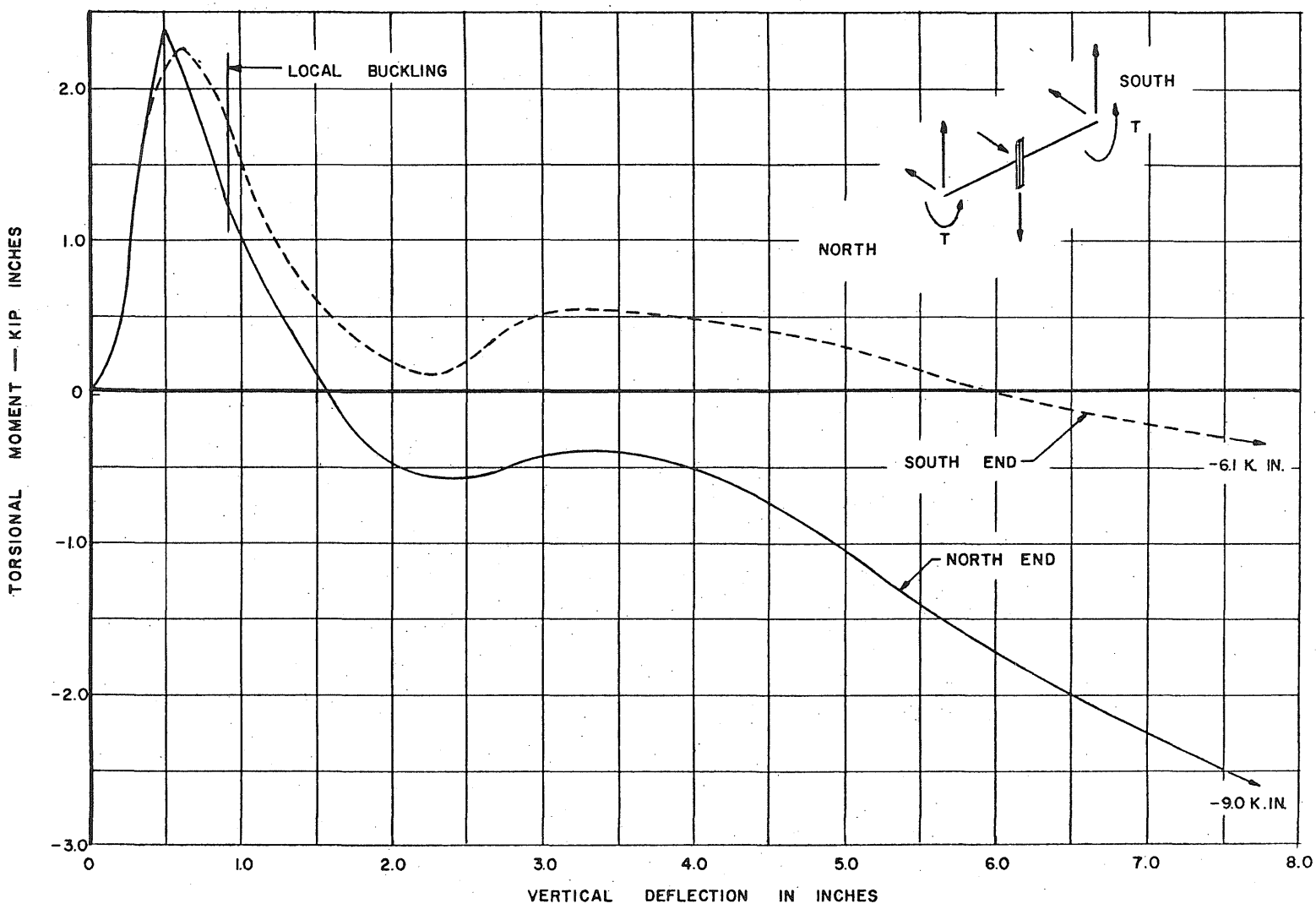

FIG. 4.23 MEASURED TORSIONAL MOMENT — VERTICAL DEFLECTION RELATIONSHIPS

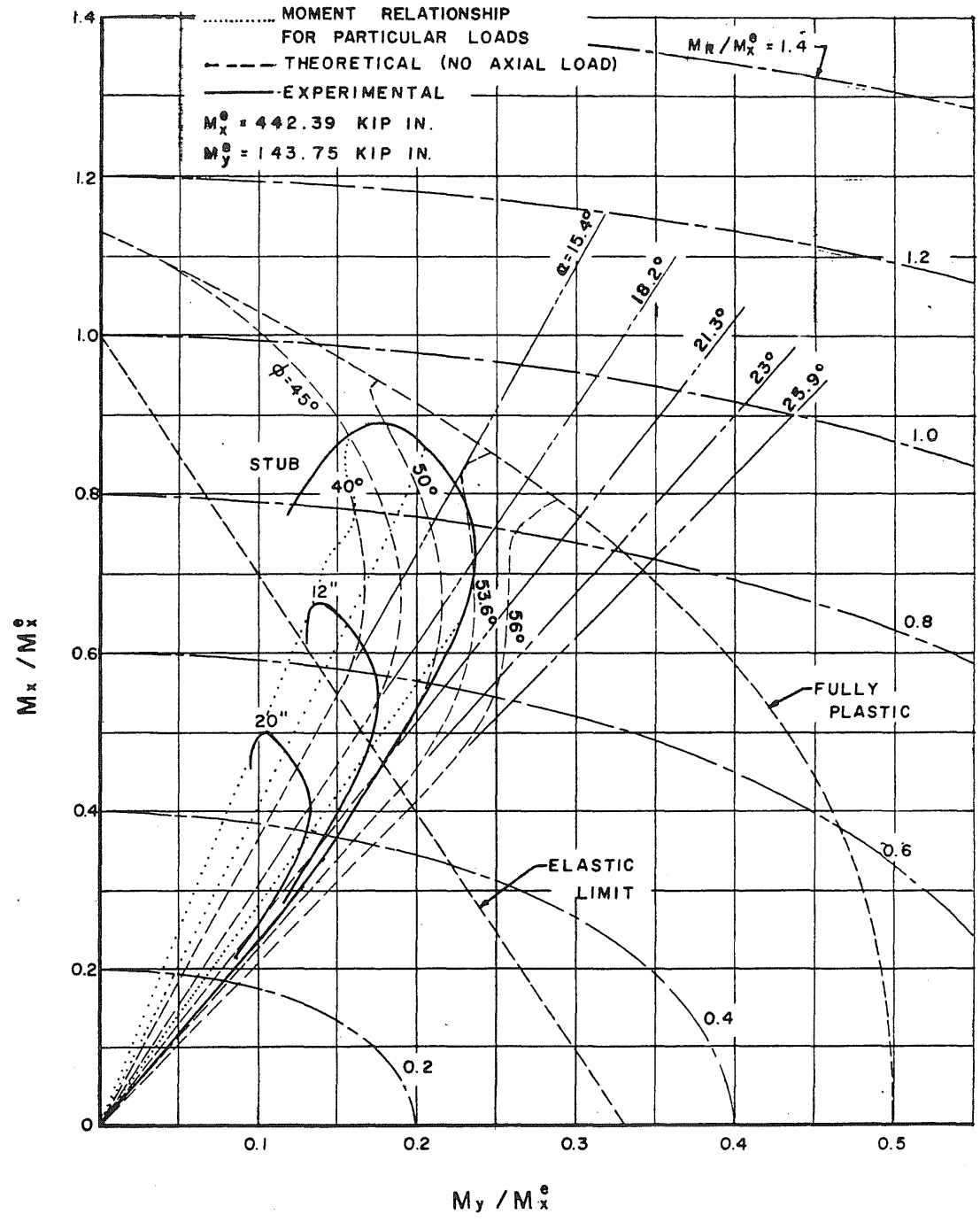

FIG.4.24 MOMENT INTERACTION RELATIONSHIP FOR SPECIMEN 4XYIS6B

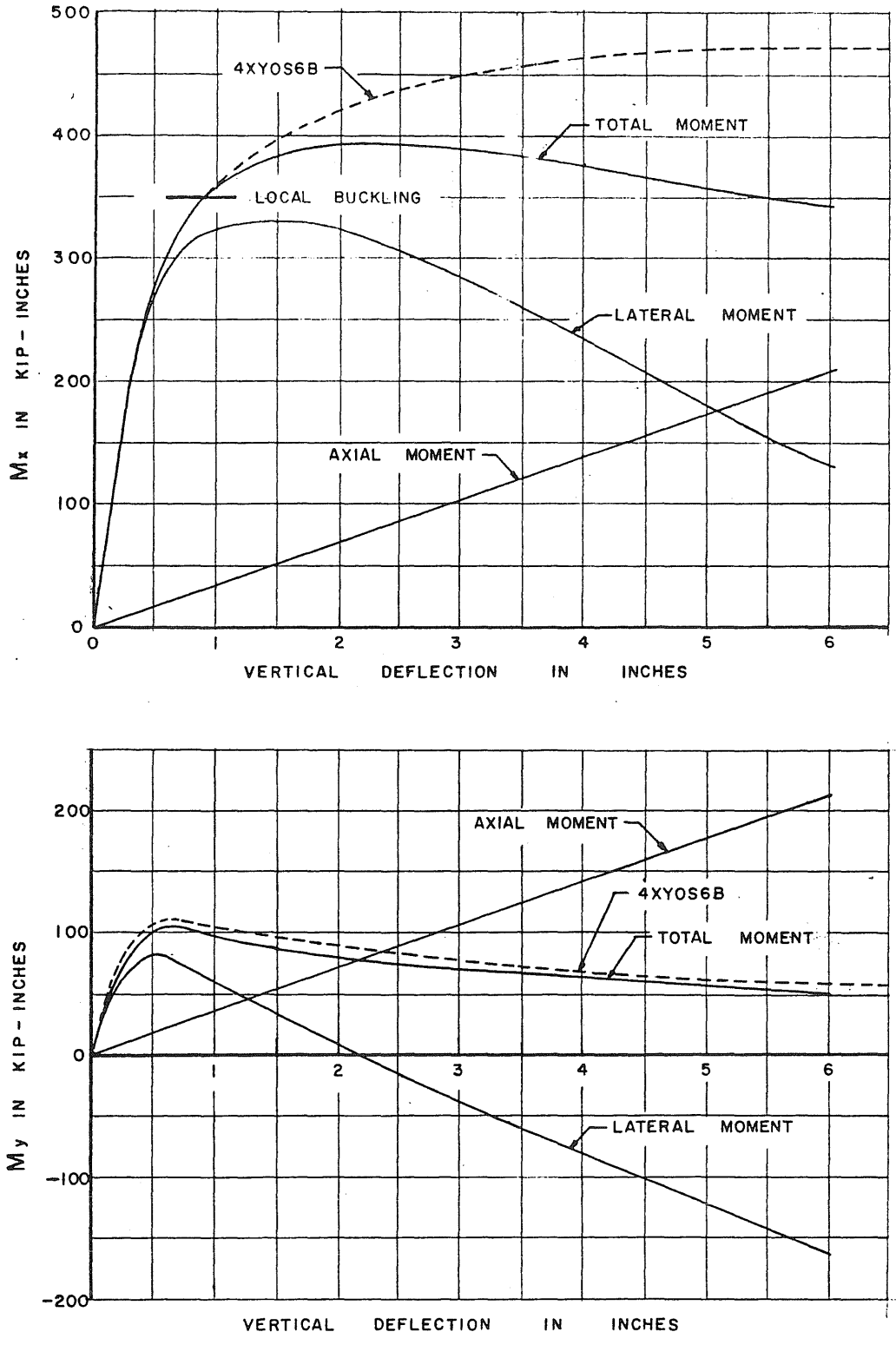

FIG. 4.25 MOMENT — DEFLECTION RELATIONSHIPS FOR SPECIMEN 4XYIS6B

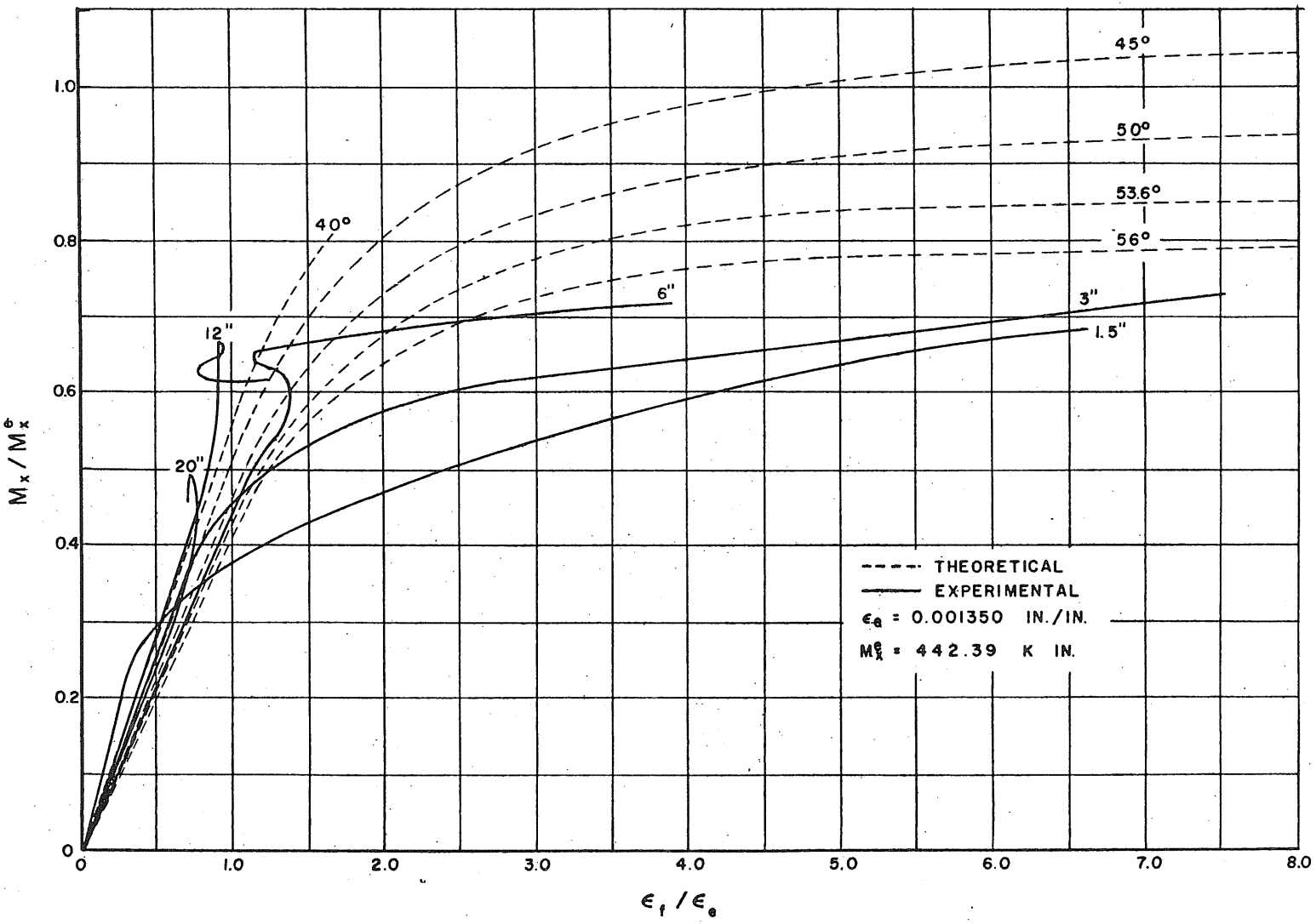

FIG. 4.26 MOMENT — FLEXURAL STRAIN RELATIONSHIP FOR SPECIMEN 4XYIS6B

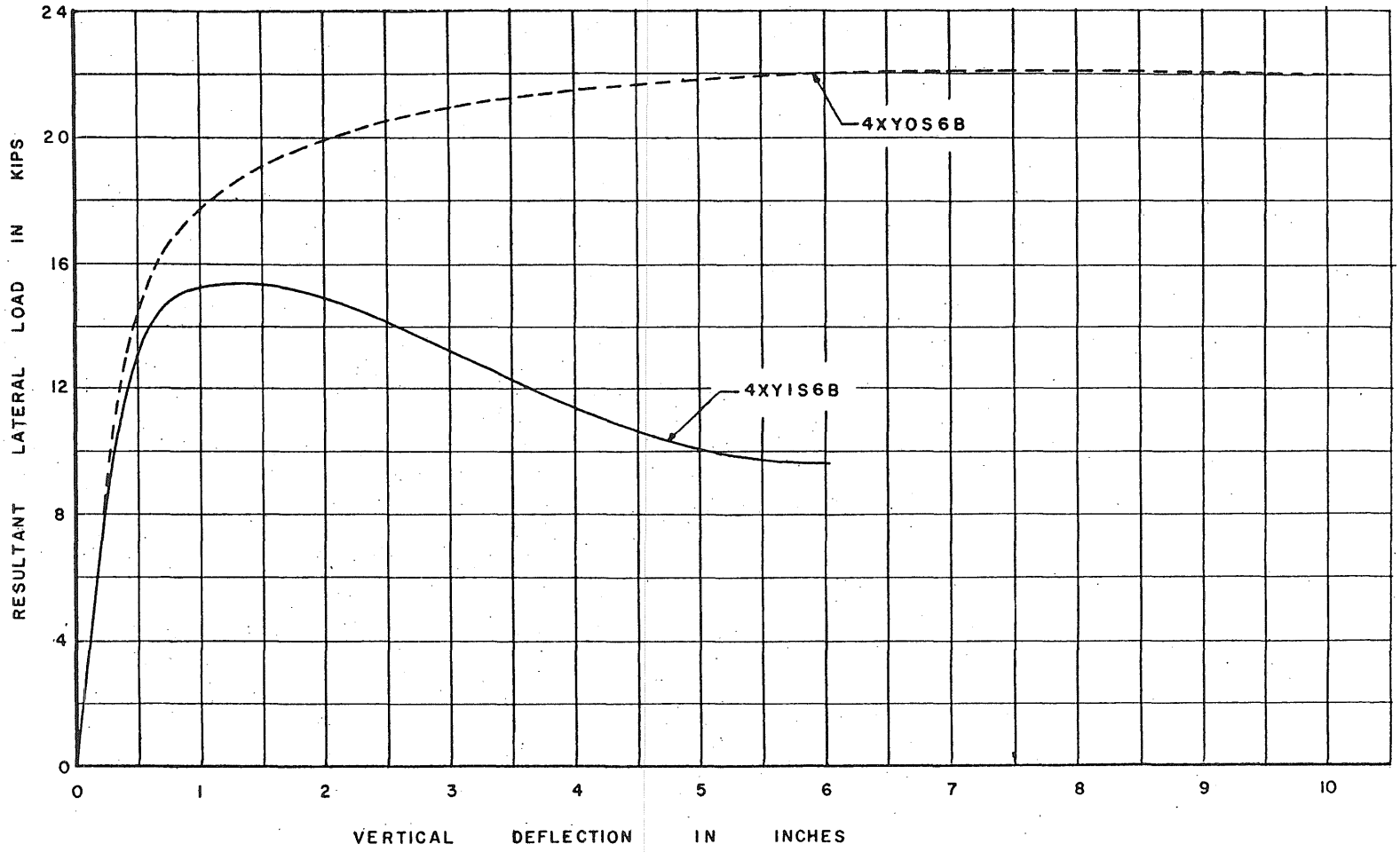

FIG. 4.27 RESULTANT LATERAL LOAD — VERTICAL DEFLECTION RELATIONSHIP FOR SPECIMENS 4XYIS6B AND 4XYOS6B

5. DYNAMIC RESPONSE OF BEAMS

5.1 INTRODUCTION

The study of the response of dynamically loaded beams requires the evaluation of the dynamic resisting function. Thus the problem is to define the parameters which affect the dynamic resistance and to correlate these parameters with those that determine the static resistance.

For a dynamically loaded beam, the resistance in the form of a moment-curvature, moment-deflection or similar type of relationship requires knowledge of the elastic resistance, a criterion for determining when inelastic action starts, and the nature of the resistance after yielding. The first requirement, knowledge of the elastic resistance, has been rigorously studied by many investigators and offers no serious problem for this program. For this region of the resistance, simplifications in the form of single-degree-of-freedom models can be made and reasonable estimates of the response computed without difficulty.

The establishment of a criterion to determine when yielding starts has been found to be of considerable importance in estimating the dynamic resistance. Statically, the yield stress, as determined by static tension tests of the material, provides the required criterion for the structures of interest here. However, when the material is loaded dynamically the upper yield stress at which general yielding starts depends on variables such as the strain rate, the excess stress, and the past loading history. The studies by Clark and Wood[1]*,[2],

---

* Numbers in parentheses refer to correspondingly numbered articles in the Bibliography at the end of this section.

have shown that mild steel can be subjected to high stresses without yielding for some time. In their study, the applied stress at yielding is related to the time required for the material to yield. Unfortunately, the stress-time relationship in a dynamically loaded beam rarely is constant and the available data are not applicable. In order to overcome this difficulty, a criterion, based on the available data, has been formulated. This criterion, which is, in a sense, empirical, is described in the next section.

The nature of the dynamic resistance after yielding is still somewhat doubtful. Some information is contained in the work by E. A. Davis[3] and Manjoine[4], which has been summarized by Nadai[5]. These data indicate that the resistance after yielding is sensitive to the strain rate and history of the strain. However, a considerable amount of further work will be required before the significance of this variability can be noted.

When the required parameters and their inter-relationship in the formulation of the resistance are known, any of the available analyses techniques can be used if proper consideration is given to the time-dependence of the phenomenon. However, further study is required before definite recommendations can be made.

5.2 CRITERION FOR DETERMINING THE DYNAMIC YIELD STRESS

Recent studies of the dynamic upper yield stress for mild steel by Clark and Wood[1],[2] have shown that, for constant stress conditions, a stress greater than the static upper yield stress can be sustained by the material for some time before yielding occurs. In their investigations

the delay time, the time during which the material is subjected to the increased stress without yielding, is reported as a function of the stress. These tests indicate, as shown in Fig. 5.1, that the log of the delay time is a linear function of the stress. In this section, an analytical statement of the criterion for yielding, based on these data, will be presented.

In the criterion it is assumed that the condition of the material with respect to general yielding can be described by a parameter φ such that when $\varphi \geq \varphi_c$ general yielding occurs and when $\varphi < \varphi_c$ the material is essentially elastic. The parameter φ is assumed to be related to instantaneous excess stress, $\delta\sigma$, which is the applied stress minus the static upper yield point, by

$$\frac{d\varphi}{dt} = f\left(\frac{\delta\sigma}{\sigma_y}\right) = f(z) \qquad (1)$$

where σ_y = the static upper yield point of approximately 40 ksi.

$\sigma - \sigma_y$ = the excess stress = $\delta\sigma$.

Thus it is assumed that the time rate of change of φ is some unknown function of the excess stress ratio z.

From the test results reported by Clark and Wood, the function f(z) can be determined. For the constant stress condition, we have the relation $z = z_m$, where z_m is the stress ratio of the applied stress, and Eq. (1) becomes:

$$\frac{d\varphi}{dt} = f(z_m) \qquad (2)$$

If the time is measured so that when t = 0, φ = 0, then, from Eq. (2),

$$\varphi = f(z_m)t \tag{3}$$

When the time equals the delay time t_d, φ equals φ_c and general yielding occurs. Therefore f(z) is, from Eq. (3),

$$f(z) = \frac{\varphi_c}{t_d}$$

From the Clark and Wood test results the relationship between the delay time and the stress is

$$t_d = e^{-kz}$$

where σ_y = 40,000 psi

k = 12.28

so that the function f(z) can be written as

$$f(z) = \varphi_c \, e^{kz} \tag{4}$$

From (4) the general expression for the criterion of yielding is

$$\frac{\varphi}{\varphi_c} = \int_o^t e^{kz(\tau)} \, d\tau + C \tag{5}$$

where $z = z(\tau)$ is the stress time history and yielding occurs when $\varphi/\varphi_c = 1.0$.

Because of the form of f(z), analytical solutions for arbitrary loading conditions are difficult to obtain. However, expressions for the change in φ are readily obtained for conditions of constant stress

and constant strain-rate. Since the changes in φ can be summed for intervals for which one of these conditions occur, it is possible to determine approximately when yielding occurs by replacing the given stress or strain-time relationship by a series of straight lines and summing, from the start of the loading, the changes in φ for each interval. When the sum equals one, general yielding occurs.

For a constant stress test in which $z = z_m$, the value of φ at any time t is

$$\frac{\varphi}{\varphi_c} = te^{kz_m} + C$$

where C is an arbitrary constant determined by the initial conditions. If the conditions are such that when $t = 0$, $\varphi/\varphi_c = \varphi_o/\varphi_c$ then

$$C = \frac{\varphi_o}{\varphi_c}$$

and the change in

$$\frac{\delta\varphi}{\varphi_c} = \frac{\varphi - \varphi_o}{\varphi_c} = te^{kz_m}$$

However, since $t_d = e^{-kz_m}$ Eq. (6) can be written as

$$\frac{\delta\varphi}{\varphi_c} = \frac{t}{t_d} \qquad (7)$$

For constant strain rate conditions, the loading is

$$z(t) = z_o + \frac{\dot{\epsilon}}{\epsilon_y} t$$

where z_o = the excess stress ratio at t = 0

$\dot{\epsilon}$ = the strain rate in in. per in. per sec.

ϵ_y = the strain corresponding to the static upper yield stress.

The change in φ for this condition is, from (5),

$$\frac{\delta\varphi}{\varphi_c} = \frac{\varphi - \varphi_o}{\varphi_c} = \frac{\epsilon_y}{k\dot{\epsilon}} \left[e^{kz} - e^{kz_o} \right] \qquad (8)$$

where z = the excess stress ratio at the end of the interval,

z_o = the stress ratio at the start of the interval and

$\varphi_o/\varphi_c = \varphi/\varphi_c$ at the start of the interval.

5.3 DYNAMIC TEST OF SPECIMEN 46 D 3 I 7.5

5.3.1 Introduction

This specimen was tested to determine when yielding occurred and to obtain information on the nature of the dynamic resistance after yielding.

The specimen similar to the one shown in Fig. 5.2, was a simply supported beam, with an effective span of 80 in., formed from a 3 I 7.5 section oriented in the strong direction with respect to the applied lateral load. The lateral load was applied by a 500 lb weight falling from a predetermined height and was measured by means of a dynamometer placed between the weight and the stub system at the center of the beam. The specimen was subjected to a series of loadings so that a variety of energy input conditions, as summarized in Table 5.1, could be studied.

5.3.2 Instrumentation

In this test the applied load, the deflected shape, and the maximum fiber strain along the length of the beam were recorded as functions of time on magnetic oscillographs. A diagram of the load and strain-recording system is shown in Fig. 5.3. The load dynamometer was an axially-loaded aluminum tube in which the load was measured by means of an SR-4 strain indicating bridge located near the specimen end of the tube. The effective strain indicated by the bridge output was related to the load applied to the specimen by statically loading the dynamometer. This procedure[6] has been shown to be satisfactory.

The maximum fiber strains were measured at ten locations along the length of the beam. A majority of the measurements were made at sections close to the stub where yielding was initiated. At each location, two gages, one on the tension and the other on the compression flange, were connected into a single bridge circuit whose output was proportional to the flexural strain component.

The deflected shape of the specimen was obtained by measuring the deflection-time relationship at the midpoint, one quarter, and three eighths points of the beam. These deflections were measured with the slide wire gages shown in Fig. 5.4. Static calibrations indicate that these gages are satisfactory for these tests. The complete deflection recording system is shown schematically in Fig. 5.5.

Since fifteen channels of records were made in this test an interlocking timing system was used to provide a consistent zero for the time scales. The interlocking system, shown in Fig. 5.6, was used

also to provide the time scale. The timing signal of 400 cps was recorded by one galvanometer in each oscillograph and the interlock was provided by the switch driven at synchronous speed which provided steps in the time trace.

5.3.3 Test Procedure

As was mentioned earlier, this specimen was subjected to a series of loadings obtained by dropping the 500 lb weight from various heights. For this beam all of the heights used should have produced measurable inelastic behavior. In performing the tests, the weight was raised to the desired height and the instruments checked. Before releasing the weight the oscillographs were started and recording continued throughout the initial loading and for several of the loadings caused by the rebounding of the weight. These later loadings, however, caused elastic response of the beam and any inelastic deformation was a result of the initial load. After the test, the final positions of the traces were recorded and the instrumentation checked. Calibration of the strain and load circuits were obtained by shunting the bridge arm with a known resistance. The deflection records were calibrated by changing the resistance of one of the arms of the bridge. The output of the bridge for the changes in resistance was related to the equivalent deflection during the static calibration of the gage.

5.3.4 Test Results

The load-time and deflection-time relationships for the various heights of drop are shown in Figs. 5.7 and 5.8, respectively. The load-time relationship shows that as the height of drop increased

the length of the pulse and the amplitude increased. However, for the last tests, the 24 and 30 in. drops, the load amplitude did not change appreciably but the pulse length increased markedly. The deflection records indicate an increase in duration and an increase in the maximum deflection with the height of drop.

The strain-time relationships for the section 2.5 in. from the stub are shown in Fig. 5.9 for the various heights of drop. These traces indicate that when yielding, indicated by permanent set, becomes general the character of the strain history is changed. This is indicated by comparing the traces for the 12 and 24 in. drops with the other traces. It should be noted that in the 6 in. drop, yielding did not occur even though strains in excess of the static elastic limit yield strain existed for an appreciable time.

In the lower part of Fig. 5.9, the strain-time relationship for various sections along the beam are shown for the 24 in. drop. As before, the strain history at the section where yielding occurs are considerably different than that of the sections that remain elastic. The strains at the 6.25 in. section, which just started to yield, and the strains at greater distances from the stub indicate one of the features noted throughout the tests. Apparently, when general yielding occurs at a section, in this case the 2.5 and 3.75 in. sections, Fig. 5.9, there is a tendency for relaxation of the strains to occur in the elastic portions of the beam. Thus the 12.5, 20 and 30 in. sections strains indicate that the maximum strain occurred approximately 18 milliseconds after the start of the test while the 3.75 in. section strain, which

yielded appreciably, reached a maximum 50 milliseconds after the atart of the loading. At the 6.25 in. section, where yielding just started, the maximum strain occurred between these time limits. The maximum center deflection for this test occurred at about 47 milliseconds after the start of the test.

Since rather complete information of the maximum fiber strains were obtained for this specimen the yield criterion, described previously, was used to determine the yield stresses at various locations along the beam. In Table 5.1 are summarized the results of this analysis. The dynamic yield stresses indicated are based on a static upper yield point of 40,000 psi. This summary shows that the dynamic yield stresses for this specimen were considerably greater than the static yield stress. In the case of the 24 and 30 in. heights of drop, the dynamic yield stress was equal to approximately the ultimate tensile strength as measured in a static tensile test of the material.

The nature of the dynamic resistance after yielding is still unknown. However, two possibilities exist: the resistance is of the same form as the static resistance but corresponds to some higher stress; or, the dynamic resistance decays from the resistance at yield to some lower level.

In order to determine if the dynamic resistance could be similar to the static resistance, the response of the beam was computed assuming some resisting function and using the measured applied load. In these computations the beam was replaced by the single-degree-of-freedom model shown in Fig. 5.10. The elastic stiffness of the model

was adjusted so that the period of the model and the beam were the same. After yielding the model was assumed to develop a resisting moment equal to the fully plastic moment of the beam section that corresponded to selected yield stresses. In determining the response of the model, the experimentally measured load was applied and the response computed using a step-by-step numerical integration procedure. The assumed resisting functions are shown in Fig. 5.11-a. In Fig. 5.11-b the computed responses are compared with the experimentally measured center deflection. These results indicate that the response is sensitive to the magnitude of the resistance as has been reported previously[7]. It should be noted that the relative magnitudes of the deflection for points where the velocity is small in the computed responses are not similar to the relative magnitudes measured in the test.

A second form of the resistance can be approximated by using the dynamic yield stresses determined previously and the deflection-time record. For the same single-degree-of-freedom model the new resisting function can be obtained as follows. The elastic range is the same as previously used. This range is terminated at the moment corresponding to the dynamic yield stress. A second point on the resisting function is, approximately, the point on a line through the measured permanent set of the center deflection, parallel to the elastic portion of the resistance, where the deflection equals the maximum measured deflection. Two resisting functions passing through this point are shown in Fig. 5.12a With these resistances and the experimental load, the computed response of the model would be as shown in Fig. 5.12b. This form of the resisting

functions seems to provide a better approximation to the response, particularly with reference to the relative magnitudes of the deflections.

5.3.5 Conclusions

From this test, and in part from the previous tests, it has been found that mild steel beams can be subjected to considerable excess stress without yielding. This phenomenon of delayed yield results in the dynamic resistance at yielding being significantly higher than the static yield resistance. The amount of increase appears to depend on the strain history of the material during the time in which it is subjected to the excess stress.

After yielding occurs, the dynamic resistance apparently decays and approaches a lower resistance which is somewhat higher than the static resistance. The nature of the resistance in this range is still uncertain and further work is required before the parameters which influence the resistance are quantitatively defined.

5.4 BIBLIOGRAPHY

1. Wood, D. S., and Clark, D. S., "The Influence of Temperature Upon the Time Delay for Yielding in Annealed Mild Steel," Proc. ASM, (1951)

2. Vreeland, T., Wood, D.S., and Clark, D. S., "A Study of the Mechanism of the Delayed Yield Phenomenon," Proc. ASM, (1952)

3. Davis, E. A., "The Effect of the Speed of Stretching and Rate of Loading on the Yielding of Mild Steel," Journ. Applied Mech., Vol. 5, Dec. (1938)

4. Manjoine, M. J., "Influence of Rate of Strain and Temperature on Yield Stresses of Mild Steel," Journ. of Applied Mech., Dec. (1944)

5. Nadai, A., "Theory of Flow and Fracture of Solids," Vol. 1, Second Edition, McGraw-Hill

6. Howland, F. L., "The Development of an Apparatus for Applying Pulse Loads to Structures," M.S. Thesis, University of Illinois, (1952)

7. Brooks, N. B. and Newmark, N. M., "The Response of Simple Structures to Dynamic Loads," Civil Engineering Studies, Structural Research Series No. 51, Univ. of Illinois, for Contract N6ori-07(06), Task Order VI, Project NR-064-183

TABLE 5.1

SUMMARY OF THE TEST RESULTS

Drop Number	Weight Used For Applying Load lbs	Height of Drop in.	Center Deflection in.		Minimum Fiber Stress At Initiation of Yielding					
					1-1/4 in. Section		2-1/2 in. Section		3-3/4 in. Section	
			Maximum	Permanent Set	$\frac{\sigma_{yd}}{\sigma_y}$ (1)	σ_{yd} psi	$\frac{\sigma_{yd}}{\sigma_y}$	σ_y psi	$\frac{\sigma_{yd}}{\sigma_y}$	σ_y psi
0	← Calibration →									
1	500	3	0.59	0	Elastic		Elastic		Elastic	
2	500	3	0.59	0	Elastic		Elastic		Elastic	
3	500	6	0.84	0.05	1.58	63,200	Elastic		Elastic	
4	500	6	0.87	0.06	1.58	63,200	Elastic		Elastic	
5	500	12	1.34	0.59	1.68	67,200	Elastic		Elastic	
6	500	12	1.38	----	1.68	67,200	1.51	60,400	1.40	56,000
7	← Calibration →									
8	500	24	2.14	1.38	Gage	Out	1.76	70,400	1.64	65,600
9	500	3	2.75	1.90	Gage	Out	Gage	Out	1.74	69,600

(1) Ratio of the Dynamic Stress At Initiation of Yield To the Static Upper Yield Stress for $\sigma_y \cong 40{,}000$ psi

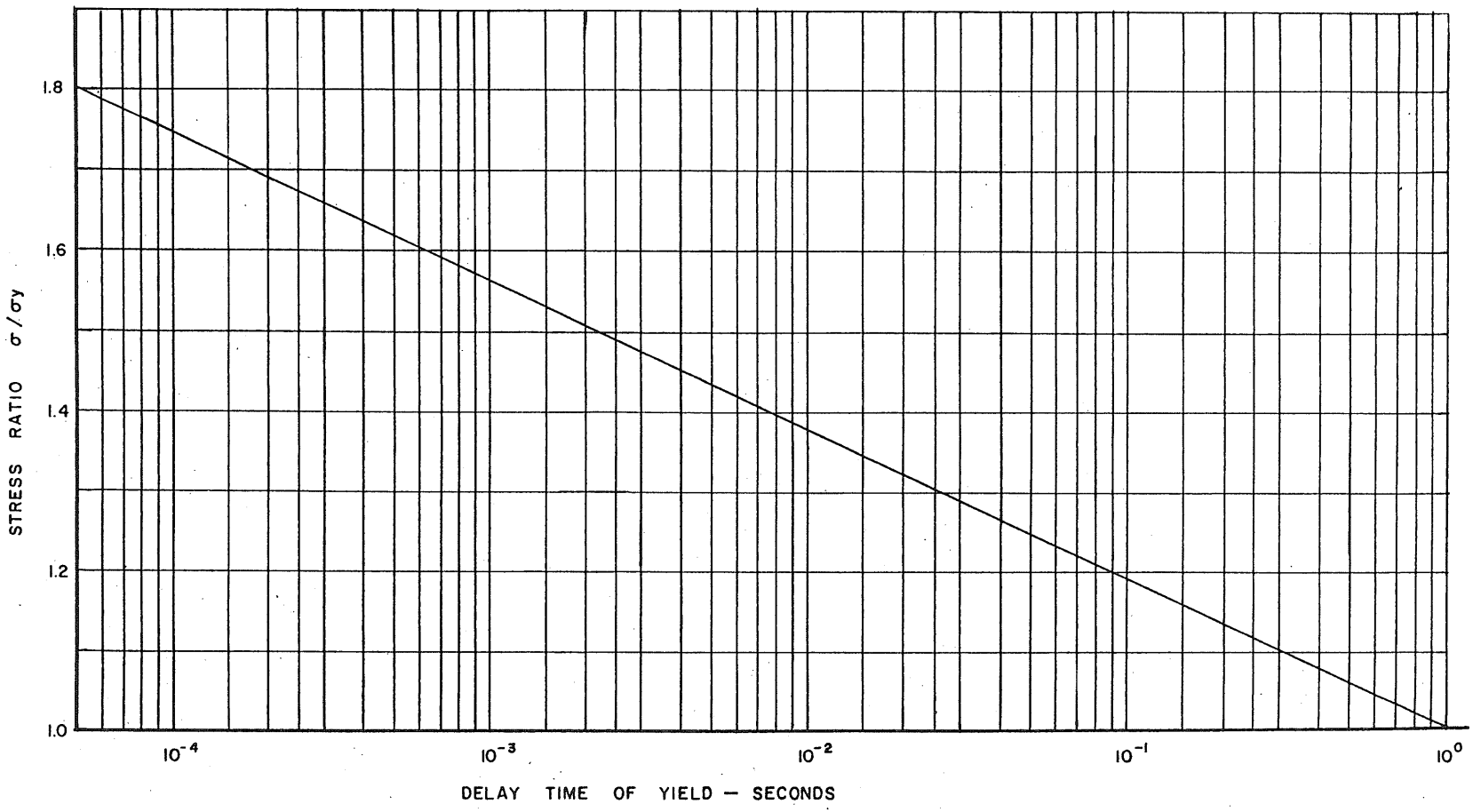

FIG. 5.1 STRESS RATIO- DELAY TIME

(From D.S. Wood and D.S. Clark, "The Influence Of Temperature Upon The Time Delay For Yielding In Annealed Mild Steel", Trans. A.S.M., Vol. 43, 1951)

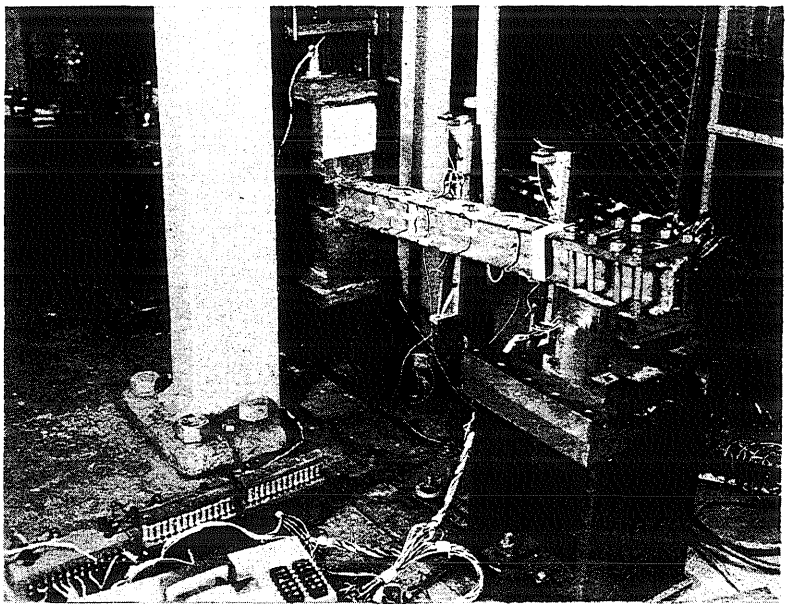

Fig. 5.2. Typical Test Specimen and Apparatus

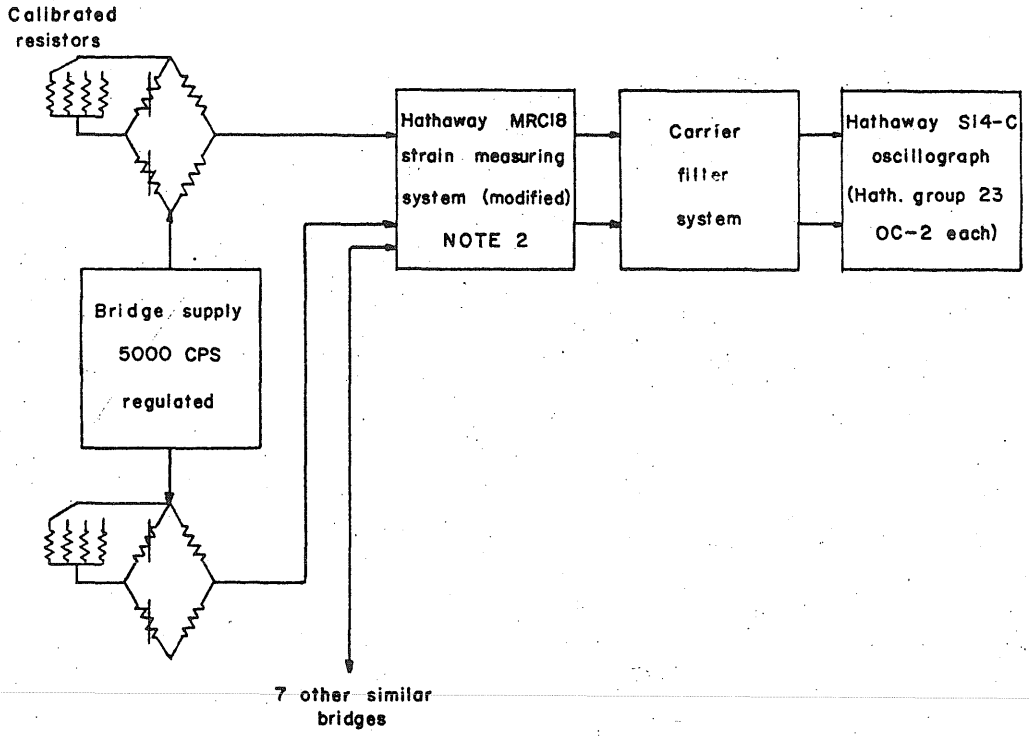

NOTE 1

Total of 7 channels of strain equipment used. (6 for strain measurements and 1 for load measurements).

NOTE 2

Standard Hathaway MRC 18 unit modified to reduce cross-talk between channels and to provide carrier supply oscillator with approximately 0.01 % regulation.

FIG. 5.3 LOAD AND STRAIN MEASURING CHANNELS

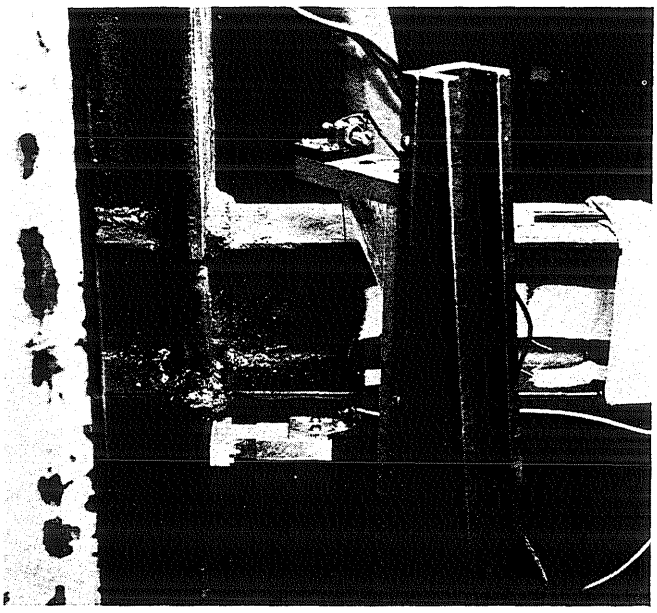

Fig. 5.4. Slide Wire Deflection Gage

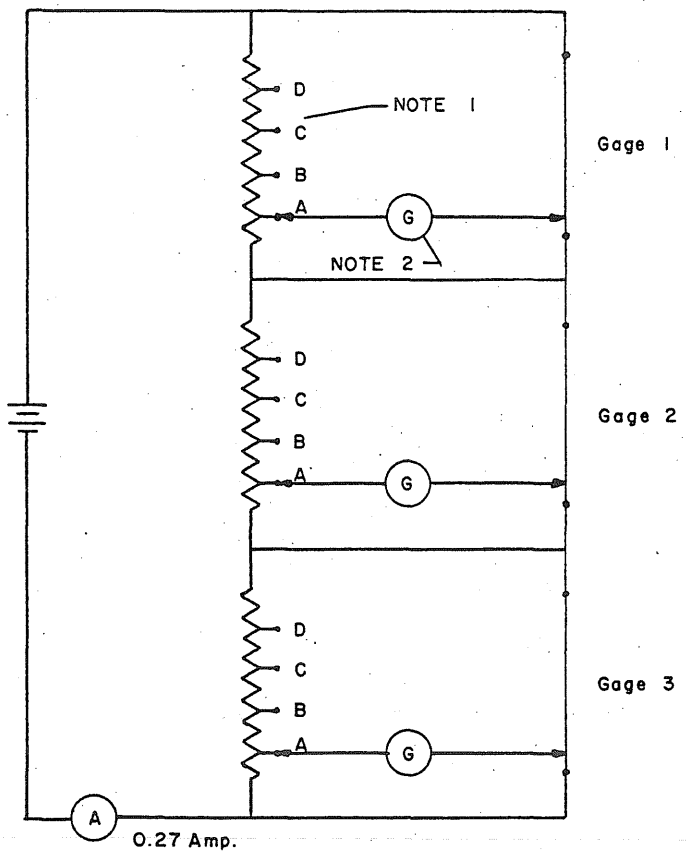

NOTE 1

Connections to B, C, and D for calibration purposes. Nominal values: B= 0.5" ; C= 2.0"; D= 4.0". Precise values taken from gage calibration curves. "A" is the balance position at zero deflection.

NOTE 2

Recording galvanometers are Hathaway Type OC2 , group 23 units used in Hathaway S14-C magnetic oscillographs.

FIG.5.5 DEFLECTION GAGE SYSTEM

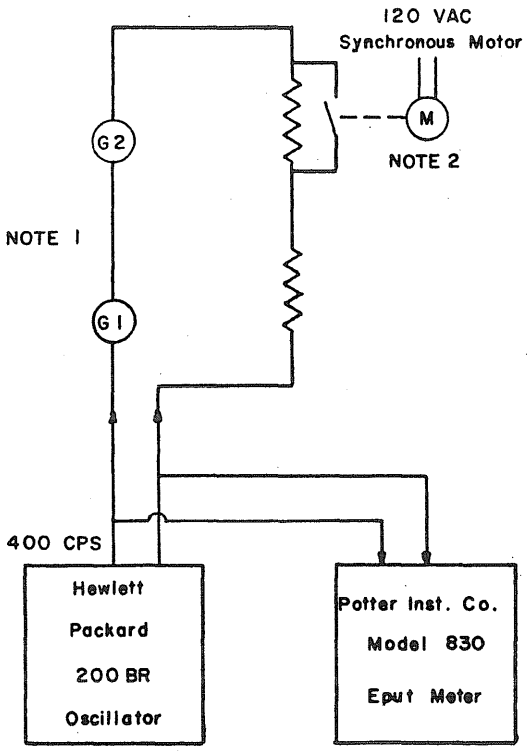

NOTE 1

G1 and G2 are Hathaway OC2 group 23 galvanometers. One galvanometer is located in each Hathaway S14—C oscillograph.

NOTE 2

Switch driven at synchronous speeds modulating the amplitude of the timing signal with steps every 0.02 min. and a step omitted once each 0.1 minute.

FIG. 5.6 TIMING AND RECORDING OF SYNCHRONIZING TRACES

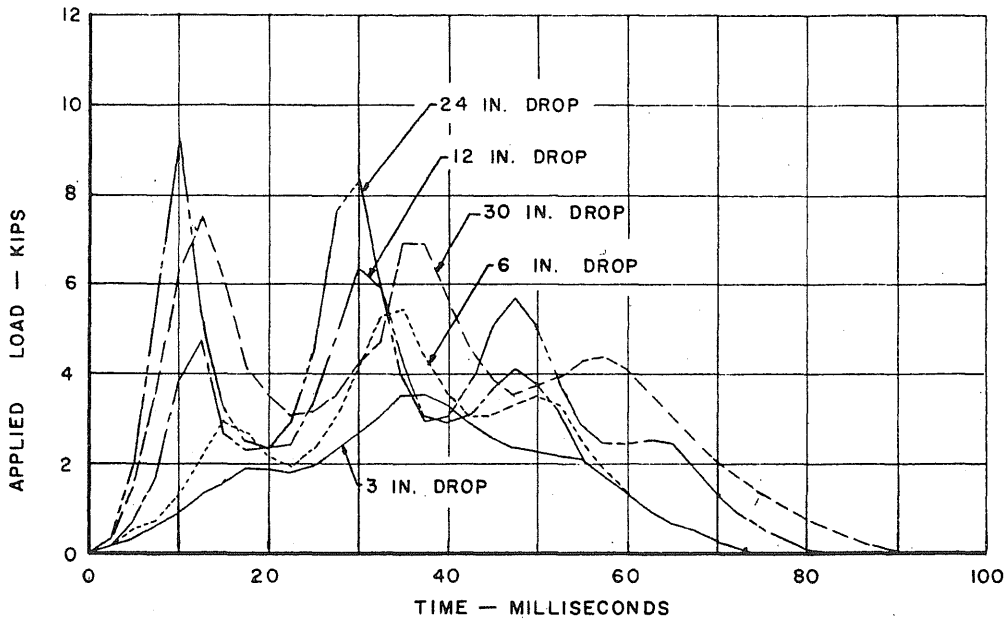

FIG. 5.7 LOAD TIME RELATIONSHIPS

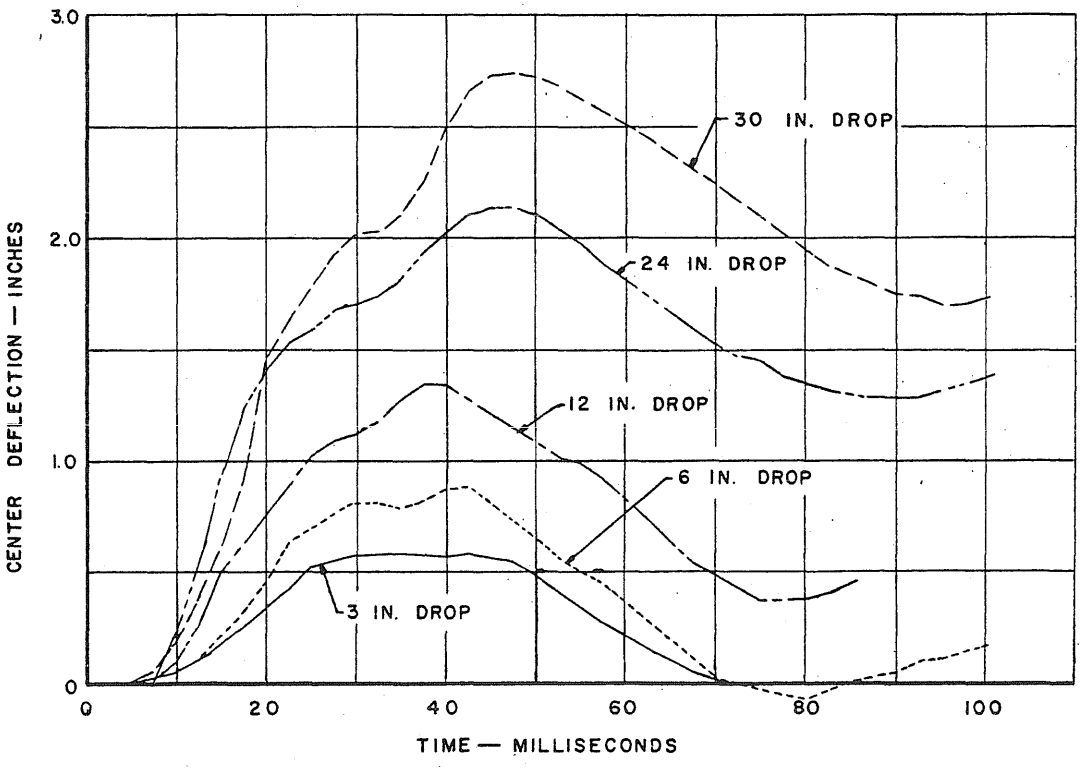

FIG. 5.8 CENTER DEFLECTION - TIME RELATIONSHIP

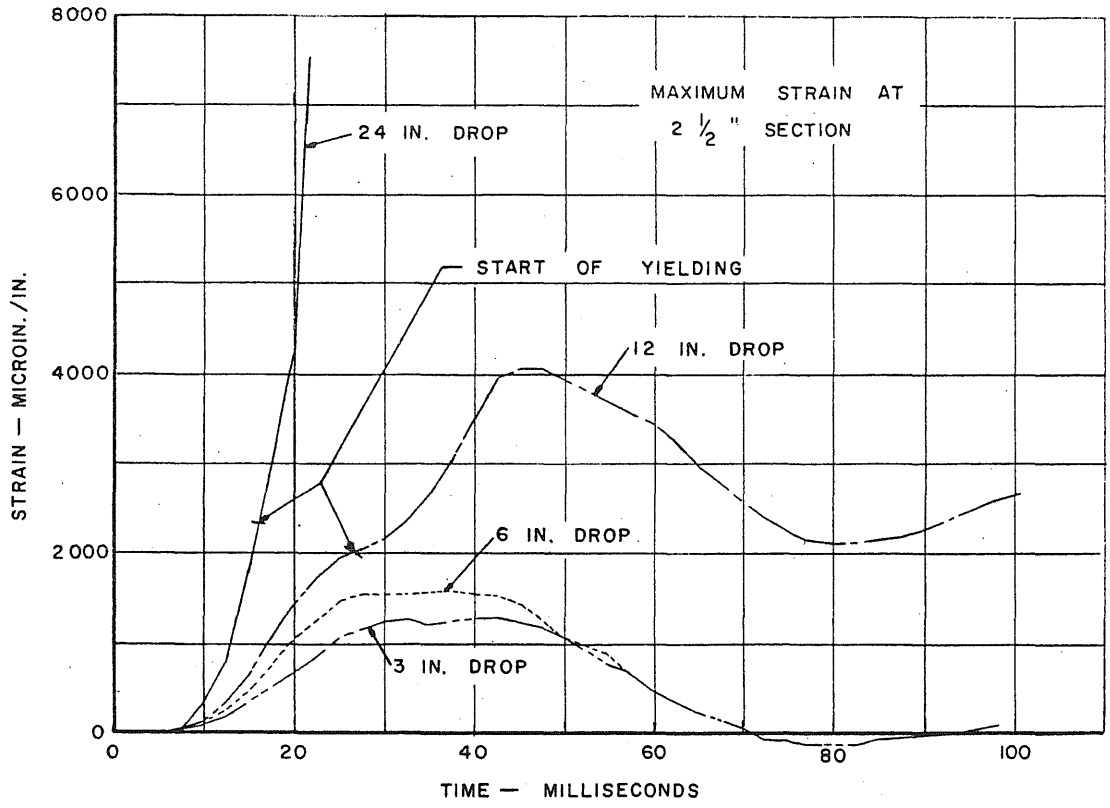

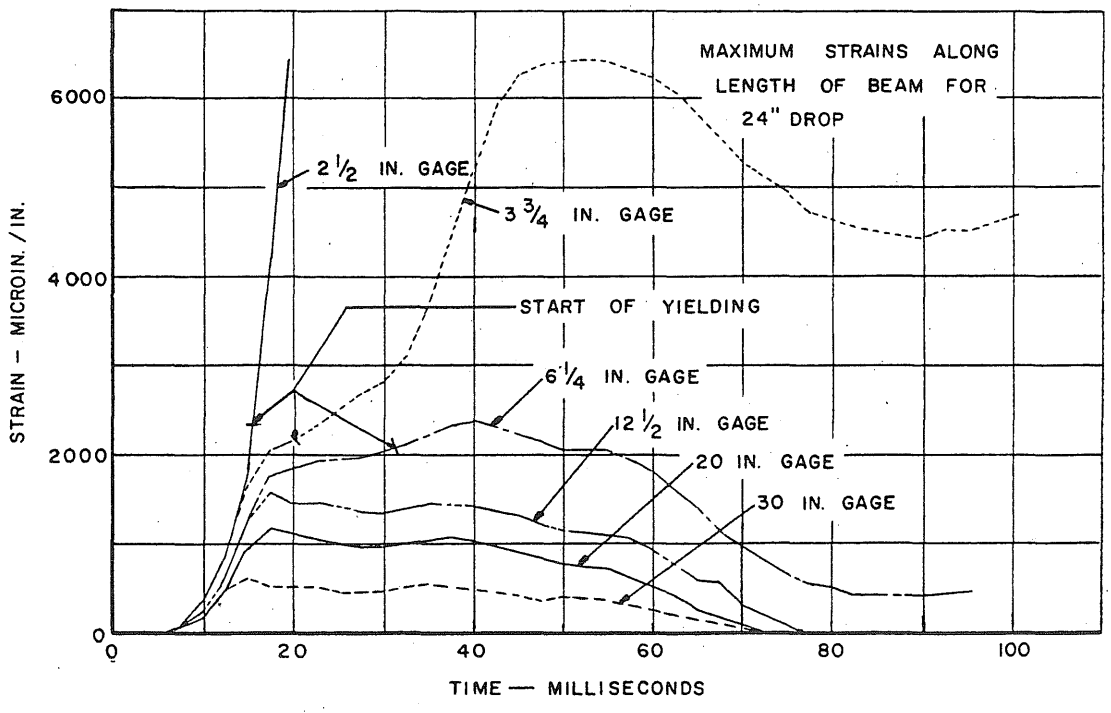

FIG. 5.9 STRAIN – TIME RELATIONSHIPS

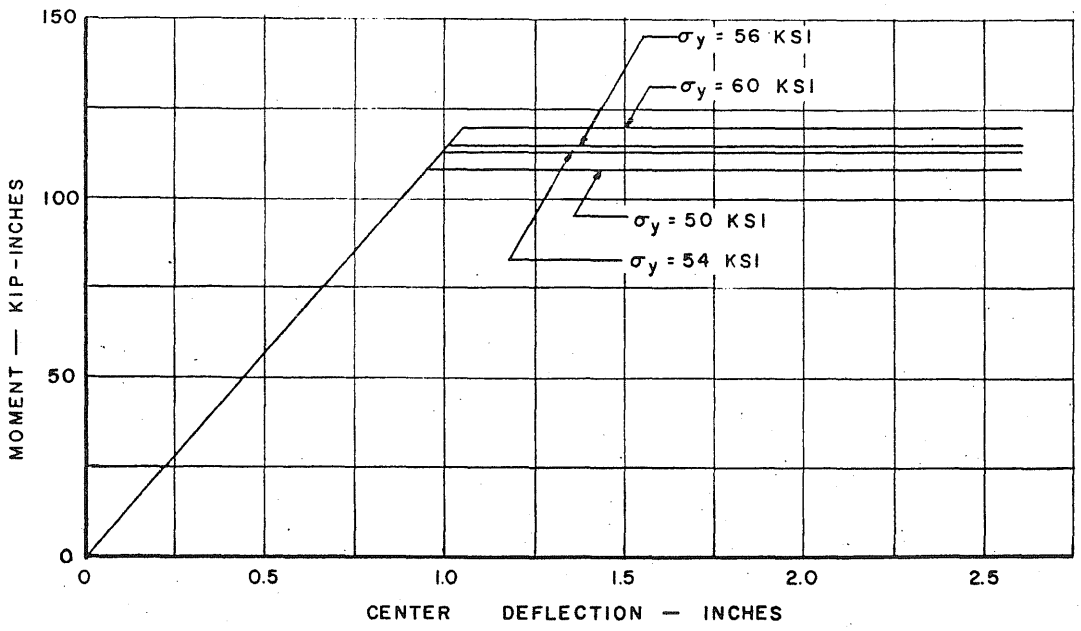

FIG. 5.11 a. ASSUMED RESISTING FUNCTION

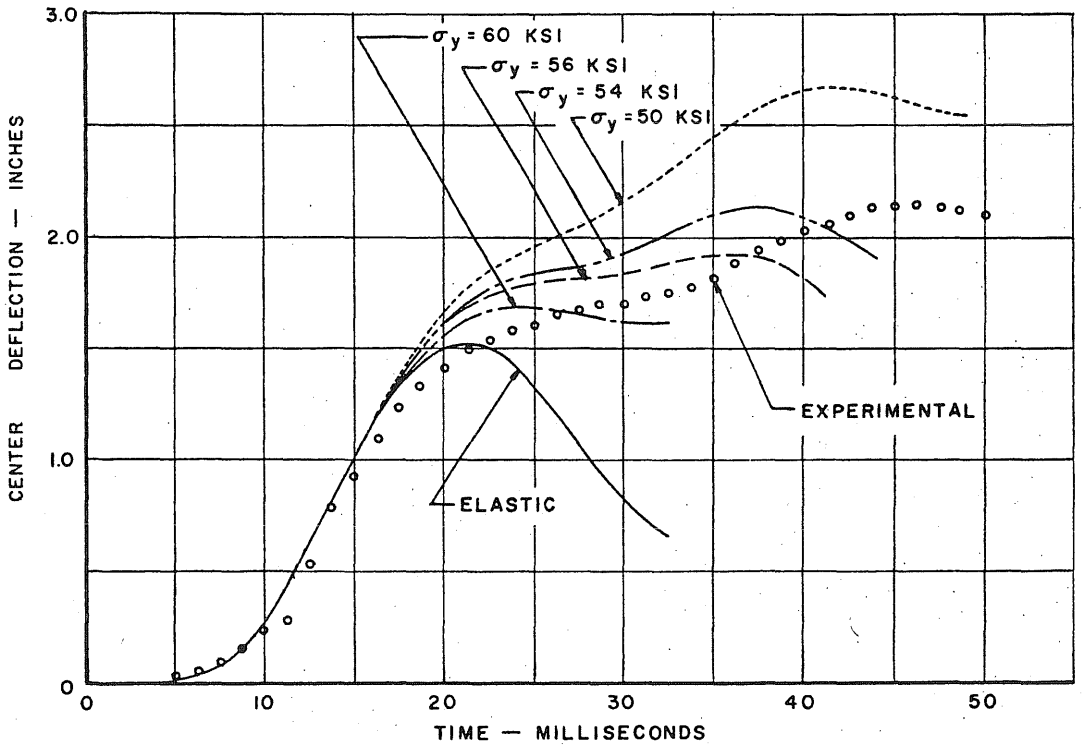

FIG. 5.11 b. COMPARISON OF THE COMPUTED AND MEASURED RESPONSE

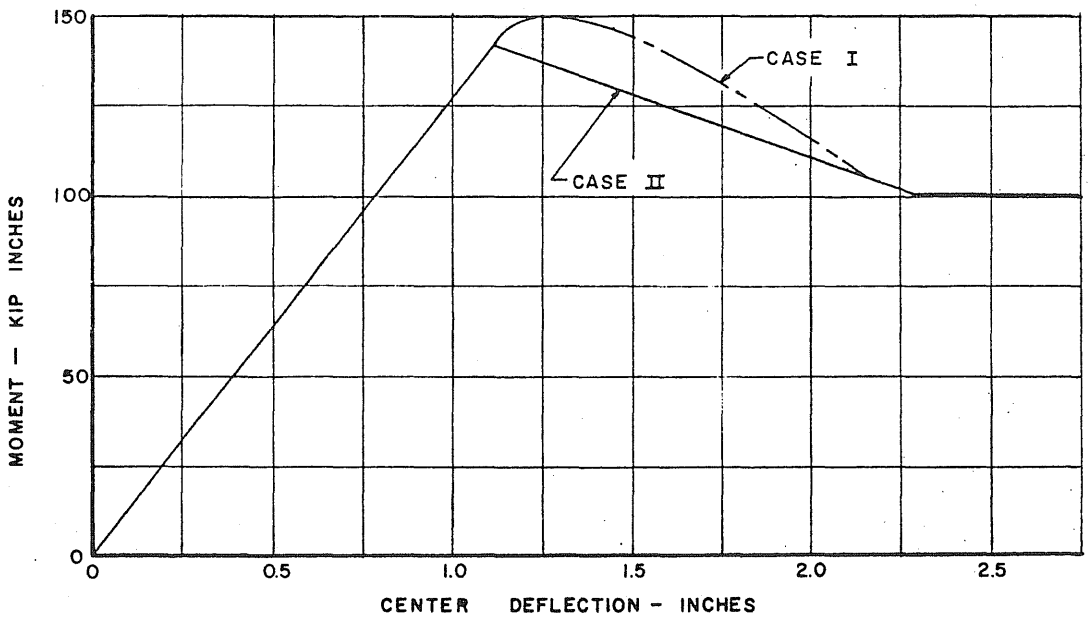

FIG. 5.12 a. ASSUMED RESISTING FUNCTIONS

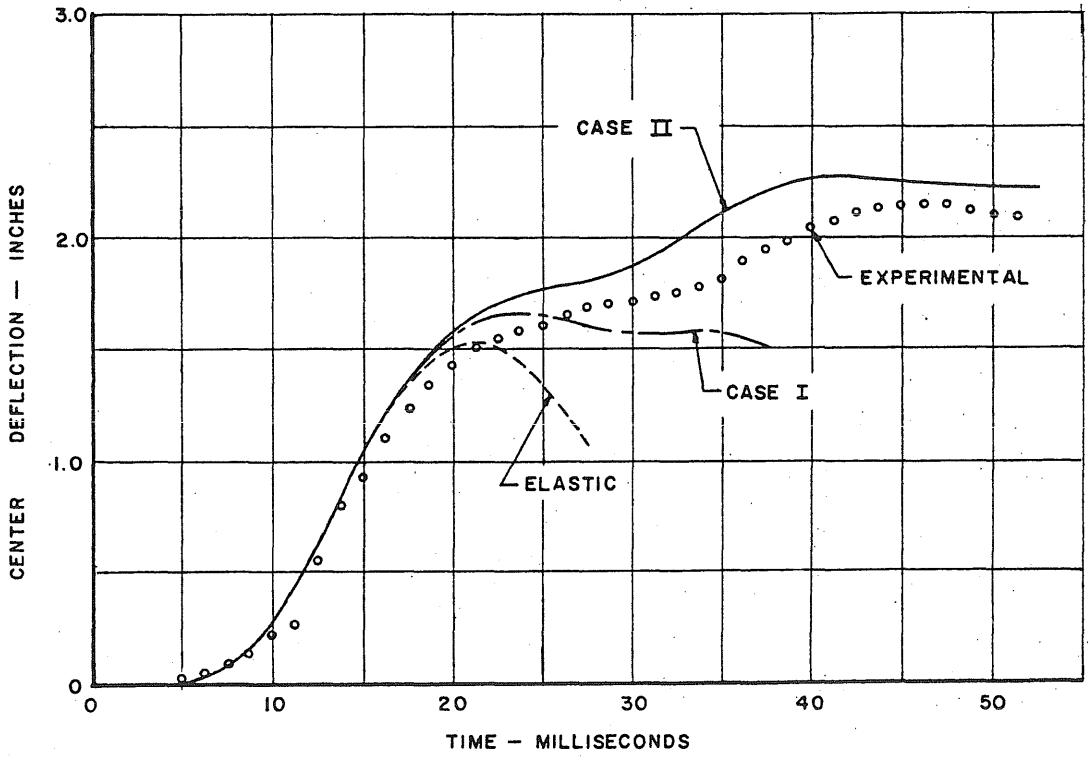

FIG. 5.12 b. COMPARISON OF THE COMPUTED AND MEASURED RESPONSE